



National Library  
of Canada

Acquisitions and  
Bibliographic Services Branch

395 Wellington Street  
Ottawa, Ontario  
K1A 0N4

Bibliothèque nationale  
du Canada

Direction des acquisitions et  
des services bibliographiques

395, rue Wellington  
Ottawa (Ontario)  
K1A 0N4

Number of microfiches

Number of microfiches

## NOTICE

## AVIS

The quality of this microform is heavily dependent upon the quality of the original thesis submitted for microfilming. Every effort has been made to ensure the highest quality of reproduction possible.

La qualité de cette microforme dépend grandement de la qualité de la thèse soumise au microfilmage. Nous avons tout fait pour assurer une qualité supérieure de reproduction.

If pages are missing, contact the university which granted the degree.

S'il manque des pages, veuillez communiquer avec l'université qui a conféré le grade.

Some pages may have indistinct print especially if the original pages were typed with a poor typewriter ribbon or if the university sent us an inferior photocopy.

La qualité d'impression de certaines pages peut laisser à désirer, surtout si les pages originales ont été dactylographiées à l'aide d'un ruban usé ou si l'université nous a fait parvenir une photocopie de qualité inférieure.

Reproduction in full or in part of this microform is governed by the Canadian Copyright Act, R.S.C. 1970, c. C-30, and subsequent amendments.

La reproduction, même partielle, de cette microforme est soumise à la Loi canadienne sur le droit d'auteur, SRC 1970, c. C-30, et ses amendements subséquents.

UNIVERSITY OF ALBERTA

EFFECT OF MIXING ON THE KINETICS OF POLYMER-AIDED FLOCCULATION

BY

XIUGUO YANG



A THESIS SUBMITTED TO THE FACULTY OF GRADUATE STUDIES AND  
RESEARCH IN PARTIAL FULFILLMENT OF THE REQUIREMENTS FOR THE  
DEGREE OF MASTER OF SCIENCE

IN

ENVIRONMENTAL ENGINEERING  
DEPARTMENT OF CIVIL ENGINEERING

EDMONTON, ALBERTA

SPRING, 1996



National Library  
of Canada

Acquisitions and  
Bibliographic Services Branch

395 Wellington Street  
Ottawa, Ontario  
K1A 0N4

Bibliothèque nationale  
du Canada

Direction des acquisitions et  
des services bibliographiques

395, rue Wellington  
Ottawa (Ontario)  
K1A 0N4

Your file / Votre référence

Our file / Notre référence

**The author has granted an irrevocable non-exclusive licence allowing the National Library of Canada to reproduce, loan, distribute or sell copies of his/her thesis by any means and in any form or format, making this thesis available to interested persons.**

**L'auteur a accordé une licence irrévocable et non exclusive permettant à la Bibliothèque nationale du Canada de reproduire, prêter, distribuer ou vendre des copies de sa thèse de quelque manière et sous quelque forme que ce soit pour mettre des exemplaires de cette thèse à la disposition des personnes intéressées.**

**The author retains ownership of the copyright in his/her thesis. Neither the thesis nor substantial extracts from it may be printed or otherwise reproduced without his/her permission.**

**L'auteur conserve la propriété du droit d'auteur qui protège sa thèse. Ni la thèse ni des extraits substantiels de celle-ci ne doivent être imprimés ou autrement reproduits sans son autorisation.**

ISBN 0-612-10769-8

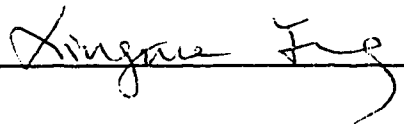
**Canada**

UNIVERSITY OF ALBERTA  
LIBRARY RELEASE FORM

NAME OF AUTHOR: XIUGUO YANG  
TITLE OF THESIS: EFFECT OF MIXING ON THE KINETICS OF  
POLYMER-AIDED FLOCCULATION  
DEGREE: MASTER OF SCIENCE  
YEAR THIS DEGREE  
GRANTED: 1996

Permission is hereby granted to the University of Alberta Library to reproduce single copies of this thesis and to lend or sell such copies for private, scholarly, or scientific research purposes only.

The author reserves all other publication and other rights in association with the copyright in the thesis, and except as herein before provided, neither the thesis nor any substantial portion thereof may be printed or otherwise reproduced in any material form whatever without the author's prior written permission.

  
\_\_\_\_\_

PERMANENT ADDRESS:

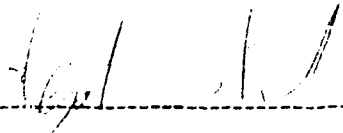
11703-133 Street  
Edmonton, Alberta  
T5M, 1H7

Date: Dec. 21, 1993

UNIVERSITY OF ALBERTA

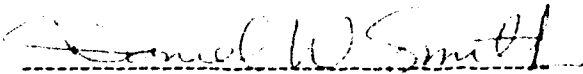
FACULTY OF GRADUATE STUDIES AND RESEARCH

The undersigned certify that they have read, and recommended to the Faculty of Graduate Studies and Research for acceptance, a thesis entitled **Effect of Mixing on the Kinetics of Polymer-Aided Flocculation** submitted by **Xiuguo Yang** in partial fulfillment of the requirements for the degree of **Master of Science in Environmental Engineering**.



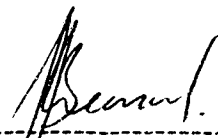
-----

Dr. Stephen J. Stanley (Co-supervisor)



-----

Dr. Daniel W. Smith (Co-supervisor)



-----

Dr. Jerry J. Leonard

Date: Dec. 20, 1995

## **ABSTRACT**

This study focused on a thorough evaluation of polymer-aided flocculation. It included the investigation of optimum experimental process conditions, and the role of mixing in the flocculation. Mathematical models were developed to describe both the rate of the flocculation, and the rate of polymeric floc growth. The impacts of mixing on kinetic parameters were predicted by mathematical models, and an optimum mixing condition was determined as a result of the kinetic analyses. Moreover, the structures of a kaolin aggregate, a alum floc and a polymeric floc were observed using scanning electron microscope, and performance of alum flocculation and polymer-aided flocculation were compared. The results confirm the conclusions that mixing has a greater impact on the kinetics of polymer-aided flocculation; the rate of polymer-aided flocculation follows a first order kinetic model with respect to primary particle concentration; and the rate of polymeric floc growth obeys a log-normal equation.

## ACKNOWLEDGEMENTS

My foremost thanks go to my co-supervisors Dr. D. W. Smith and Dr. S. J. Stanley for their valuable guidance, encouragement, and financial support throughout the course of this research. The great contributions of Dr. S. J. Stanley with various aspects of this research, specially in experimental designs and participation of lab work, are sincerely appreciated. I would also like to thank the other member of my committee, Dr. J. J. Leonard, for his helpful suggestions.

A special thanks would like to give to Nick Chernuka and Garry Solonyenko for their technical assistance in the lab work.

I would also like to express my appreciation to: Mr. S. Suthaker for the computer supervision, Mr. Dennis Prince for the cooperation with photography, and Mrs. Honghui Zhu for providing the polymers .

## TABLE OF CONTENTS

1 INTRODUCTION .....	1
1.1 Background .....	1
1.2 Scope of Investigation.....	4
2 RESEARCH OBJECTIVES .....	6
3 REVIEW OF LITERATURE .....	7
3.1 Characteristics of Fine Particles.....	7
3.1.1 General Characteristics of Fine Particles .....	7
3.1.2 Characteristics of Kaolin Particles .....	8
3.2 Mechanisms of Coagulation and Flocculation .....	10
3.2.1 General Mechanisms of Coagulation and Flocculation .....	10
3.2.2 Mechanisms of Polymer Flocculation.....	11
3.3 Mechanisms of Mixing .....	13
3.4 Types of Coagulant System .....	15
3.5 Types of Coagulant .....	16
3.5.1 Inorganic Coagulants .....	16
3.5.2 Organic Coagulants.....	18
3.6 Factors Influencing Polymer Performance .....	20
3.6.1 Polymer Molecular Weight .....	20
3.6.2 Polymer Molecular Structure .....	21
3.6.3 Ionic Group and Charge Density .....	22
3.6.4 Polymer Dosage .....	23
3.6.5 Polymer Concentration .....	24
3.6.6 Ionic Strength of Suspension.....	24



3.6.7	Degree of Polymer Hydrolysis.....	24
3.6.8	Experimental Process Conditions .....	25
3.7	General Review of the Kinetics of Flocculation .....	26
3.7.1	Kinetics of Perikinetic Flocculation.....	27
3.7.2	Kinetics of Orthokinetic Flocculation .....	28
3.7.2.1	Rate of Aggregation .....	29
3.7.2.2	Rate of Floc Breakup .....	36
3.7.2.3	Overall Kinetics of Orthokinetic Flocculation.....	37
3.7.2.4	Kinetics of Polymer Flocculation .....	38
3.7.3	Kinetics of Floc Growth.....	38
3.8	Safety Regulations Regarding Polymer Use in Drinking Water	
Treatment	.....	40
<b>4</b>	<b>METHODS AND APPARATUS .....</b>	<b>42</b>
4.1	Preparation of Solutions.....	42
4.1.1	Kaolin Suspension.....	42
4.1.2	Alum Solution .....	42
4.1.3	Polymer Stock Solution .....	43
4.1.4	Polymer Feed Solution .....	43
4.2	Experimental Apparatus.....	43
4.2.1	Reactor .....	43
4.2.2	PH Meter .....	45
4.2.3	Turbidity Meter .....	45
4.2.4	Particle Size Analyzer .....	45
4.2.5	Scanning Electron Microscope .....	48
4.3	Experimental Methods .....	49

<b>5 RESULTS AND DISCUSSIONS .....</b>	<b>50</b>
<b>5.1 Evaluation of Kaolin Particle Size and Size Distribution .....</b>	<b>50</b>
<b>5.2 Methods of Data Analysis.....</b>	<b>51</b>
5.2.1 Particle Size Distribution .....	51
5.2.2 Mean Particle Diameter .....	51
5.2.3 Flocculation Efficiency .....	59
<b>5.3 Selection of an Optimum Polymer as a Coagulant Aid .....</b>	<b>59</b>
<b>5.4 Determination of Optimum Experimental Conditions.....</b>	<b>62</b>
5.4.1 Optimum pH .....	62
5.4.2 Optimum Alkali Dose .....	71
5.4.3 Method for Polymer Addition.....	76
5.4.4 Reactor Volume .....	79
<b>5.5 Effect of Mixing on the Kinetics of Polymer-Aided Flocculation.....</b>	<b>83</b>
5.5.1 Effect of Mixing on the Rate of Polymer-Aided Flocculation.....	83
5.5.1.1 Model Simulation and Residual Examination.....	83
5.5.1.2 Effect of Mixing on the First Order Rate Constant.....	95
5.5.2 Effect of Mixing on the Rate of Polymeric Floc Growth .....	99
5.5.2.1 Mechanism of Polymeric Floc Growth .....	99
5.5.2.2 Effect of Mixing on Floc Buildup Time .....	110
5.5.2.3 Effect of Mixing on Floc Growth Constants.....	116
5.5.2.4 Effect of Mixing on Mean Floc Growth Rate .....	119
<b>5.6 Effect of Mixing on Particle Size Distribution Function .....</b>	<b>130</b>
<b>5.7 Effect of Mixing on the Maximum Mean Floc Diameter .....</b>	<b>132</b>
<b>5.8 Comparison between Alum Flocculation and Polymer Aided     Flocculation.....</b>	<b>137</b>
<b>6 CONCLUSIONS .....</b>	<b>153</b>

7 LIMITATIONS AND SUGGESTIONS OF THE STUDY .....	155
8 REFERENCES.....	158
9 APPENDIX .....	177
Appendix A Reactor Calibration Plot .....	177
Appendix B Polymeric Floc Growth Curves on Semilogarithmic Scale .....	177
Appendix C Model for Effect of Mixing on the First Order Rate Constant .....	183
Appendix D Determination of the Power Law Slope Coefficient .....	190
Appendix E Determination of the $d_{max}$ Growth Constant.....	196
Appendix F The Data of Determination of Experimental Conditions .....	208
Appendix G Kinetic Data of Polymer-Aided Flocculation.....	213

## LIST OF TABLES

Table 4.1 Channel Setting of the Particle Size Analyzer .....	46
Table 5.1 Nomenclature Mean Particle Diameters $\bar{D}_{p,q}$ .....	53
Table 5.2 Process Conditions for the Determination of the Optimum Polymer and the Optimum Dose Combination .....	60
Table 5.3 Model Simulation Process ( $\bar{G}_f=80 \text{ s}^{-1}$ ).....	85
Table 5.4 The Examination of Serial Correlation in Residuals .....	93
Table 5.5 Effect of Mixing on the First Order Kinetic Constant (K).....	95
Table 5.6 Model Simulation Process for the Effect of Mixing on $t_b$ .....	113
Table 5.7 Model Simulation Process for the Effect of Mixing on $t_o$ .....	127
Table 5.8 Comparison between Alum flocculation with Polymer-Aided Flocculation.....	139

## LIST OF PLATES

Plate 4.1	Equipment Apparatus.....	44
Plate 5.1	Shape of a Polymeric Floc at a High Mixing Rate ( $\bar{G}_c = \bar{G}_f = 400 \text{ s}^{-1}$ ).....	140
Plate 5.2	Shape of a Polymeric Floc with a Big Size( $d \cong 150 \mu\text{m}$ ).....	141
Plate 5.3	Shape of a Polymeric Floc with a Small Size( $d \cong 10 \mu\text{m}$ ).....	142
Plate 5.4	Shape of a Alum Floc with a Big Size( $d \cong 70 \mu\text{m}$ ).....	143
Plate 5.5	Microstructure of Kaolin Aggregate.....	144
Plate 5.6	Microstructure of a Polymeric Floc formed at a high Mixing Rate ( $\bar{G}_c = \bar{G}_f = 400 \text{ s}^{-1}$ ).....	145
Plate 5.7	Microstructure of a Big Alum Floc ( $\bar{G}_c = \bar{G}_f = 400 \text{ s}^{-1}$ ).....	146

## LIST OF FIGURES

Figure 5.1 Particle Size Distribution of the Kaolin Particles .....	50
Figure 5.2 Flocculation Curve at $\bar{G}_f=80 \text{ s}^{-1}$ .....	52
Figure 5.3 Evaluation of Mean Particle Diameters ( $d_i$ = Channel Setting) .....	56
Figure 5.4 Evaluation of Mean Particle Diameters ( $d_i$ = Arithmetic Mean)).....	57
Figure 5.5 Comparison of D(6,3) Values Expressed by Different $d_i$ .....	58
Figure 5.6 Effect of pH on Maximum Mean Floc Diameter and Particle Removal Efficiency .....	65
Figure 5.7 Effect of pH on Turbidity Removal Rate .....	66
Figure 5.8 Particle Size Distributions at pH=8 .....	69
Figure 5.9 Particle Size Distributions at pH=8 (on Semilogarithmic Scale) .....	70
Figure 5.10 Effect of Alkali Dosage on Particle Removal Efficiency and D(6,3) .....	73
Figure 5.11 Effect of Alkali Dosage on Particle Settling Rate .....	74
Figure 5.12 Effect of Lag Time on Particle Removal Efficiency (E), and Maximum Particle Size ( $d_{max}$ ).....	77
Figure 5.13 Effect of Lag Time on Particle Settling Rate .....	78
Figure 5.14 Effect of Reactor Volume on the Rate of Polymeric Floc Growth .....	80
Figure 5.15 The Curves of Mean Floc Growth Rate.....	81
Figure 5.16 Polymeric Floc Growth Curves .....	82
Figure 5.17 Kinetic Curves of Polymer-Aided Flocculation ( $20 \leq \bar{G}_f \leq 50 \text{ s}^{-1}$ ).....	86
Figure 5.18 Kinetic Curves of Polymer-Aided Flocculation ( $60 \leq \bar{G}_f \leq 100 \text{ s}^{-1}$ ).....	87
Figure 5.19 Kinetic Curves of Polymer-Aided Flocculation ( $125 \leq \bar{G}_f \leq 200 \text{ s}^{-1}$ ).....	88
Figure 5.20 Kinetic Curves of Polymer-Aided Flocculation ( $225 \leq \bar{G}_f \leq 400 \text{ s}^{-1}$ ).....	89
Figure 5.21 Residuals Plotted against Fitted Values.....	91
Figure 5.22 Residuals Plotted against Independent Parameter .....	91
Figure 5.23 Normal Plot of the Residuals .....	92

Figure 5.23	Normal Plot of the Residuals .....	92
Figure 5.24	Histogram Plot of the Residuals .....	92
Figure 5.25	The Model Simulation Diagram ( $\bar{G}_f = 80 \text{ s}^{-1}$ ).....	94
Figure 5.26	Effect of Mixing on the First Order Rate Constant .....	96
Figure 5.27	Linear Regression of the First Order Rate Constants .....	98
Figure 5.28	Polymeric Floc Growth Curves at $20 \leq \bar{G}_f \leq 60 \text{ s}^{-1}$ .....	100
Figure 5.29	Polymeric Floc Growth Curves at $70 \leq \bar{G}_f \leq 150 \text{ s}^{-1}$ .....	101
Figure 5.30	Polymeric Floc Growth Curves at $175 \leq \bar{G}_c = \bar{G}_f \leq 225 \text{ s}^{-1}$ .....	102
Figure 5.31	Polymeric Floc Growth Curves at $100 \leq \bar{G}_f \leq 400 \text{ s}^{-1}$ .....	103
Figure 5.32	Polymeric Floc Growth Curves at $450 \leq \bar{G}_c = \bar{G}_f \leq 800 \text{ s}^{-1}$ .....	104
Figure 5.33	Polymeric Floc Growth Curves at $1000 \leq \bar{G}_c = \bar{G}_f \leq 1600 \text{ s}^{-1}$ .....	105
Figure 5.34	Polymeric Floc Growth Curves on Semilogarithmic Scale .....	107
Figure 5.35	Effect of Mixing Rate on Transfer Points .....	108
Figure 5.36	Effect of Mixing on the Floc Buildup Time $t_b$ .....	112
Figure 5.37	Residuals Plotted against Fitted Values.....	114
Figure 5.38	Residuals Plotted against Independent Parameter .....	114
Figure 5.39	The Histogram Plot of the Residuals .....	115
Figure 5.40	The Normal Plot of the Residuals.....	115
Figure 5.41	Effect of Mixing on the Floc Growth Constants.. .....	117
Figure 5.42	Curves of Mean Polymeric Floc Growth Rate at $\bar{G}_f = 20$ to $40 \text{ s}^{-1}$ .....	120
Figure 5.43	Curves of Mean Polymeric Floc Growth Rate at $\bar{G}_f = 60$ to $100 \text{ s}^{-1}$ .....	121
Figure 5.44	Curves of Mean Polymeric Floc Growth Rate at $\bar{G}_f = 150$ to $200 \text{ s}^{-1}$ .....	122
Figure 5.45	Curves of Mean Polymeric Floc Growth Rate at $\bar{G}_f = 300$ to $400 \text{ s}^{-1}$ .....	123
Figure 5.46	Effect of Mixing on Maximum Mean Floc Growth Rate .....	124
Figure 5.47	Effect of Mixing on Critical Flocculation Time .....	125
Figure 5.48	Residuals Plotted against Fitted Values ( $t_0$ ).....	128
Figure 5.49	Residuals Plotted against Independent Parameter .....	128

Figure 5.50 Normal Plot of the Residuals .....	129
Figure 5.51 Histogram Plot of the Residuals .....	129
Figure 5.52 Effect of the Degree of Flocculation on the Power Law Slope Coefficient .....	132
Figure 5.53 Polymeric Floc Growth Process .....	133
Figure 5.54 Effect of Mixing on the Maximum Mean Floc Diameter .....	134
Figure 5.55 Effect of Mixing on $d_{\max}$ Growth Constants .....	135
Figure 5.56 Effect of Mixing on Particle Removal Efficiency in Alum Flocculation .....	147
Figure 5.57 Effect of Mixing on the Growth Rate of Alum Flocs .....	148
Figure 5.58 Effect of Polymer on Particle Removal Efficiencies at $\bar{G}_f=40 \text{ s}^{-1}$ .....	149
Figure 5.59 Effect of Polymer on Particle Removal Efficiencies at $\bar{G}_f=70 \text{ s}^{-1}$ .....	150
Figure 5.60 Effect of Polymer on the Rate of Floc Growth at $\bar{G}_f=40 \text{ s}^{-1}$ .....	151
Figure 5.61 Effect of Polymer on the Rate of Floc Growth at $\bar{G}_f=70 \text{ s}^{-1}$ .....	152



## LIST OF SYMBOLS

$A_0$	Power law density coefficient
$\bar{D}_{-1,0}$	Harmonic mean diameter ( $\mu\text{m}$ )
$\bar{D}_{0,0}$	Geometric mean diameter ( $\mu\text{m}$ )
$\bar{D}_{1,0}$	Arithmetic mean diameter ( $\mu\text{m}$ )
$\bar{D}_{2,0}$	Mean surface diameter ( $\mu\text{m}$ )
$\bar{D}_{3,0}$	Mean volume diameter ( $\mu\text{m}$ )
$\bar{D}_{2,1}$	Diameter-weighted mean diameter ( $\mu\text{m}$ )
$\bar{D}_{3,2}$	Surface-weighted mean diameter ( $\mu\text{m}$ )
$\bar{D}_{4,3}$	Volume-weighted mean diameter ( $\mu\text{m}$ )
$\bar{D}_{3,1}$	Diameter-weighted mean surface diameter ( $\mu\text{m}$ )
$\bar{D}_{4,2}$	Surface-weighted mean surface diameter ( $\mu\text{m}$ )
$\bar{D}_{5,3}$	Volume-weighted mean surface diameter ( $\mu\text{m}$ )
$\bar{D}_{4,1}$	Diameter-weighted mean volume diameter ( $\mu\text{m}$ )
$\bar{D}_{5,2}$	Surface weighted mean volume diameter ( $\mu\text{m}$ )
$\bar{D}_{6,3}$	Volume-weighted mean volume diameter ( $\mu\text{m}$ )
$\bar{D}_{1,1}$	Diameter-weighted geometric mean diameter ( $\mu\text{m}$ )
$\bar{D}_{2,2}$	Surface-weighted geometric mean diameter ( $\mu\text{m}$ )
$\bar{D}_{3,3}$	Volume-weighted geometric mean diameter ( $\mu\text{m}$ )
$D(6,3)_0$	$D(6,3)$ at $t_f = 0$ min. ( $\mu\text{m}$ )
$D(6,3)_{t_1}$	Mean floc diameters at $t_f = t_1$ ( $\mu\text{m}$ )
$D(6,3)_{t_2}$	Mean floc diameters at $t_f = t_2$ ( $\mu\text{m}$ )
$D(6,3)$	Volume-weighted mean volume diameter at $t_f$ ( $\mu\text{m}$ )
$D_i$	Statistical values of diameter

E	$(1 - \frac{n_t}{n_0}) \times 100\%$ = particle removal efficiency
$\bar{G}_c$	Mean velocity gradient in fast mixing process
$\bar{G}_f$	Mean velocity gradient in slow mixing process
K	First order rate constant
K	Rate constant of floc collision
$K_1$	Aggregation constant
$K'$	Rate constant of floc aggregation
$K_2''$	Floc breakup constant
$K_A$	Overall flocculation constant or general aggregation constant
$K_B'$	Floc breakup coefficient
$K_F$	$= - \frac{\alpha \epsilon a^3}{\pi} = \text{constant}$
$K_T$	Theoretic isotropic turbulence first order rate constant
$K_s$	Theoretic Smoluchowski first order rate constant
L	Constant which values are dependent on the floc size
$N_1$	turbidity of effluent (NTU)
$N_0$	Turbidity of influent (NTU)
$N_0/N_1$	Turbidity removal
$N_t$	Total particle concentration,(count/mL)
P	Total power dissipated (W)
$\frac{R_{t_2+t_1}}{2}$	= $(\Delta d/\Delta t)$ ; mean polymeric floc growth rate at the midpoint of flocculation interval of $t_1$ to $t_2$ ( $\mu\text{m}/\text{min.}$ )
$(\frac{R_{t_2+t_1}}{2})_{\text{max}}$	= $(\Delta d/\Delta t)_{\text{max}}$ , maximum mean floc growth rate ( $\mu\text{m}/\text{min.}$ )
T	Absolute temperature (K)
V	Volume of reactor ( $\text{m}^3$ )
d	Diameter of particle ( $\mu\text{m}$ )
$d_i$	$d_1 i^{1/3}$ = diameter of i-fold particles ( $\mu\text{m}$ )

$d_j$	$d_j j^{1/3}$ = diameter of j-fold particles ( $\mu\text{m}$ )
$\bar{d}$	Arithmetic mean particle diameter ( $\mu\text{m}$ )
$d'$	Constant ( $\mu\text{m}$ )
$d_p$	Diameter of particles ( $\mu\text{m}$ )
$d_1$	Diameter of primary particles ( $\mu\text{m}$ )
$d_i$	Floc diameter ( $\mu\text{m}$ )
$\frac{dn_m}{dt}$	Rate of change of number concentration of particles of size $d_m$ (count/mL·s)
$dN$	Number of particles per unit fluid volume in size range $d_p$ to $d_p+d(d_p)$ (count/mL)
$dn_1/dt$	Diminution rate of the primary particle concentration of $n_1$ (count/mL·s)
$d_{\text{max}}$	Maximum mean floc diameter ( $\mu\text{m}$ )
$k$	Boltzmann's constant
$m$	$d_{\text{max}}$ growth constant
$n$	Primary particle concentration ( $d \leq 10 \mu\text{m}$ ) (count/mL)
$n_i$	Number of particles with diameter $d_i$ (count/mL)
$n_j$	Concentration of particles of size of $d_j$ (count/mL)
$\dot{n}(d_p)$	Particle size distribution function
$q$	Fraction of the surface covered by adsorbed polymer segment
$t_b$	Floc buildup time (min., or sec.)
$t_f$	Flocculation time (min., or sec.)
$t_j$	Transfer points on the floc growth Curves (min., or sec.)
$t_o$	Critical flocculation time when the maximum mean floc growth rate [ $(R_{\frac{d_2-d_1}{2}})_{\text{max}}$ ] reaches (min., or sec.)
$\mu'$	Absolute viscosity ( $\text{N} \cdot \text{s}/\text{m}^2$ )

$\epsilon$	Power input or dissipation per unit mass of fluid
$\dot{a}$	Ratio of particle collision radius to its physical radius,
$\dot{\epsilon}$	Size distribution function
$\phi$	Volume fraction, or volume of primary particles per unit volume of suspension.
$a$	Collision efficiency
$b$	Power law slope coefficient that characterizes size distributions
$g$	Kinematic viscosity
$\mu$	Floc growth constant (min. <sup>-1</sup> )
$\Delta d$	Channel width ( $\mu\text{m}$ )
$\Delta N$	Differential particle concentration (counts/ mL)

# 1 INTRODUCTION

## 1.1 Background

Particles are ubiquitous in natural waters. Some of them may be contaminants themselves, while others may be transporting contaminants which may affect human health and aquatic ecosystems. The recognition that particulate matter in drinking water may impact public health has recently resulted in more stringent drinking water guidelines. Turbidity, which is a general measure of the quantity of particles in water, is one of the measures used to assess drinking water quality, and allowable limits continue to decrease. There is also a requirement to remove very fine particles ( $d \leq 10 \mu\text{m}$ ), as these particles have been associated with microbial contaminants and generally are difficult to remove. As a result, water utilities and researchers have begun to search for methods to optimize the coagulation, flocculation and sedimentation processes, which is generally the most economical method of removing large quantities of particulate matter from water.

One of the realistic and cost-effective strategies to optimize the coagulation, flocculation and sedimentation processes is to investigate coagulant alternatives. This has been driven by the knowledge that conventional alum coagulation has been found to have two major disadvantages: 1) not effective at removal of the fine particles; 2) the high dosage of alum required which can result in the excessive volume of sludge and the high residual aluminum concentrations in finished water. The alum sludge is difficult to dewater, and it constitutes a possible ecological hazard (Bosanac, et al 1993). Although there is still great controversy associated with it, the significance of residual aluminum in drinking water has been linked to a number of neurological disorders such as Alzheimer's disease (Selvapathy, 1992), and as a result, residual aluminum is being considered for inclusion in drinking water guidelines and standards (Leony, 1992).

A number of alternatives are available to overcome the above disadvantages, which include: 1) the use of non-aluminum based metal salts (iron salts) as coagulants; 2) the adjustment of pH, when alum is used, to minimize residual aluminum concentrations; 3) the use of polymerized alum salts; 4) the use of a cationic metal-polysilicate complex; and 5) the use of polymer as a coagulant or a coagulant aid. The first four alternatives will eliminate or reduce residual alum concentrations, and increase flocculation efficiency. However, the dosages required are still high resulting a large volume of sludge. The priority to address the above concerns is to use a polymer in the coagulation process as a primary coagulant, or as a coagulant aid to reduce the dosage of alum required. The use of polymers provides the following advantages:

- (1) Polymer flocculation has been shown to be excellent at the removal of fine particles (Namasivayam and Kanagarathinam, 1992), and increases the strength and density of flocs over that of inorganic coagulant alone (Levine, and Friesen, 1987). The improved floc characteristics result in increased floc settling rates with an additional benefit that flocculation occurs over a wider pH range (Benedek, 1976). This can lead to a decrease in the size of the settling basins (Gilman, 1979-b) due to the reduction in the detention time required for clarification, or allow for greater production in existing systems.
- (2) The use of polymers has been found to reduce water treatment costs due to lower inorganic coagulant dosages required, and a smaller volume of sludge produced. This reduces chemical costs and overall sludge disposal costs. Furthermore, the sludge formed also tends to have better dewatering properties, which further reduces sludge handling cost and the environmental problems associated with the final disposal of sludge (King and Blankenship, 1979; Tascchi, 1977).

Review of available literature found that a great quantity of work has been carried out on the study of polymer flocculation. However, this research focused on a less well studied component of polymer coagulation and flocculation, specifically the study of the kinetics of polymer-aided flocculation. The study included an investigation of the types of kinetic models which best described polymer-aided flocculation, the effect of mixing on kinetic rates, and the characteristics of the formed floc. These factors were investigated for different mixing conditions. Although the work was more fundamental in nature, results should aid in the selection of polymer-inorganic coagulant combinations, and highlight the importance of mixing in the process.

## 1.2 Scope of Investigation

The primary objective of this study was to improve the removal efficiency of fine particles from drinking water. There is a concern that conventional alum coagulation methods used in many large water treatment plants are not effective at the removal of fine particles ( $d \leq 10 \mu\text{m}$ ). Furthermore, higher doses of alum produce larger volumes of sludge. This study investigated the use of small dosages of polymer in combination with alum in order to address the above problems.

As a polymer was used in conjunction with alum, it functioned as a coagulant aid. Synthetic raw water with an aqueous suspension made of kaolin particles was used for the theoretical study to assess kinetics and the role of mixing on these kinetics. Identical experimental conditions were utilized in preparing the kaolin suspension in order to produce a consistent raw water source which would allow comparisons between various treatments. The concentration of kaolin suspension was chosen at 20 mg/L with turbidity of 19.5 NTU to simulate natural raw waters. Different polymer-inorganic coagulant combinations and process conditions were evaluated to determine optimum conditions. Using these optimum conditions, the impacts of mixing on flocculation kinetics were evaluated under a wide range of mixing intensities ( $20 \leq \overline{G}_f \leq 1600 \text{ s}^{-1}$ ).

The kinetics of polymer-aided flocculation was evaluated by the rate of polymer flocculation and the rate of polymeric floc growth. Kinetic models which best fit observed results were developed. The rate of polymer aided flocculation was evaluated by a first order rate constant determined from the model parameter. The rate of polymeric floc growth was evaluated by three methods: 1) a mean floc growth rate for a specific flocculation time, 2) a floc growth constant for each stage of floc growth process, and 3) a floc buildup time for the overall floc growth process. The overall coagulation and



flocculation process was characterized in terms of maximum mean floc diameter and floc buildup time. The above kinetic parameters were determined from flocculation curves and floc growth curves. The flocculation curves were plotted based on the number of particle counts, and the floc growth curves were plotted based on the mean particle diameter.

Also investigated were: the effects of pH, alkalinity, reactor volume, and method of polymer addition on the efficiency of fine particle removal. The effect of mixing on the maximum mean particle diameter, and on the particle size distribution function was also examined. Moreover, the characteristics of formed flocs, the rate of floc growth, and the maximum mean particle diameter were compared between alum flocculation and polymer aided flocculation where a polymer was used in conjunction with alum.

## 2 RESEARCH OBJECTIVES

The major objective of this study was to improve the efficiency of polymer-aided flocculation. It was accomplished by determining the optimum experimental process conditions, and investigating the impact of mixing on the kinetics of polymer-aided flocculation through the study of the rate of flocculation and the rate of polymeric floc growth. The detailed objectives are described as follows:

- (1) Select the optimum polymer and the optimum combination doses of alum-polymer.
- (2) Investigate the major factors affecting the efficiency and the kinetics of polymer-aided flocculation, which include pH, alkalinity, mixing intensity, reactor volume, and the method of polymer addition.
- (3) Evaluate the methods to represent particle sizes and size distributions.
- (4) Propose mathematical models to describe the rate of polymer-aided flocculation and the rate of polymeric floc growth.
- (5) Evaluate the impact of mixing on the kinetics of polymer-aided flocculation in order to determine the optimum  $\overline{G}_f$ -value through the study of mixing on the kinetic parameters: a first order rate constant (K), a floc growth constant ( $\mu$ ), a  $d_{\max}$  growth constant, a floc buildup time ( $t_b$ ), and a critical flocculation time ( $t_0$ ).
- (6) Evaluate the impact of mixing on a maximum mean floc diameter ( $d_{\max}$ ) in order to determine the critical  $\overline{G}_f$ -value.
- (7) Evaluate the impact of mixing on the particle size distribution function in order to achieve good performance for flocculation.
- (8) Compare the performance of alum flocculation with polymer-aided flocculation.

### **3 REVIEW OF LITERATURE**

The literature review presented reviewed major aspects of polymer-aided flocculation. Major topics included are: characteristics of fine particles; mechanisms of coagulation; mechanisms of mixing; types of coagulant systems; types of coagulants; factors influencing polymer performance; a general review of the kinetics of flocculation; and safety regulations regarding polymer use in drinking water.

#### **3.1 Characteristics of Fine Particles**

##### **3.1.1 General Characteristics of Fine Particles**

Most fine particles ( $d \leq 10 \mu\text{m}$ ) in natural waters tend to be negatively charged (Niehof, 1972; Hunter, 1979). The negative charge may arise due to the reaction of surface groups on the particles with protons and solutes in water, or because of isomorphous replacement (imperfections within the structure of the particle). A negatively charged particle is surrounded by a diffuse layer where an excess of positive charges accumulate in the interfacial region. Ions of opposite charge accumulating in the interfacial region together with the primary charge form an electrical double layer. Particles of the same charge will tend to repel each other and cannot be effectively agglomerated to form larger and more settleable floc. This type of solution is termed an electrostatically stabilized suspension. The addition of a coagulant is necessary in order to destabilize the particles by reducing repulsive forces. Once destabilized, particles can be mixed to promote inter-particle contact and form larger flocs.

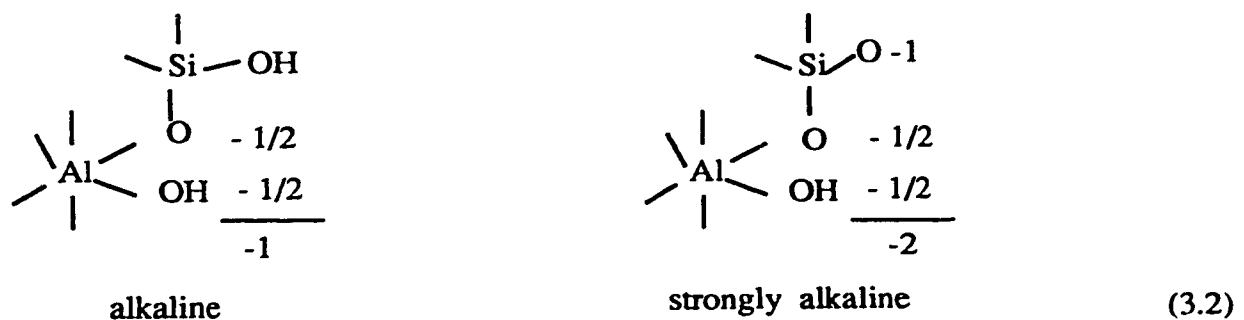
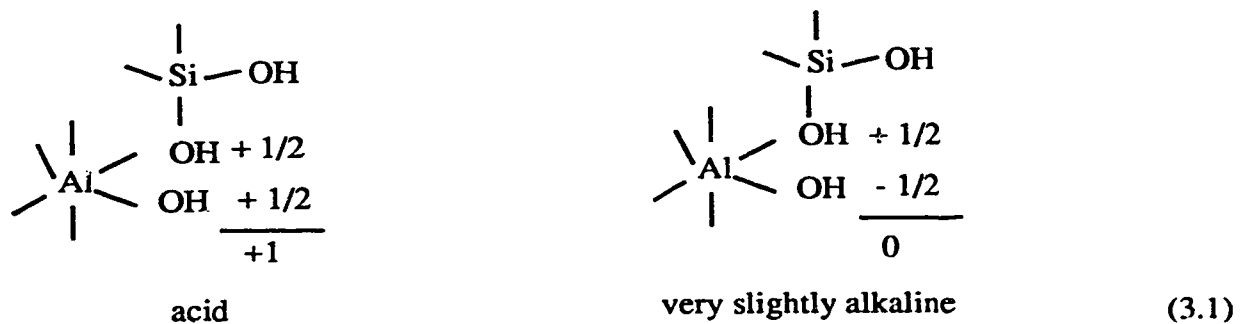
### 3.1.2 Characteristics of Kaolin Particles

In this study a synthetic water was used to produce consistent conditions for experiments. Particles used in this water were kaolin clay. As a result a brief review of characteristics of kaolin clay particles is presented. Kaolin clay particles are a major type of particle that tend to exist in natural raw water. It contains theoretically 46.54 % of  $\text{SiO}_2$ , 39.50% of  $\text{Al}_2\text{O}_3$ , and 13.96 % of  $\text{H}_2\text{O}$ . The layer structure of kaolin particles was presented by Theng (1979). The structure of the kaolin particle consists of two single layers: a tetrahedral silicon sheet cross-linked with an octahedral aluminum sheet. These two sheets are bound together by hydrogen bonding to form a common layer. The hydrogen bonding forms between the exposed oxygen and hydroxyl groups, which are presented in the tetrahedron silicon sheet and the octahedral aluminum sheet respectively. However, Cruz et al (1972) considered that the interlayer attraction was largely electrostatic in origin.

Theoretically, the layered structure of the kaolin particle should reveal that the kaolin layers are electrically neutral. In reality, however, most if not all kaolin particles carry a net surface charge because the double sheet layers can be broken from surface erosion to expose alumina and silica oxides along their edges. The pH-independent negative charges are produced by isomorphous substitution within the structure. They make up a major part of the total charge. A small amount of pH-dependent negative charges are formed due to exposed silica. Positive charges on the edge, or on the cleavage face, of the crystal are ascribable to exposed alumina. Therefore, the total net surface charge of the kaolin particles may be negatively or positively charged depending on the pH of the medium.

The isoelectric point of the edge alumina is  $\text{pH}= 7.8$ , and that of the edge silica

lies in between 1.8 to 2.4 (Michaelis, 1955). Outside the range of pH=1.8 to 7.8, kaolin particles are positively charged. The positive charge results from both silica and alumina being deprotonated. Inside the range of pH=1.8 to 7.8, the silica is negative and alumina is positive with the resulting net charge being negative (Schofield, 1953; and Samson, 1954). The detailed description about variations in charge characteristics of the edge surface of kaolin-type crystals under acid and alkaline conditions were given as follows (Theng, 1979):



Therefore, the kaolin suspension is electrostatically stabilized and undergoes “slow” coagulation. For this reason, coagulants are required to initiate coagulation.

## **3.2 Mechanisms of Coagulation and Flocculation**

### **3.2 1 General Mechanism of Coagulation and Flocculation**

In this study, coagulation refers to the chemical process of particle destabilization, and flocculation refers to the physical process of producing contacts. The general mechanism of coagulation and flocculation includes four stages:

- (1) **Compression of the Double Layer.** Compression of the double layer is described by the electrostatic model of Derjaguin, Landau, Verwey, and Overbeek (DLVO theory), which states that the addition of indifferent electrolytes, ions of opposite electrical charge to the colloids can compress the electrical double layer to the point that attractive van der Waals' forces prevail and precipitation occurs (Bruno, 1958). The amount of electrolyte required to achieve coagulation by this mechanism is practically independent of the concentration of the indifferent electrolyte, but is dependant upon the valence of the indifferent electrolyte. Based on the empirical Schulze-Hardy rule and the theoretical DLVO model, Amirtharajah & O'Melia (1990) concluded that the higher ion charges, the less the ion dosages required. However, when alum is added to the suspension, it does not function solely as indifferent electrolyte, it also undergoes hydrolysis reactions in addition to electrostatic ones.
  
- (2) **Adsorption to Produce Charge Neutralization.** Adsorption and charge neutralization occur when a chemical species of opposite charge to that of the colloid adsorbs onto the surface of particle. This will reduce the particle charge, the particles will coagulate by virtue of attractive forces ( Vladimir et

al, 1974). Destabilization by this mechanism is stoichiometric, and the required dosage of coagulant is proportional to the charge of the coagulant.

(3) Enmeshment in a Precipitate or Sweep Coagulation. When metal salts such as alum or iron salts are used in a certain pH range, they will precipitate as metal hydroxides [e.g.  $\text{Al}(\text{OH})_3$  (s) or  $\text{Fe}(\text{OH})_3$  (s)], colloidal particles can be enmeshed in these precipitates as they are formed by colliding with them in the process. This has been termed “sweep-floc” coagulation by Packham (1965). An inverse relationship exists between optimum coagulant dosage and colloid concentration. At a high colloid concentration a lower dosage of coagulant is needed. At lower colloid concentration more coagulant is required. The conditions for optimum coagulation do not correspond to a minimum zeta potential (Sheludko, 1966).

(4) Adsorption to Permit Interparticle Bridging. Destabilization by bridging occurs when segments of a polymer chain adsorb on more than one particle, thereby linking the particles together. Polymer bridging can occur between dissimilarly, and similarly charged materials. Bridging of negatively charged colloids by high-molecular-weight cationic and anionic polymers are examples of the first and second kind of bridging, respectively.

### **3.2.2 Mechanisms of Polymer Flocculation**

Polymer flocculation refers to destabilization by the bridging mechanism. From the survey of literature, it was found that the major mechanism of polymer flocculation included both adsorption and interparticle bridging (Ruehrwein and Ward, 1952; Michaelis, 1954, and Morellos, 1955; La Mer and Smellie, 1957; Healy and La Mer,

1962; La Mer and Healy, 1963; Kane et al, 1963; and O'Melia, 1969). The polymer adsorption is accomplished by: 1) transport of particles more close to the polymer chain, 2) collision between particle and polymer, and 3) adherence. As low bonding energy per segment suffices to render the affinity of particle on the segment, most of the collisions result in adherence. Collision and adherence are fast reaction processes, and the rate of polymer adsorption is governed by the transport processes. The primary mechanisms for the transport are: 1) perikinetic flocculation driven by thermal forces, 2) orthokinetic flocculation due to bulk fluid and turbulent motions, and 3) differential settling due to larger particles overtaking smaller particles. The orthokinetic flocculation is the dominant mechanism in polymer flocculation with mixing input. The rate of particle transport is dependent on the mixing intensity and mixing has an impact on both the length of the segment of the polymer chain and the conformation of the long chain polymer.

When a polymer molecule comes into contact with a clay particle, some of the reactive groups on the polymer chain adsorb on the particle surface, leaving other portions of the molecule extending into the solution. If a second particle with some vacant adsorption sites contacts these extended loops and tails, attachment can occur. A particle-polymer-particle aggregate is formed in which the polymer serves as a bridge (Gregory, 1978). More polymer molecules continue to adsorb onto these and other particles, until thousands or even millions are tied together in large masses called flocs. Depending on the rate that polymer molecules are introduced into the suspension, a more or less tightly knit or dense network of flocs can be found that will settle readily when liquid turbulence is minimized (Amirtharajah, 1990).

It is essential to recognize that adsorbed polymers can act to either stabilize or destabilize the solution, depending on the relative quantities of polymer and solid



particles, the affinities of the polymer for the solid and for water, electrolyte type and concentration. A stabilizing polymer may contain two types of groups, one of which has a high affinity for the solid surface and a second, hydrophilic group that is left “dangling” in the water. Effective bridging requires that absorbed polymers extend far enough from the particle surface to attach to other particles and also that some free surface is available for adsorption of the extended segments. If excess polymer is added and adsorbed, the particles are restabilized by surface saturation and can be sterically stabilized (Lyklema, 1978).

Another noteworthy feature is that the flocculation of dilute clay suspensions by polymers can be facilitated when the clay particles have previously been brought close together by electrolyte addition. This view is supported by the electrostatic model of Derjaguin, Landau, Verwey, and Overbeek (DLVO theory) which was previously discussed. Therefore, when polymer is used in conjunction with alum, the flocculation efficiency can be improved, and the chemical cost may be decreased. The combined coagulant system may be better than a single coagulant system for the flocculation of dilute clay particle suspension.

### **3.3 Mechanism of Mixing**

The overall mixing operations in a water treatment plant process includes two stages: rapid mixing and slow mixing. The rapid mixing disperses coagulants uniformly and quickly so as to cause the destabilization of the particles. When alum is used, the hydrolyzed species of alum are formed and adsorb onto the particle surfaces in the rapid mixing process. The slow mixing transforms the destabilized smaller particles into flocs or larger aggregates. The formation of flocs is principally by transport mechanisms due

to velocity gradients ( $\bar{G}$ ). The term  $\bar{G}$  was defined by Camp and Stein (1943) in terms of power input per unit volume as:

$$\bar{G} = \left[ \frac{P}{\mu V} \right]^{1/2} \quad (3.3)$$

where  $P$  is the total power dissipated (W),  $\mu$  is the absolute viscosity (Ns/m<sup>2</sup>), and  $V$  is the volume of the tank (m<sup>3</sup>). Equation (3.3) may also be expressed as:

$$\bar{G} = \left[ \frac{\epsilon}{\gamma} \right]^{1/2} \quad (3.4)$$

where  $\epsilon$  is the average rate of energy dissipation per unit mass, and  $\gamma$  is kinematic viscosity.

Literature reports that  $\bar{G}$  was often used as the critical parameter for controlling the rate of orthokinetic flocculation (Amirtharajah, 1991), and  $\bar{G}t$ , which is the product of mean velocity gradients and flocculation time, was used as the factor to control the degree of flocculation (Camp, 1953). If the variation of the initial particle concentration exists,  $\bar{G}n_1^0$  and  $\bar{G}n_1^0 t$  were used instead of  $\bar{G}$  and  $\bar{G}t$  where  $n_1^0$  is initial primary particle concentration (Tambo et al, 1970-b and 1979). Experience indicated that low  $\bar{G}$ -values are used if sedimentation follows; whereas, higher  $\bar{G}$ -value are used if direct filtration follows (Amirtharajah et al, 1991). It has also been found that  $\bar{G}t$  can be used to describe by the total shear flow. It gives an indication of the total work applied to the process, and used to characterize the performance of the flocculation. However, the optimum  $\bar{G}t$  is influenced by the kind of impeller system and the type of chemical system (Amirtharajah

et al, 1991).

It should be noted however that although  $\bar{G}$  has long been used in the study of flocculation and coagulation, there recently has been considerable work published that has questioned the use of  $\bar{G}$  (Cleasby, 1984; Clark, 1985; Hanson and Cleasby, 1990; Han and Lawler, 1992; Clark et al 1994; Stanley, 1995). Many of these studies have highlighted that “local” hydrodynamics within the reactor, especially in the impeller zone, may be more important than vessel-average parameters such as  $\bar{G}$ .

Although the above limitations of  $\bar{G}$  is important to consider, research is still in the preliminary stage of finding a parameter to replace  $\bar{G}$ , and as a result  $\bar{G}$  will be used in this work, recognizing some of the limitations associated with it.

### **3.4 Types of Coagulant System**

Four types of coagulant system have been used in water treatment:

- (1) A single coagulant system where inorganic or organic coagulant is used alone as a primary coagulant;
- (2) A mixed coagulant system where two or three different kinds of inorganic coagulants are used together;
- (3) A combination coagulant system where an inorganic coagulant is used in conjunction with a polymer; and
- (4) A dual polymer system in which the addition of a low molecular-weight and high charge density cationic polymer is followed by a high-molecular weight and low charge density anionic or nonionic polymer.

Literature reveals that a combined coagulation system (an inorganic coagulant plus a polymer ) reduces the optimum inorganic and/or organic coagulant dosages considerably (Hespanhol & Selleck, 1975), and it is more economical than single or dual coagulant systems. It also reduces the residual aluminum concentrations, and reduces the ecological problems of the final disposal (Prendivile, 1992; Geothals, 1979; Schwartz, 1975). However, the floc formed by a dual polymer process has a higher strength because the cationic polymer acts as a coagulant and a coagulant aid simultaneously.

### **3.5 Types of Coagulant**

Historically, a great number of coagulants have been used in water treatment. They are mainly categorized into inorganic coagulants and organic coagulants.

#### **3.5.1 Inorganic Coagulants**

Inorganic coagulants are divided into four generations which are described as follows.

The first generation of inorganic coagulants are mainly alum and iron salts (Reynolds, 1982). They are still the most widely used coagulants in drinking water treatment. Alum is more often used than iron salts because it is readily available, costs less, and has higher effectiveness. Also, alum is superior for color removal, and it is colorless when overdosed (Helfrich ,1992; Packham & Ratnayaka, 1992). Ferric salts, however, are more effective at low temperature and over a wider pH range (from 4 to 12). They also produce water with lower turbidity, TOC and THMFT (trihalomethane formation potential), and lower sludge volume (Helfrich, 1992; Prendiville, 1992).

Although those inorganic coagulants are relatively inexpensive in comparison to other types of coagulants, they still have definite disadvantages such as higher dosage requirement, higher residual aluminum concentration, and a larger volume of sludge which is difficult to dewater.

The second generation of inorganic coagulants are polymerized aluminum salts. They appeared in the 1970's, and introduced a clear improvement compared with the first generation of inorganic coagulants. This is because they combined the properties of a primary coagulant and a coagulant aid. Moreover, polymerized aluminum salts are less sensitive to the pH of raw water, require lower dosage, retain desired properties at low temperature, produce higher density flocs, and create lower volumes of sludge than that of the first generation coagulants (Kaeding, 1992).

It has also been found that the use of polymerized aluminum salts is particularly favored for waters with high levels of turbidity. However, these hydrolyzed salts, just like simple salts, leave traces of residual aluminum in the treated water, in concentrations that vary according to the characteristics of the raw water. This may cause a problem in drinking water treatment.

The third generation of coagulants have been synthesized which are high basicity (HB) or high OH/Al ratio polymerized aluminum salts. They limit the residual aluminum concentration while maintaining excellent flocculation properties. The high basicity polymerized aluminum salts appreciably reduce residual aluminum concentration when the water being treated has a high pH. This is because the more intense pre-hydrolysis of these coagulants leads to the formation of polycationic species (particularly  $Al_{13}$  ions) in great concentration, and simultaneously leads to a reduction in the concentration of monomeric and dimeric cationic species. It was reported that the residual aluminum

concentrations are reduced by 30 to 35 % compared with alum salts when the natural waters were tested (Pouillot and Suty, 1992).

The last type of inorganic coagulant is a cationic metal-polysilicate complex which has a higher particle removal efficiency than that of a conventional polymerized aluminum salts due to the much stronger bridge-forming capability of the complex (Hashimoto et al , 1991). It can be used to remove both coarse colloidal or suspended matter and minute colloids without generating toxicity.

### **3.5.2 Organic Coagulants**

Organic flocculants, called polyelectrolytes or polymers, are mainly linear water-soluble high-molecular-weight ( $10^7$ ) organic compounds containing ionizable groups along the carbon chains. The flexibility and polyfunctionality of the chain allow the polymer to adopt various shapes or conformational states at the surface, and to be attached to the solid by a number of segment-surface bonds.

Organic coagulants originally used in water treatment were natural polymers such as starches, cellulose derivatives, polysaccharide gums, and proteins. They are nontoxic substances and with low costs, but the efficiency of coagulation was too low to meet stricter drinking water regulations.

Synthetic polymers came into use in water treatment over two decades ago, and are increasingly being used in drinking water treatment plants as coagulants or coagulant aids (Letterman and Pero, 1990; Kerhalkar et al, 1990; Bansal, 1988; Leu, 1988; Prasad & Belsare, 1982; AWWA, 1982; SPCUUS, 1982, and Vaidya & Bulusu, 1981, Robinson 1974 , Schwartz 1975 and Haff 1976, Glaser & Edzwald 1979, Decook 1980, Bowie

1977 & Gilman et al 1979). The particle removal efficiencies are much higher than that of natural polymers (Gilman, 1979-a) or inorganic coagulants (Prendivile, 1992; Namasivayam and Kanagarathinam, 1992; Decook, 1980; Robinson, 1974). There are three types of synthetic polymers employed on a widespread basis in water treatment: cationic, anionic and nonionic.

Cationic polymers are polymers that contain positively charged groups such as imino ( $-\text{CH}_2-\text{N}^+\text{H}_2-\text{CH}_2-$ ), amino ( $-\text{N}^+\text{H}_3$ ), quaternary amino ( $-\text{N}^+\text{R}_3$ ). They are the most common type used as primary coagulants, coagulant aids, or both to destabilize negatively charged particles (Gutcho, 1977; Committee Report, 1982).

Anionic polymers are polymers that contain negatively charged functional groups. Most commercial anionic polymers are polyacrylamides with the carboxylate moiety ( $-\text{COO}^-$ ) in the solution. The polyacrylamides with high-molecular-weights ( $10^6$  to  $10^7$ ) are more often used as coagulant aids in conjunction with inorganic coagulants. Some experiments, however, have indicated that they can still function as primary coagulants to destabilize the negatively charged kaolin particles (Michaelis, 1954; Michaelis and Morellos, 1955). The possible explanations are described as: first of all, hydrogen bonding is formed between the kaolin and carboxylate, amide, hydroxyl or other groups (Hespanhol and Selleck, 1975); secondly, ion-exchange reaction between kaolin clay particles and the exchangeable ions held around the outside of the two cross-linked layers of kaolin particles are occurred (Hespanhol and Selleck, 1975); and finally, the bridge over the gap is formed by repulsive interaction (Amirtharajah and O' Melia, 1990). However, the flocculation efficiency is low (Brown, 1981) when anionic polymers are used as primary coagulants. A critical electrolyte concentration, thus, is needed to initiate flocculation.

Nonionic polymers are the polymers containing no charge species. These polymers include: polyvinyl alcohol, polyacrolein, and pure polyacrylamide. As nonionic polymers tend to adopt a random coil conformation in solution, the molecular weight of the nonionic polymer must be very high ( $10^6$  to  $10^7$ ) in order to offer the coil dimension. It is more effective if a nonionic polymer is used in conjunction with an inorganic coagulant, resulting in a lower optimum polymer dosage and a broader optimum dosage range.

### **3.6 Factors Influencing Polymer Performance**

A number of factors have been found to affect the performance of a polymer in water treatment. These include: 1) characteristics of the polymer: molecular weight, molecular structure, ionic groups, charge density, coagulant dose, the concentration and degree of hydrolysis; 2) characteristics of medium: ionic strength, pH and alkalinity, and 3) process conditions: mixing intensity ( $\bar{G}$ ), mixing time, polymer loading method, the sequence and position of polymer addition. Each will be described separately below.

#### **3.6.1 Polymer Molecular Weight**

The efficiency of polymer flocculation is strongly dependent on the polymer molecular weight. It is controlled more often by the effective length of the segment of the chain than by the amount adsorbed. For linear polymers, the higher the molecular weight, the higher the flocculation efficiency, and the lower the optimum polymer dose. This is because the chain of a linear polymer has a greater geometric extension, exposes more active groups, and increases the probability of adsorption and bridging (Link & Booth, 1960; Hespanhol & Selleck, 1975; Levine and Friesen, 1987). On the other hand,



the increase in the molecular weight retards flocculation since it gives a rise in steric stabilization which reduces the van der Waals attraction forces between colliding colloidal particles ( Katchalski, 1951), and decreases the efficiency of collision between the primary particles and polymer molecules. Therefore, a maximum molecular weight exists for a system for optimum performance. La Mer & Healy (1963) have verified the above conclusion experimentally using a suspension of a calcium phosphate. It was found that the efficiency of flocculation of a calcium phosphate suspension was maximum when the molecular weight of the polyacrylamide used as a coagulant was about  $3 \times 10^6$  ; and it decreased abruptly when the molecular weight was above this value.

It is sufficient to point out that the anionic and nonionic polymers with high molecular weight ( $10^6$  to  $10^7$ ) more often function as coagulant aids, and the long chain anionic polymers are more effective than that of short chain polymer with the same degree of hydrolysis ( Ghosh et al 1985). Also, cationic polymers with low molecular weight ( $< 10^5$ ) are often used in water treatment for saving of cost, because it was reported that lower molecular weight cationic polymers were more effective than similar molecular weight polymers with negative or no charge (Singley, 1972).

### **3.6.2 Polymer Molecular Structure**

The structure of a polymer chain influences the extent of interparticle bridging. Both linear and branched polymers are used as coagulants or coagulant aids, but the linear polymers are more effective than branched polymers when molecular weight and chemical type are comparable (Levine and Friesen , 1987). Generally, if a polymer is nonionic, its molecular chain will be in the form of a random coil in the neutral suspension (around pH=7). Thus, only part of the polymer chain comes in contact with

clay particles resulting in low flocculation efficiency. The extent of the extension of polymer chain is strongly dependent on pH and alkalinity of the suspension; mixing intensity ( $\bar{G}$ ). The higher the pH, the more extended the polymer chain is. Also, mixing imposed on the system will enhance the extension of the polymer chain.

### **3.6.3 Ionic Group and Charge Density**

The ionic group and charge density on the polymer chains affect the efficiency of flocculation as they determine the interactions occurring between the different ionic groups and the colloidal suspensions. It is necessary to determine the mechanism of flocculation in order to choose the optimum polymer.

A cationic polymer has the advantage as a primary coagulant over anionic and nonionic types for negatively charged colloid particles such as kaolin and montmorillonite clays. This is because it acts as both a neutralizer, reducing the zeta potential, and a bridging agent, strengthening the flocs (Hespanhol & Selleck, 1975; Brown, 1981).

A nonionic polymer can act as a primary coagulant, but the addition of an electrolyte (eg. calcium or alum) to the suspension is required to compress the double layer, and reduce the zeta potential to the isoelectric point at which the maximum destabilization occurs. However, an exception was found for the coagulation of kaolin suspensions where the maximum destabilization did not occur at the isoelectric point, but at negative values of the zeta potential from  $-0.7$  to  $0.0 \mu\text{ cm/ volt-sec}$  (Black et al, 1966).

Although the charges are like, an anionic polymer still can act as a primary coagulant to destabilize negatively charged colloid particles such as kaolin. An anion

exchange, where the carboxylate ions replace adsorbed anions on the kaolin surface , mainly contributes to this coagulation process (Ruehrwein and Ward, 1952). However, when an anionic polymer was used as a primary coagulant, the optimum dosage was high, and the efficiency of the flocculation was low (Hespanhol & Selleck,1975). For this reason, it is not widely utilized as a primary coagulant in water treatment.

An anionic polymer demonstrates good performance only after its electrokinetic potential has been sufficiently reduced by addition of a suitable electrolyte or a polymer of opposite sign ( Posselt & Reidies, 1964; Krone, & Johnson, 1965; Dale, 1973; and Levine & Friesen, 1987). This conclusion has been confirmed experimentally in a number of tests using an anionic polymer in conjunction with alum to coagulate kaolin suspensions. The experimental results have shown that the efficiency of flocculation was much better than that of a sole anionic polymer and, in addition, the optimum polymer dosage was lowered, and the optimum dosage range was broader (Black et al, 1959; Birkner & Edzwald, 1959; Hespanhol & Selleck,1975).

#### **3.6.4 Polymer Dosage**

The efficiency of polymer flocculation is affected significantly by polymer dose. The optimum polymer dosage is strongly dependent on the charge density of polymer, suspended particle concentration, and mixing conditions. Also, it is directly related to the fraction of the surface covered by polymer segment ( $q$ ). It was reported that the optimum dose occurred at  $q = 0.5$ , and at the optimum dosage most of the polymer added was adsorbed on the solid phase with little left in solution (Hespanhol & Selleck, 1975). Overdosing polymer could cause either the reduction of the adsorption sites on the surface of the polymer, or the restabilization of the particles. The flocculation efficiency thus decreased, and the treatment costs increased (Levine & Friesen, 1987). The

literature indicates that cationic polymers should be effective at lower dosage than that of anionic or nonionic ones, since cationic polymers can act to neutralize particle charge as well as to provide inter-particle bridging.

### **3.6.5 Polymer Concentration**

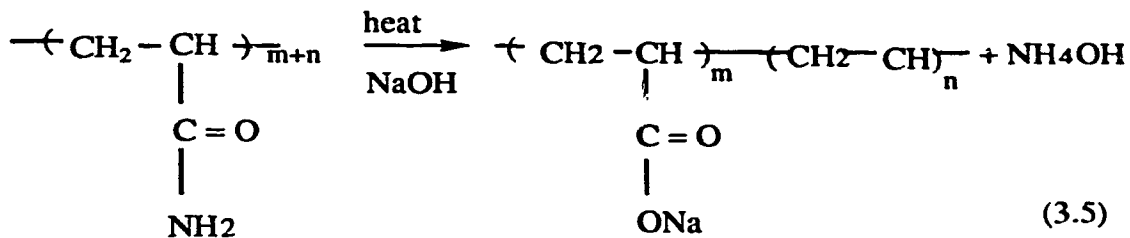
Polymer feed concentration impacts the degree of polymer hydrolysis and dispersion. High concentration of polymer stock solution is suggested in order to avoid hydrolysis reactions, but it should be diluted prior to the addition in order to disperse the polymer homogeneously, and eliminate overdosing in certain areas.

### **3.6.6 Ionic Strength of Suspension**

Ionic strength has two antagonistic influences on polymer flocculation: 1) it reduces the electrostatic energy of repulsion between the clay particles, and brings about the reaction of charge neutralization, and 2) it reduces the extension of the polymer chain. The reduction of the repulsion forces and the extension of the polymer chain aids polymer adsorption. The charge neutralization results in the destabilization of the particles. However, the coiling of the polymer chain decreases the ability of bridging. These factors are competitive, and as a result an optimum ionic strength exists.

### **3.6.7 Degree of Polymer Hydrolysis**

Nonionic polymer based on polyacrylamide often undergoes hydrolysis reactions in alkaline solution. The hydrolysis process is described as:



polyacrylamide

hydrolyzed polyacrylamide

The hydrolyzed polyacrylamide is an anionic polymer. The charge density is determined by the degree of ionization. The degree of ionization is expressed by the degree of hydrolysis of polyacrylamide  $\left[ \left( \frac{n}{m+n} \right) \cdot 100\% \right]$ , which is the fraction of the polymer chain ionized by the replacement of amide groups with carboxylate groups. The degree of hydrolysis of a polyacrylamide is strongly dependent on pH and alkalinity of the suspension. There exists an optimum degree of hydrolysis at which the maximum flocculation efficiency occurs. It has been reported that the optimum hydrolysis degree of polyacrylamide is proportional to one-half carboxylate group per amide group (Hespanhol and Selleck, 1975).

### 3.6.8 Experimental Process Conditions

The experimental conditions which include pH, alkalinity, and mixing intensity all have a significant impacts on polymer flocculation. At a given ionic strength, the pH and alkalinity of the suspension determine the zeta potential, the degree of hydrolysis, the intermediate products and the solubility of the chemical species involved, as well as the optimum polymer dose. Tomi & Bagster (1978) reported that the optimum polymer dose and the maximum floc size are inversely related to  $\bar{G}$ -values or  $\bar{G}t$ -values in the slow mixing process. The review found that only a limited knowledge about these factors and the effects they have on performance is available. More research is required in this area.

### **3.7 General Review of the Kinetics Of Flocculation**

The models for the kinetics of flocculation were categorized as follows: 1) in terms of the flocculation modes associated with different mixing floc patterns: random flocculation, contact flocculation, and pellet flocculation (Amirtharajah and Clark, 1991) and; 2) in terms of particle transport mechanisms: brownian diffusion (perikinetic flocculation), fluid shear (orthokinetic flocculation), and differential settling.

Historically, much of the work has been done in the study of kinetic models for the flocculation with inorganic coagulants starting in 1916 (Smoluchowsky, 1916; Overbeek, 1952; Gillespie, 1960 ; Nielsen, 1964; Friedlander, 1977; O'Melia, 1978; Lawler, 1979; Lawler et al, 1980; O'Melia and Bowman, 1984; Valioulis & List ,1984; Ali 1985; Francois, 1988 ; Weilenmann and O'Melia, 1989, and Amirtharajah & O'Melia, 1990 ). These models were based on the measurement of particle size distributions, and were illustrated as the diminution of the number concentration of primary particles.

The kinetic model for perikinetic flocculation was first studied by Smoluchowsky (1916), and has been further developed by many researchers (Overbeek, 1952; Gillespie, 1960 ; Friedlander, 1977; O'Melia, 1978; and Amirtharajah & O'Melia, 1990). The latest expression of the model for perikinetic flocculation in heterodispersed suspension was given by Amirtharajah & O'Melia (1990).

Kinetic models for orthokinetic flocculation have been investigated by Fair and Gemmel (1964), Harris and Kaufman (1966), Argaman and Kaufman (1970), Parker et al (1972), Tomi and Bagster (1978). The above models were proposed and analyzed based on the rate of aggregation with some considering the rate of floc breakup and some giving

no consideration to this phenomena. Overall kinetic models were proposed by Argaman & Kaufman (1966 , 1970); Hespanhol & Selleck (1975), which considered both the impacts of floc formation and floc breakup. The Argaman and Kaufman's model was further improved by Amirtharajah & O'Melia (1990).

It is sufficient to emphasize that the above models were proposed on the studies of the flocculation with inorganic coagulants. Little information on the kinetics of polymer aided flocculation or polymer flocculation have been found in the literature reviewed.

The kinetics of perikinetic flocculation will be reviewed briefly in this study as it is not the major transport mechanism in most water treatment applications, but the kinetics of orthokinetic flocculation are within the scope of this research, thus it will be discussed in more detail.

### 3.7.1 Kinetics of Perikinetic Flocculation

The kinetic model for perikinetic flocculation was first studied by Smoluchowsky (1916), and has been further developed by many other researchers (Overbeek, 1952; Gillespie, 1960 ; Friedlander, 1977; O'Melia, 1978; and Amirtharajah & O'Melia, 1990). The expression of the model for perikinetic flocculation in heterodispersed suspension was given (Amirtharajah & O'Melia, 1990) as:

$$\frac{dn_1}{dt} = -\frac{2}{3} \alpha \frac{kT}{\mu'} \frac{(d_i + d_j)^2}{d_i d_j} n_i n_j \quad (3.6)$$

where

- $dn_1/dt$  = diminution of the primary particle concentration of  $n_1$   
 $n_i, n_j$  = concentrations of particles of sizes of  $d_i, d_j$   
 $k$  = Boltzmann's constant  
 $T$  = absolute temperature  
 $\mu$  = fluid viscosity  
 $\alpha$  = collision efficiency

The correction factor  $\alpha$  is used to account for electrostatic effects and/or the hydrodynamic effects. It has been predicted by several models (Fuchs, 1934; Spielman, 1970 & 1978; Valioulis & List, 1984; and Amirtharajah & O'Melia, 1990). If flocculation occurs in a monosized suspension, Equation 3.6 can be simplified to

$$\frac{dn_1}{dt} = - \alpha \frac{4kT}{3\mu} n_1^2 \quad (3.7)$$

Equation 3.7 indicates that the driving force in the perikinetic flocculation is thermal forces, since the interparticle collision frequency is a function of temperature. Additionally, it also demonstrates that the kinetics of perikinetic flocculation for a monosized suspension without floc breakup is a second order process with respect to primary particle concentration; and it is independent of fluid flow, gravity, or the particle size.

### 3.7.2 Kinetics of Orthokinetic Flocculation

The kinetic models for orthokinetic flocculation have been investigated by Fair and Gemmel (1964), Harris and Kaufman (1966), Argaman and Kaufman (1970), Parker et al (1972), and Tomi and Bagster (1978). The models were proposed and analyzed



based on the rate of aggregation both with and without consideration of the rate of floc breakup.

### 3.7.2 1 Rate of Aggregation

The rate of aggregation is represented by the diminution of the number concentration of the primary particles. It can be described by two particle collision models with the assumption that the collisions occur between the particles of two different sizes, which gives the collision frequency of the binary orthokinetic flocculation as (Friedlander, 1977):

$$N_{ij} = -\frac{1}{6} (d_i + d_j)^3 \bar{G} n_i n_j \quad (3.8)$$

For a monosized suspension of spherical primary particles with  $d_i = d_j$ ,  $n_i = n_j = n_1$ ,  $\phi = \frac{\pi d^3}{6} n_1$ , the Equation 3.8 reduces to:

$$\frac{dn_1}{dt} = -K_A \bar{G} n_1 \quad (3.9)$$

where

$$K_A = \frac{4}{\pi} \phi \quad (3.10)$$

is the overall flocculation constant or general aggregation constant,  $\phi$  is a volume fraction, which is the volume of primary particles per unit volume of suspension.

When the mixing intensity ( $\bar{G}$ ) is fixed, Equation 3.9 can be modified as

$$\frac{dn_1}{dt} = -K_s n_1 \quad (3.11)$$

where

$$K_s = \frac{4}{\pi} \phi \bar{G} \quad (3.12)$$

is the theoretical Smoluchowski first order rate constant depending on system chemistry and mixing physics.

Equation 3.11 shows that the kinetics of orthokinetic flocculation for a monosized suspension without floc breakup is a first order process with respect to primary particle concentration. However, the experimental verification of the above first order kinetic model indicates that the experimentally determined rate constants are only 36 to 38 per cent of the values predicted by the Smoluchowski theory (Swift and Friedlander, 1964). This discrepancy might be a result of residual interparticle repulsive forces or due to hydrodynamic interactions that become important when the particles are in close proximity to each other (Birkner and Morgan, 1968). Therefore, the collision efficiency factor ( $\alpha$ ) is used to correct the Smoluchowski first order kinetic equation which gives the same expression as Equation 3.10 but  $K_s$  is expressed differently as:

$$K_s = \frac{4}{\pi} \alpha \phi \bar{G} \quad (3.13)$$

Equation 3.13 also indicates that the mean velocity gradient  $\bar{G}$  is the most important parameter influencing the kinetics of orthokinetic flocculation. Increasing  $\bar{G}$  accelerates the aggregation of the primary particles, and tends to form the flocs with smaller sizes and higher densities (Amirtharajah and O'Melia, 1990).

For the special case of isotropic turbulence, the collision frequency between particles was studied by Saffman and Turner (1956) who proposed the kinetic equation at the initial phase of flocculation as:

$$\frac{dN_t}{dt} = -K_T N_t \quad (3.14)$$

where

$$K_T = 1.24 N_t \quad (3.15)$$

where  $K_T$  is the theoretical isotropic turbulence first order rate constant, and  $N_t$  is total particle concentration.

It is important to recognize that the above two first order kinetic equations are valid only during the initial phase of the flocculation where all the particles are monosized. The accuracy of the above models will decrease with the broadening of the particle size distribution spectrum of the system as the flocculation reaction proceeds.

When collisions occur between particles of different sizes, different models have been developed by Harris et al (1966), Lawler (1980); Amirtharajah & O'Melia (1990); and Amirtharajah and Clark (1991). Among them, Harris et al (1966) proposed the kinetic model for orthokinetic flocculation by assuming an upper limit  $p$  for the floc size and no floc breakup:

$$\frac{dn_1}{dt} = - \frac{\alpha \dot{\epsilon} \phi \dot{a}^3}{\pi} \overline{G} n_1 \quad (3.16)$$

where

$\dot{a}$  = the ratio of particle collision radius to its physical radius, and

$$\dot{\epsilon} = \frac{\sum_{i=0}^{p-1} n_i (i^{1/3} + 1)^3}{\sum_{i=0}^p i n_i} \quad \text{is the size distribution function}$$

The  $\dot{\epsilon}$  is a measure of the degree to which the size distribution deviates from a primary particle.

Assuming

$$K_F = - \frac{\alpha \dot{\epsilon} \dot{a}^3}{\pi} \quad (3.17)$$

and a constant pH,  $\phi$  is proportional to coagulant concentration,

$$K_F \phi = K_A \quad (3.18)$$

Based on Equation 3.18, Equation 3.16 can be written as:

$$\frac{dn_1}{dt} = -K_A \overline{G} n_1 \quad (3.19)$$

where  $K_A$  is the overall flocculation constant or general aggregation constant.

Equation 3.19 has the same form as Equation 3.9, except that the overall flocculation constant or general aggregation constant  $K_A$  in Equation 3.19 contains the size distribution function. With the assumption of no floc breakup, both equations show that the kinetics of orthokinetic aggregation is a first order process whether the primary particles are monosized or have a size distribution. Furthermore, both equations show that  $\bar{G}$  is a main parameter affecting the kinetics of orthokinetic flocculation.

It is important to emphasize that the Smoluchowski's orthokinetic model shown in Equation 3.19 has been used successfully in systems where the interacting particles can be considered as porous, allowing fluid flow through the particles (Spielman, 1978). An excellent example for this case is that of alum flocs, which are loosely bound aggregates. So far no paper has reported if it can be applied in polymer flocculation. This being the case, the mode of the kinetics of polymer aided flocculation or polymer flocculation should be investigated.

Lawler's generalized model (Lawler, 1980) for orthokinetic flocculation of the binary collisions between particles of different sizes is presented based on the expression given by Amirtharajah & O'Melia (1990):

$$\frac{dn_m}{dt} = \frac{\alpha \bar{G}}{6} \left[ \sum_{i+j=m} (d_i + d_j)^3 n_i n_j - n_m \sum_{i=1}^{\infty} (d_i + d_j)^3 n_i \right] \quad (3.20)$$

where  $\frac{dn_m}{dt}$  is the rate of change of number concentration of particles of size  $d_m$ .

With the availability of particle size analyzers, the use of the above model enables the determination of particle size distributions through the flocculation and sedimentation processes.

Lawler et al (1980, 1984) modeled the expected changes in particle size distributions in flocculation process as part of an integral design model of a water treatment plant. The model was tested with measurements of particle sizes in a softening plant, and calibrated with one set of data to determine  $\alpha$ , chosen as a fitting parameter. Another set of data was used for model verification. They concluded that the model predictions tend to fit the measured results for either the small or large particles but not for both.

The  $\alpha$ -value can be determined by two methods: 1) measuring the volume fraction ( $\Phi$ ) using a particle size analyzer (Francois, 1988), then calculating the  $\alpha$ -value from the expression of rate constant; and 2) using nonlinear regression by the computer. The detailed analytical procedures of the nonlinear regression were given as follows:

- (1) The particle size distribution that was initially measured experimentally is used as input to the above model, a trial value of  $\alpha$  is selected based on the empirical expression of a collision efficiency.
- (2) The change in total particle number concentration over time is predicted.
- (3) This change is compared to the measured results over time.
- (4) The model parameter  $\alpha$  is selected by varying  $\alpha$  systematically in repetitive calculations until the minimum value of the sum of the squares of the

differences between calculated and measured number concentrations is obtained.

A stability factor ( $\alpha$ ) was defined by Weilenmann and O' Melia (1989) as the ratio of the rate at which particles attach to each other. It can be used to compare the degree of destabilization of the suspension (Hahn & Stumm, 1970 ) by assuming that for an ideal stable colloid,  $\alpha=0$ , and for a completely destabilized suspension,  $\alpha =1$ . The higher the value of  $\alpha$ , the greater the degree of destabilization of the suspension.

The model which described the collision between i- and j-fold particles in random flocculation can be found in Amirtharajah and Clark's paper (1991) as:

$$N_{ij} = K \left( \frac{d_i}{2} + \frac{d_j}{2} \right)^3 n_i n_j = K' d_1^3 (i^{1/3} + j^{1/3})^3 n_i n_j \quad (3.21)$$

where:

$d_1$  = diameter of primary particle (cm)

$d_i$  =  $d_1 i^{1/3}$  = diameter of i-fold particles (cm)

$d_j$  =  $d_1 j^{1/3}$  = diameter of j-fold particles (cm)

$n_i$  = number concentration of i-fold particles (count / cm<sup>3</sup>)

$n_j$  = number concentration of j-fold particles (counts / cm<sup>3</sup>)

$K$  = rate constant of floc collision which is proportional to the  $\bar{G}$ -value

$K'$  = rate constant of floc aggregation which is proportional to the  $\bar{G}$ -value

Since collision between i- and j-fold particles in random flocculation is not a concern in this study, the detailed information about this model is not provided.

### **3.7.2.2 Rate of Floc Breakup**

The rate of floc breakup is expressed using the increase of the number concentration of primary particles caused by floc breakup. A quantitative treatment of floc breakup rate as a part of the overall kinetic model of orthokinetic flocculation was studied by several researchers, and different floc breakup models were proposed. These include the Filament Fracture Model, Surface Erosion Model and Generalized Model.

The Filament Fracture Model (Thomas, 1964) is based on the assumption that, under turbulent flow conditions, the principle mechanism leading to floc rupture is pressure differences on opposite sides of the floc, which cause bulgy deformation and rupture. The breakup of the floc is resisted by yield stress, which increases with the energy dissipation per unit mass of fluid. Francois (1987) reported that flocs with dimensions of the order of magnitude of the turbulence scale for inertial conversion will be ruptured to large fragments, and that the breakup of the flocs will follow the filament fracture model.

The Surface Erosion Model (Argaman and Kaufman, 1970) is based on the assumption that floc breakup is due to surface erosion of primary particles from the flocs by shear, and that the floc erosion is proportional to the shearing stress and the surface area of a floc. It was found (Francois, 1987) that flocs subjected to viscous forces will be ruptured by erosion of small particles from the floc structure, and the floc breakup can be described by the surface erosion model.



The Generalized Model for floc breakup rate in orthokinetic flocculation (Amirtharajah and O'Melia, 1990) takes the two breakup mechanisms of splitting and erosion into account based on the models of Parker et al (1972) and Pandya and Spielman (1982). It gives the simplest expression of the rate of breakup function as:

$$\frac{dn_1}{dt} = K_B' \bar{G}^L \quad (3.22)$$

where  $K_B'$  is the floc breakup coefficient and the exponent  $L$  is the constant which values are dependent on the floc size. Thus,  $L$  has a value of 4 for unstable flocs greater than the microscale range, and equals 2 for flocs smaller than the microscale range .

Equation (3.22) shows that floc breakup has zero-order kinetics with respect to the concentration of the primary particles, and that the mixing intensity is the major factor impacting on the rate of floc breakup. Also, the rate of floc breakup increases with the increasing of the  $\bar{G}$  - value in orthokinetic flocculation.

### 3.7.2.3 Overall Kinetics of Orthokinetic Flocculation

It is well known that floc breakup occurs more often under shear, and that the rate of floc breakup is an essential part of the kinetics of the flocculation process in turbulent mixing. Therefore, two contradictory impacts which are floc formation and floc breakup are included in many overall kinetic models (Argaman & Kaufman, 1966, 1970; Hespanhol & Selleck, 1975; Amirtharajah & O'Melia, 1990). The improved Argaman and Kaufman's model was given by Amirtharajah & O'Melia (1990) as:

$$\frac{dn_1}{dt} = - K_A \bar{G} n_1 + K_B \bar{G}^L \quad (3.23)$$

where  $K_A$  and  $K_B$  are the overall flocculation constant and the floc breakup constant.

### 3.7.2.4 Kinetics of Polymer Flocculation

Although polymer flocculation has been carried out for more than two decades, only a few studies on the kinetics of polymer flocculation were reported. La Mer et al's (1957, 1962, and 1963) overall kinetic model for polymer flocculation with floc breakup was developed based on the surface covered fraction  $q$ . It was assumed that at  $q = 0$  where no polymer was adsorbed, thus no bridge could be formed ; at  $q = 1$  where the surface of a particle was fully covered with polymer; and at  $q = 0.50$  where polymer bridging would reach maximum . The model gives:

$$\frac{dn_1}{dt} = - K_1 n_1^2 q(1-q) + K_2 R \theta^{-1} (1-\theta)^{-1} \quad (3.24)$$

where the first part in the right side is the aggregation rate. The second part is the disaggregation rate;  $K_1$  is the aggregation constant,  $K_2$  is floc breakup constant ,  $q$  is the fraction of the surface covered by adsorbed polymers , and  $(1-q)$  is the function of the surface uncovered.

### 3.7.3 Kinetics of Floc Growth

In contrast to the literature on the kinetics of flocculation, only very little

information is available on the kinetics of floc growth. The models used to describe the kinetics of floc growth can be divided into two types: 1) conceptual models, and 2) mathematical models.

The conceptual models reviewed by Stanley (1995) shows that two new methods of analyzing the kinetics of floc growth have been studied in recent work. One of them is through the use of a multi-level floc model which divides the floc growth process into four levels: primary particles --> flocculi--> flocs --> agglomerates (Francois & Van Haute, 1985; Clark & Flora, 1991). The other method of describing floc growth process and kinetics is through the use of fractal dimensions of the floc (Clark & Flora, 1991). A relatively recent model which uses fractal dimensions is the random cluster -cluster aggregation model ( Botet et al., 1986 ). The conceptual models described above aid to understand floc formation and growth process in a conceptual sense rather than quantitatively described by mathematical model.

Few mathematical models for the kinetics of floc growth have been developed. Fair and Gemmell (1964) have developed a floc growth kinetics model for orthokinetic flocculation by assuming various upper particle size limits and floc breakup models on Smoluchowski's equation. It was found that the floc growth approached a steady value if the velocity gradient-particle concentration product was not large enough to cause floc breakup , and the floc growth became fluctuating if the velocity gradient-particle concentration product was large enough to cause floc breakup and reformation. The breakup of flocs appeared to be a first-order relationship between particle size and time (Bhaskar et al, 1993). Francois (1988) proposed a floc growth kinetic model by fitting the evolution of alum floc diameter with time on a semilogarithmic scale, a quantification of floc growth can be described as:

$$d_i = d' \exp (\mu t_f) \quad (3.25)$$

where  $d_i$  is a floc diameter,  $d'$  is a constant,  $t_f$  is flocculation time,  $\mu$  is floc growth constant.

To this time, these models have been used to study inorganic flocs with a small sizes. Based on a review of the literature, the investigation of kinetic models for polymeric flocs with big sizes, high strength and density is suggested.

### **3.8 Safety Regulations Regarding Polymer Use in Drinking Water Treatment**

Polymer flocculants are considered to be no hazard to human's health when their doses are limited to maximum 1 ppm in the drinking water treatment (Reuter and Landscheidt, 1988, Mallevalle et al 1984, EPA Report, 1975). They do not remain in the treated water like an additive, but are removed from the water almost completely. Therefore, United States, Great Britain, Federal Republic of Germany have given official permission for the use of polymers in drinking water treatment. Some other countries have also adopted this position. However, some contaminants in polymers such as the residual monomers, unreacted chemicals used to form the monomer units, and the products of reactions that transform or degrade residual monomers (i.e. acrylamide and epichlorohygrin ) are considered to be toxic since chronic exposure to them can cause animal carcinogens. As a general rule, the use of acrylamide-containing polyelectrolytes in drinking water treatment is considered to be safe if the content of monomeric acrylamide is limited less than 0.05% (Reuter and Landscheidt, 1988). The evaluation of the residual content of monomeric acrylamide is important to ensure the minimal risk to human health and well-being. Detailed analysis methods can be found elsewhere

(Ohnishi ,1985; Wang et al ; 1978; and Letterman & Pero, 1990). It has also been found that polymers are generally noncorrosive on metals such as stainless steel used in processing equipment (Gutcho, 1977).

## 4 METHODS AND APPARATUS

### 4.1 Preparation of Solutions

All the solutions except for the standard solutions of 1N NaOH and 1N HCl were prepared on a daily basis using identical conditions in order to minimize the variations of the primary particle concentrations and the particle size distributions, and to reduce the hydrolysis and photodegradation reactions of the chemicals.

#### 4.1.1 Kaolin Suspension

The kaolin stock suspension (4000 mg/L) was prepared daily by mixing the fine kaolin particles (K<sub>2</sub>-500, Fisher Scientific Co.) with tap water. The vessel used was 2L jar and flat blade impeller ( see section 4.2.1 and Plate 4.1). The suspension was mixed for four hours at an impeller speed of 400 rpm ( $\bar{G}=840 \text{ s}^{-1}$ ) in order to disperse the agglomerates caused by the adhesion of individual particles and to maintain the uniformity of the kaolin suspensions. For use, the stock solution was diluted to a suspension of 20 mg/L to permit the turbidities (approximate 19.5 NTU) of the suspension to be close to natural raw waters. The initial particle concentrations and turbidities of diluted kaolin suspensions were measured for each flocculation experiment. Results gave satisfying repetition.

#### 4.1.2 Alum Solution

A 2500 mg/L alum [ $\text{Al}_2(\text{SO}_4)_3 \cdot 18\text{H}_2\text{O}$ ] stock solution was prepared daily by adding 250 mg of alum into 100 mL of the Milli-Q<sup>®</sup> water. The solution was mixed for 1 hour with a constant mixing intensity (scale 3) using a magnetic stirrer. The 250 mg/L of alum feed solution was prepared by diluting stock alum solution with Milli-Q<sup>®</sup> water by a ratio of 1:10 using volumetric glassware.

#### **4.1.3 Polymer Stock Solution**

A Percol LT 20 which is nonionic form of polyacrylamide was used as a flocculant aid. A 2500 mg/L of the polymer stock solution was prepared, at ambient conditions, by first rapidly agitating 100 mL of Milli-Q<sup>®</sup> water into vortex, then adding 250 mg solid grade polymer into the Milli-Q<sup>®</sup> water. After which the polymer solution was mixed for 2 hours at lower mixing rate. The mixing rate and time were consistent each time. It is important to note that the polymer chains can break apart if the mixing rate or time is too great.

#### **4.1.4 Polymer Feed Solution**

The stock polymer solution was diluted prior to being added into the reactor in order to avoid creating a large concentration gradient. The dilution ratio used for polymer feed solution was 1:10 resulting in a feed solution with a concentration of 250 mg/L.

### **4.2 Experimental Apparatus**

#### **4.2.1 Reactor**

The reactor used in this research is known as a Hudson jar (Hudson and Wagner,

1981). The two-liter square jar (115 mm × 115 mm × 150 mm ) was mixed using a 76 mm diameter flat blade impeller. This apparatus has been the standard since its introduction by Hudson & Wagner (1981). Plate 4.1 shows the reactor along with the mixer and the particle size analyzer.

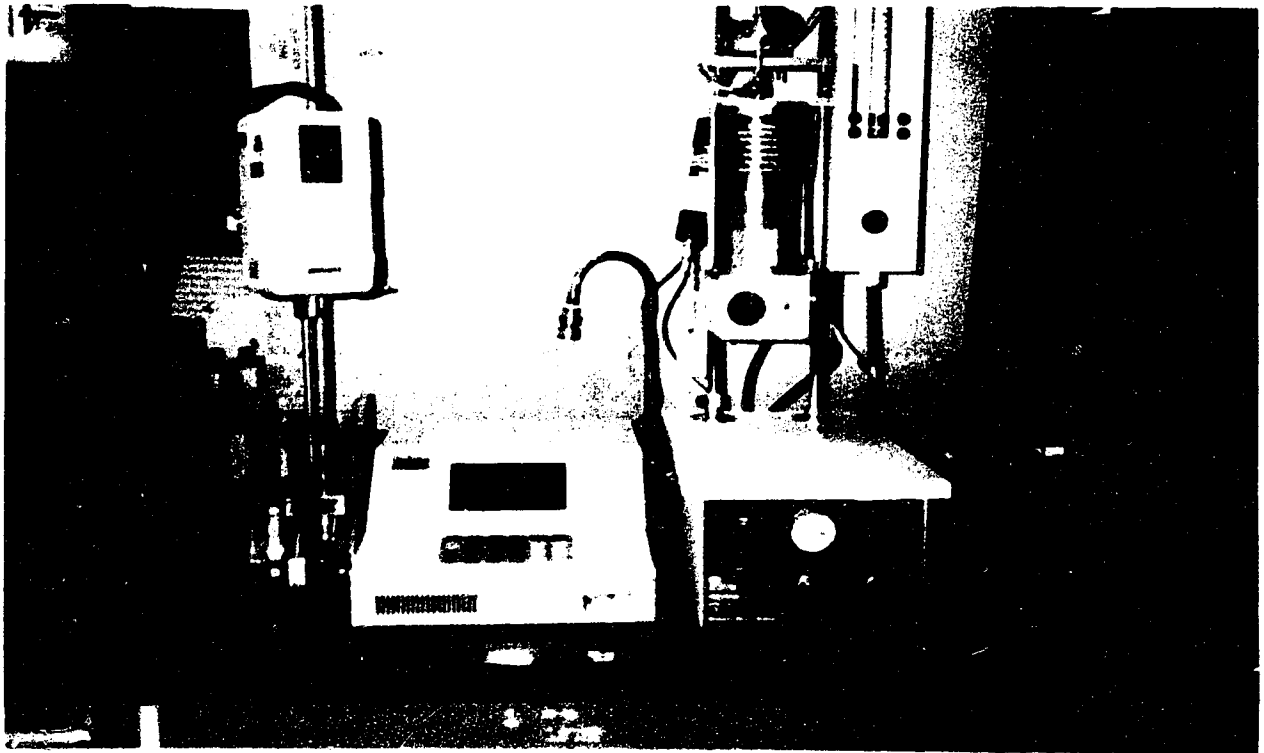


Plate 4.1 Equipment Apparatus



#### **4.2.2 PH Meter**

The pH of the suspension was measured with a Fisher Scientific Accumet<sup>®</sup> pH meter 25. The pH meter was calibrated using pH= 4 , pH=7 and pH=10 standard buffer solutions provided by Fisher Scientific. Calibration was performed on a daily basis.

#### **4.2.3 Turbidity Meter**

The turbidity of the suspension was determined using a Hach Turbidimeter (Model 2100 A). The turbidity meter was calibrated using manufacturer supplied formazin suspension standards prior to the measurement and between each measurement , as suggested by the supplier.

#### **4.2.4 Particle Size Analyzer**

Particle sizes and size distributions were analyzed with a light-blockage particle size analyzer (HIAC/ROYCO MODEL 8000A) which is also shown in Plate 4.1. This employs a laser-light source along with advanced data acquisition and processing systems. The HRLD-150 light-obscuration sensor was used in the particle size analyzer. The sensor ranges from 1 to 150  $\mu\text{m}$  with the resolution of 1  $\mu\text{m}$ . The sensor was calibrated using latex particles in water with flow rate of 25 mL/min. The optimum concentration range was 0 to 18, 000 count/mL. A 10 mL sample was analyzed in each run, but a minimum of 35 ml of sample was required for each measurement because of the large tare (dead volume) held in the tubes (about 25 mL).

The particle size analyzer sizes particles into eight user-specified channels. The number of particles counted in each channel and the particle size distribution are strongly

dependent on the channel setting. The lowest size channel was set at the smallest size limit for the sensor in use to verify that the maximum recommended particle concentration was not exceeded. The fixed channel settings were utilized in order to obtain consistent results. The channel settings employed throughout our study are presented in Table 4.1.

**Table 4.1 Channel Setting of the Particle Size Analyzer**

Channel Number	Channel Setting ( $\mu\text{m}$ )
1	1
2	5
3	10
4	20
5	30
6	40
7	50
8	60

Table 4.1 demonstrates that a successive and non-uniform class-size intervals were selected. The narrow channel widths were set for the lower sizes which allowed the most particles to be detected, but wide widths were chosen for the higher channels where relatively few particles were detected. This is because the particles in the kaolin suspension had wide particle size distribution during the process of flocculation where there existed a great number of fine particles and small number of bigger flocs.

Using this set of channel settings, the particle size analyzer's ability to define the particle size distribution of a sample was limited by its resolution capabilities rather than the channel settings chosen by the analyst. Particle counts were normalized for channel width when the particle size distribution graphs were plotted in the evaluation of the impact of pH on the flocculation, which can eliminate the impact of channel width on the particle size distribution .

The particle size analyzer was calibrated and standardized before being used for measurements. Internal and external calibrations were performed. The internal calibration curve of latex particles in water was selected for these flocculation experiments. The particle size analyzer was calibrated from time to time during the process of measurement. The external calibration standards (d=2.08, 9.70, 19.81  $\mu\text{m}$ , distributed by Coulter Source INC., and manufactured by EPICS Division of Coulter Corporation) were used to standardized the analyzer.

The standard solutions used to standardize the particle size analyzer were prepared by gently mixing the standard particles with Milli-Q<sup>®</sup> water and surfacant for 30 minutes to ensure complete dispersion, where the addition of surfacant aids to disperse the standard particles. The concentration of the standard suspension was controlled at approximately 4500 counts/mL which is 25% of the manufacturer's recommended maximum concentration. The use of this concentration limited the coincidence errors to less than 3 %.

After the standard suspensions were well mixed, samples were taken and exposed for at least one minute to remove the bubbles. The samples were analyzed in triplicate using the particle size analyzer. The channel settings of particle size analyzer were: the lowest size channel was set at the smallest size limit for the sensor in use to verify that the maximum recommended particle concentration was not exceeded, and remaining channels were set up in 1- $\mu\text{m}$  increments around the mean calibration sphere diameter. The data were taken following the procedures described below:

- (1) Perform instrument warm-up procedure for 30 minutes. Then execute the field standardization using the "auto-adjustment" prior to the initiation measurement in order to ensure low noise in the data.

- (2) Flush the sampling line and the sensor volume five times using Milli-Q® water prior to the initial measurement, record the particle counts from the past 2 or 3 flushes. If the total background counts were greater than that of the clean system, more flushing was required until the counts dropped to the level of a clean system. This was necessary to eliminate the possibility of contamination of samples by residuals in the sampling line and the sensor volume of the particle size analyzer.
- (3) Adjust the sample flow rate to 25 mL/min using Milli-Q® water or a test sample. The flow rate was checked and adjusted periodically throughout the experiment to maintain a constant flow rate. Adjustments were made very slowly via a potentiometer on the pump controller.
- (4) Take an aliquot of approximately 40 mL of the sample from the side sampler in the reactor every three minutes from the beginning of flocculation. Expose the sample for 1 minute to remove bubbles, then measure immediately with very gentle mixing while the big flocs were present, and without mixing when the flocs were very fine.
- (5) Flush the sampling line several times with Milli-Q water between each test, and also prior to instrument shutdown for the removal of all residual particles.

#### **4.2.5 Scanning Electron Microscope**

The shapes and microstructures of the flocs and primary particles were observed and photographed using Scanning Electron Microscope (HITACHI SEM-2500 ).

### **4.3 Experimental Methods**

The diluted kaolin suspension was used as simulated raw water. A polymer was utilized in conjunction with alum. The dilute kaolin suspension was brought to the desired initial alkalinity first. The pH of the suspension was then adjusted to the desired range using standard solutions of 1 N HCl and 1 N NaOH.

All experiments were performed using a jar-test apparatus. The procedures used in the study of the kinetics of polymer-aided flocculation is described as follows: 1) 2L of the 20 mg/L kaolin was added to the jar, and mixed at an impeller speed of 100 rpm for 10 minutes; 2) the initial pH and turbidity were measured; 3) the alkalinity was increased by adding  $\text{NaHCO}_3=100$  mg/L; 4) the pH of the kaolin suspension in the reactor was adjusted to the optimum value of pH=8; 5) alum and polymer were added simultaneously near the impeller to ensure complete dispersion; 6) the desired rapid mixing rate was set on the mixer; 7) the mixer was started immediately after polymer addition; 8) once the required rapid mixing time was reached, the mixing rate was reduced to the value required for the slow mixing rate, and the time for slow mixing was documented; 9) the suspension was sampled every three minutes from the side sampler; and 10) samples were analyzed as described previously.

## 5 RESULTS AND DISCUSSIONS

### 5.1 Evaluation of Kaolin Particle Size and Size Distribution

The size and size distribution of the kaolin particles used in this study (K<sub>2</sub>-500, Fisher Scientific Co.) were analyzed using a particle size analyzer as no data are available from the manufacturer.

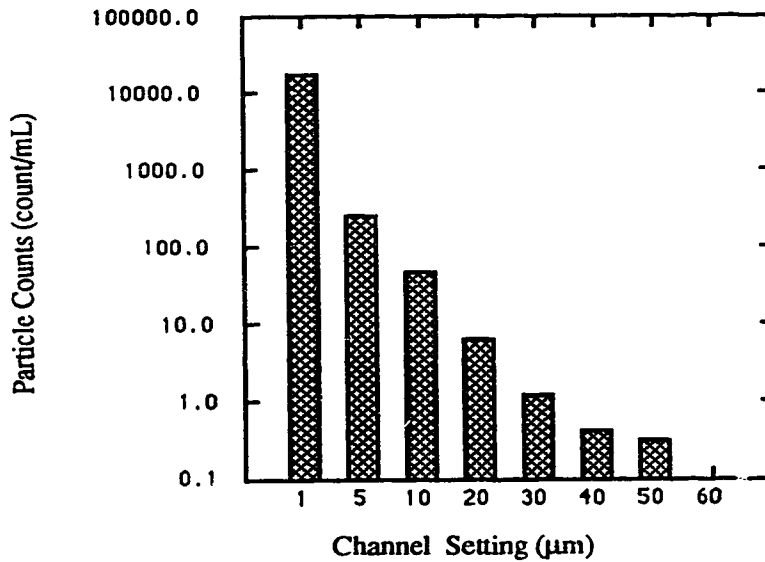


Figure 5.1 Particle Size Distribution of the Kaolin Particles

Figure 5.1 shows that the particle size of the unflocculated kaolin was far from uniform. It covers a wide range from 1 up to 50 μm. However, 98% of the kaolin particles were found to have a particle size of less than 5 μm, and 99.7% less than 10 μm. The size of the kaolin particles, thus, is assumed to be in the range of 1 to 10 μm.

## **5.2 Methods of Data Analysis**

### **5.2.1 Particle Size Distribution**

Data on particle size distributions were usually analyzed graphically and mathematically in order to transform the raw data into useful information for applications such as treatment plant process optimization and control, treatment plant unit design, and establishment of water quality criteria . Ropp et al (1985) presented a brief review of different graphical methods that can be used to display particle size distribution. These methods included a two-parameter distribution function (Petroll et al 1986), a three-parameter log-normal distribution function (Laapas, 1985), and a four-parameter log-hyperbolic function (Durst & Macagno, 1986). Among them, the two-parameter distribution function using log-normal equation was selected in this study because it showed the simple linear relationship between the particle counts and flocculation times on semilogarithmic scale (see Figure 5.2).

### **5.2.2 Mean Particle Diameter**

The size of an irregular coagulated floc was often evaluated by the projected diameter (or called equivalent diameter) which includes: projected area diameter, perimeter diameter, Feret diameter, and Martin diameter (Tambo, 1991). The projected area diameter (also called the Heywood diameter ) was usually given by measurements through photometric methods. The perimeter diameter was useful in evaluating the shape factor of an irregular particle. Feret and Martin diameters were often used to evaluate floc size when many flocs were measured (Tambo, 1991). The project area diameter was given by the particle size analyzer used in this research.

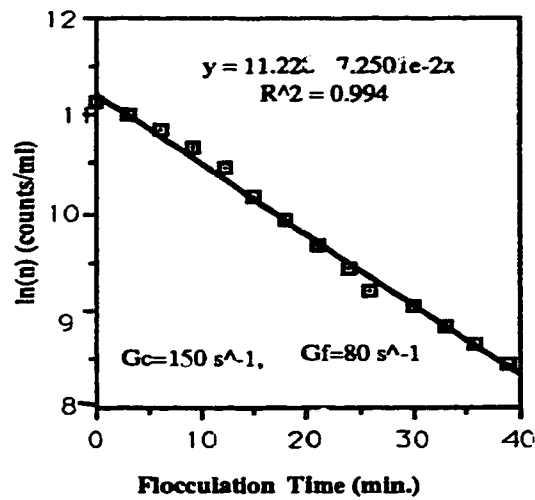


Figure 5.2 Flocculation Curve at  $\bar{G}_f=80 \text{ s}^{-1}$  [primary particle concentrations ( $d \leq 10 \mu\text{m}$ ) against flocculation times plotted on semilogarithmic scale)

Experience has shown that it was often more convenient to use one or more mean diameters to represent the whole size distribution for the purpose involved. Various types of mean particle diameters were used in the literature, which could afford measures of the spread or variability among the particles in respect of both size and size distribution. Each has its own characteristics, and was useful under specific circumstances. The nomenclature which covers the whole field of mean particle diameters was Alderliesten (1984) and was presented in Table 5.1.



**Table 5.1 Nomenclature Mean Particle Diameters  $\bar{D}_{p,q}$**

<b>Systematic Code</b>	<b>Names</b>
$\bar{D}_{-1,0}$	Harmonic mean diameter
$\bar{D}_{0,0}$	Geometric mean diameter
$\bar{D}_{1,0}$	Arithmetic mean diameter
$\bar{D}_{2,0}$	Mean surface diameter
$\bar{D}_{3,0}$	Mean volume diameter
$\bar{D}_{2,1}$	Diameter-weighted mean diameter
$\bar{D}_{3,2}$	Surface-weighted mean diameter
$\bar{D}_{4,3}$	Volume-weighted mean diameter
$\bar{D}_{3,1}$	Diameter-weighted mean surface diameter
$\bar{D}_{4,2}$	Surface-weighted mean surface diameter
$\bar{D}_{5,3}$	Volume-weighted mean surface diameter
$\bar{D}_{4,1}$	Diameter-weighted mean volume diameter
$\bar{D}_{5,2}$	Surface weighted mean volume diameter
$\bar{D}_{6,3}$	Volume-weighted mean volume diameter
$\bar{D}_{1,1}$	Diameter-weighted geometric mean diameter
$\bar{D}_{2,2}$	Surface-weighted geometric mean diameter
$\bar{D}_{3,3}$	Volume-weighted geometric mean diameter

P.S. 1)  $p = -1, 1, 2, 3, 4, 5,$  and  $6$ ; 2)  $q = 0, 1, 2,$  and  $3$

The general expression of systematic code for mean diameter  $\bar{D}_{p,q}$  was formulated by Alderliesten (1984) as:

$$\bar{D}_{p,q} = \left[ \frac{\sum_i n_i D_i^p}{\sum_i n_i D_i^q} \right]^{1/(p-q)} \quad p \neq q \quad (5.1)$$

where  $n_i$  = the number of particles with diameter  $D_i$ , and for  $q=p$ ,  $\bar{D}_{p,p}$  can be expressed as:

$$\bar{D}_{p,p} = \exp \left[ \frac{\sum_i n_i D_i^p \ln D_i}{\sum_i n_i D_i^p} \right] \quad (5.2)$$

The types of mean diameters used play a central role, and it was, therefore, very important to select the proper one for analysis of experimental results. Four different mean particle diameters which relate to the volume of a floc are the most relevant to this study. These include:  $\bar{D}(1,0)$ ,  $\bar{D}(3,0)$ ,  $\bar{D}(4,3)$ , and  $\bar{D}(6,3)$ . The detailed expressions are given as:

$$\bar{D}_{1,0} = \frac{\sum_i n_i D_i}{\sum_i n_i} \quad (5.3)$$

$$\bar{D}_{3,0} = \left[ \frac{\sum_i n_i D_i^3}{\sum_i n_i} \right]^{1/3} \quad (5.4)$$

$$\bar{D}_{4,3} = \frac{\sum_i n_i D_i^4}{\sum_i n_i D_i^3} \quad (5.5)$$

$$\bar{D}_{6,3} = \left[ \frac{\sum_i n_i D_i^6}{\sum_i n_i D_i^3} \right]^{1/3} \quad (5.6)$$

where  $D_i$  is the statistical value of diameter. It can be expressed using the threshold settling data or the midpoint of each successive class-size interval. Figures 5.3 to 5.5 demonstrate that using midpoint is superior, because it gives the floc growth curves which more closely approximate the experimental phenomena. Therefore, it was used throughout this study.

The above four expressions were evaluated by comparing the floc growth curves shown in Figures 5.3 to 5.4. The analysis of the figures indicates that the trend of floc growth curve derived from  $\bar{D}_{1,0}$  is not the correct representation for the floc growth process observed, and also can not be used to evaluate the kinetics of floc growth. The trends derived from  $\bar{D}_{3,0}$ ,  $\bar{D}_{4,3}$  and  $\bar{D}_{6,3}$  are similar, and consistent with the experimental phenomena observed except for the difference of the distinctness between each trend.

The trend from  $\bar{D}_{6,3}$  was used as it provided clearly three stages of floc growth, which have been reported in the literature. Therefore, all the mean particle diameters were evaluated by  $\bar{D}_{6,3}$ .

Figures 5.3 to 5.5 also show that the mean floc diameter is a relative value. It depends on the method of measurement and evaluation. Therefore, much care should be taken when different mean particle diameters are compared.

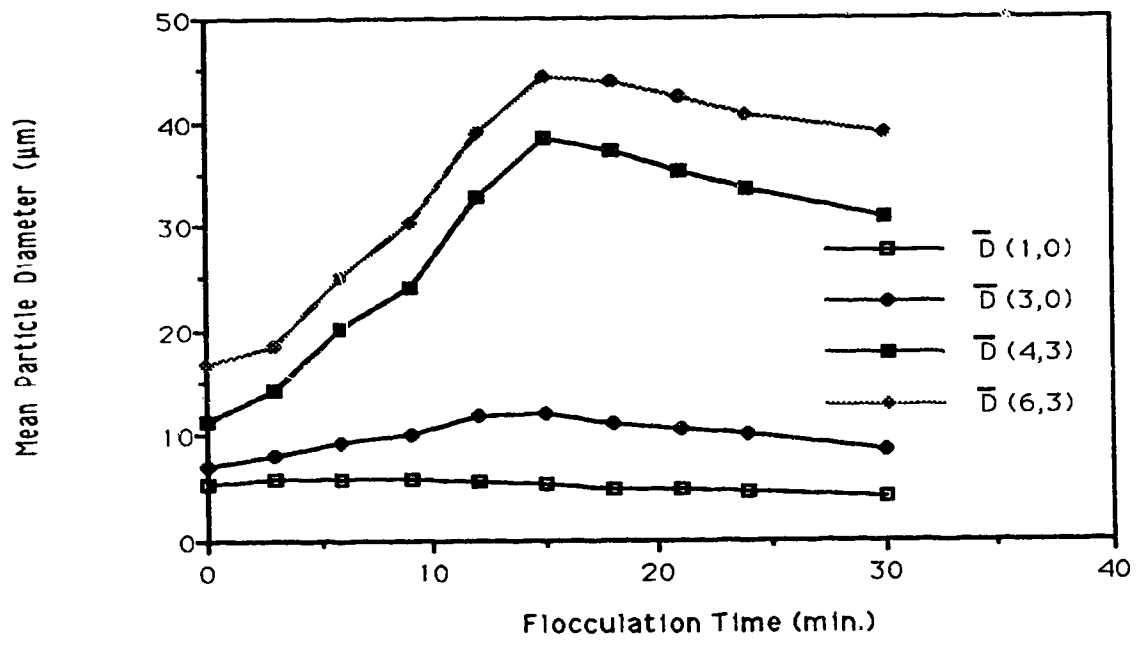


Figure 5.3 Evaluation of Mean Particle Diameters ( $d_j$ = channel setting,  $\bar{G}_c=150 \text{ s}^{-1}$  for 2 min.,  $\bar{G}_f=30 \text{ s}^{-1}$  for 30 min., alum=5 mg/L, polymer=0,5 mg/L,  $\text{NaHCO}_3=100 \text{ mg/L}$ )

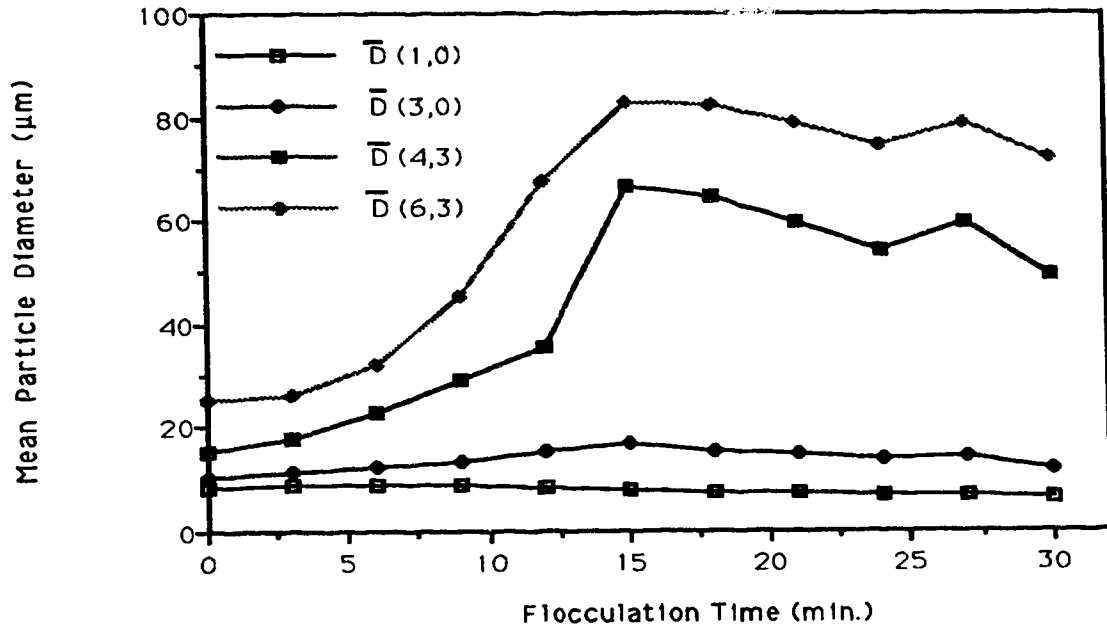


Figure 5.4 Evaluation of Mean Particle Diameters ( $d_i$ = arithmetic mean of the near channel settings,  $\bar{G}_c=150 \text{ s}^{-1}$  for 2 min.,  $\bar{G}_f=30 \text{ s}^{-1}$  for 30 min., alum=5 mg/L, polymer=0,5 mg/L,  $\text{NaHCO}_3=100 \text{ mg/L}$ )

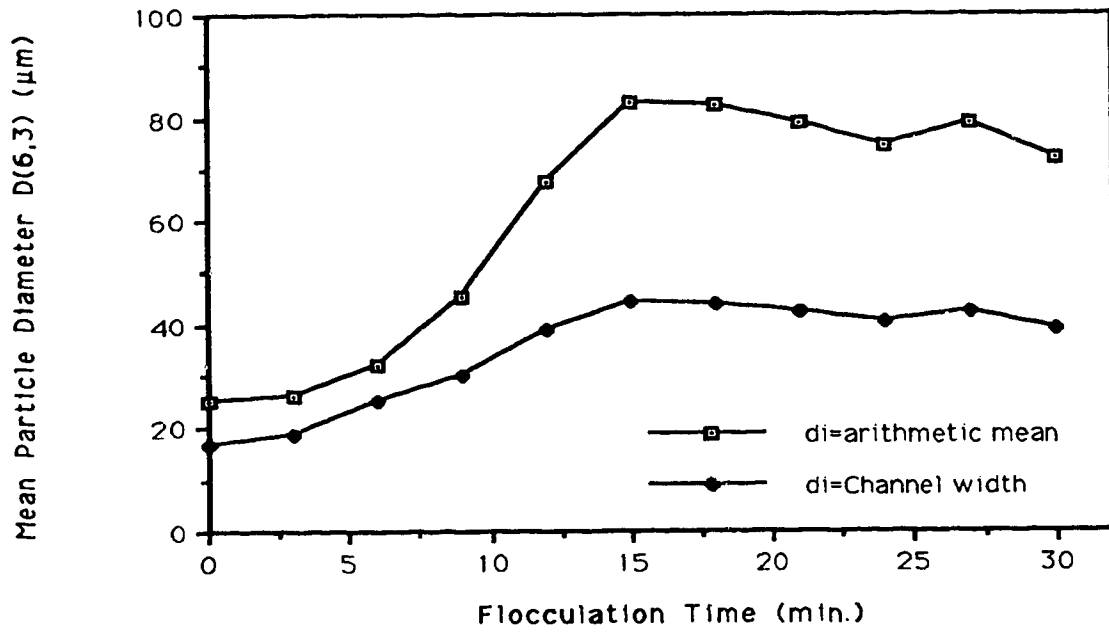


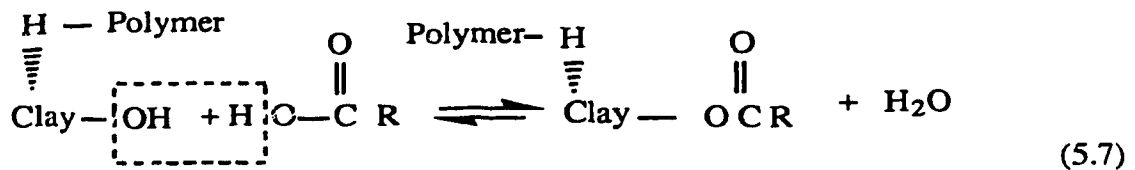
Figure 5.5 Comparison of D(6,3) Values Expressed by Different Types of  $d_i$   
 $(\bar{G}_c=150 \text{ s}^{-1}$  for 2 min.,  $\bar{G}_f=30 \text{ s}^{-1}$  for 30 min., alum=5 mg/L, polymer=0.5 mg/L,  $\text{NaHCO}_3=100 \text{ mg/L}$ )

### **5.2.3 Flocculation Efficiency**

Historically, there are many methods to measure the efficiency of flocculation: (1) using the reduction of sediment density (Michaelis, 1954); (2) using sediment volume (Michaelis, 1954); (3) using settling rates ( Link & Booth, 1960); (4) using filtration rates (Kane et al, 1963, Smellie and La Mer, 1958); (5) using turbidity removal ( $N_0/N_1$  ) where  $N_0$  and  $N_1$  are the turbidities of influent and effluent (Timasheff, 1966); (6) using turbidity removal rate ( $N_0/N_1$  vs  $t$  ); and (7) using the removal ratio of the number of primary particle concentration. Among them, the flocculation efficiency expressed by the removal of turbidity is a quick and effective method. It was used to select the optimum polymer, to determine the optimum alum-polymer doses combination and optimum process conditions. The flocculation efficiency, expressed by the removal ratio of the primary particle concentration, was the more accurate method, and was used to compare the effectiveness between alum flocculation and polymer-aided flocculation.

### **5.3 Selection of an Optimum Polymer as a Coagulant Aid**

The selection of an optimum polymer as a coagulant aid was based on the following factors: 1) the characteristics of kaolin suspension; 2) the chemistry of alum hydrolysis; and 3) the constituent, characteristics, availability and cost of a polymer. The theoretical analysis led to the conclusion that carboxyl-containing polymers with hydroxyl groups were the priority since the adsorption of the polymer by kaolin clay particles occurs not only by hydrogen bonding, but also by chemical bonding. As the chemical bonds are much stronger than hydrogen bonds, the strength of a floc may be improved dramatically as a consequence, and a high flocculation efficiency may be achieved.



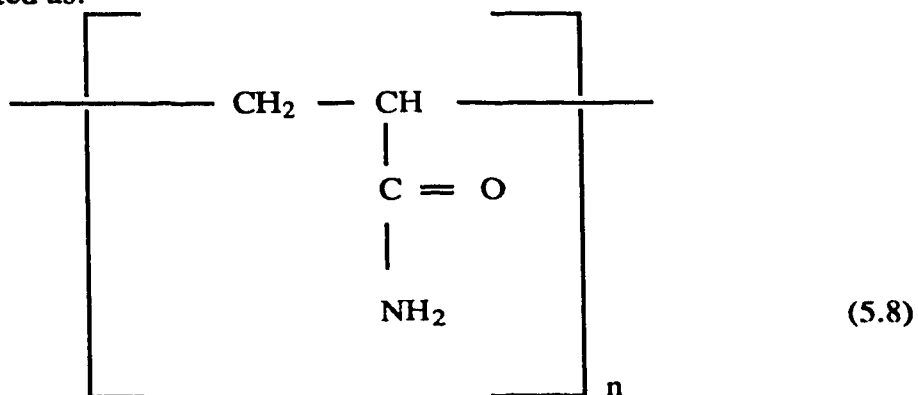
Polyacrylamides are carboxyl-containing polymers with hydroxyl groups. The commercially available polyacrylamides were the PAM series and the Percol LT series with different ionic groups, molecular weights, and charge densities. Screening polymer tests were performed among the following types of the polymers: PAM A-303, PAM C-412, Percol LT-20 (nonionic), LT22 (medium cationic), LT 27 (medium anionic). Different alum-polymer combinations and different dose combinations were examined using jar-tests in terms of the efficiency of flocculation expressed by the rate of turbidity removal. The process conditions for screening tests were listed in Table 5.2. The results found that Percol LT 20 had the lowest optimum dose (0.5 mg/L), and the highest flocculation efficiency at pH=8. Thus, Percol LT 20 was the alternative chosen throughout this study.

Table 5.2 Process Conditions for Determination of Optimum Polymer and Optimum Dose Combination

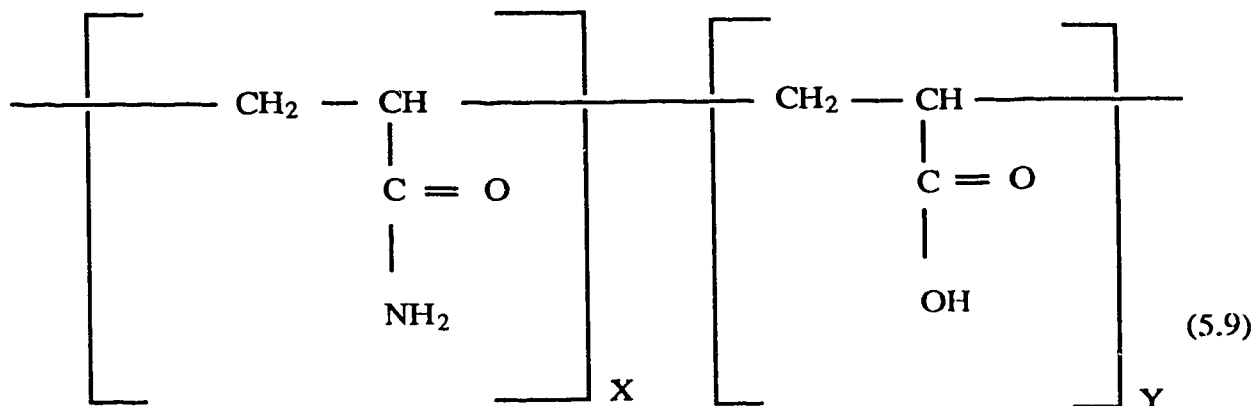
Parameter	Data
Kaolin (mg/L)	20
NaHCO <sub>3</sub> (mg/L)	100
Alum (mg/L)	1.0 to 20
Polymer (mg/L)	0.1 to 1.0
pH	8
Rapid Mixing Rate (rpm)	100
Rapid Mixing Time (min.)	2
Slow Mixing Rate (rpm)	30
Slow Mixing Time (min.)	30



Percol LT 20 is a nonionic form of polyacrylamide with a high molecular weight, its structure is postulated as:



Some of its amide groups can be hydrolyzed to carboxylic acid at alkaline suspension (pH>7), and the hydrolyzed polyacrylamide has the structure:



The anionic structure shown in Equation (5.10) may be formed by the ionization of the carboxylic groups in hydrolyzed polyacrylamide macromolecules, and the anionic character becomes strong as the degree of hydrolysis increases.



particles, governs the degree of hydrolysis, ionic groups, charge density and steric structure of a polymer. Therefore, it is necessary to evaluate the effect of pH on the flocculation efficiency, and determine the optimum pH.

In order to minimize the number of the experimental runs, the range of pH tested was predicted first based on the alum coagulation diagram (Amirtharajah, 1990; Mills, 1982), and related literature (Clark & Srivastava, 1993; Baes & Mesmer, 1976; Hespanhol & Selleck, 1975).

At lower values of pH ( $\text{pH} < 6$ ), the dominant soluble species at equilibrium with alum are cationic monomers of  $\text{Al}(\text{H}_2\text{O})_6^{3+}$  and  $\text{Al}(\text{OH})_2^+$ . These cationic monomers can destabilize the primary particles through the charge neutralization reaction, but the efficiency of fine particle removal was low due to the absence of sweep-floc coagulation.

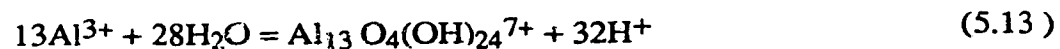
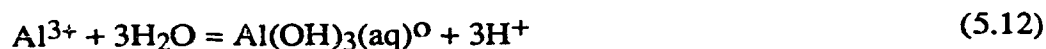
At the pH range of 6 to 7, although the positively charged polymeric species of aluminum such as  $\text{Al}_2(\text{OH})_2^{4+}$ ,  $\text{Al}_3(\text{OH})_4^{5+}$ ,  $\text{Al}_6(\text{OH})_{15}^{3+}$ ,  $\text{Al}_8(\text{OH})_{20}^{4+}$ ,  $\text{Al}_{13}\text{O}_4(\text{OH})_{24}^{7+}$ , are thought to exist, and improve flocculation by charge neutralization. Metal hydroxide particles  $[\text{Al}(\text{OH})_3]$  formed are not in great enough concentration to produce a rapid growth of floc particles. This tends to lead to smaller floc size, and low flocculation efficiency.

The pH range from 7.0 to 10.0 was selected as the most informative and interesting range to be tested in this study since sweep-floc coagulation may occur at some point of this range. Jar-tests were used to determine the optimum pH based on the assessment of the maximum mean floc size ( $d_{\text{max}}$ ), flocculation efficiency (E), and particle settling rate (R).

Figures 5.6 and 5.7 show that pH has a great impact on flocculation performance. The critical pH occurred at pH=8 where  $E_{max}$ ,  $d_{max}$ , and  $R_{max}$  were achieved. These three parameters tend to increase with the increase in pH at pH < 8, but decrease with the increase in pH at pH > 8. This is because the efficiency of polymer aided flocculation in conjunction with alum is determined by three mechanisms: 1) adsorption of hydrolysis species on the kaolin particles causing charge neutralization; 2) sweep-floc coagulation enhancing the precipitation of solid hydroxides to a greater extent; and 3) bridging by the long-chain polymers promotes physically the kinetics of flocculation, and producing more settleable flocs. The reaction extent of each mechanism controls the performance of flocculation.

At pH < 8, the changes in E,  $d_{max}$ , and R with pH were dominated by the sweep-floc coagulation. The extent of the sweep-floc coagulation tended to increase as pH increased in the range of pH=7.5 to 8 resulting in more Al(OH)<sub>3</sub> precipitating out, which aided flocculation.

At pH=8, the performance of flocculation was at an optimum as the above three mechanisms occurred simultaneously resulting in the maximum values of E,  $d_{max}$ , and R. Clark (1993) demonstrated that at pH=8, the dominant alum hydrolysis reactions are



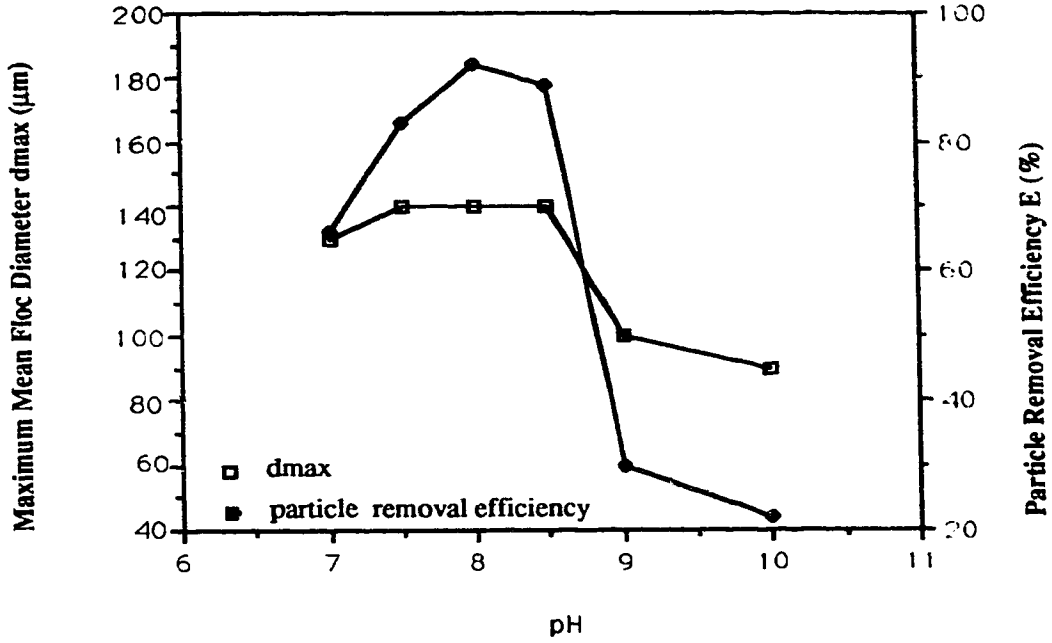


Figure 5.6 Effect of pH on Maximum Mean Floc Diameter and Particle Removal Efficiency (polymer = 0.5 mg/L, alum = 5 mg/L, kaolin = 12.5 mg/L, NaHCO<sub>3</sub> = 100 mg/L, 100 rpm for 1 min., 30 rpm for 30 min. )

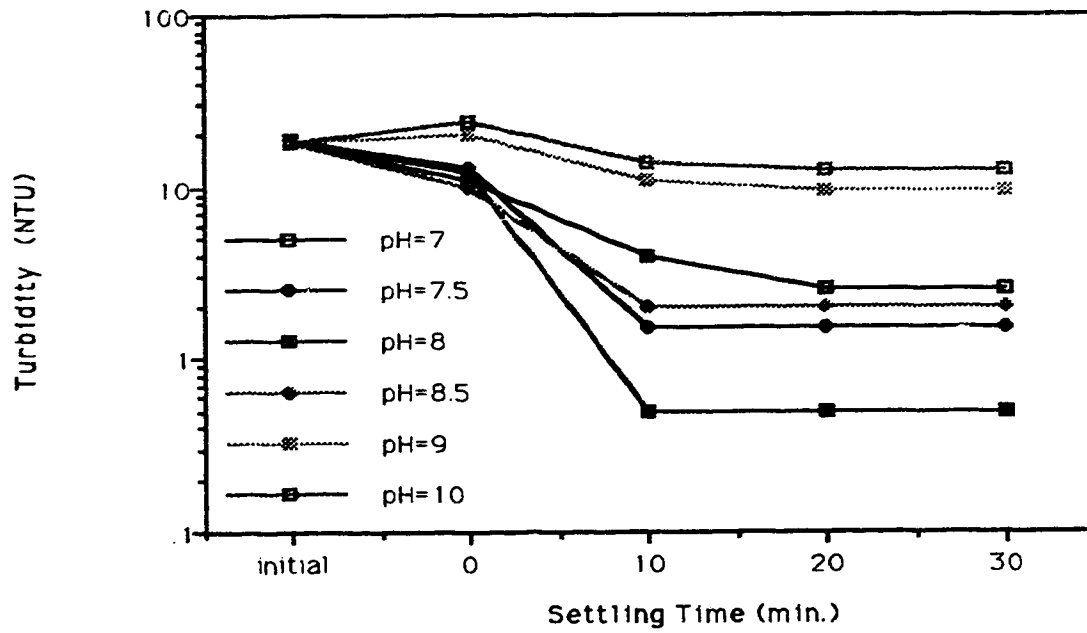


Figure 5.7 Effect of pH on Turbidity Removal Rate (polymer = 0.5 mg/L, alum =5 mg/L, kaolin = 12.5 mg/L, NaHCO<sub>3</sub> = 100 mg/L, 100 rpm for 1 min., 30 rpm for 30 min. )

The intermediate hydrate species of  $\text{Al}(\text{OH})_2^+$  and polymeric forms of aluminum  $\text{Al}_{13}\text{O}_4(\text{OH})_{24}^{7+}$  were responsible for the charge neutralization reaction, and the precipitates of  $\text{Al}(\text{OH})_3(\text{aq})^0$  were responsible for the sweep-floc coagulation. As discussed, this type of coagulation significantly improves the flocculation efficiency since  $\text{Al}(\text{OH})_3$  precipitates provided a greater number of adsorption sites resulting in the fine particles adsorbing and enmeshing on the surface. Moreover, at  $\text{pH}=8$ , the conformation of the polymer chain was near the optimum state which gave the optimum dimension of the segment of the chain benefiting both adsorption and bridging.

At  $\text{pH} > 8$ , the performance deteriorated with increase in  $\text{pH}$ , and a very poor performance was observed at  $\text{pH} > 8.5$ . This is contributed to by the following two factors:

- 1) Less destabilized particles were formed at  $\text{pH} > 8$ . The kaolin particles carried a small amount of  $\text{pH}$ -dependent negative charges due to exposed silica as well as positive charges on the edge of cleavage faces of the crystal ascribable to exposed alumina. The net charge of kaolin particles at the  $\text{pH}$  range of 6 to 7.8 was negative (Schofield, 1953; and Samson, 1954). The kaolin particles tended to lose negative charge at  $\text{pH}=7.8$  as the edge alumina reaches isoelectric point at this  $\text{pH}$ . The kaolin particles became positively charged at  $\text{pH} > 7.8$ . These particles were destabilized through the adsorption of negatively charged ions in the suspension. The amount of negative ions was thus the factor governing the efficiency of flocculation. Although the polymer used possessed some negative charge, and more anionic intermediate metal hydrate molecules such as  $[\text{Al}(\text{OH})_4]^-$  were formed from the hydrolysis of alum at  $\text{pH} > 8$ , the negative ions were still under dosed resulting in low efficiency of particle destabilization.

2) No sweep-floc coagulation occurred. At  $\text{pH} > 8$ , the amount of  $\text{Al}(\text{OH})_3$  precipitated tended to be reduced, and at  $\text{pH}=8.5$ , the hydrolysis species was dominated by  $[\text{Al}(\text{OH})_4]^-$ , which promotes a charge neutralization reaction rather than sweep-floc coagulation.

The above analysis demonstrates that the optimum pH with respect to  $\text{Al}(\text{OH})_3$  formation occurred at  $\text{pH}=8.0$ . This pH was used throughout this study. The particle size distributions at different stages of the coagulation and flocculation processes are presented in Figures 5.8 and 5.9 in order to visualize the efficiency of the flocculation at  $\text{pH}=8.0$ . The above figures show that most of the fine particles ( $d \leq 10 \mu\text{m}$ ) were aggregated into settleable flocs, and a very short settling time ( $t_f < 10 \text{ min.}$ ) resulted in finished water with a turbidity less than 1 NTU.



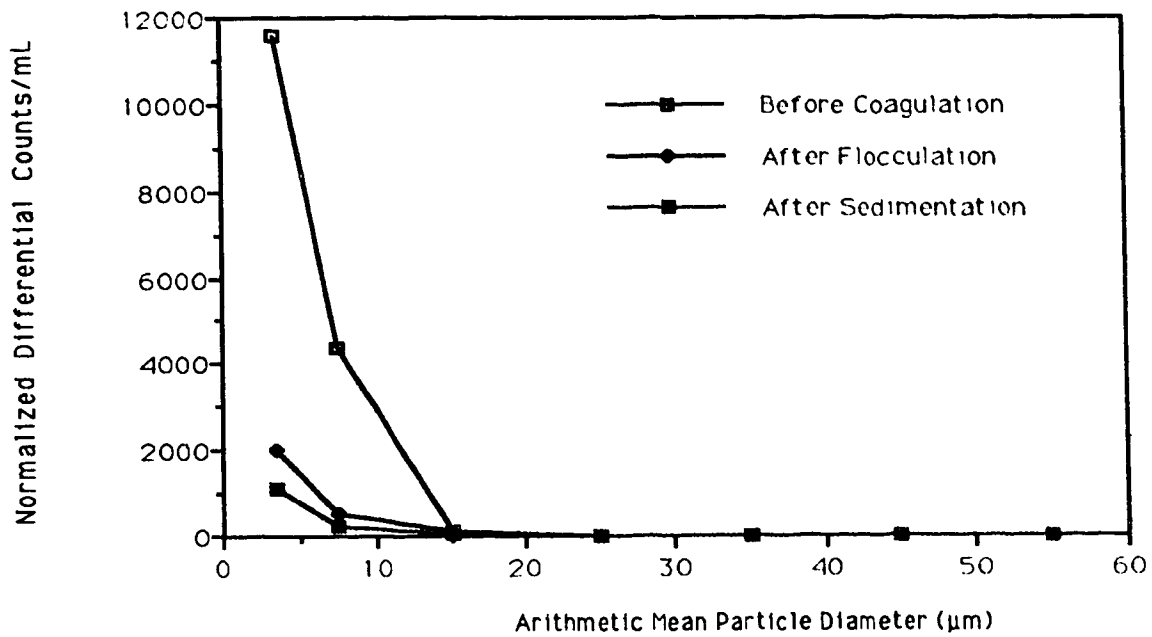


Figure 5.8 The Particle Size Distributions at pH=8 (polymer = 0.5 mg/L, alum =5 mg/L, kaolin = 12.5 mg/L, NaHCO<sub>3</sub> = 100 mg/L, 100 rpm for 1 min., 30 rpm for 30 min. )

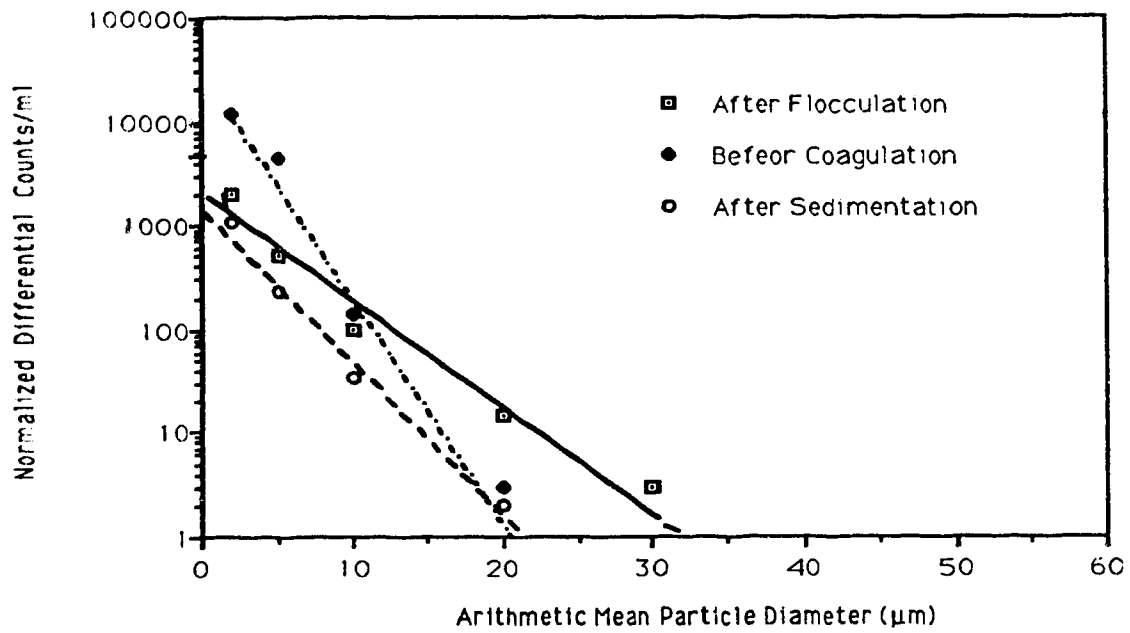
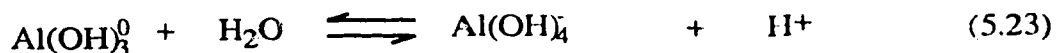
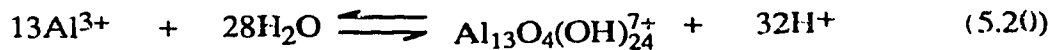
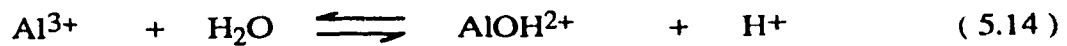


Figure 5.9 Particle Size Distributions at pH=8 and on Semilogarithmic (polymer = 0.5 mg/L, alum = 5 mg/L, kaolin = 12.5 mg/L, NaHCO<sub>3</sub> = 100 mg/L, 100 rpm for 1 min., 30 rpm for 30 min. )

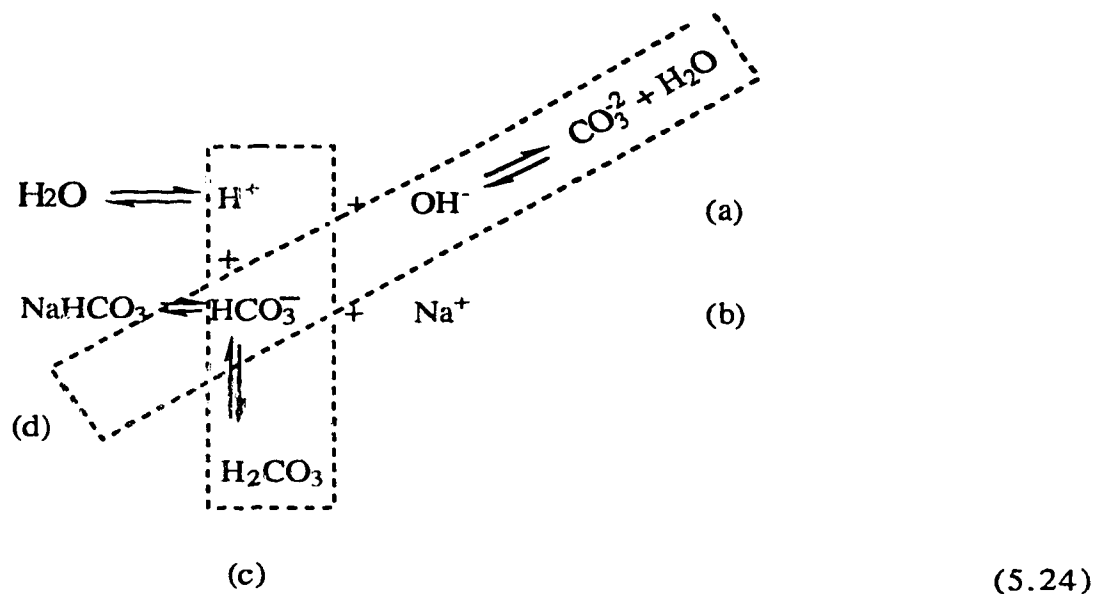
### 5.4.2 Optimum Alkali Dose

The main purpose of the addition of alkali ( $\text{NaHCO}_3$ ) was to buffer the kaolin suspension, or to keep the pH of the suspension from going down as the result of alum addition, as alum acts as an acid due to the hydrolysis reactions (Amirtharajah and O' Melia, 1990):



Equations 5.14 to 5.23 demonstrate that the formation of  $\text{H}^+$  ions lowers the pH of the suspension to different degrees depending on alum dose and the initial alkalinity of suspension. The experimental results showed that pH decreased from 8 to 7.8 after 5 mg/L of alum was added into the suspension without alkali addition. Therefore, the alkali was used to buffer the suspension.

$\text{NaHCO}_3$  was selected to address above problem. The mechanism of  $\text{NaHCO}_3$  in buffering the suspension is explained by Equation 5.24:



The equilibria between Equations 5.24 (a), (b), (c) and (d) exist at a constant pH. The addition of alum gave a rise in the number of  $\text{H}^+$  ions. The excess  $\text{H}^+$  ions reacted with the  $\text{HCO}_3^-$  ions produced from the dissociation of  $\text{NaHCO}_3$  yielding to  $\text{H}_2\text{CO}_3$  which is a very weak acid, or reacted with  $\text{OH}^-$  formed  $\text{H}_2\text{O}$ . As a result, the pH of the suspension remained constant. This value was determined by the buffer intensity which could be controlled by the dose of the alkalinity added into the suspension. Therefore, the optimum dose of  $\text{NaHCO}_3$  should be evaluated in order to keep a constant pH value of 8 after the alum addition.

Jar tests were used to determine the optimum alkali dose. The turbidity and the floc size and size distribution were measured. The mean particle size  $\bar{D}(6,3)$  defined by Equation 5.6), the particle removal efficiency  $[ E = (1 - \frac{n_t}{n_0}) \times 100\% ]$ , and the turbidity removal rate (R) were used to assess the performance of flocculation.

From Figures 5.10 and 5.11 it can be seen that the alkali dose has a great impact on  $\bar{D}(6,3)$ , E, and R. The values of the above three parameters tended to increase with the increased dose of  $\text{NaHCO}_3$ . The optimum dose occurred at  $\text{NaHCO}_3=100$  mg/L in which the best performance was achieved. The performance significantly deteriorated at  $\text{NaHCO}_3 > 100$  mg/L. This can be explained by the fact that the dose of  $\text{NaHCO}_3$  determined the buffer capacity which controlled the variation of the pH after alum addition.

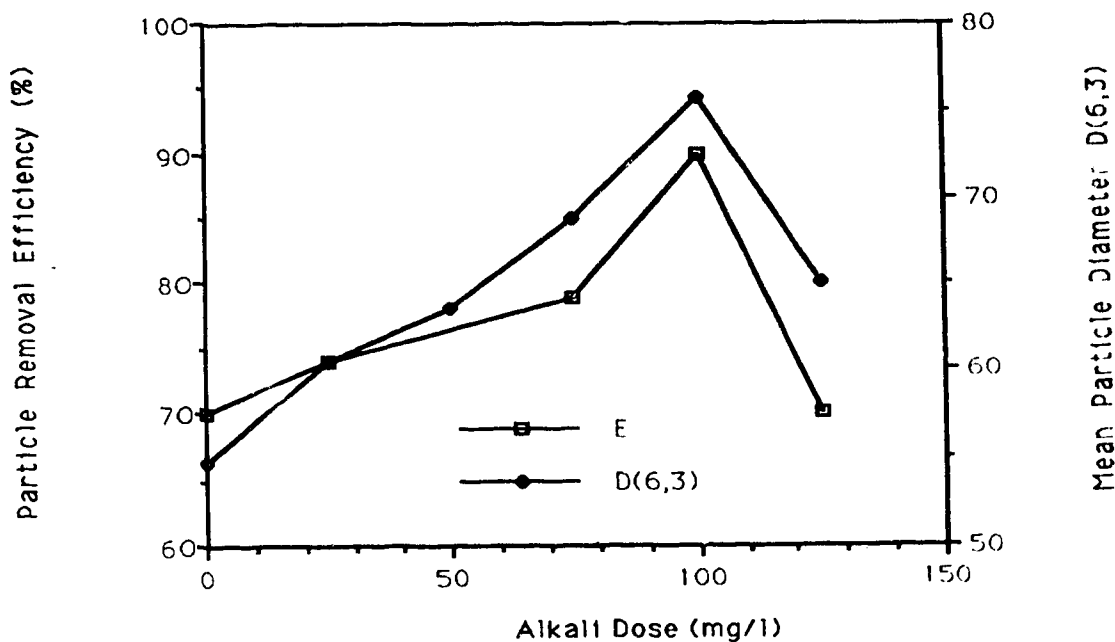


Figure 5.10 Effect of Alkali Dose on Particle Removal Efficiency and  $\bar{D}(6,3)$   
 [kaolin=20 mg/L, pH=8, alum =5 mg/L, polymer=0.5 mg/L,  $\bar{G}_c=122 \text{ s}^{-1}$   
 (100 rpm) for 1 min., and  $\bar{G}_f=23 \text{ s}^{-1}$  (30 rpm) for 30 min.]

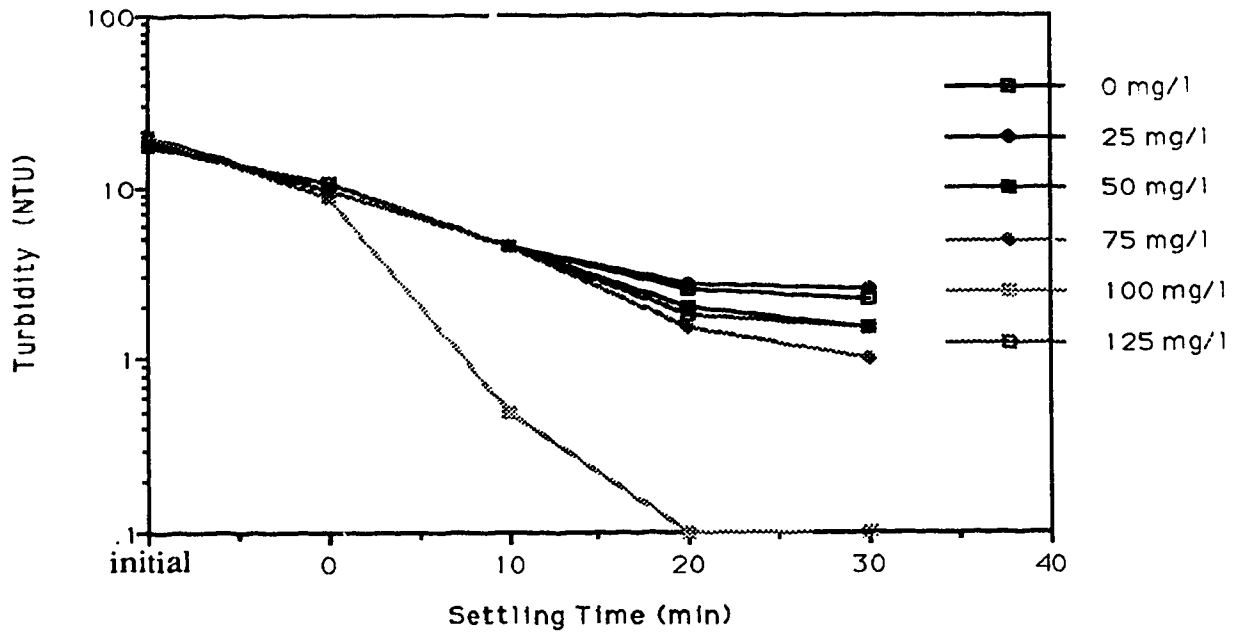


Figure 5.11 Effect of Alkali Dose on Particle Settling Rate [kaolin=20 mg/l., pH=8, alum =5 mg/L, polymer=0.5 mg/L,  $\bar{G}_c=122 \text{ s}^{-1}$  (100 rpm) for 1 min., and  $\bar{G}_f=23 \text{ s}^{-1}$  (30 rpm) for 30 min.]

Figures 5.10 and 5.11 also show that the optimum dose occurred at  $\text{NaHCO}_3 = 100$  mg/L which buffered the suspension to the optimum pH of 8. The comparison of Figures 5.6 and 5.10 leads to the conclusion that pH and alkalinity have similar effects on the flocculation performance; the higher alkali dose, the higher the pH is buffered. The increase in the alkali dose is equivalent to an increase in the final pH as the alkali dose determines the final pH after alum addition. The correlation of alkali dose and pH seems to be: at  $\text{NaHCO}_3 < 100$  mg/L, the buffered pH  $< 8$ , and at  $\text{NaHCO}_3 = 100$  mg/L, the buffered pH = 8. However, more complicated reactions exist at  $\text{NaHCO}_3 > 100$  mg/L as the excess ions of  $\text{Na}^+$  and  $\text{HCO}_3^-$  have a contradictory effect on the performance of the flocculation.

The favorable effect of  $\text{Na}^+$  ions is ascribed to the increase in the ability of adsorption through the reduction of the surface charge repulsion between polymer molecules and kaolin particles resulting from the compression of the diffuse double layer, and the reduction of length of segment of the polymer chain resulting from the coiling of the chain. The unfavorable effect of  $\text{Na}^+$  ions is that it reduces the bridging ability due to the decrease in the dimension of the segment of the polymer chain.

The favorable effects of  $\text{HCO}_3^-$  ions include the promotion of the hydrolysis of alum, and the formation of more precipitates of aluminum hydroxide which provided more surface area for fine particle adsorption and enmeshment. The adverse effect of  $\text{HCO}_3^-$  ions includes an increase in the negative charge of the kaolin surface due to the adsorption via hydrogen bonding between the  $\text{HCO}_3^-$  ions and the hydroxyl groups exposed in the octahedral aluminum sheets (Michaelis, 1954; Michaelis & Morellos, 1955; Schofield & Samson, 1953; and Hespanhol & Selleck, 1975). As a result, a higher dose of alum was required to reduce the negative electrophoretic mobility. If the alum dose remained constant, the flocculation efficiency would drop.

In conclusion, the optimum alkalinity dose occurs at  $\text{NaHCO}_3 = 100 \text{ mg/L}$ . It buffers the kaolin suspension to the optimum pH value of 8. The 100 mg/L of  $\text{NaHCO}_3$  was used in all the flocculation experiments.

#### **5.4.3 Determination of Optimum Method of Polymer Addition**

It was suspected that the sequence of coagulant addition may play an important role in polymer flocculation. A number of studies have been carried out by different researchers, but several contradictory conclusions have been drawn. It was reported that higher removal efficiency were generally obtained when alum was added ahead of the polymer rather than vice-versa (Hespanhol & Selleck, 1975). The explanation given is that alum can reduce the zeta potential by reducing the thickness of the double layer, while a polymer can enhance bridging ability and strengthen the resulting flocs. Other researchers have found that polymer should be added before the inorganic coagulants or other electrolytes which can align the clay particles, and reduce the interparticle bridging. Moreover, it was demonstrated that alum and polymer should be added at the same time. Overall, it was difficult to determine which sequence should be used. Experiments were carried out based on the different sequences and different lag times of polymer addition where lag time refers to the time period between alum addition which was conducted in rapid mixing stage and polymer addition which was performed either in the rapid mixing stage or slow mixing stage.

Based on the analyses of  $d_{\text{max}}$ , the particle removal efficiency (E), and the particle settling rate, the results shown in Figure 5.12 and 5.13 demonstrate that there was little difference between different sequences of polymer addition. Therefore, alum and polymer were added simultaneously throughout this research program.



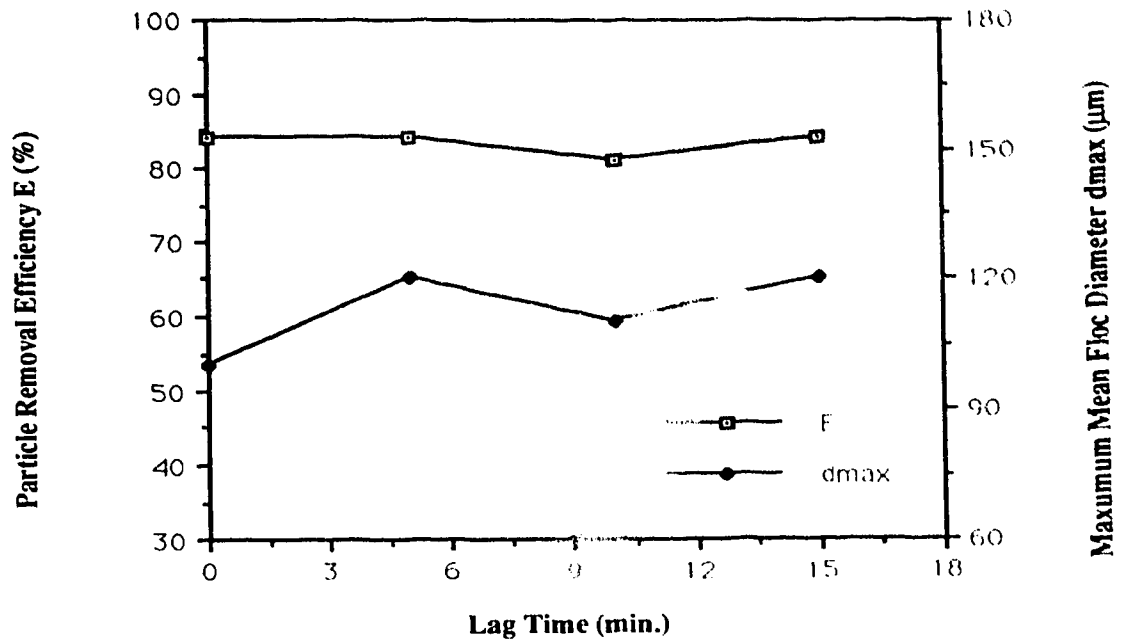


Figure 5.12 Effect of Lag Time on Particle Removal Efficiency (E), and Maximum Particle Size ( $d_{max}$ ) [kaolin=20 mg/L, pH=8,  $\text{NaHCO}_3$ =100 mg/L, alum =5 mg/L, polymer=0.5 mg/L,  $\bar{G}_c=122 \text{ s}^{-1}$  for 1 min., and  $\bar{G}_f=23 \text{ s}^{-1}$  for 30 min.]

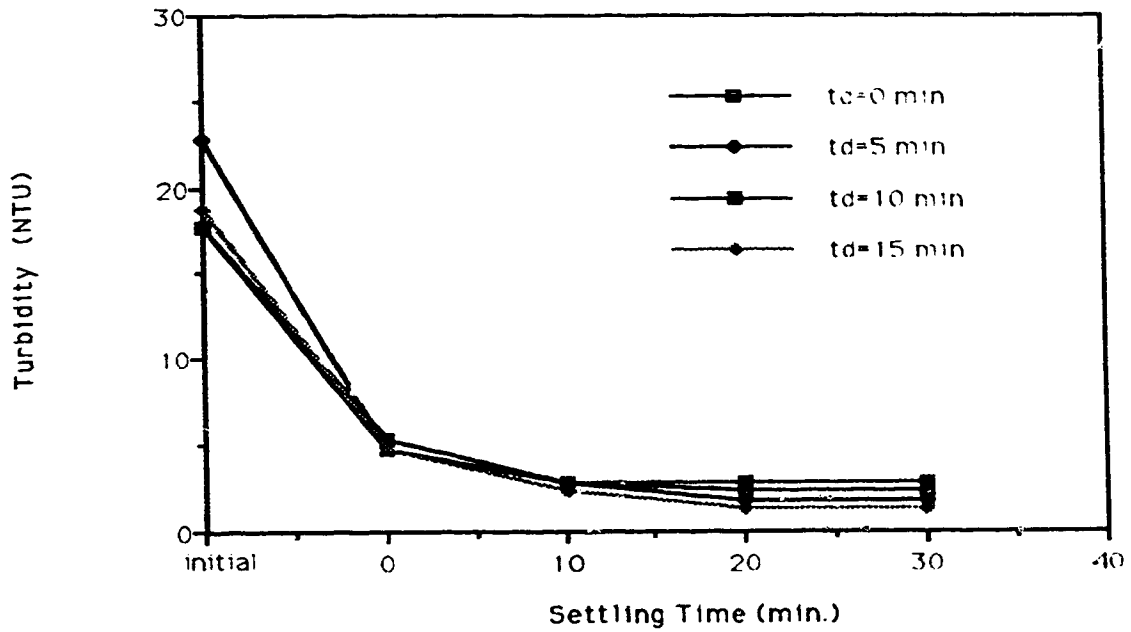


Figure 5.13 Effect of Lag Time on Particle Settling Rate [kaolin=20 mg/L, pH=8, NaHCO<sub>3</sub>=100 mg/L, alum =5 mg/L, polymer=0.5 mg/L,  $\bar{G}_c=122 \text{ s}^{-1}$  (100 rpm) for 1 min., and  $\bar{G}_f=23 \text{ s}^{-1}$  (30 rpm ) for 30 min.]

#### 5.4.4 Reactor Volume

The impact of the reactor volume on flocculation was evaluated in order to scale-up the experiment. Limited experiments were performed only on two-scales:  $V=1\text{L}$  and  $V=2\text{L}$ . The two-scale flocculation experiments were performed at the standard process conditions: kaolin=20 mg/L, alum=5 mg/L, polymer=0.5 mg/L, pH=8, and  $\text{NaHCO}_3=100\text{ mg/L}$ . The rapid mixing was conducted at  $\bar{G}_c=122\text{ s}^{-1}$  for 1 min. The slow mixing was performed in the two volume scales at two slow mixing conditions: 1) same impeller speed (68 rpm), and 2) approximately same  $\bar{G}_f$ -value ( $\bar{G}_f=99$  to  $100\text{ s}^{-1}$ ).

It should be pointed out that the  $\bar{G}_f$ -value at  $V=1\text{L}$  could not be determined from the calibration curve provided in Appendix A as this calibration curve was based on  $V=2\text{L}$ . The  $\bar{G}_f$ -value at  $V=1\text{L}$  was calculated from Equation 3.3. The calculation was based on the assumption that the same pump capacity provides the same impeller speed at different reactor volumes. The validity of the assumption was confirmed in this study. From the above relationship, it can be postulated that the total power dissipated ( $P$ ) was proportional to the impeller speed, but independent of reactor volume ( $V$ ). However, the energy dissipation rate ( $\epsilon$ ) is inversely proportional to reactor volume ( $\epsilon=P/\rho V$ ).

Figure 5.14 shows that the  $d_{\max}$  remains constant at the same impeller speed but different reactor volumes. It is consistent with the prediction made by Stanley (1995). This is because  $d_{\max}$  was determined by shearing force and yield stress, which were determined mainly by the impeller discharge zone (Stanley, 1995). The variation of the reactor volume did not change the shape and size of the impeller discharge zone, as a result  $d_{\max}$  remains constant.

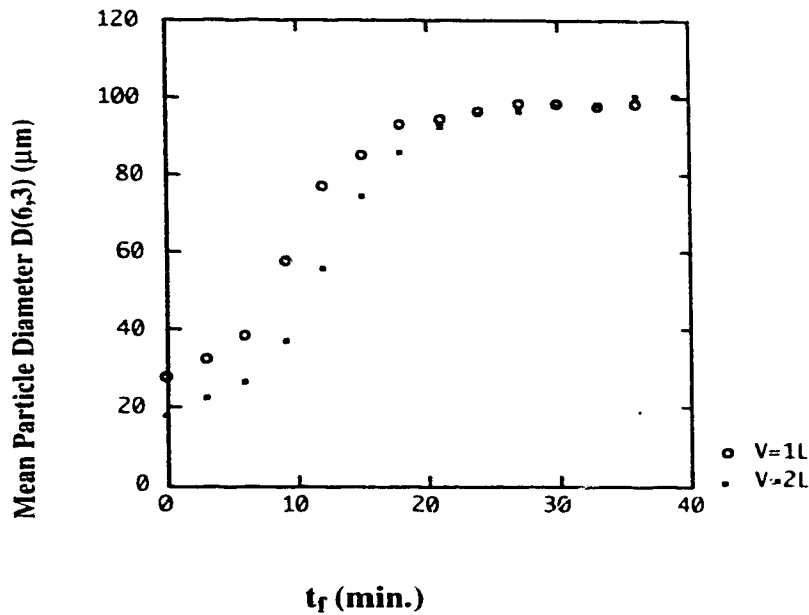


Figure 5.14 Effect of Reactor Volume on the Rate of Polymeric Floc Growth [kaolin=20 mg/L, pH=8,  $\text{NaHCO}_3$ =100 mg/L, alum =5 mg/L, polymer=0.5 mg/L,  $\bar{G}_c=122 \text{ s}^{-1}$  (100 rpm) for 1 min., and  $\bar{G}_f=70 \text{ s}^{-1}$  (68 rpm) for 40 min.]

Figure 5.15 demonstrates that, at a given impeller speed, the smaller the reactor volume, the faster the rate of floc growth. It was explained that the higher energy input providing higher efficiency of collisions in the smaller reactor. The increase of the collision efficiency promoted the floc growth.

Figure 5.16 indicates that the values of maximum mean floc diameter ( $d_{\text{max}}$ ) remained constant at  $\bar{G}_f$ -values tested. Further tests are required over a broad range of  $\bar{G}_f$ -values with different impeller speed and vessel volumes.

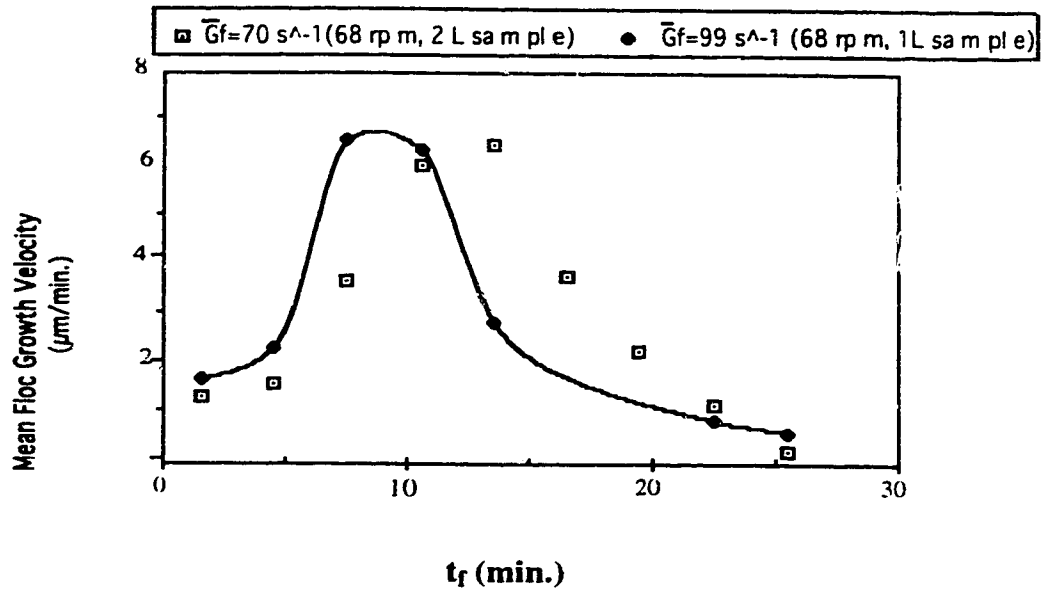


Figure 5.15 Curves of Mean Floc Growth Rates [kaolin=20 mg/L, pH=8,  $\text{NaHCO}_3=100 \text{ mg/L}$ , alum =5 mg/L, polymer=0.5 mg/L,  $\bar{G}_c=122 \text{ s}^{-1}$  for 1 min.]

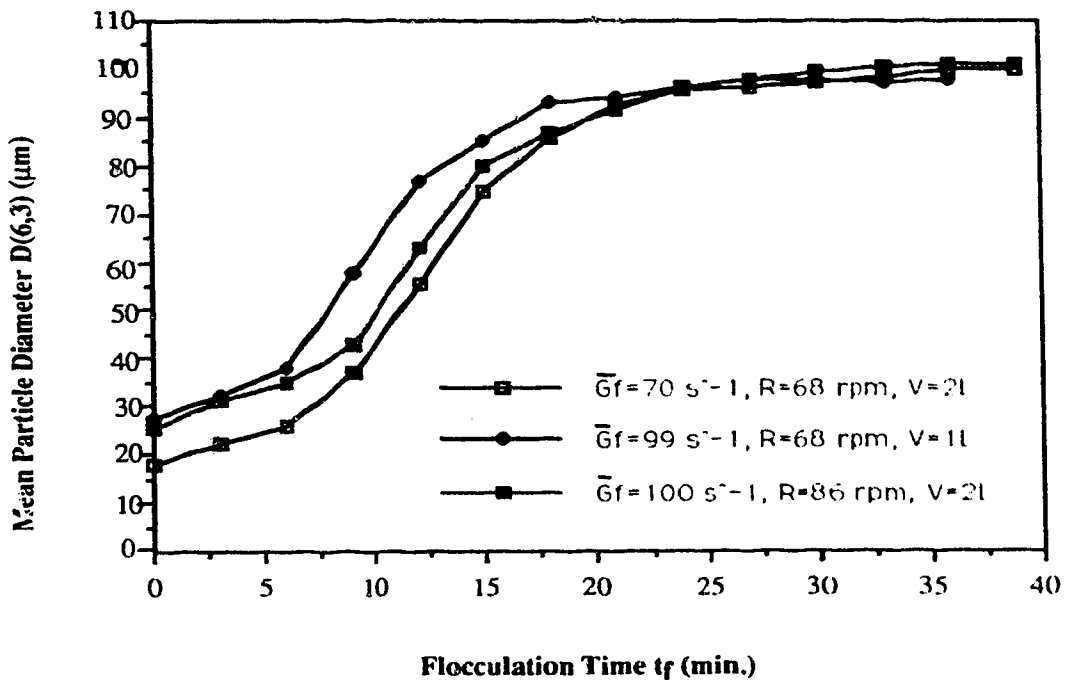


Figure 5.16 Polymeric Floc Growth Curves [kaolin=20 mg/L, pH=8,  $\text{NaHCO}_3=100$  mg/L, alum =5 mg/L, polymer=0.5 mg/L,  $\bar{G}_c=122 \text{ s}^{-1}$  (100 rpm) for 1 min.

## 5.5 Effect of Mixing on the Kinetics of Polymer-Aided Flocculation

The effect of mixing on the kinetics of polymer-aided flocculation was investigated theoretically and experimentally in two aspects: (1) the effect of mixing on the rate of polymer-aided flocculation; and (2) the effect of mixing on the rate of polymeric floc growth. The rate of polymer-aided flocculation was evaluated by a first order rate constant. The rate of the polymeric floc growth was evaluated by a mean floc growth rate ( $\frac{R_{t_2+t_1}}{2}$ ), a floc growth constant ( $\mu$ ), and a floc buildup time ( $t_b$ ). Detailed information will be given in the following sections.

### 5.5.1 Effect of Mixing on the Rate of Polymer-Aided Flocculation

The first order kinetic model was used to fit the data for the particle size distribution obtained from polymer-aided flocculation. The first order rate constant ( $K$ ) was used to evaluate the rate of flocculation. The correlation between  $K$  and  $\bar{G}_f$  was described by two mathematical models, and the accuracy of the models was compared to determine the best one to predict the impact of mixing on the rate of polymer-aided flocculation.

#### 5.5.1.1 Model Simulation and Residual Examination

The survey of literature indicated that there was no mathematical model that had been utilized directly in polymer-aided flocculation of kaolin suspensions. The first order kinetic model with respect to the primary particle concentration was proposed in this study. It had a mathematical expression:

$$\frac{dn}{dt} = -Kn \quad (5.26)$$

where  $K$  was the first order rate constant, and  $n$  was the primary particle concentration ( $d \leq 10 \mu\text{m}$ ). The integral of the model being:

$$\ln(n) = -Kt + C \quad (5.27)$$

The above first order kinetic model was proposed based on the following assumptions: (1) mixing was isotropic in the reactor, the average vessel parameter  $\bar{G}_f$  was the rate controlling factor; (2) orthokinetic flocculation dominated the mechanism of transport; (3) collisions occurred between the particles with the size range from 1 to 10  $\mu\text{m}$ ; (4) the instantaneous concentration of the primary particles was equal to the cumulative particle concentration with the size range of  $d \leq 10 \mu\text{m}$  at that moment; and (5) the breakup of the floc was negligible at  $\bar{G}_f \leq 400 \text{ s}^{-1}$  and  $t_f \leq 30 \text{ min}$ .

Based on the above assumptions, a model simulation was performed. An example of the model simulation processes was presented in Table 5.3.

The In-normal plots of particle size distributions were presented in Figures 5.17 to 5.20 in order to confirm the validity of assumption (5), and demonstrate that the rate of flocculation followed the first order kinetic model only at  $\bar{G}_f \leq 400 \text{ s}^{-1}$  and  $t_f \leq 30 \text{ min}$ . Outside this range, deviations of the data from the kinetic curves occurred. This was contributed by instrument over-concentration in the particle size analyzer at lower  $t_f$ , or by floc breakup and the dispersion of the size of the particles collided at higher  $t_f$ , which violated assumption (3).



Table 5.3 Model Simulation Process ( $\bar{G}_f = 80 \text{ s}^{-1}$ )

Model :  $\text{Ln}(n) = K * t_f + C$  (K and C are constants)

ITERATION	LOSS	PARAMETER VALUES	
0	0.9073510D+03	0.1000D+00	0.1000D+00
1	0.7752393D+03	0.5412D+00	0.1272D+00
2	0.2226684D+03	0.9345D-01	0.1145D+02
3	0.7842140D-01	-.7378D-01	0.1122D+02
4	0.6111543D-01	-.7251D-01	0.1123D+02
5	0.6111543D-01	-.7251D-01	0.1123D+02
6	0.6111543D-01	-.7251D-01	0.1123D+02

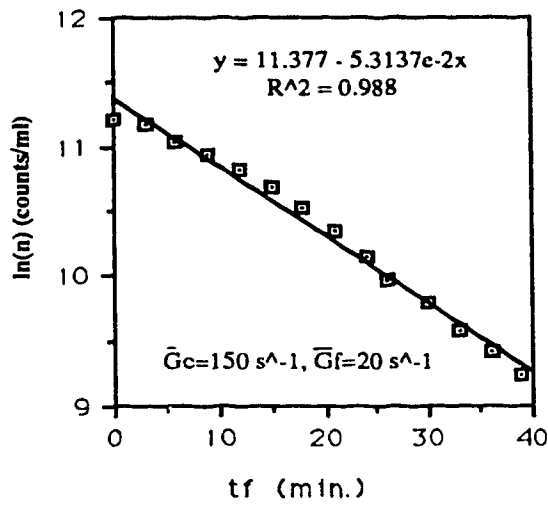
DEPENDENT VARIABLE IS  $\text{Ln}(n)$

SOURCE	SUM-OF-SQUARES	DF	MEAN-SQUARE
REGRESSION	1360.747	2	680.373
RESIDUAL	0.061	12	0.005
TOTAL	1360.808	14	
CORRECTED	10.751	13	

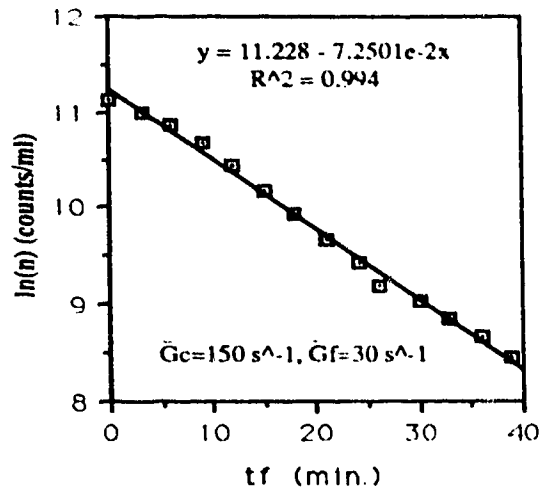
RAW R-SQUARED (1-RESIDUAL/TOTAL) = 1.000  
 CORRECTED R-SQUARED (1-RESIDUAL/CORRECTED) = 0.994

PARAMETER	ESTIMATE
K	-0.073
C	11.229

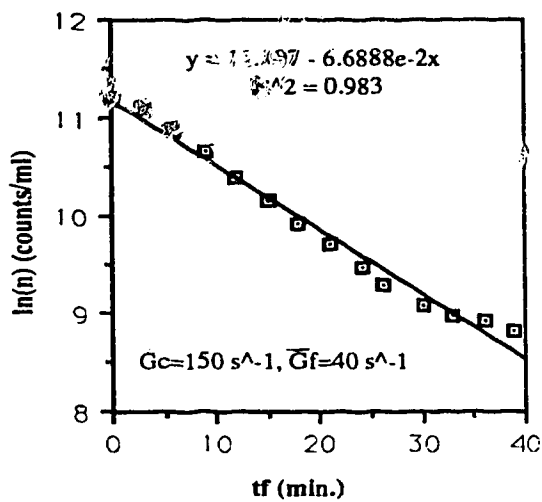
$$\text{Ln}(n) = -0.073 t_f + 11.229$$



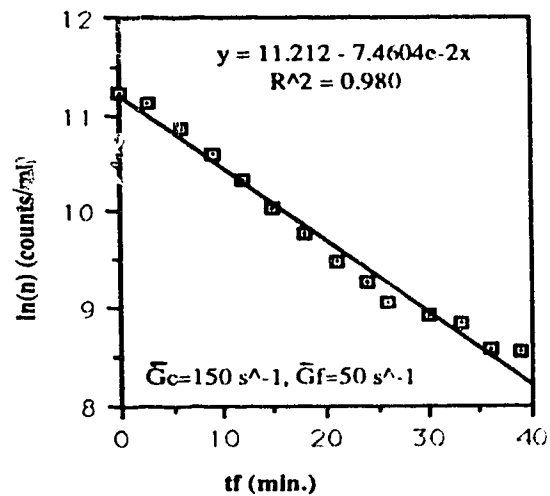
(a)



(b)

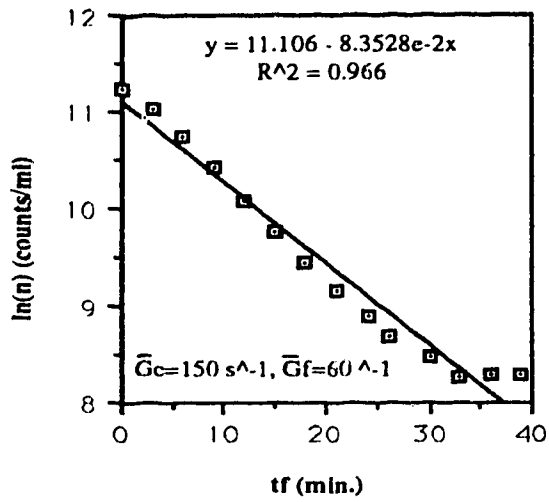


(c)

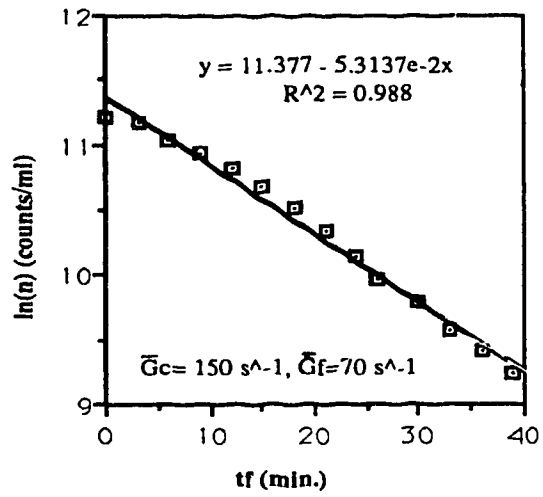


(d)

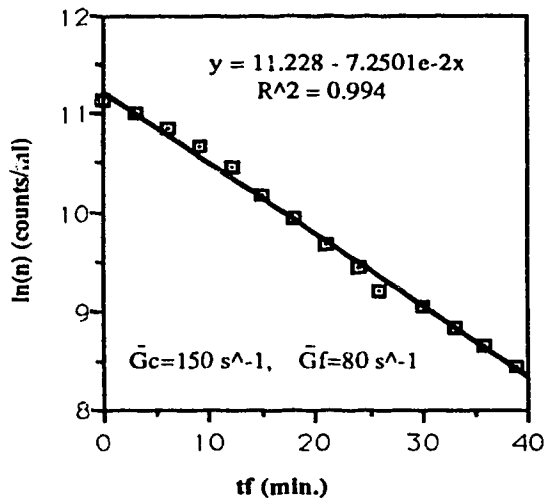
Figure 5.17 Kinetic Curves of Polymer-Aided Flocculation ( $20 \leq \bar{G}_f \leq 50 \text{ s}^{-1}$ )  
 (kaolin=20 mg/L, pH=8,  $\text{NaHCO}_3$ =100 mg/L, alum=5mg/L, polymer=0.5 mg/L)



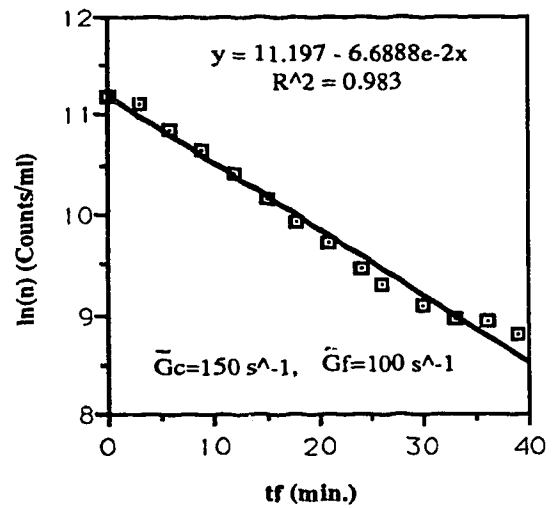
(a)



(b)

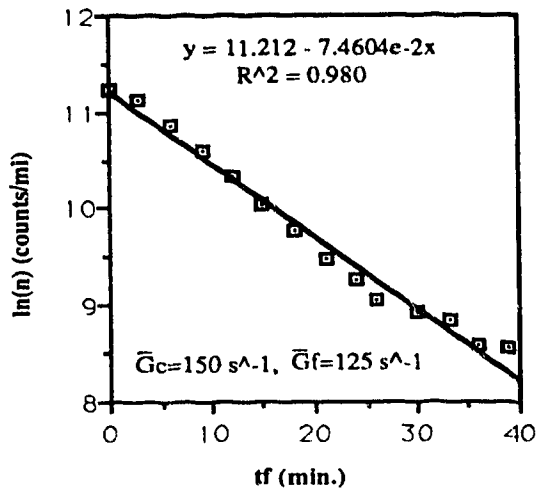


(c)

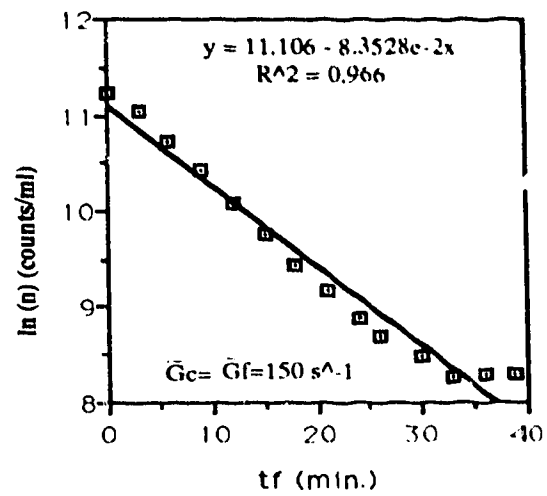


(d)

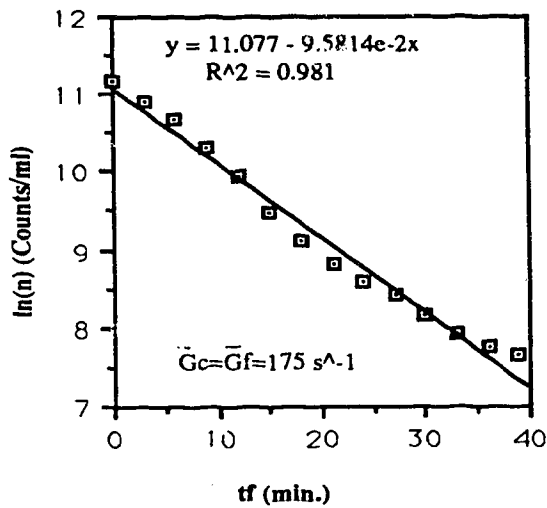
Figure 5.18 Kinetic Curves of Polymer-Aided Flocculation ( $60 \leq \bar{G}_f \leq 100 \text{ s}^{-1}$ )  
 (kaolin=20 mg/L, pH=8,  $\text{NaHCO}_3$ =100 mg/L, alum=5mg/L, polymer=0.5 mg/L)



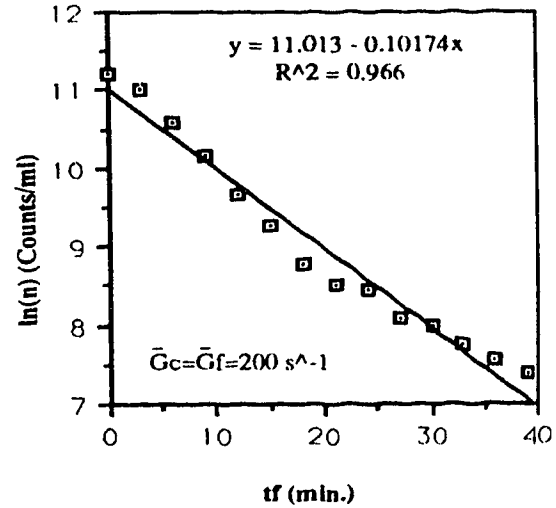
(a)



(b)

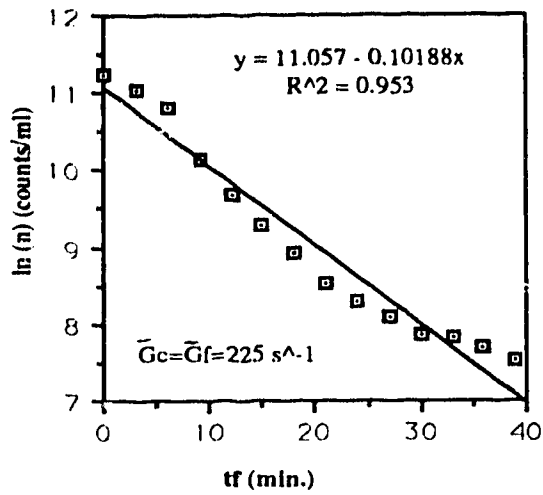


(c)

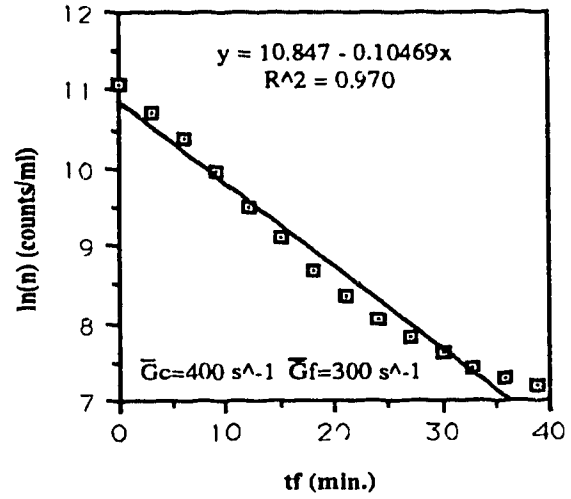


(d)

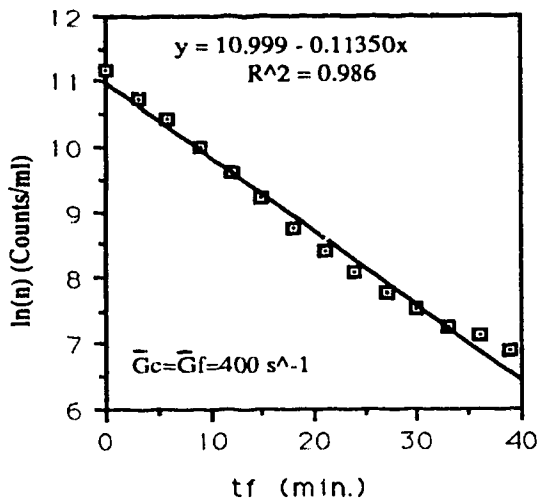
Figure 5.19 Kinetic Curves of Polymer-Aided Flocculation ( $125 \leq \bar{G}_f \leq 200 \text{ s}^{-1}$ )  
 (kaolin=20 mg/L, pH=8,  $\text{NaHCO}_3$ =100 mg/L, alum=5mg/L, polymer=0.5 mg/L)



(a)



(b)



(c)

Figure 5.20 Kinetic Curves of Polymer-Aided Flocculation ( $225 \leq \bar{G}_f \leq 400 \text{ s}^{-1}$ )  
 (kaolin = 20 mg/L, pH=8,  $\text{NaHCO}_3 = 100 \text{ mg/L}$ , alum = 5mg/L, polymer = 0.5 mg/L)

The reliability of the model was tested by examining model residuals. The residuals were checked at each  $\overline{G}_f$  from 20 to 400 s<sup>-1</sup>. Four ways were used to check the model residuals: 1) the residual were plotted against fitted value (Figure 5.21); 2) the residuals were plotted against the independent parameter (Figure 5.22) ; 3) normal plot of the residuals (Figure 5.23); and 4) histogram plot of the residuals (Figure 5.24). A valid model led to the residuals being independent and having a normal distribution with a zero mean.

Figures 5.23 and 5.24 demonstrated that the residuals had a zero mean. Figures 5.21 to 5.22 showed that the residuals were in the horizontal bands, with some pattern with the parameter it was plotted against. The independence of the residuals was further examined by checking the serial correlation in the residuals. Table 5.4 showed that the mean of series was zero, and all the points were inside the parentheses; thus the residuals were not significant. The apparent pattern in the residuals might be the result of the small number of residuals used. Therefore, the assumptions of the model errors, which was the model residual being independent, and with a zero mean, did not appear to be violated, and there was no reason to say that the model was incorrect. As a result, the first order kinetic model was considered to be adequate to use for the description of the rate of polymer-aided flocculation.

The accuracy of the model was confirmed by comparing the experimental results with the values predicted by the model. Figure 5.25 exhibited that the experimental results closely follow the theoretical predictions. This quantitative consistency indicated that the model was accurate.

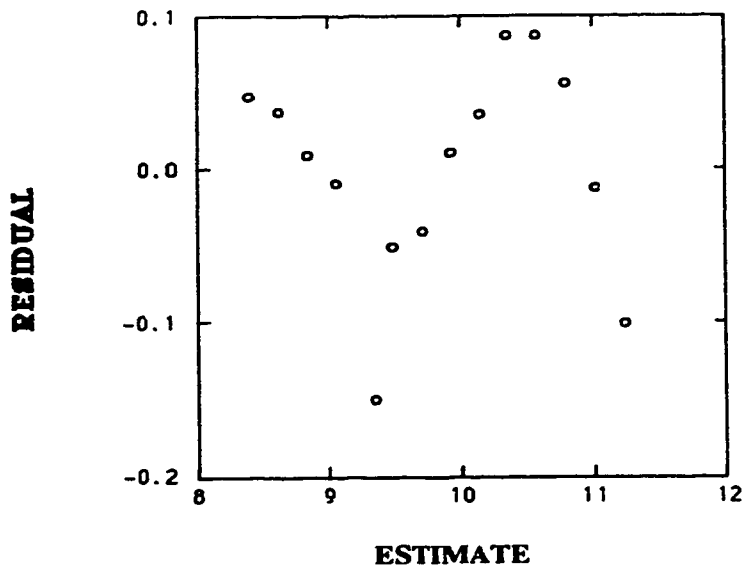


Figure 5.21 The Residuals Plotted against Fitted Value [ Ln(n)]

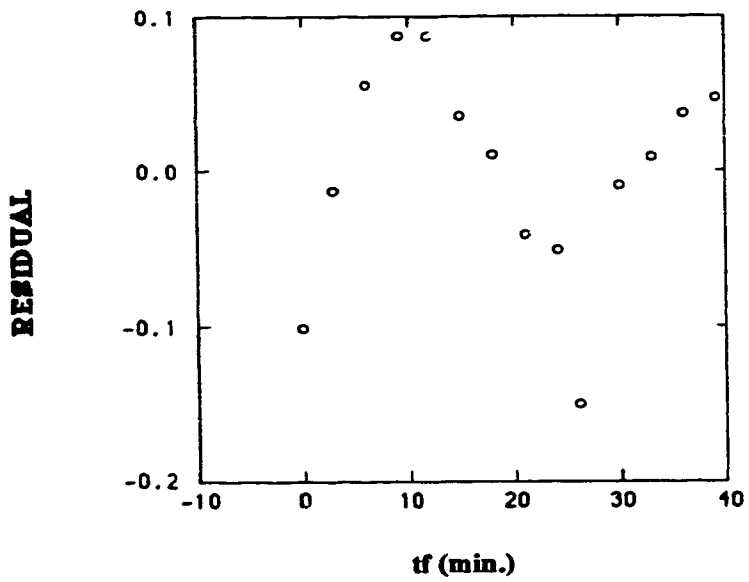


Figure 5.22 The Residuals Plotted against the Independent Parameter

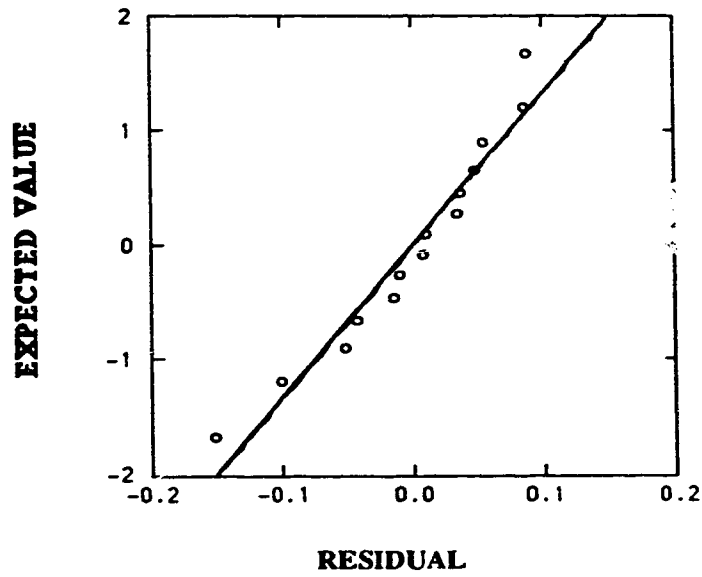


Figure 5.23 Normal Plot of the Residuals

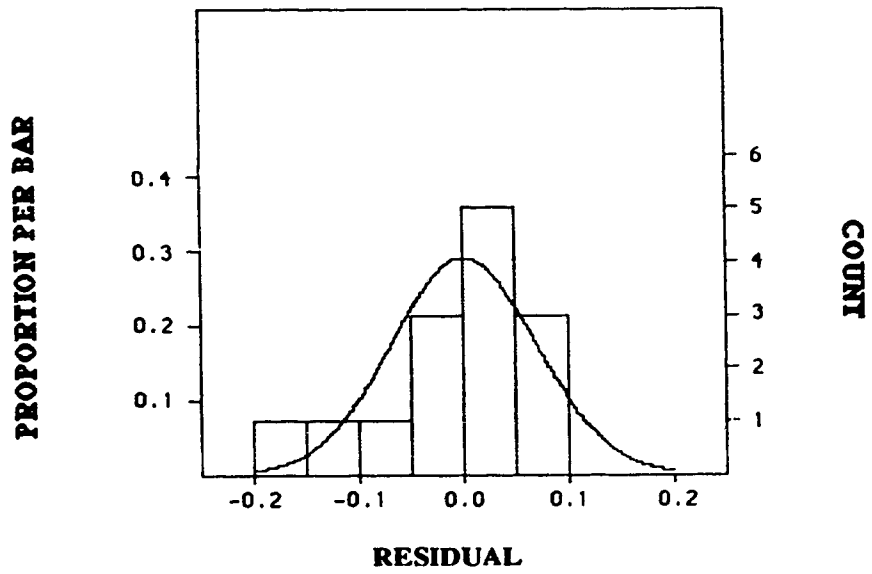


Figure 5.24 Histogram Plot of the Residuals



**Table 5.4 The Examination of Serial Correlation in Residuals**

**PLOT OF RESIDUAL**

**NUMBER OF CASES = 14**

**MEAN OF SERIES = 0.000**

**STANDARD DEVIATION OF SERIES = 0.066**

**PLOT OF AUTOCORRELATIONS**

LAG	CORR	SE	-1.0	-.8	-.6	-.4	-.2	.0	.2	.4	.6	.8	1.0
			--- --- --- --- --- --- --- --- --- ---										
1	0.483	0.267								.....			
2	0.091	0.324								..			
3	-0.332	0.325								.....			
4	-0.523	0.349								.....			
5	-0.458	0.401								.....			
6	-0.303	0.437								.....			
7	-0.027	0.452											
8	0.203	0.452								.....			
9	0.383	0.458								.....			
10	0.116	0.480								..			
11	0.019	0.482											
12	-0.072	0.483											
13	-0.079	0.483											
14	0.000	0.484											

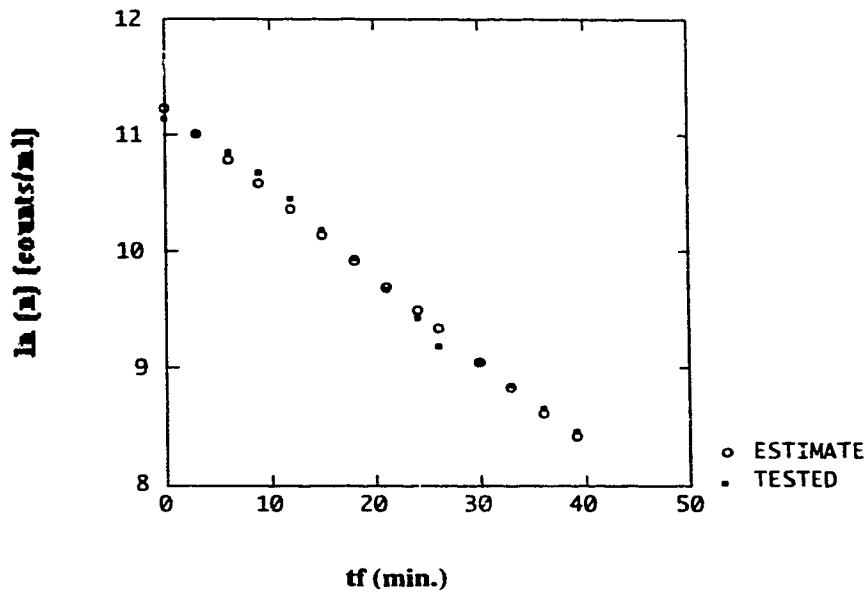


Figure 5.25 The Model Simulation Diagram ( $\bar{G}_f = 80 \text{ s}^{-1}$ )

Therefore, the rate of polymer-aided flocculation was of the first order kinetics with respect to the primary particle concentration. The conclusion was consistent with the simplified linear equation given by Argaman and Kaufman (1968) to describe the removal of primary particles from kaolin suspension upon flocculation with alum (Argaman and Kaufman, 1966 & 1970, Weber, 1972). The significances of this were; 1) it demonstrated the similarity of the kinetic mechanism of alum flocculation and polymer-aided flocculation; 2) it provided a method to evaluate the rate of polymer-aided flocculation through the first order rate constant determined from model parameters; and 3) it allowed the rate of flocculation to be compared in different situations.

It should be emphasized that the model simulation and residual examination were conducted for data generated from different mixing conditions ( $20 < \bar{G}_f < 400 \text{ s}^{-1}$ ) in order to further confirm the credibility of the model. The results were presented in Table

5.5. Table 5.5 demonstrated that the rate of polymer-aided flocculation followed the first order kinetic model at  $20 < \bar{G}_f < 400 \text{ s}^{-1}$ .

**Table 5.5 Effect of Mixing on the First Order Kinetic Constant (K)**

Parameter	$\bar{G}_f=20 \text{ s}^{-1}$	$\bar{G}_f=30 \text{ s}^{-1}$	$\bar{G}_f=40 \text{ s}^{-1}$	$\bar{G}_f=50 \text{ s}^{-1}$	$\bar{G}_f=60 \text{ s}^{-1}$
K[counts/(ml*min.)]	0.018	0.020	0.049	0.052	0.058
C(count/ml)	11.200	11.192	11.360	11.305	11.262
R <sup>2</sup>	1.000	1.000	1.000	1.000	1.000
R <sub>corr</sub> <sup>2</sup>	0.992	0.947	0.985	0.982	0.995
Residual Check	OK	OK	OK	OK	OK
Parameter	$\bar{G}_f=70 \text{ s}^{-1}$	$\bar{G}_f=80 \text{ s}^{-1}$	$\bar{G}_f=100 \text{ s}^{-1}$	$\bar{G}_f=125 \text{ s}^{-1}$	$\bar{G}_f=150 \text{ s}^{-1}$
K[counts/(ml*min.)]	0.054	0.072	0.067	0.074	0.083
C(count/ml)	11.385	11.230	11.199	11.214	11.108
R <sup>2</sup>	1.000	1.000	1.000	1.000	1.000
R <sub>corr</sub> <sup>2</sup>	0.994	0.996	0.985	0.982	0.969
Residual Check	OK	OK	OK	OK	OK
Parameter	$\bar{G}_f=175 \text{ s}^{-1}$	$\bar{G}_f=200 \text{ s}^{-1}$	$\bar{G}_f=225 \text{ s}^{-1}$	$\bar{G}_f=300 \text{ s}^{-1}$	$\bar{G}_f=400 \text{ s}^{-1}$
K[counts/(ml*min.)]	0.096	0.102	0.102	0.105	0.113
C(count/ml)	11.017	11.013	11.057	10.847	10.999
R <sup>2</sup>	1.000	0.999	0.999	0.990	1.000
R <sub>corr</sub> <sup>2</sup>	0.981	0.966	0.953	0.970	0.986
Residual Check	OK	OK	OK	OK	OK

### 5.5.1.2 Effect of Mixing on the First Order Rate Constant

As given in Equation 5.26, the first order rate constant (K) was used to evaluate the rate of polymer-aided flocculation, and could be determined from the slope of the kinetic curves (Figure 5.20). The results shown in Table 5.5 indicated that K was

affected by  $\bar{G}_f$ , and Figure 5.26 further showed that K was strongly dependent on  $\bar{G}_f$  at  $0 < \bar{G}_f \leq 200 \text{ s}^{-1}$ , but to a lesser extent at a higher  $\bar{G}_f$  ( $\bar{G}_f > 200 \text{ s}^{-1}$ ).

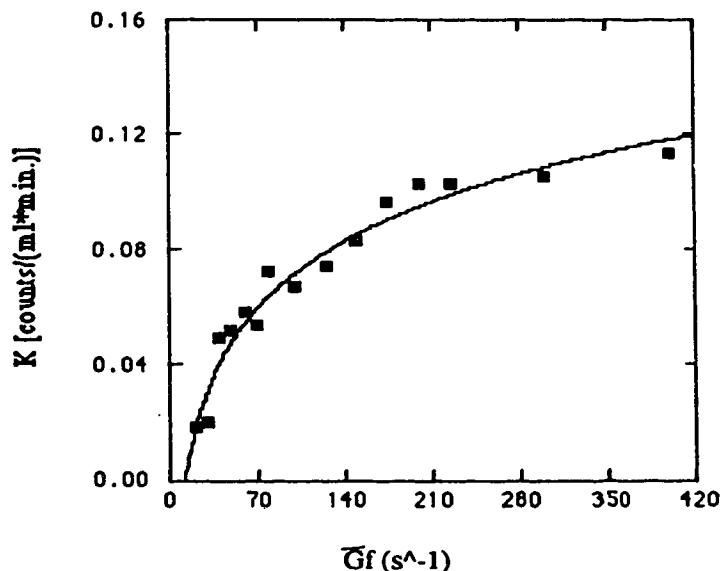


Figure 5.26 Effect of Mixing on the First Order Kinetic Constant ( $\bar{G}_c = 150 \text{ s}^{-1}$ ,  $\bar{G}_f \leq 150 \text{ s}^{-1}$ ;  $\bar{G}_c = \bar{G}_f$ ,  $\bar{G}_f > 150 \text{ s}^{-1}$ )

Two mathematical models presented in Equations 5.28 and 5.29 were tested in an attempt to describe the relationship between K and  $\bar{G}_f$  at  $20 \leq \bar{G}_f \leq 400 \text{ s}^{-1}$ . The model simulation and residual examination processes were presented in Appendix C which demonstrated that the above two models predicted the impact of  $\bar{G}_f$  on K with the same precision.

$$K = 7.967 (\bar{G}_f)^{0.004} - 8.048 \text{ [counts/(ml}\cdot\text{min.)]} \quad 20 \leq \bar{G}_f \leq 400 \text{ s}^{-1} \quad (5.28)$$

$$K = 0.033 \text{ Ln}(\bar{G}_f) - 0.082 \text{ [counts/(ml}\cdot\text{min.)]} \quad 20 \leq \bar{G}_f \leq 400 \text{ s}^{-1} \quad (5.29)$$

Therefore, both models could be used to predict the impact of mixing on the rate of polymer-aided flocculation.

From Figure 5.26 it was seen that  $\bar{G}_f$  had a significant impact on K at  $20 \leq \bar{G}_f \leq 200 \text{ s}^{-1}$ , which was approximated by the linear model shown in the following equation:

$$K = 0.00041 \bar{G}_f + 0.024 \quad 20 \leq \bar{G}_f \leq 200 \text{ s}^{-1} \quad (5.30)$$

and plotted in Figure 5.27. By comparing Equation 5.30 with Equation 5.31 being:

$$K = K_A \bar{G}_f \quad (5.31)$$

which was proposed based on alum flocculation (Argaman & Kaufman 1968; Amirtharajah & O'Melia 1990), it was found that both models were linear. They both showed that K was directly proportional to  $\bar{G}_f$ , where the ratio constant  $K_A$  was called the overall flocculation constant. This was explained by the fact that a high  $\bar{G}_f$  increased particle - particle contacts. The comparison also led to the conclusion that the polymer-aided flocculation and alum flocculation followed the same kinetic mechanism, and the role of the polymer in the flocculation was to bridge the fine flocs resulting in bigger and denser flocs which hastened the rate of sedimentation.

In conclusion, the kinetics of polymer-aided flocculation was accurately described by a first order kinetic model with respect to the primary particle concentration ( $d \leq 10 \mu\text{m}$ ) at  $0 < \bar{G}_f \leq 400 \text{ s}^{-1}$  and  $0 \leq t_f \leq 30 \text{ min}$ .

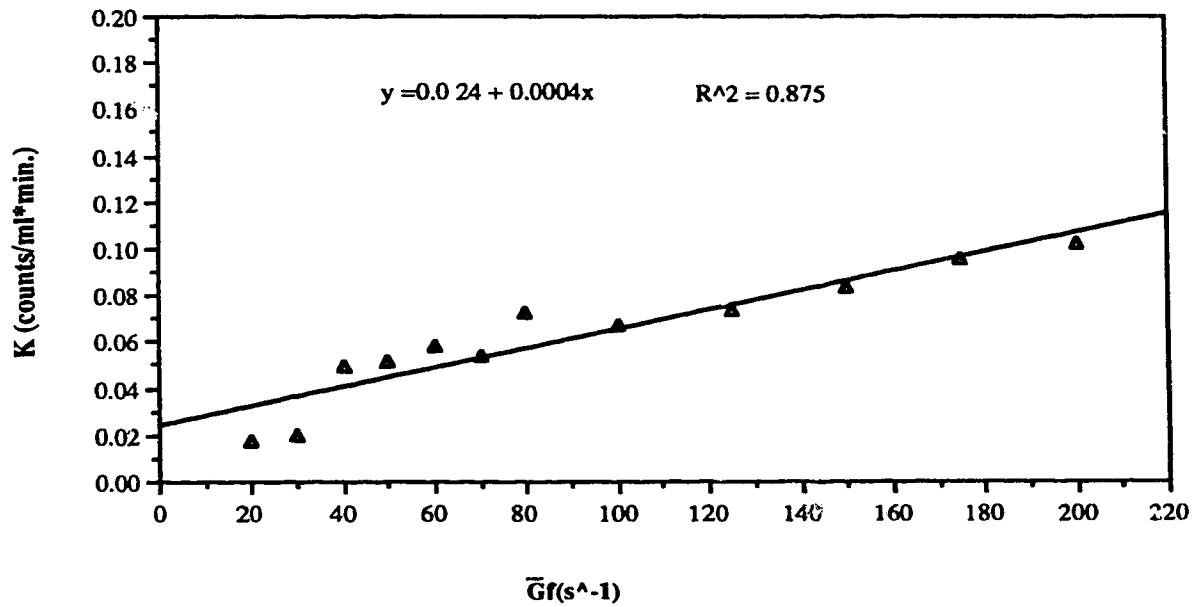


Figure 5.27 Linear Regression of the First Order Rate Constants ( $20 \leq \bar{G}_f \leq 200 \text{ s}^{-1}$ )  
 (kaolin=20 mg/L, pH=8,  $\text{NaHCO}_3$ =100 mg/L, alum=5mg/L,  
 polymer=0.5 mg/L)

## 5.5.2 Effect of Mixing on the Rate of Polymeric Floc Growth

The rate of polymeric floc growth was evaluated by three methods: 1) the mean floc growth rate ( $\bar{R}_{\frac{t_2+t_1}{2}}$ ) for the specific flocculation time; 2) the floc growth constant ( $\mu$ ) for each stage of the floc growth process; and 3) the floc buildup time ( $t_b$ ) for the overall flocculation process. These kinetic parameters were determined from floc growth curves plotted on the basis of mean particle diameter  $D(6,3)$ .

### 5.5.2.1 Mechanism of Polymeric Floc Growth

The floc growth curves in the  $\bar{G}_f$  range from 20 to 1600  $s^{-1}$  were plotted on a normal-scale and a semi-logarithmic scale.

Normal-scale plots (Figures 5.28 to 5.32) showed that similar sigmoid-shape curves were obtained at  $20 \leq \bar{G}_f \leq 800 s^{-1}$  with the exception of different values of  $d_{max}$  and  $t_b$ . It also demonstrated that the size of the floc grew during the course of the flocculation until the ultimate size ( $d_{max}$ ) was reached, and it remained constant for a given time before the size fluctuation occurred. However, Figure 5.33 showed that the curves fluctuated up and down at  $\bar{G}_f > 800 s^{-1}$  due to the breakup and regrowth of the floc.

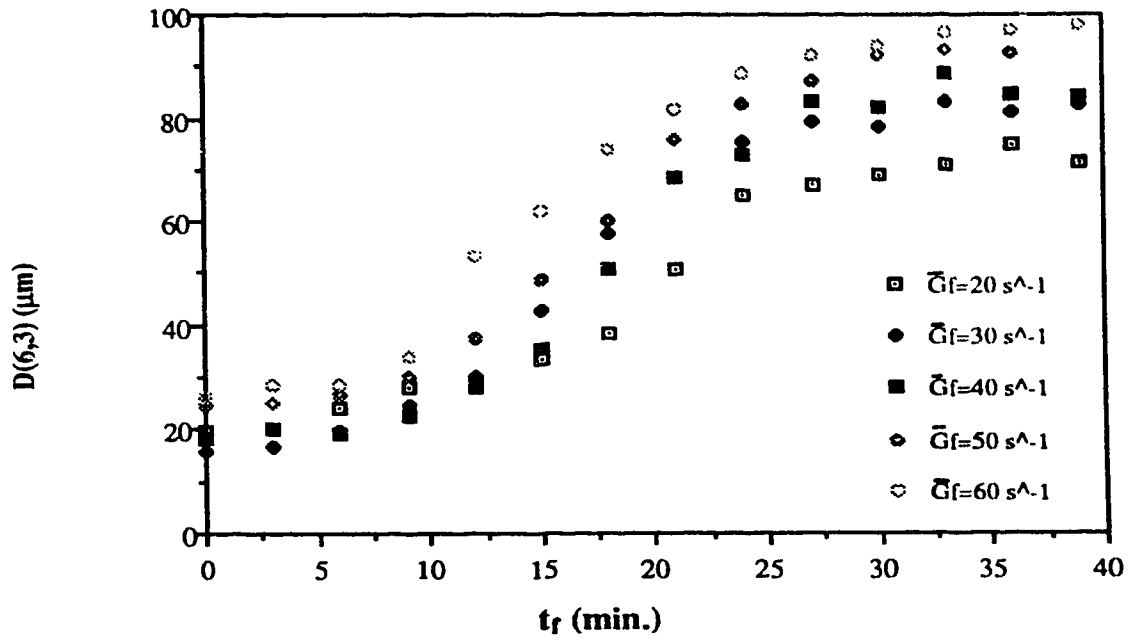


Figure 5.28 Polymeric Floc Growth Curves at  $20 \leq \bar{G}_f \leq 60 \text{ s}^{-1}$  (kaolin=20 mg/L, pH=8,  $\text{NaHCO}_3$ =100 mg/L, alum=5 mg/L, polymer=0.5 mg/L,  $\bar{G}_c=150 \text{ s}^{-1}$  for 1 min.)



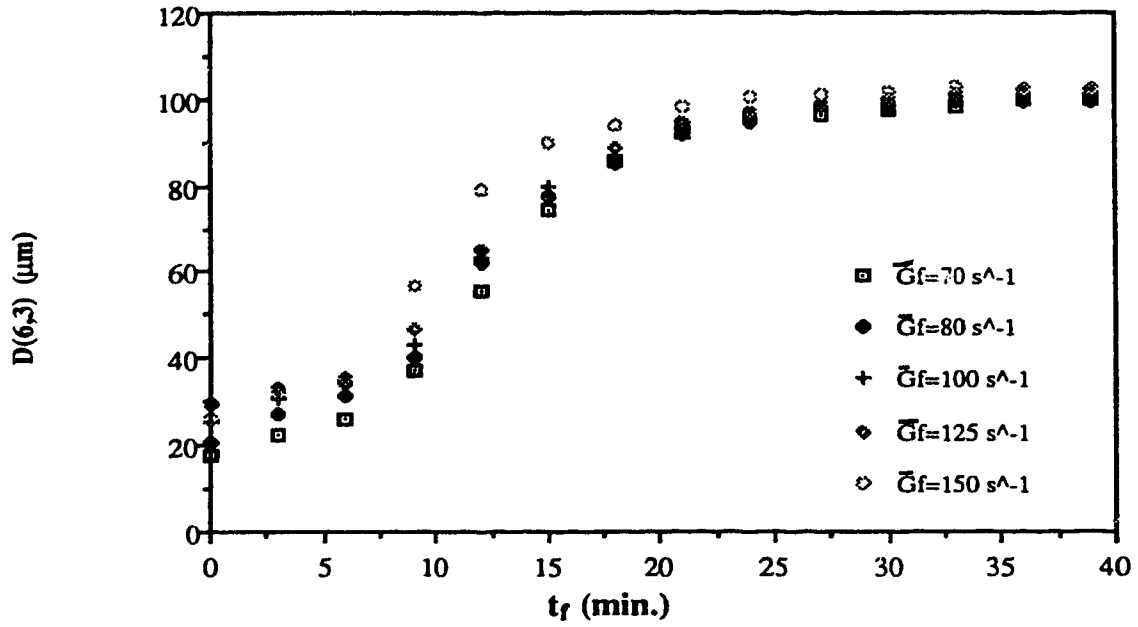


Figure 5.29 Polymeric Floc Growth Curves at  $70 \leq \bar{G}_f \leq 150 \text{ s}^{-1}$  (kaolin=20 mg/L, pH=8,  $\text{NaHCO}_3$ =100 mg/L, alum=5 mg/L, polymer=0.5 mg/L,  $\bar{G}_c = 150 \text{ s}^{-1}$  for 1 min.)

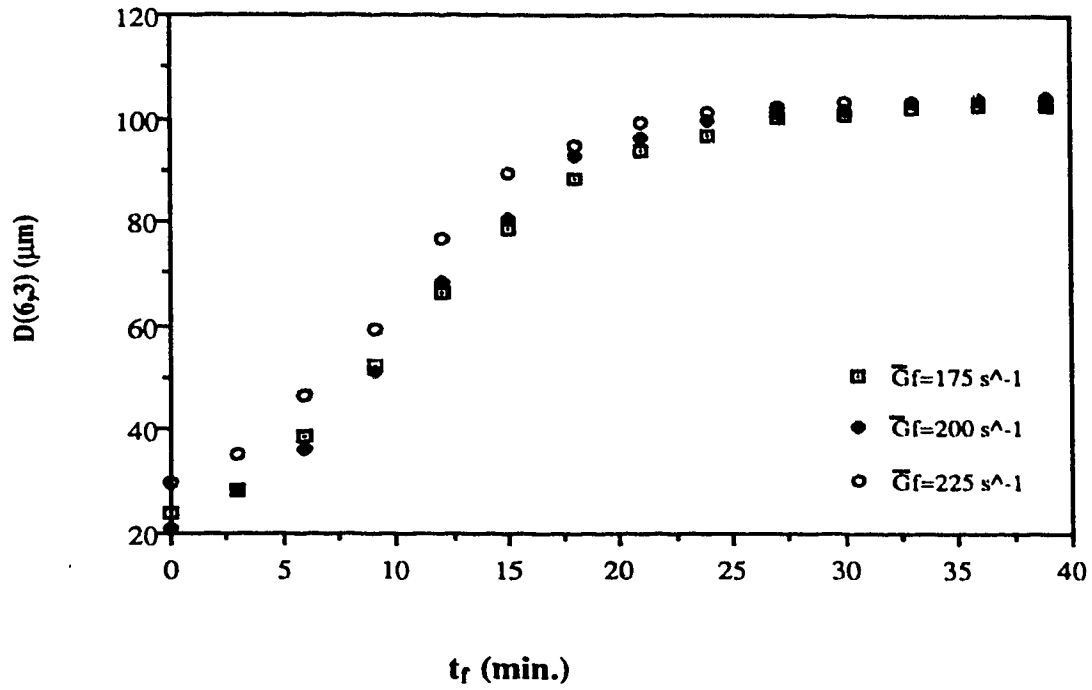


Figure 5.30 Polymeric Floc Growth Curves at  $175 \leq \bar{G}_c = \bar{G}_f \leq 225 \text{ s}^{-1}$   
 (kaolin=20 mg/L, pH=8,  $\text{NaHCO}_3$ =100 mg/L, alum=5 mg/L,  
 polymer=0.5 mg/L)

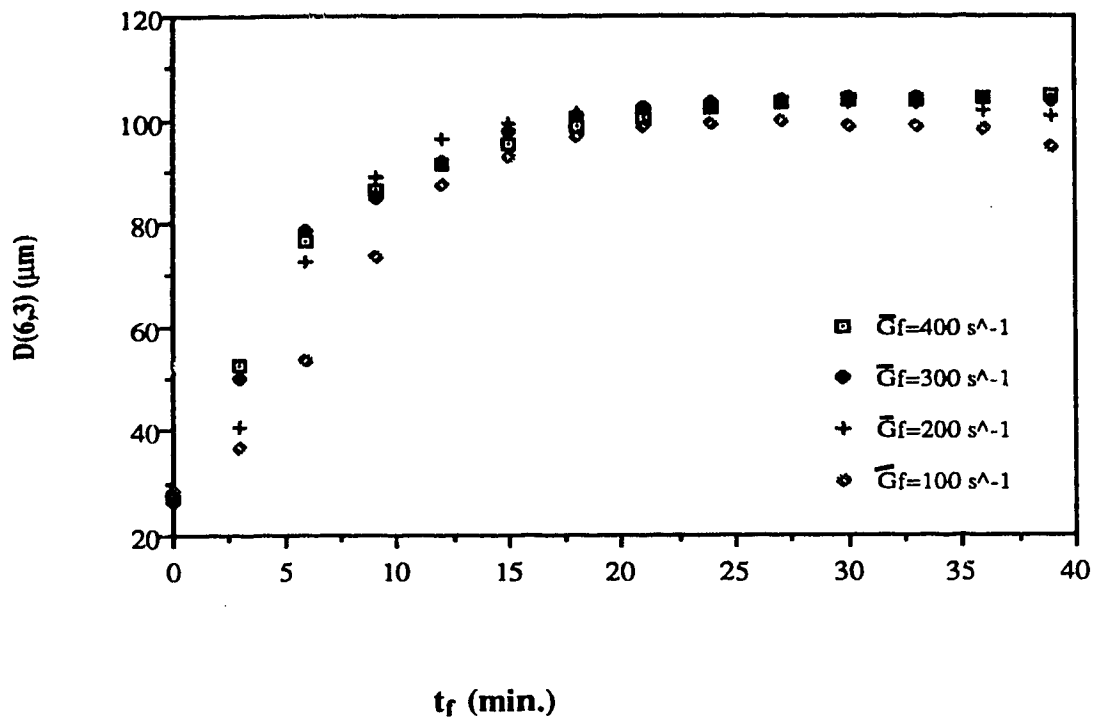


Figure 5.31 Polymeric Floc Growth Curves at  $100 \leq \bar{G}_f \leq 400 \text{ s}^{-1}$  (kaolin=20 mg/L, pH=8,  $\text{NaHCO}_3$ =100 mg/L, alum=5 mg/L, polymer=0.5 mg/L,  $\bar{G}_c$ =400  $\text{s}^{-1}$  for 1 min.)

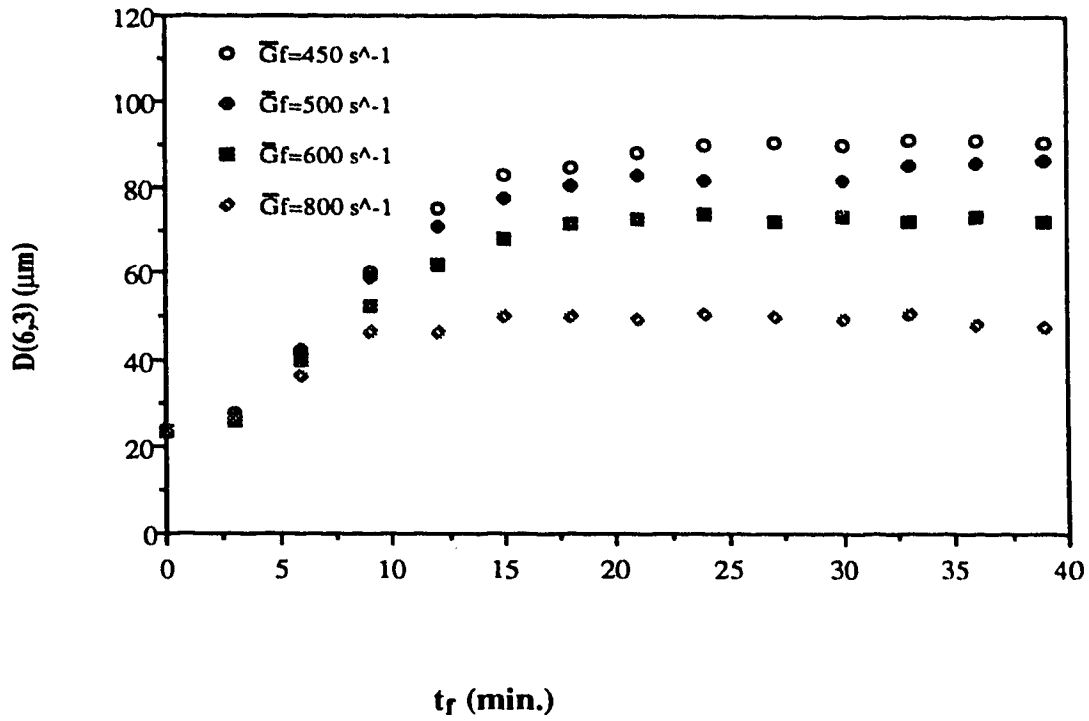
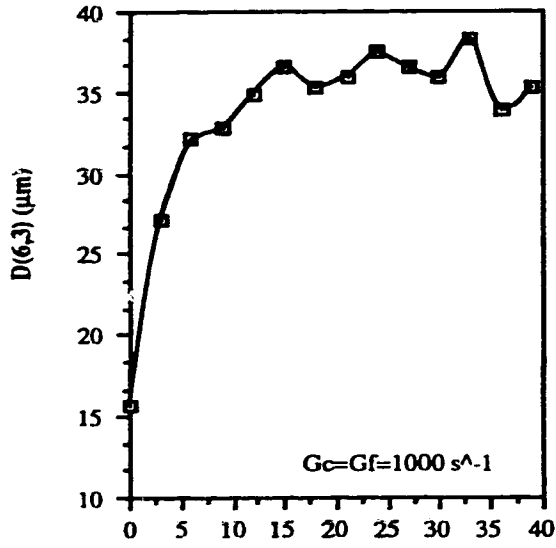
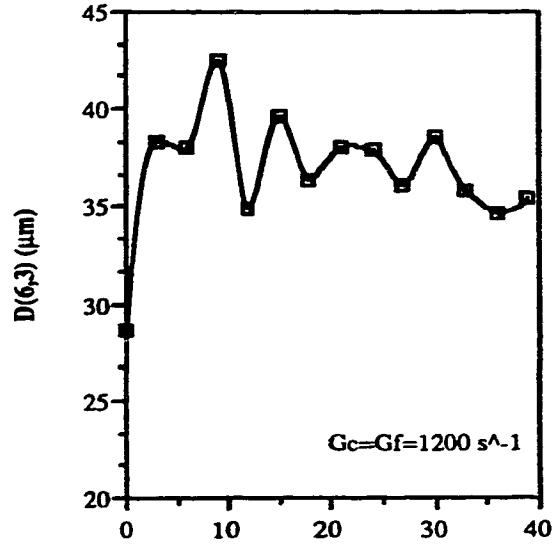


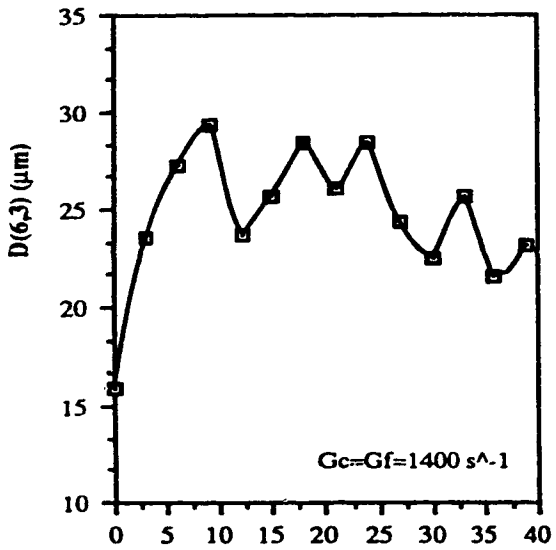
Figure 5.32 Polymeric Floc Growth Curves at  $450 \leq \bar{G}_c = \bar{G}_f \leq 800 \text{ s}^{-1}$  (kaolin=20 mg/L, pH=8,  $\text{NaHCO}_3$ =100 mg/L, alum=5 mg/L, polymer=0.5 mg/L)



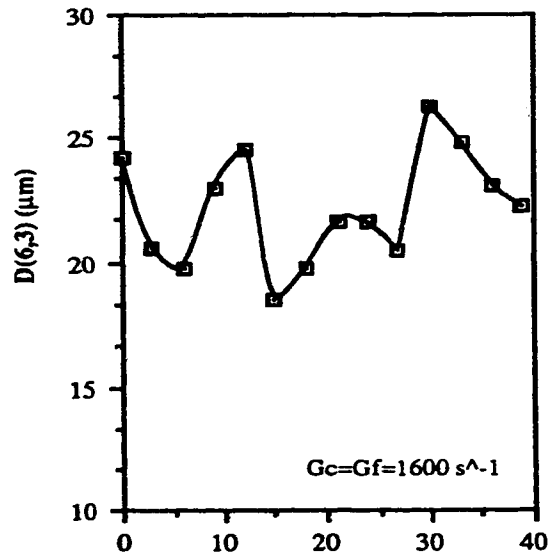
tf (min)  
(a)



tf (min)  
(b)



tf (min)  
(c)

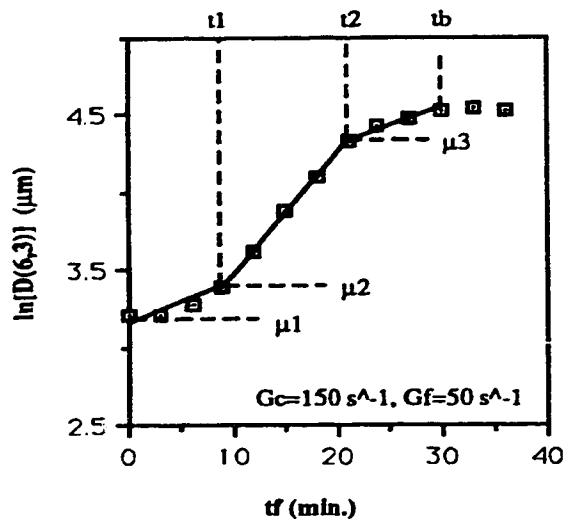


tf (min)  
(d)

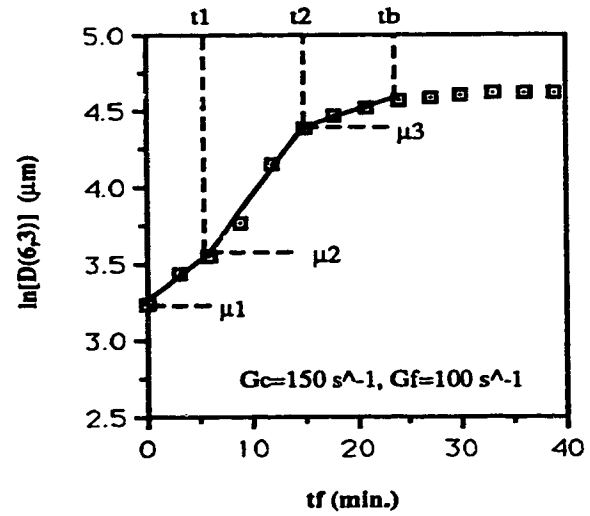
Figure 5.33 Polymeric Floc Growth Curves at  $1000 \leq \bar{G}_c = \bar{G}_f \leq 1600 \text{ s}^{-1}$   
(kaolin=20 mg/L, pH=8,  $\text{NaHCO}_3$ =100 mg/L, alum=5 mg/L,  
polymer=0.5 mg/L)

Semi-log plots were represented in Figure 5.34 and Appendix B. The figures showed that the curves could be divided into several stages, and a simple straight line relationship existed in each stage on a log - normal plot. It indicated that the polymeric floc growth followed a log-normal relationship.

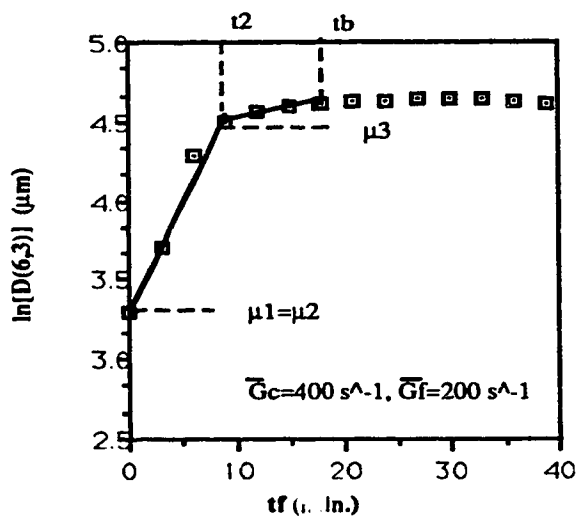
The deflections in the curve were used to divide the overall curve into a number of stages. Figure 5.35 demonstrated that the number and the location of the stages were dependent on the  $\bar{G}_f$ -value. The variations in the number of stages were shown in Figure 5.34 plus figures presented in Appendix B. The figures showed that four stages were observed in the overall polymeric floc growth curves at  $20 \leq \bar{G}_f < 175 \text{ s}^{-1}$ , three stages at  $175 \leq \bar{G}_f < 600 \text{ s}^{-1}$ , and two stages at  $\bar{G}_f > 600 \text{ s}^{-1}$ . This was because the first two stages appeared to merge at  $175 \leq \bar{G}_f < 600 \text{ s}^{-1}$ , and the first three stages seemed to amalgamate at  $\bar{G}_f > 600 \text{ s}^{-1}$ .



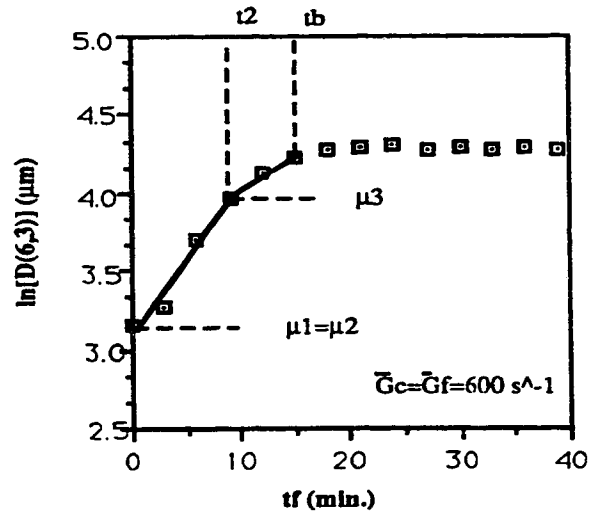
(a)



(b)



(c)



(d)

Figure 5.34 Polymeric Floc Growth Curves on Semi-logarithmic Scale (kaolin=20 mg/L, pH=8,  $\text{NaHCO}_3=100 \text{ mg/L}$ , alum=5 mg/L, polymer=0.5 mg/L)

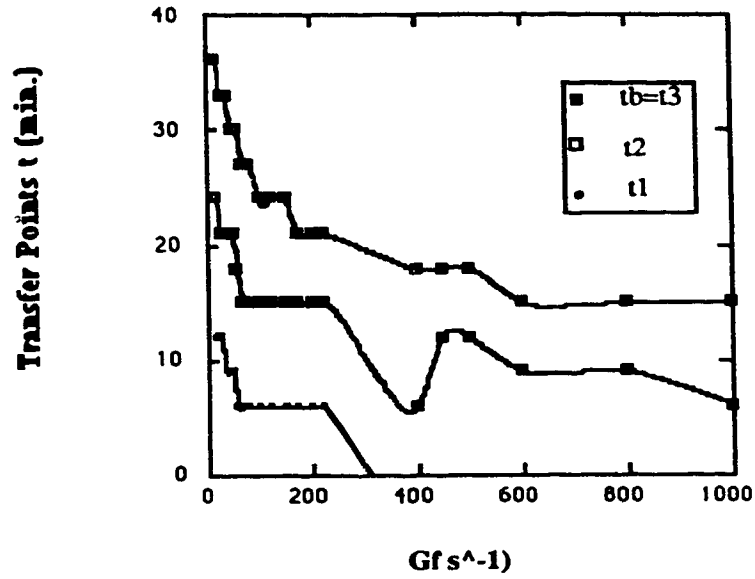


Figure 5.35 Effect of Mixing Rate on Transfer Points ( $\bar{G}_c = 150 \text{ s}^{-1}$ ,  $0 < \bar{G}_f \leq 150 \text{ s}^{-1}$ ;  $\bar{G}_c = \bar{G}_f$ ,  $150 < \bar{G}_f \leq 1000 \text{ s}^{-1}$ , kaolin=20 mg/L,  $\text{NaHCO}_3=100 \text{ mg/L}$ , pH=8, alum = 5mg/L, polymer=0.5 mg/L)

P.S. Transfer points divided a floc growth curve into several stages.



It was believed that each stage in the floc growth curve had a physical meaning. The physical meaning was postulated based on the mechanism of the polymeric floc growth and on the comparison with the alum floc growth curve given by Francois (1988). The physical meanings in the first four stages were postulated in this study as: (1) adsorption, 2) rapid floc growth, (3) slow floc growth, and (4) stabilization. The detailed descriptions of the physical meaning in each stage were given as follows.

At the first stage up to  $t_1$ , adsorption was the dominant mechanism, and primary particles were aggregated by enmeshment. Two types of adsorption were postulated to occur simultaneously: (1) individual kaolin particles were absorbed onto alum hydrolysis species, and onto the polymer chains; (2) the microflocs formed from the kaolin particles and the alum hydrolysis species were absorbed onto polymer chains. These adsorption reactions occurred with the aid of electrostatic forces, hydrogen bonding, chemical interactions, or ion exchange. The extent and rate of the adsorption reactions were significantly dependent on the surface chemistry and the conformation of a polymer chain which were determined by the pH and alkalinity of the suspension and the mixing conditions. The optimum alkali dose maintained the optimum pH, and at the optimum pH more precipitates of aluminum hydroxide were produced, which enmeshed fine flocs and unsettleable particles. The higher the  $\bar{G}_f$ -value, the more rapid the adsorption reaction occurred as the rate of adsorption was limited by transport processes rather than adsorption processes.

In the second stage from  $t_1$  to  $t_2$ , polymer bridging was the dominant mechanism resulting in rapid floc growth. The efficiency of the bridging was dependent on the length of the segment of the polymer chain, the saturation of the surface of the polymer chain, and the supply of primary particles and microflocs. The sufficient surface area of

the polymer chain and adequate supply of primary particles and microflocs led to the growth of the floc with a rapid speed.

In the third stage from  $t_2$  to  $t_3$ , polymer bridging was still the dominant mechanism. However, the growth rate declined until the moment  $t_b$  ( $t_b = t_3$ ) due to the depletion of the supplies of the primary particles, microflocs and the surface of the polymer chain. The  $t_b$  was called floc buildup time. The rate equilibrium between floc growth and breakup was established, and the floc reached a critical size ( $d_{max}$ ) at  $t_b$ .

In the fourth stage ( $t_f > t_b$ ), the equilibrium of floc growth and floc breakup was established, and  $d_{max}$  was maintained for a period of time if  $\bar{G}_f \leq 800 \text{ s}^{-1}$ .

Results also showed that when a longer flocculation time ( $t_b > 40 \text{ min.}$ ) or a higher  $\bar{G}_f$  value ( $800 < \bar{G}_f \leq 1600 \text{ s}^{-1}$ ) were used, the stable stage disappeared, and floc growth curves fluctuated up and down due to the breakup and regrowth of the floc (Figure 5.33).

The above analyses were supported by Tomi and Bagster (1978). Also the sigmoid-shape curves of polymeric floc growth was similar to that of the inorganic floc growth described by Tambo and Watanabe (1979) and Francois (1988). The significance of the study of the mechanism for polymeric floc growth lied in better understanding of the factors that affect the kinetics of the polymeric floc growth, and demonstrated that kinetic mechanisms or mathematical models derived from the inorganic floc were applicable to the polymeric floc.

#### **5.5.2.2 Effect of Mixing on Floc Buildup Time**

As previously described, the floc buildup time ( $t_b$ ) was the time when the floc reaches a critical size ( $d_{max}$ ). It was a simple, convenient parameter used to evaluate the overall rate of floc growth as  $t_b$  included all the factors which affect the rate of floc growth, and was used to compare various process conditions. The shorter the  $t_b$  was, the higher the rate of floc growth.

A mathematical model was proposed in this study in order to quantitatively describe the correlation between  $t_b$  and  $\bar{G}_f$ . The model simulation process was presented in Table 5.6. The model residuals were examined using the same method previously described. Figures 5.37 to 5.40 exhibit that the residuals were independent with zero mean and constant variance. Thus, the model was adequate. Therefore the impact of  $\bar{G}_f$  on  $t_b$  was described by following equation:

$$t_b = - 5.702 \ln (\bar{G}_f) + 52.062 \quad (5.32)$$

Figure 5.36 showed that  $t_b$  decreased significantly with  $\bar{G}_f$  at  $\bar{G}_f \leq 200 \text{ s}^{-1}$ , but only slightly at  $\bar{G}_f > 200 \text{ s}^{-1}$ . The conclusion was consistent with that derived from the analysis of the impact of mixing on the first order rate constant (see Section 5.5.1.2). Both analyses state the same result that the rate of the floc growth and the rate of flocculation was hastened by raising the value of  $\bar{G}_f$  at the range of  $\bar{G}_f \leq 200 \text{ s}^{-1}$ . Also, it has been confirmed by Figure 5.54, the increase in the  $\bar{G}_f$  at  $\bar{G}_f \leq 200 \text{ s}^{-1}$  did not cause the reduction of  $d_{max}$ . Therefore, the significance of the study of the impact of  $\bar{G}_f$  on  $t_b$  lied in the knowledge of the concept that the kinetic rates was controlled simply by  $\bar{G}_f$  only in a certain  $\bar{G}_f$  range. This  $\bar{G}_f$  range for the polymer-aided flocculation occurred at  $\bar{G}_f \leq 200 \text{ s}^{-1}$ .

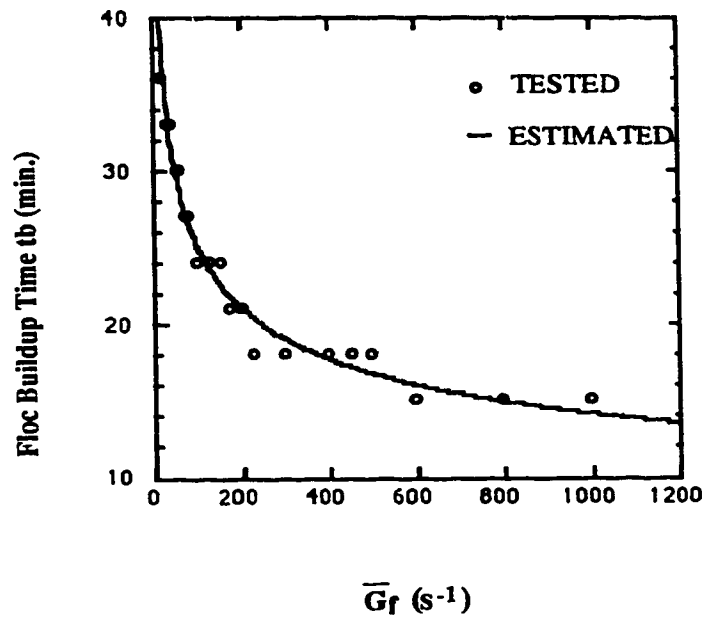


Figure 5.36 Effect of Mixing on Floc Buildup Time  $t_b$  ( $\bar{G}_c=150 s^{-1}$ ,  $20 \leq \bar{G}_f \leq 150 s^{-1}$ ;  $\bar{G}_c=\bar{G}_f$ ,  $150 < \bar{G}_f \leq 1000 s^{-1}$ , kaolin=20 mg/L,  $NaHCO_3=100$  mg/L, pH=8, alum=5mg/L, polymer=0.5 mg/L)

**Table 5.6 Model Simulation Process for Effect of Mixing on  $t_b$**

Model:  $t_b = M * \ln(\bar{G}_f) + N$  (M and N are constants)

ITERATION	LOSS	PARAMETER VALUES	
0	0.1110935D+05	0.1000D+00	0.1000D+00
1	0.3696160D+04	0.5469D+01	0.1232D+01
2	0.1381692D+04	-.1299D+02	0.9056D+02
3	0.3735924D+02	-.5665D+01	0.5166D+02
4	0.3640889D+02	-.5700D+01	0.206D+02
5	0.3640635D+02	-.5702D+01	0.5206D+02
6	0.3640635D+02	-.5702D+01	0.5206D+02

DEPENDENT VARIABLE IS  $t_b$

SOURCE	SUM-OF-SQUARES	DF	MEAN-SQUARE
REGRESSION	11600.594	2	5800.297
RESIDUAL	36.406	18	2.023
TOTAL	11637.000	20	
CORRECTED	825.770	19	

RAW R-SQUARED (1-RESIDUAL/TOTAL) = 0.997  
 CORRECTED R-SQUARED (1-RESIDUAL/CORRECTED) = 0.956

PARAMETER	ESTIMATE
M	-5.702
N	52.062

$$t_b = - 5.702 \ln(\bar{G}_f) + 52.062$$

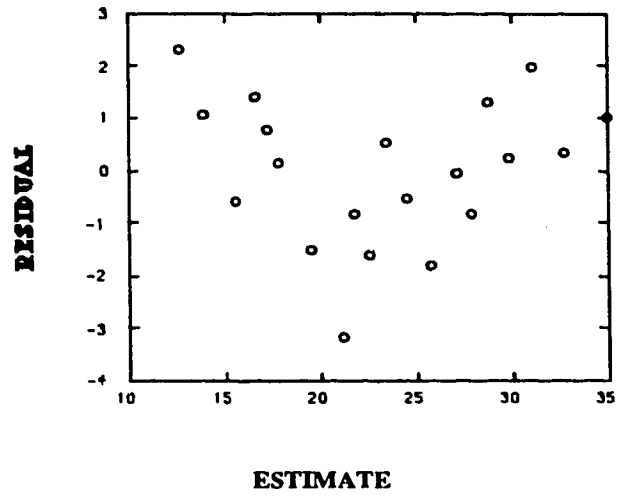


Figure 5.37 The Residuals Plotted against Fitted Value

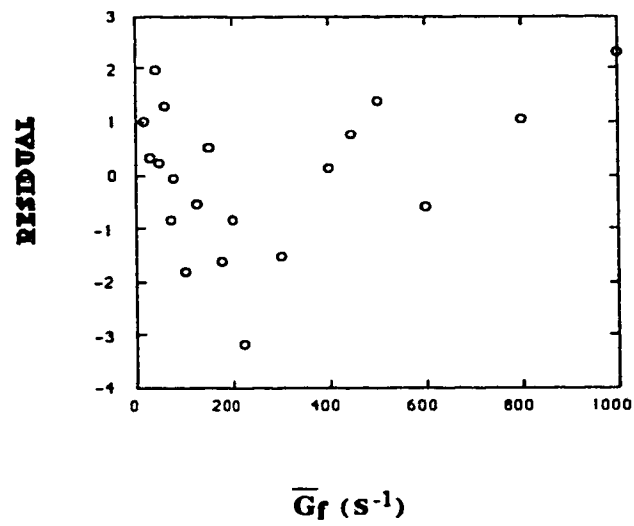


Figure 5.38 The Residuals Plotted against the Independent Parameter

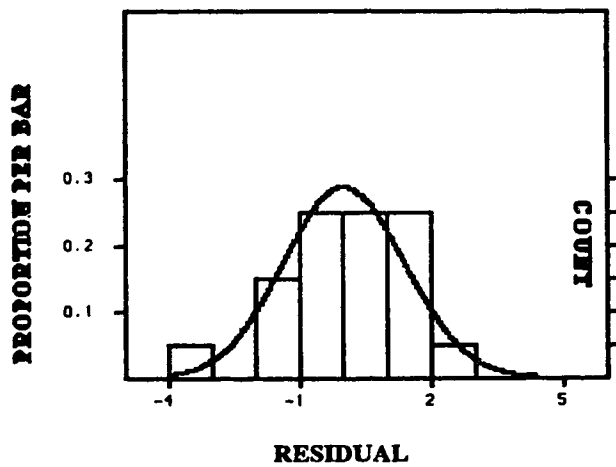


Figure 5.39 The Histogram Plot of the Residuals

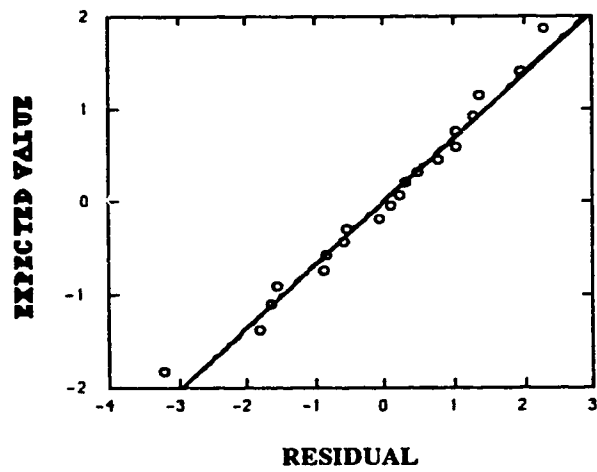


Figure 5.40 The Normal Plot of the Residuals

### 5.5.2.3 Effect of Mixing on Floc Growth Constants

Figure 5.35 and Appendix B demonstrated that a simple straight line was obtained in each stage of the plot of  $\ln D(6,3)$  versus  $t_f$ . It was postulated that

$$\ln D(6,3) = -\mu t_f + \ln D(6,3)_0 \quad (5.33)$$

which can be reorganized to

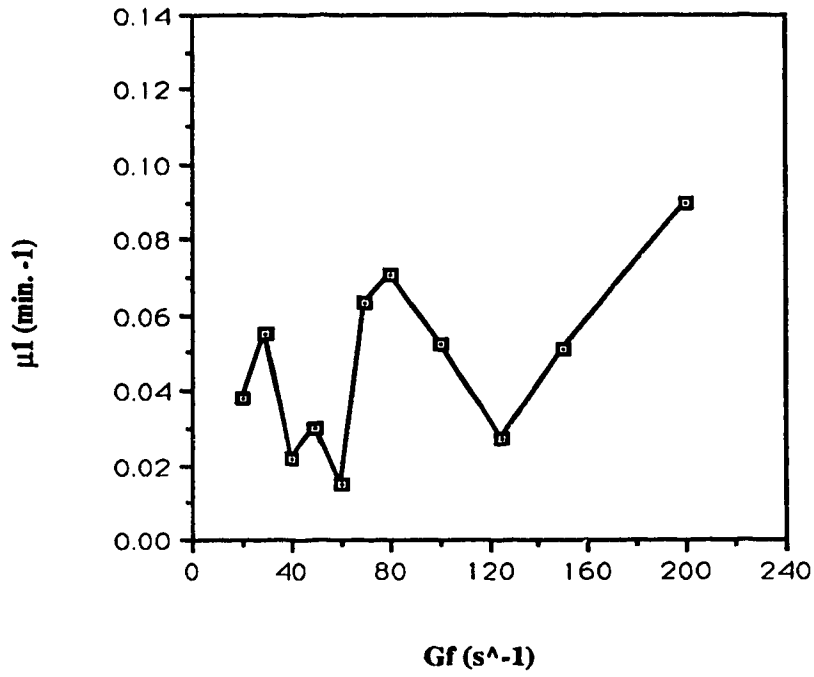
$$D(6,3) = D(6,3)_0 e^{-\mu t_f} \quad (5.34)$$

where  $D(6,3)$  was the mean particle diameter at flocculation time  $t_f$  and  $D(6,3)_0$  was  $D(6,3)$  at  $t_f=0$ .  $\mu$  was the floc growth constant used to evaluate the rate of the floc growth, and was determined either from the slope of the floc growth curves shown in Figure 5.35 and Appendix B, or from the mathematical model given in Equation 5.34. The above two methods gave the same results which were shown in Figure 5.41 where  $\mu_i$  ( $i=1, 2$  and  $3$ ) were used to stand for the floc growth constants in the first stage (adsorption), the second stage (rapid growth), and the third stage (slow growth).

From Figure 5.41 it was seen that  $\bar{G}_f$  had a significant impact on  $\mu_1$  and  $\mu_2$ , but to a lesser extent on  $\mu_3$ .

Figure 5.41-a showed that the trend of variation of  $\mu_1$  with  $\bar{G}_f$  was not obvious; which demonstrated that this method of kinetic analysis was not appropriate to use for the investigation of kaolin-alum-polymer adsorption theories. The study of the equilibrium thermodynamics was suggested, but it was beyond the scope of this study.





(a)

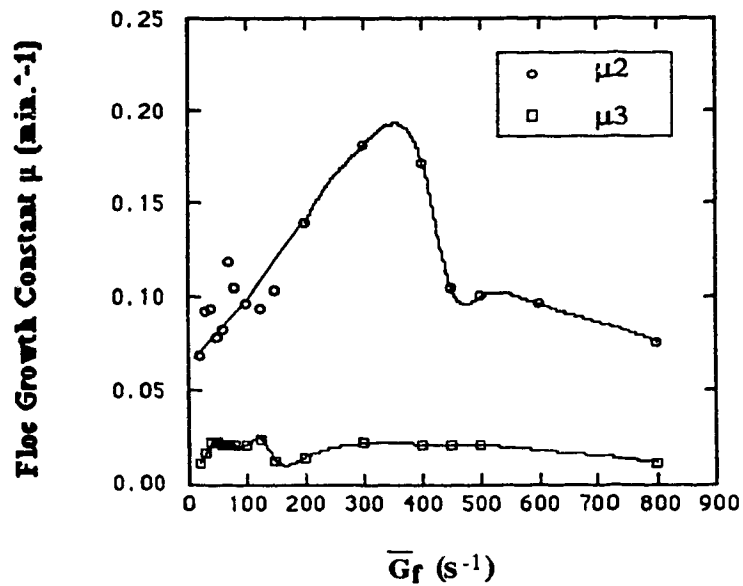


Figure 5.41 Effect of Mixing on Floc Growth Constants ( $\bar{G}_c=150 s^{-1}$ ,  $20 \leq \bar{G}_f \leq 150 s^{-1}$ ;  $\bar{G}_c=\bar{G}_f$ ,  $150 < \bar{G}_f \leq 200 s^{-1}$ , kaolin=20 mg/L,  $NaHCO_3=100$  mg/L, pH=8, alum=5mg/L, polymer=0.5 mg/L)

Figure 5.41-b showed that  $\mu_2$  increased as  $\bar{G}_f$  increases at  $0 < \bar{G}_f \leq 300 \text{ s}^{-1}$ . The possible explanation was that the growth of the floc occurred only if the collision of the particles could bring about the adherence of the particles. The collision was governed by transport processes, and the adherence was controlled by affinity. Alum acted as the “anchoring joints” on a long chain polymer that could be in contact with a surface by many segments simultaneously, and low bonding energy per segment sufficed to render the affinity of several segments together. As a result, adherence was a rapid and irreversible process, and the polymer adsorption and the growth of the floc were governed by transport processes. A high  $\bar{G}_f$  led to a higher collision rate due to the strong bulk fluid and turbulent motions, which resulted in a high value of  $\mu_2$ .

However, Figure 5.41 also demonstrated that  $\mu_2$  tended to decrease nonlinearly with the increase in  $\bar{G}_f$  at  $\bar{G}_f > 300 \text{ s}^{-1}$ . This could be caused mainly by two factors: 1) steric hindrance, and 2) floc breakup. The steric hindrance which lowered the ability of adsorption was caused by the increase in the dimension of the segment of the chain, as the polymer chain tended to be stretched at high  $\bar{G}_f$ . The floc breakup was due to the breaking of a polymer chain, and the increased shearing stress, and pressure force. A stretched polymer chain tended to reach its critical size, and might be broken apart under shear, which reduced the bridging ability. A high shearing stress gave a rise to the rate of surface erosion of primary particles from the floc, and the higher pressure force caused a more significant bulgy deformation and rupture; as a result, the floc breakup became substantial at  $\bar{G}_f > 300 \text{ s}^{-1}$  resulting in the decrease of  $\mu_2$ .

Figure 5.41 also showed that  $\bar{G}_f$  only had a slight impact on  $\mu_3$  as it was controlled by the supplies of particles and microflocs, and the availability of the surface of the polymer. The number of the particles and microflocs were limited, and the

saturation degree of the surface of polymer was high in this stage. Thus, a low and approximately constant  $\mu_3$  was observed.

The major significance of the investigation of the impact of mixing on the floc growth constants  $\mu_j$  was to better control the floc growth rate by using the proper  $\bar{G}_f$ -value. Also, the floc growth constants  $\mu_j$  were used to compare the rate of floc growth in each stage under different experimental conditions.

#### 5.5.2.4 Effect of Mixing on Mean Floc Growth Rate

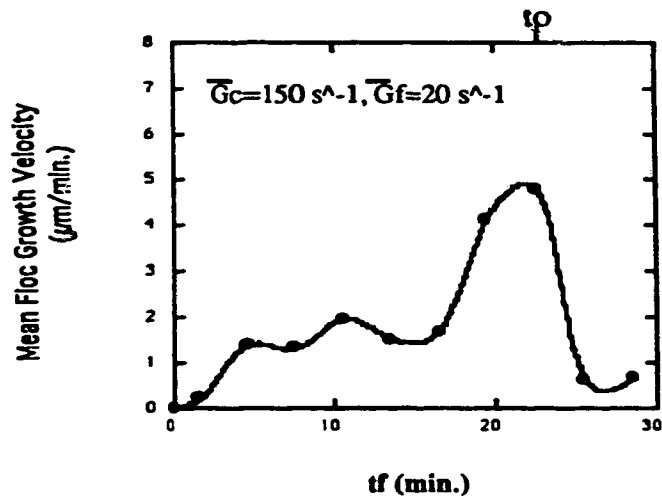
The mean polymeric floc growth rate was defined by the following equation in this study:

$$R_{\frac{t_2+t_1}{2}} = \frac{D(6,3)_{t_2} - D(6,3)_{t_1}}{t_2 - t_1} \quad (5.35)$$

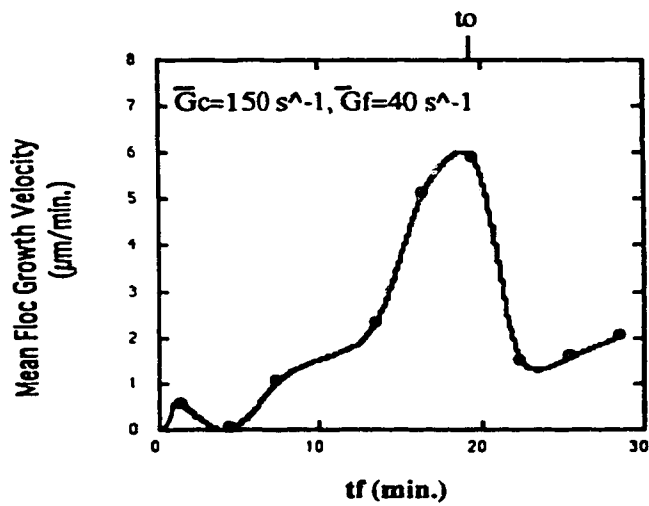
where  $R_{\frac{t_2+t_1}{2}}$  ( $\mu\text{m}/\text{min.}$ ) was the mean polymeric floc growth rate at mean flocculation time  $\frac{t_2+t_1}{2}$ ;  $D(6,3)_{t_2}$  and  $D(6,3)_{t_1}$  were the mean floc diameters at the flocculation times of  $t_2$  and  $t_1$  (min.), respectively. The curves of  $R_{\frac{t_2+t_1}{2}}$  against  $\frac{t_2+t_1}{2}$  were plotted at  $20 \leq \bar{G}_f \leq 400 \text{ s}^{-1}$ .

Figures 5.42 to 5.45 demonstrated that  $R_{\frac{t_2+t_1}{2}}$  was in a state of flux during the course of flocculation. It tended to increase at  $t_f < t_0$  until  $(R_{\frac{t_2+t_1}{2}})_{\text{max}}$  occurred at  $t_f = t_0$ , then tended to decrease. The  $t_0$  was called the critical flocculation time, and was used to characterize the variation rate of  $R_{\frac{t_2+t_1}{2}}$ . From Figures 5.42 to 5.45 it was seen that the

values of  $\frac{R_{t_2+t_1}}{2}$ ,  $(\frac{R_{t_2+t_1}}{2})_{\max}$  and  $t_0$  were dependent on  $\bar{G}_f$ . The impacts of  $\bar{G}_f$  on  $(\frac{R_{t_2+t_1}}{2})_{\max}$  and  $t_0$  were presented in Figures 5.46 and 5.47.



(a)



(b)

Figure 5.42 The Curves of Mean Polymeric Floc Growth Rate at  $\bar{G}_f = 20$  to  $40 \text{ s}^{-1}$  (kaolin=20 mg/L,  $\text{NaHCO}_3=100 \text{ mg/L}$ , pH=8, alum=5mg/L, polymer=0.5 mg/L)

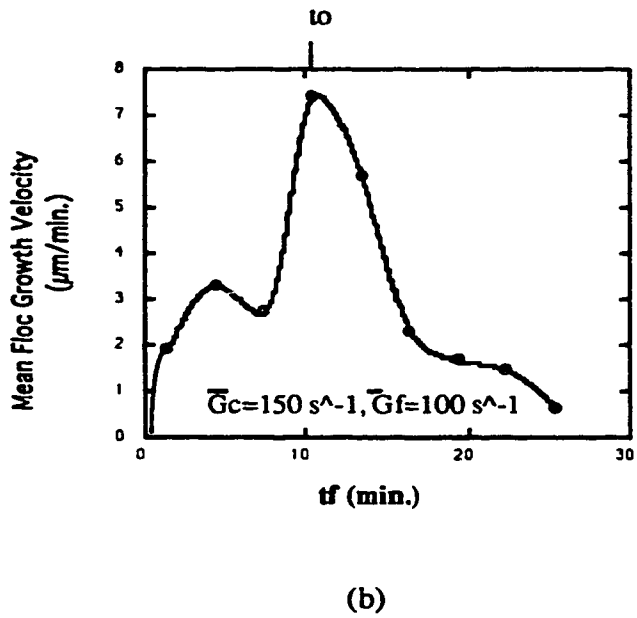
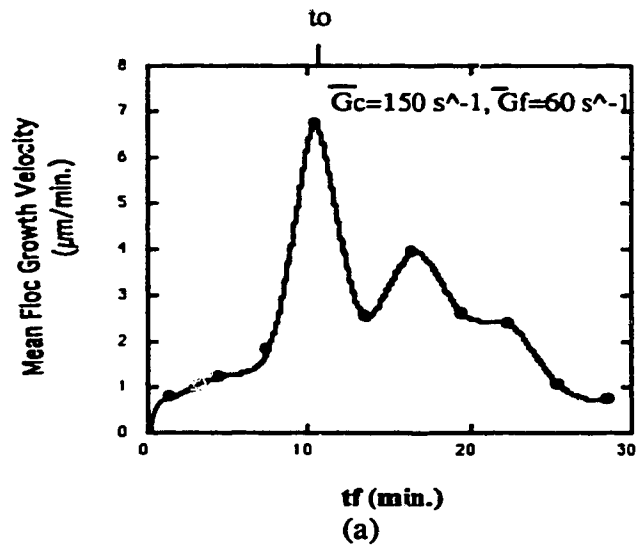
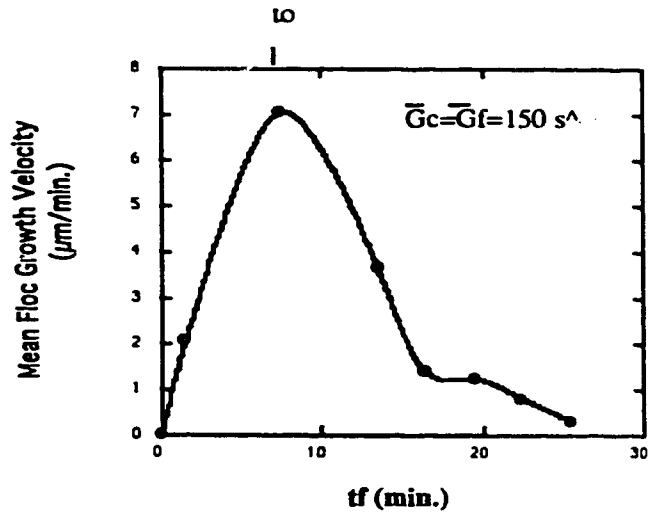
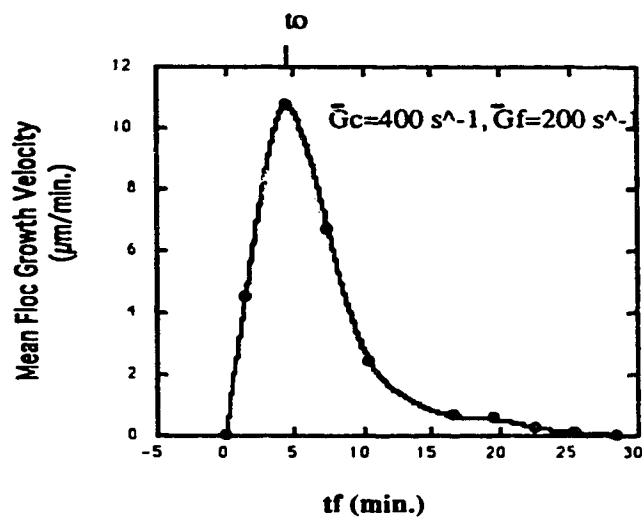


Figure 5.43 The Curves of Mean Polymeric Floc Growth Rate at  $\bar{G}_f = 60$  to  $100 \text{ s}^{-1}$  ( kaolin=20 mg/L,  $\text{NaHCO}_3=100 \text{ mg/L}$ ,  $\text{pH}=8$ , alum=5mg/L, polymer=0.5 mg/L)

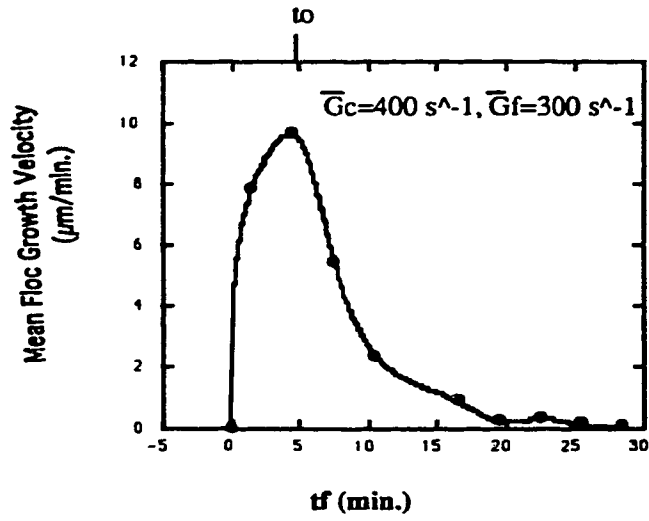


(a)

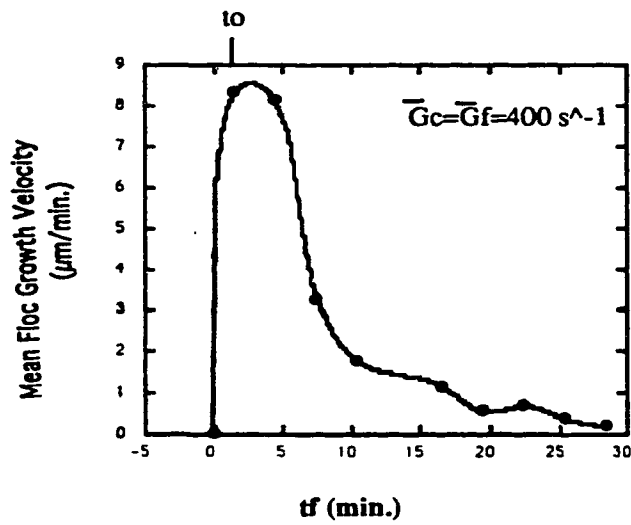


(b)

Figure 5.44 The Curves of Mean Polymeric Floc Growth Rate at  $\bar{G}_f = 150$  to  $200 \text{ s}^{-1}$  ( kaolin=20 mg/L,  $\text{NaHCO}_3$ =100 mg/L, pH=8, alum=5mg/L, polymer=0.5 mg/L)



(a)



(b)

Figure 5.45 The Curves of the Mean Polymeric Floc Growth Rate at  $\bar{G}_f = 300$  to  $400 \text{ s}^{-1}$  ( kaolin=20 mg/L,  $\text{NaHCO}_3$ =100 mg/L, pH=8, alum=5mg/L, polymer=0.5 mg/L)

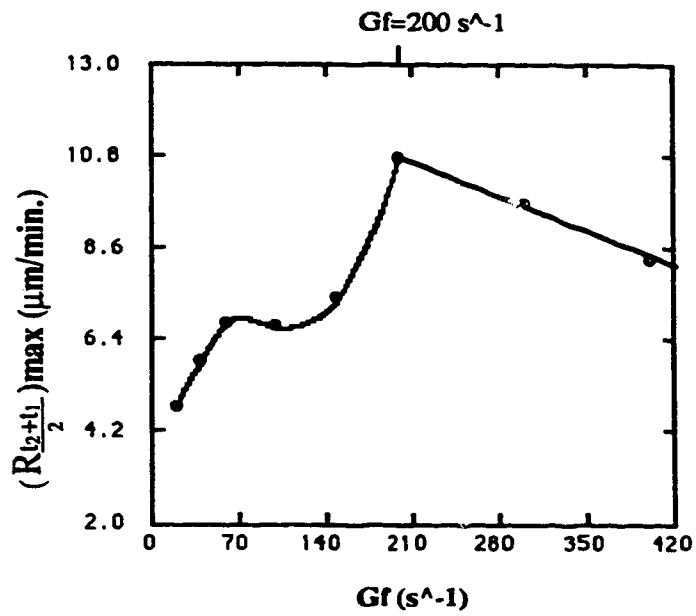


Figure 5.46 Effect of Mixing on Maximum Mean Floc Growth Rate ( $\bar{G}_c = 150 \text{ s}^{-1}$ ,  $20 \leq \bar{G}_f \leq 150 \text{ s}^{-1}$ ;  $\bar{G}_c = 400 \text{ s}^{-1}$ ,  $150 < \bar{G}_f \leq 400 \text{ s}^{-1}$ , kaolin=20 mg/L, pH=8,  $\text{NaHCO}_3=100 \text{ mg/L}$ , alum=5 mg/L, polymer=20 mg/L)



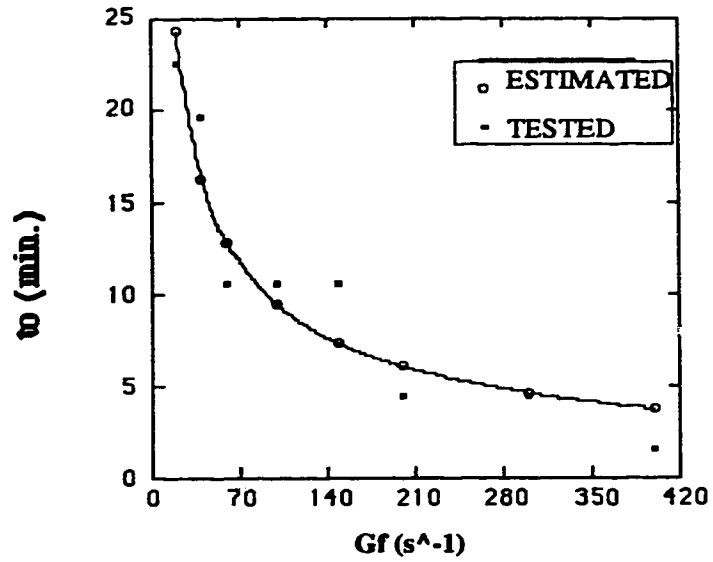


Figure 5.47 Effect of Mixing on Critical Flocculation Time ( $\bar{G}_c=150 \text{ s}^{-1}$ ,  $20 \leq \bar{G}_f \leq 150 \text{ s}^{-1}$ ;  $\bar{G}_c=400 \text{ s}^{-1}$ ,  $150 < \bar{G}_f \leq 400 \text{ s}^{-1}$ , kaolin=20 mg/L, pH=8,  $\text{NaHCO}_3=100 \text{ mg/L}$ , alum=5 mg/L, polymer=20 mg/L)

Figure 5.46 showed that  $(R_{\frac{t_2+t_1}{2}})_{\max}$  increased nonlinearly with the increase in  $\bar{G}_f$ , and the maximum value of  $(R_{\frac{t_2+t_1}{2}})_{\max}$  occurred at  $\bar{G}_f=200 \text{ s}^{-1}$ . The value of  $(R_{\frac{t_2+t_1}{2}})_{\max}$  decreased linearly as increased  $\bar{G}_f$  at  $\bar{G}_f > 200 \text{ s}^{-1}$ . The above conclusion confirms the fact that the first order rate constant  $K$  tended to increase slowly and floc build-up time  $t_b$  tended to decrease slowly at  $\bar{G}_f > 200 \text{ s}^{-1}$  as previously discussed.

Figure 5.47 demonstrated that  $t_0$  decreased nonlinearly with the increase in  $\bar{G}_f$  at  $0 < \bar{G}_f \leq 400 \text{ s}^{-1}$ . The nonlinear regression was performed in order to quantitatively describe the correlation between  $t_0$  and  $\bar{G}_f$ . The regression process was presented in Table 5.7, and the residual examination shown in Figures 5.48 to 5.51 confirmed that the impact of  $\bar{G}_f$  on  $t_0$  could be predicted by the following equation:

$$t_0 = 87.101 (\bar{G}_f)^{-0.163} - 30.752 \quad (5.36)$$

Experience has shown that  $t_0$  was directly proportional to the floc appearance time which was the elapsed time required for the very first fine flocs to appear. However, the  $t_b$ , as discussed, was the time when  $d_{\max}$  was reached. Comparison of Figure 5.36 with Figure 5.50 led to the conclusion that  $\bar{G}_f$  had a consistent impact on the floc buildup time  $t_b$  and the critical flocculation time  $t_0$ .

In conclusion, the analyses of the impacts of  $\bar{G}_f$  on the first order rate constant  $K$ , the maximum mean floc growth rate  $(R_{\frac{t_2+t_1}{2}})_{\max}$ , the floc build up time  $t_b$  and the critical flocculation time  $t_0$  all pointed to the same conclusion that the rate of polymer-aided flocculation and the rate of polymeric floc growth increased significantly with  $\bar{G}_f$  at  $\bar{G}_f \leq 200 \text{ s}^{-1}$ , and slightly at  $200 < \bar{G}_f \leq 400 \text{ s}^{-1}$ . As a result, the kinetics of polymer-aided flocculation was controlled by mixing intensity only at  $\bar{G}_f \leq 200 \text{ s}^{-1}$ .

**Table 5.7 Model Simulation for Effect of Mixing on  $t_0$**

Model:  $t_0 = M * (\bar{G}_f)^N + C$  (M, N and C are constants)

ITERATION	LOSS	PARAMETER VALUES		
0	0.2899619D+02	0.8709D+02	-.1627D+00	-.3075D+02
1	0.2899619D+02	0.8710D+02	-.1626D+00	-.3075D+02
2	0.2899619D+02	0.8710D+02	-.1626D+00	-.3075D+02

DEPENDENT VARIABLE IS  $t_0$

SOURCE	SUM-OF-SQUARES	DF	MEAN-SQUARE
REGRESSION	1231.005	3	410.335
RESIDUAL	28.996	5	5.799
TOTAL	1260.000	8	
CORRECTED	378.000	7	

RAW R-SQUARED (1-RESIDUAL/TOTAL) = 0.977  
 CORRECTED R-SQUARED (1-RESIDUAL/CORRECTED) = 0.923

PARAMETER	ESTIMATE
M	87.101
N	-0.163
C	-30.752

$$t_0 = 87.101 * (\bar{G}_f)^{-0.163} - 30.752$$

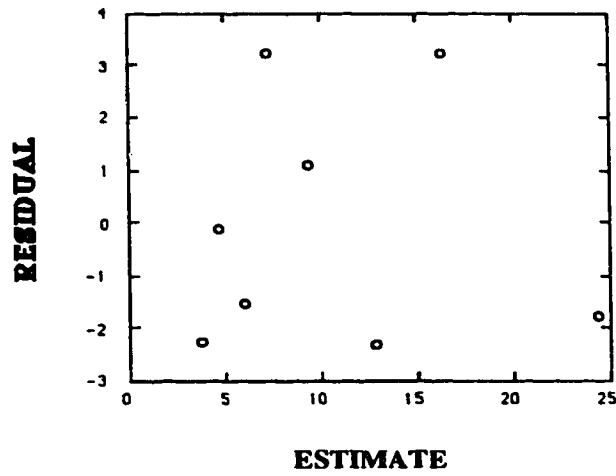


Figure 5.48 The Residuals Plotted against Fitted Value ( $t_0$ )

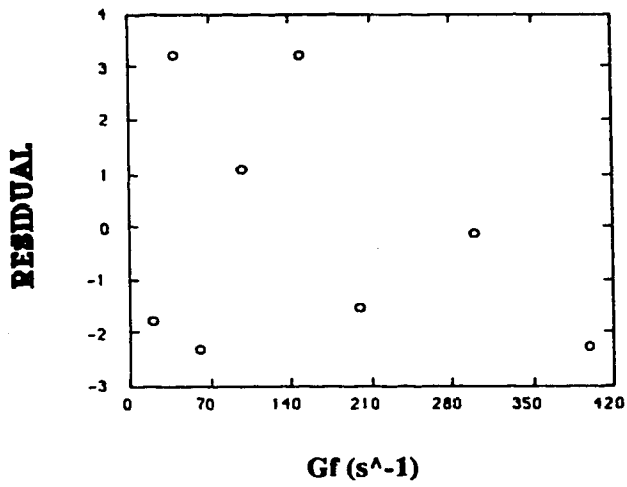


Figure 5.49 The Residuals Plotted against the Independent Parameter

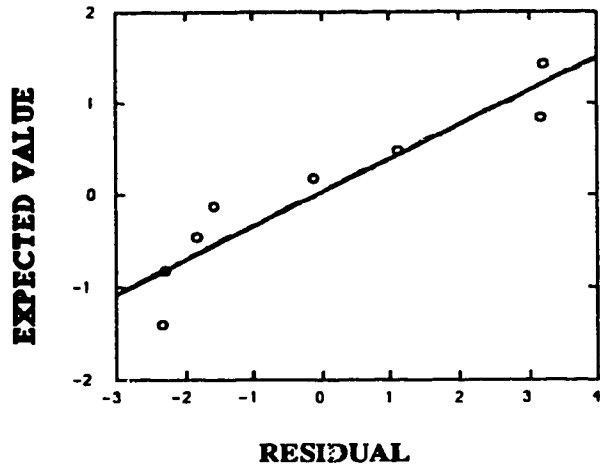


Figure 5.50 Normal Plot of the Residuals

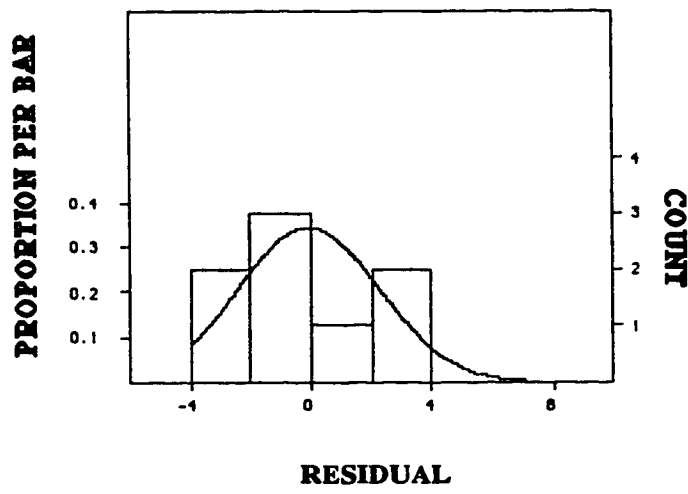


Figure 5.51 Histogram Plot of the Residuals

## 5.6 Effect of Mixing on Particle Size Distribution Function

In the previous analyses  $D(6,3)$  and  $d_{\max}$  were used to assess flocculation performance. It was also important to assess the variation in particle size which was accomplished through the use of particle size distribution function. The particle size distribution function given by O' Melia (1978) was :

$$\frac{dN}{d(d_p)} = \dot{n} (d_p) \quad (5. 37)$$

where  $dN$ = number of particles per unit fluid volume in size range  
 $d_p$  to  $d_p+d(d_p)$ , count/mL  
 $d_p$  = diameter of particles,  $\mu\text{m}$   
 $\dot{n} (d_p)$  = particle size distribution function, count/mL  $\cdot \mu\text{m}^{-1}$

It was assumed that particle size distributions in the kaolin suspension tested followed a power law function, Equation 5. 37 was represented (Hargesheimer et al 1992) as:

$$\frac{dN}{d(d_p)} = \dot{n} (d_p) = A_o(\bar{d})^{-\beta} \quad (5. 38)$$

where:  $\bar{d}$  = arithmetic mean particle diameter ( $\mu\text{m}$ )  
 $A_o$  = power law density coefficient which is related  
to the total concentration of particles

$\beta$  = power law slope coefficient that characterizes size distributions

The value of the power law slope coefficient ( $\beta$ ) was determined graphically from the slope of the straight-line shown in the following equation:

$$\log \left[ \frac{\Delta N}{\Delta d} \right] = \log A_o - \beta \log (\bar{d}) \quad (5.39)$$

where:  $\Delta N$  = differential particle concentration (counts/ mL)

$\Delta d$  = channel width ( $\mu\text{m}$ )

$\bar{d} = \frac{\Delta d}{2}$  ( $\mu\text{m}$ ), midpoint of each successive class-size intervals

The diagrams of  $\log \left( \frac{\Delta N}{\Delta d} \right)$  versus  $\log (\bar{d})$  were plotted using the data collected from the first seven channels, and straight lines were obtained. The  $\beta$  values were determined graphically from the slopes of the straight lines shown in Appendix D. It was notable that the differential counts at the eighth channel were eliminated from the determination of  $\beta$  values as the arithmetic mean size for the largest size range was difficult to define, and it was dependent on the sensor size range capabilities. Also, only the  $\beta$  values at  $0 < \bar{G}_{ftb} < 3 \times 10^5$  were determined, because the trend of particle size distribution function tended to be flat at  $\bar{G}_{ftb} > 2 \times 10^5$ , the linear relationship disappeared at the end of the curves (see Appendix D). Figure 5.52 indicated that  $\beta$  was inversely proportional to  $\bar{G}_{ftb}$ . The low regression coefficient ( $R^2 = 0.722$ ) was contributed by the end parts of the curves, which tended to be flat at higher  $\bar{G}_{ftb}$ .

The  $\beta$  had important applications in water treatment, because it was used to estimate particle size distribution in the suspension, determine the dominant transport process that influenced the particles in that water (Amirtharajah and O'Melia, 1990). It was also used to determine the efficiency of alternative flocculants (Leu and Ghosh, 1988; Lawler and Wilkes, 1984), and flocculation efficiency. The parameter  $\beta$  provided an indication of changes in particle size distribution in a sample, so that it was possible to compare particle size distributions under different experimental conditions, and degrees of flocculation.

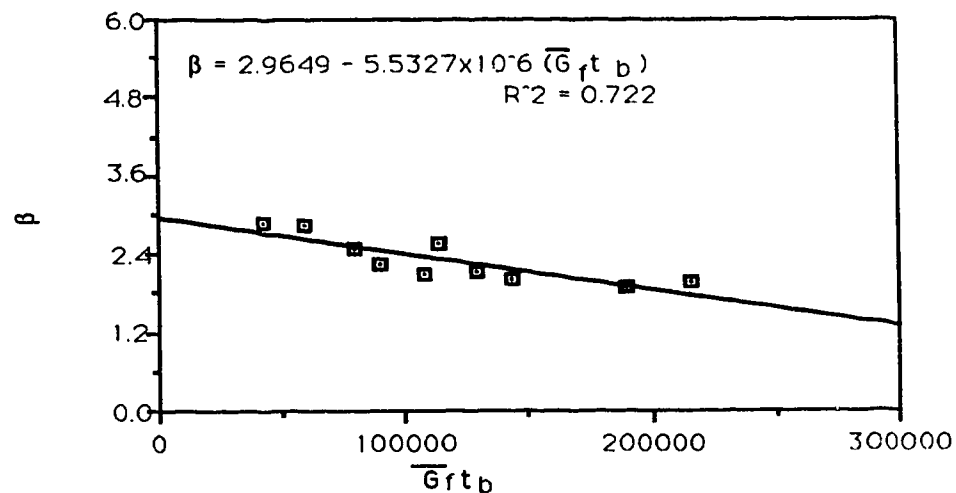


Figure 5.52 Effect of Degree of Flocculation on Power Law Slope Coefficient

### 5.7 Effect of Mixing on Maximum Mean Floc Diameter

As shown in Figure 5.53, the maximum mean floc diameter ( $d_{max}$ ) was the equilibrium size in the stabilization stage of the floc growth process ( $t_f > t_b$ ). It was determined by two opposing factors; the mechanical strength and the applied breaking



forces. The mechanical strength was contributed by chemical bond, hydrogen bond, van der Waals attraction, and bridging. The breaking forces included shearing force and the pressure force. The size of the floc reached  $d_{\max}$  as the equilibrium between these two kinds of opposing forces was established. The  $d_{\max}$  decreased if floc breakup became significant.

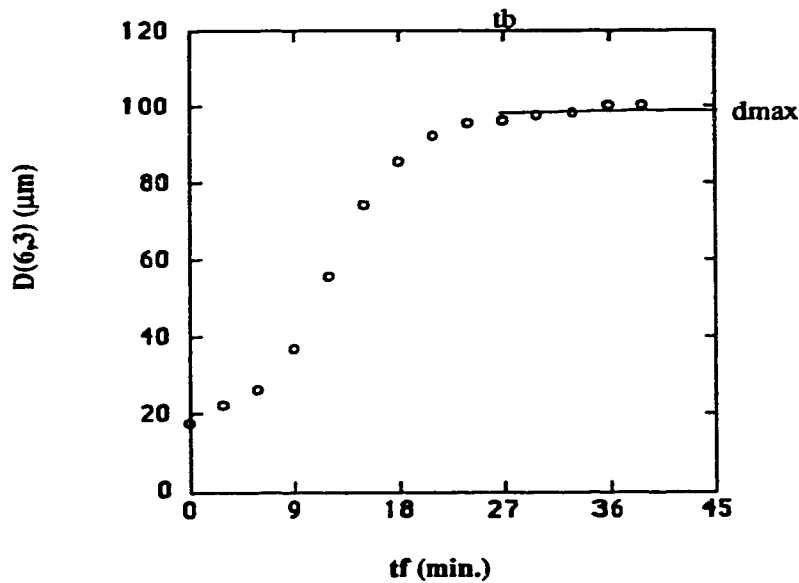


Figure 5.53 Polymeric Floc Growth Process ( $\bar{G}_c=150 \text{ s}^{-1}$ ,  $\bar{G}_f=70 \text{ s}^{-1}$ , kaolin=20 mg/L, pH=8,  $\text{NaHCO}_3=100 \text{ mg/L}$ , alum=5mg/L, polymer=0.5 mg/L)

Figure 5.54 showed that a nonlinear relationship existed between  $d_{\max}$  and  $\bar{G}_f$ .

The mathematical model:

$$d_{\max}=a (\bar{G}_f)^m +b \tag{5.40}$$

was used to fit the data. The model simulation process was presented in Appendix E.

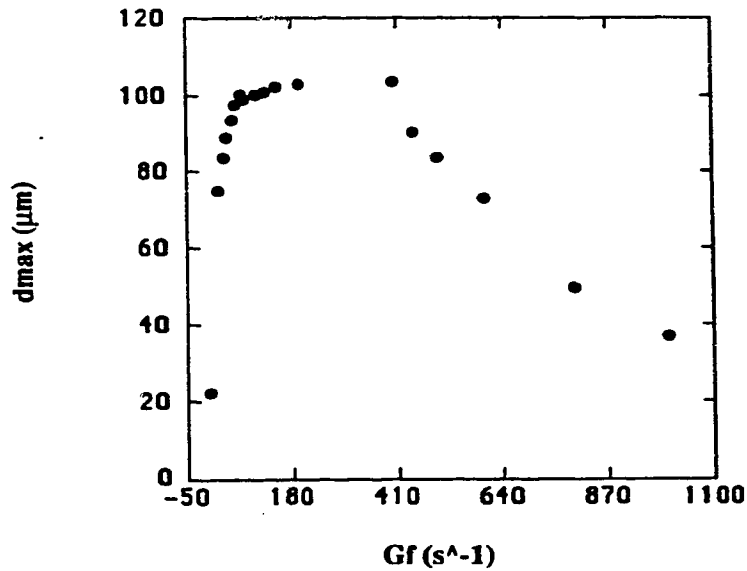


Figure 5.54 Effect of Mixing on Maximum Mean Floc Diameter ( $\bar{G}_c = 150 \text{ s}^{-1}$ ,  $20 \leq \bar{G}_f \leq 150 \text{ s}^{-1}$ ,  $\bar{G}_c = \bar{G}_f > 150 \text{ s}^{-1}$ , kaolin=20 mg/L, pH=8,  $\text{NaHCO}_3=100 \text{ mg/L}$ , alum=5mg/L, polymer=0.5 mg/L)

The exponent  $m$  in Equation 5.40, called a  $d_{\text{max}}$  growth constant, was determined from the model parameter. It was used to quantitatively evaluate the rate of the variation of  $d_{\text{max}}$ . Figure 5.55 showed that  $m$  was dependent on  $\bar{G}_f$ , the positive  $m$ -value was obtained at  $0 < \bar{G}_f \leq 400 \text{ s}^{-1}$ , and the negative  $m$ -value was obtained at  $\bar{G}_f > 400 \text{ s}^{-1}$ . It also demonstrated that  $m$  remained constant in a certain range of  $\bar{G}_f$ .

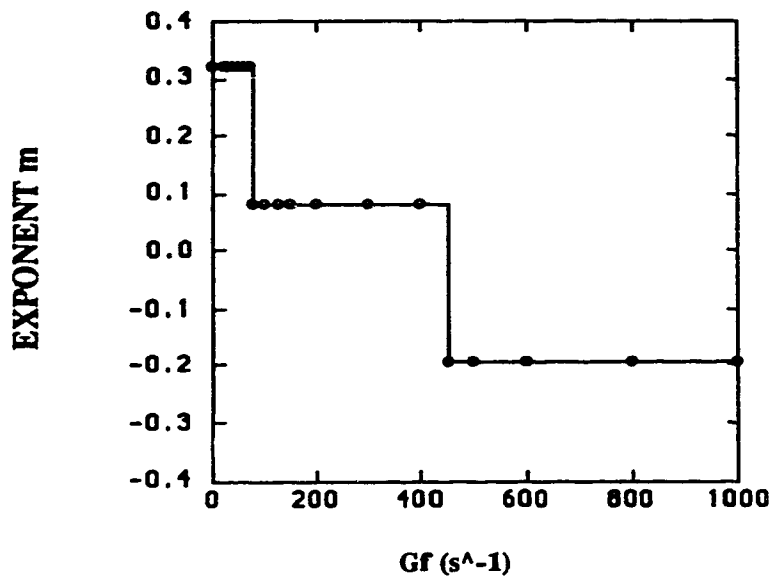


Figure 5.55 Effect of Mixing on  $d_{\max}$  Growth Constants ( $\bar{G}_c = 150 \text{ s}^{-1}$ ,  $20 \leq \bar{G}_f \leq 150 \text{ s}^{-1}$ ,  $\bar{G}_c = \bar{G}_f > 150 \text{ s}^{-1}$ , kaolin=20 mg/L, pH=8,  $\text{NaHCO}_3=100 \text{ mg/L}$ , alum=5mg/L, polymer=0.5 mg/L)

The positive  $m$ -value showed that  $d_{\max}$  tended to increase at  $0 < \bar{G}_f \leq 400 \text{ s}^{-1}$ . It was well known that  $d_{\max}$  was achieved by the kinetic equilibrium of floc growth and floc breakup in a turbulence field, and  $d_{\max}$  was determined by mechanical strength and hydrodynamic force provided by mixing. As the polymeric floc has high strength, it was more resistant to shearing, the increase in  $\bar{G}_f$  improved the collision efficiency, and bridging ability due to the stretch of the polymer chain at higher  $\bar{G}_f$ . As a result,  $d_{\max}$  tended to increase at  $0 < \bar{G}_f \leq 400 \text{ s}^{-1}$ .

The higher positive m-value obtained at  $\bar{G}_f=20$  to  $70 \text{ s}^{-1}$  showed that the growth rate of  $d_{\max}$  was rapid in this range. This indicated that the strength of the floc was greater than hydrodynamic forces being placed on it.

The smaller positive m-value obtained at  $\bar{G}_f=70$  to  $400 \text{ s}^{-1}$  was postulated that the two types of opposing factors increased simultaneously with the increase in  $\bar{G}_f$ . One was positive, and the other was negative. The positive factor was contributed by the increase in the length of the segment of the chain and collision efficiency. The increase in the length resulted in a high bridging ability, and the increase in collision efficiency improved adsorption efficiency. The negative factors were contributed by the surface stress, and steric hindrance. The surface stress may cause floc breakup, and steric hindrance may lower the adsorption ability. The  $d_{\max}$  was balanced by these factors, it thus increased slowly.

The negative m-value showed that  $d_{\max}$  tended to decrease at  $\bar{G}_f \geq 400 \text{ s}^{-1}$ . In this zone hydrodynamic forces exceed the strength of the floc. Plate 5.1 demonstrated that the polymeric floc was significantly sheared at  $\bar{G}_f=400 \text{ s}^{-1}$ , the breakup of the floc may occur at the weak part of the floc.

It should be stressed that the m-values derived from this study were based on the  $d_{\max}$  which was the maximum mean particle diameter determined from the floc growth curves of D(6,3) versus  $t_f$ . It can not be compared with the m-values for aluminum hydroxide kaolin flocs given by Tambo et al (1970, 1979) due to the difference of the basis of statistics. Even based on the same statistics, the m-value for the polymeric floc was different from that for alum floc, which was predicted by Amirtharajah et al (1991).

Alum floc was formed through the aggregation of the primary particles by adsorption and enmeshment, the growth of the floc was more slow due to the absence of polymer as a bridge. Also, the alum floc was much more fragile than that of the polymeric floc, and was much more easily broken up under shear. It was postulated that the  $m$ -value for the alum floc was smaller than that for the polymeric floc derived above.

### **5.8 Comparison between Alum Flocculation and Polymer-Aided Flocculation**

In this study, alum flocculation was the flocculation completed by sole alum coagulant, and polymer-aided flocculation was defined as the flocculation accomplished by a polymer in conjunction with alum. The laboratory experiments enabled the two coagulant systems to be compared in identical experimental conditions. The flocculation efficiency ( $E$ ), mean floc size [ $D(6,3)$ ], and  $d_{\max}$  were used to assess the performance of the flocculation systems. The shapes and structures of a kaolin aggregate, an alum floc and a polymeric floc were observed and photographed using a Scanning Electron Microscope (HITACHI SEM-2500), and were shown in Plates 5.2 to 5.7.

Plates 5.2 and 5.3 showed that polymeric flocs yielded in the same experimental run had a size distribution and shape difference. The biggest floc was approximately 150  $\mu\text{m}$ , but the smallest floc was only about 15  $\mu\text{m}$ . Plates which were not presented also demonstrated that the shape of the polymeric floc tended to be irregular with the increased floc size or  $\overline{G}_f$ -value.

The microstructures of an aggregate of kaolin particles, an alum floc and a polymeric floc were presented in Plates 5.4 to 5.7 in order to compare the compaction of the flocs. Plates 5.4 and 5.7 demonstrated that the alum floc had a loose and fragile structure, but the polymeric floc contained denser and stronger structure which could also

be seen in Plates 5.2 and 5.3. Other plates which were not provided showed that the higher the  $\overline{G}_f$ -value, the more compact the polymeric floc was. Therefore, the use of the polymer as a coagulant aid significantly improved the settle ability of the floc. As a result it provided higher quality of water before filtration, which should increase the efficiency of filtration.

The evaluations of E, D(6,3), and  $d_{max}$  in two systems were conducted in the optimum experimental conditions: kaolin=20 mg/L, alum=5mg/L, pH=8, alkalinity=100 mg/L as NaHCO<sub>3</sub>, and  $\overline{G}_c=150 \text{ s}^{-1}$ . Two levels of mixing intensity were used. One was  $\overline{G}_f=40 \text{ s}^{-1}$ , which was the optimal  $\overline{G}_f$  for alum flocculation, and the other was  $\overline{G}_f=70 \text{ s}^{-1}$ , which was the favored  $\overline{G}_f$  for the polymer-aided flocculation.

The conclusive results drawn from Figures 5.56 to 5.61 were tabulated in Table 5.8 which showed that the values of E, D(6,3), and  $d_{max}$  of the polymeric floc were much higher than those of the alum floc. The experimental evidence demonstrated that the use of the polymer dramatically reduced the settling time as it took 30 to 50 min. to settle most of the alum flocs, but only 2 to 5 min. to settle polymeric flocs. The E of polymer flocculation was as high as 99%, the suspension had a low turbidity of less than 1 NTU. Therefore, the polymer-aided flocculation was superior over alum flocculation, and it was highly recommended for water treatment.

**Table 5. 8 Comparison Alum Flocculation with Polymer-Aided Flocculation**

$\bar{G}_f$ ( $s^{-1}$ )	Maximum Mean Floc Diameter $d_{max}$ ( $\mu m$ )		$R = E_{max.2} / E_{max.1}$
	$d_{max.1}$	$d_{max.2}$	
	(polymer=0 mg/L) (alum flocculation)	(polymer=0.5 mg/L) (polymer-aided flocculation)	
40	27.36	84.67	3
70	21.83	98.3	4.5
$\bar{G}_f$ ( $s^{-1}$ )	Particle Removal Efficiency E (%) (at $t_f=27$ min.)		$R = E_{max.2} / E_{max.1}$
	$E_{max.1}$	$E_{max.2}$	
	(polymer=0 mg/L) (alum flocculation)	(polymer=0.5 mg/L) (polymer-aided flocculation)	
40	23	68	3
70	31	71	2.3

\* The data of particle removal efficiencies were collected after flocculation rather than after sedimentation.

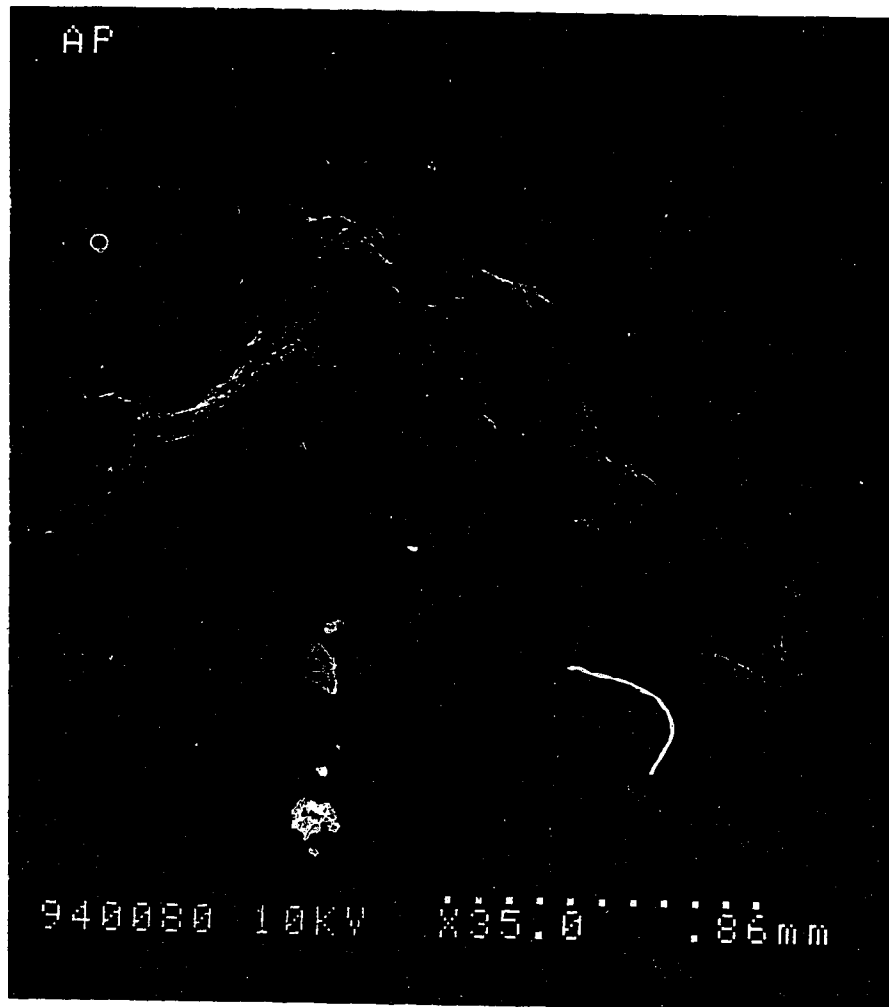


Plate 5.1 Shape of a Polymeric Floc at a High Mixing Rate (kaolin = 20 mg/L, alum = 5 mg/L, polymer = 0.5 mg/L,  $\text{NaHCO}_3 = 100 \text{ mg/L}$ ,  $\bar{G}_c = \bar{G}_f = 400 \text{ s}^{-1}$ , and  $t_f = 30 \text{ min.}$ )



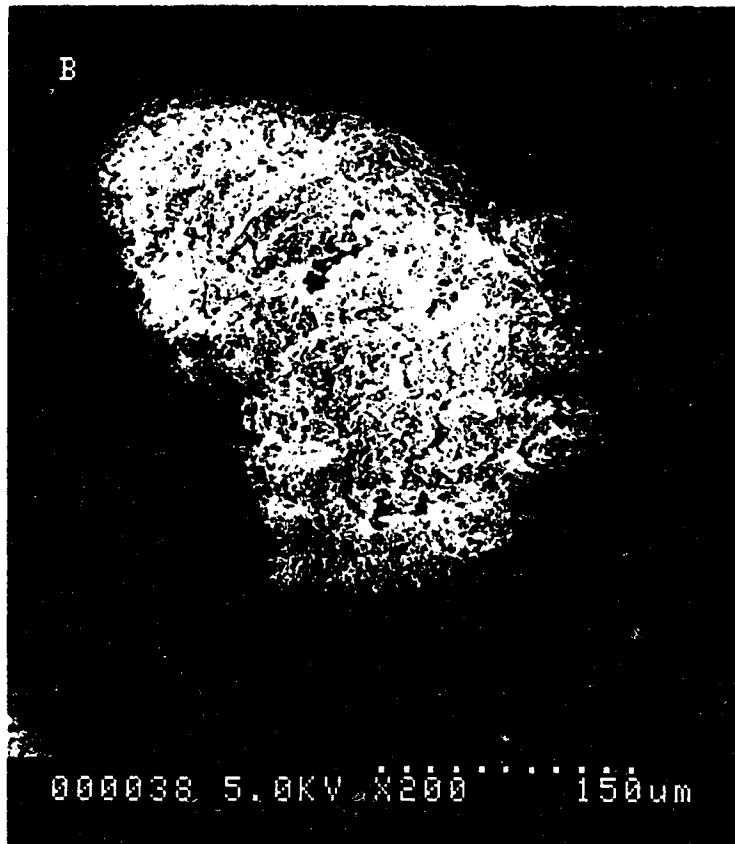


Plate 5.2 Shape of a Polymeric Floc with Big Size ( $d \cong 150 \mu\text{m}$ ) (kaolin = 20 mg/L, alum= 5 mg/L, polymer = 0.5 mg/L,  $\text{NaHCO}_3 = 100 \text{ mg/L}$ ,  $\bar{G}_c = 200 \text{ s}^{-1}$ ,  $\bar{G}_f = 30 \text{ s}^{-1}$ ,  $t_c = 1 \text{ min}$ , and  $t_f = 30 \text{ min}$ .)

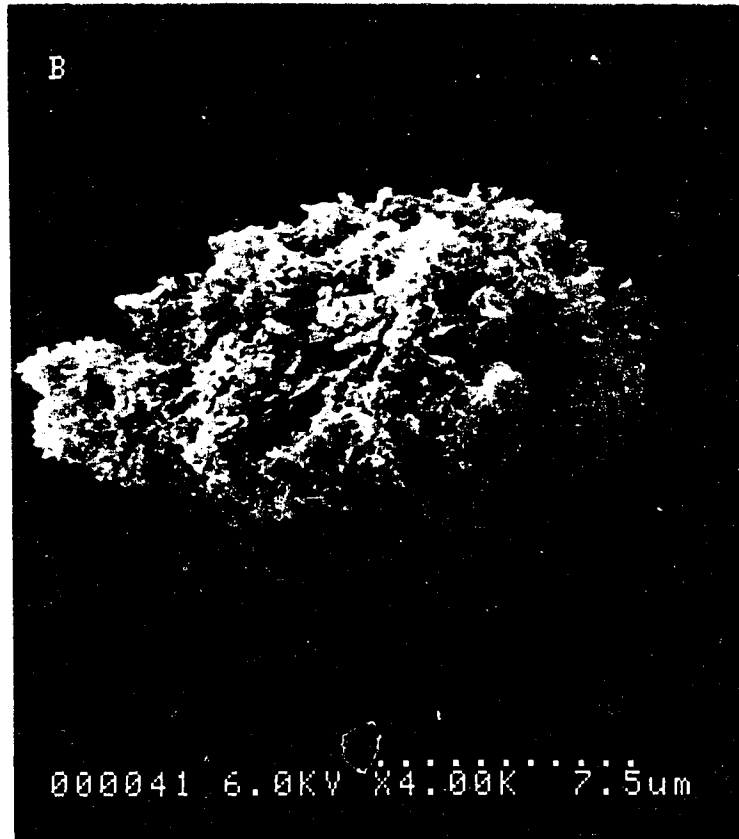


Plate 5.3 Shape of a Polymeric Floc with Small Size ( $d \approx 10 \mu\text{m}$ ) (kaolin = 20 mg/l., alum = 5 mg/L, polymer = 0.5 mg/L,  $\text{NaHCO}_3 = 100 \text{ mg/L}$ ,  $\bar{G}_c = 200 \text{ s}^{-1}$ ,  $\bar{G}_f = 30 \text{ s}^{-1}$ ,  $t_c = 1 \text{ min}$ , and  $t_f = 30 \text{ min}$ .)

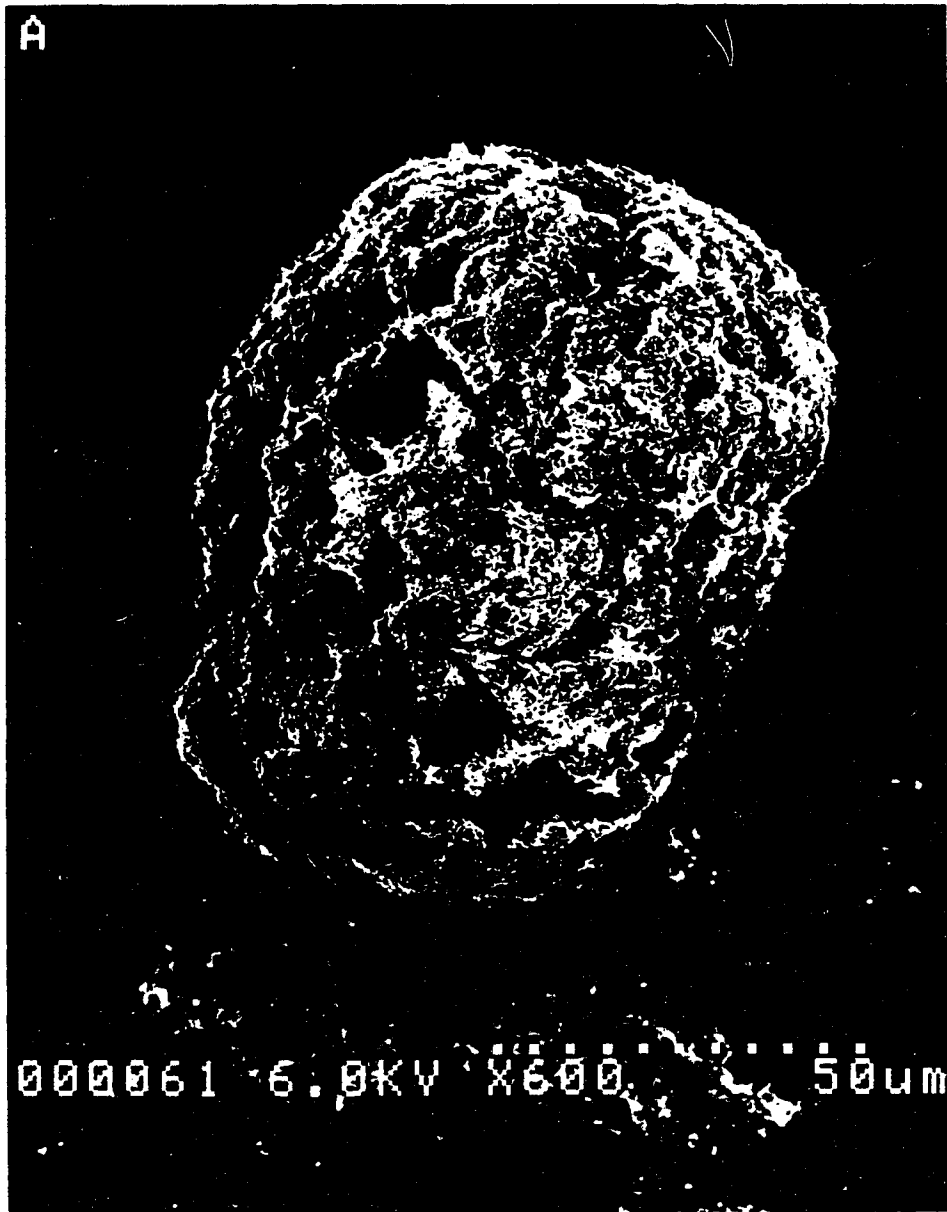


Plate 5.4 Shape of a Alum Floc with Big Size ( $d \cong 70 \mu\text{m}$ ) (kaolin = 20 mg/L, alum= 5 mg/L, polymer = 0.5 mg/L,  $\text{NaHCO}_3 = 100 \text{ mg/L}$ ,  $\bar{G}_c = 200 \text{ s}^{-1}$ ,  $\bar{G}_f = 30 \text{ s}^{-1}$ ,  $t_c = 1 \text{ min}$ , and  $t_f = 30 \text{ min}$ .)

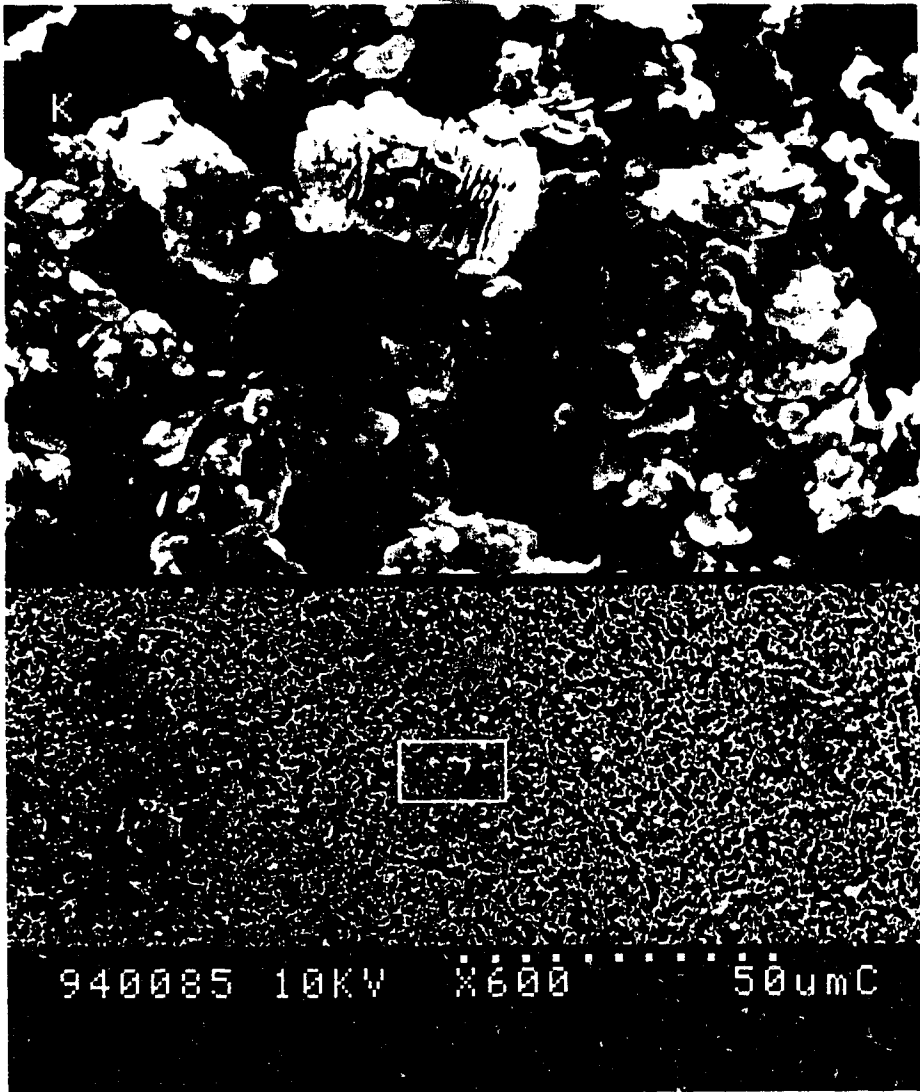


Plate 5.5 The Microstructure of Kaolin Aggregate

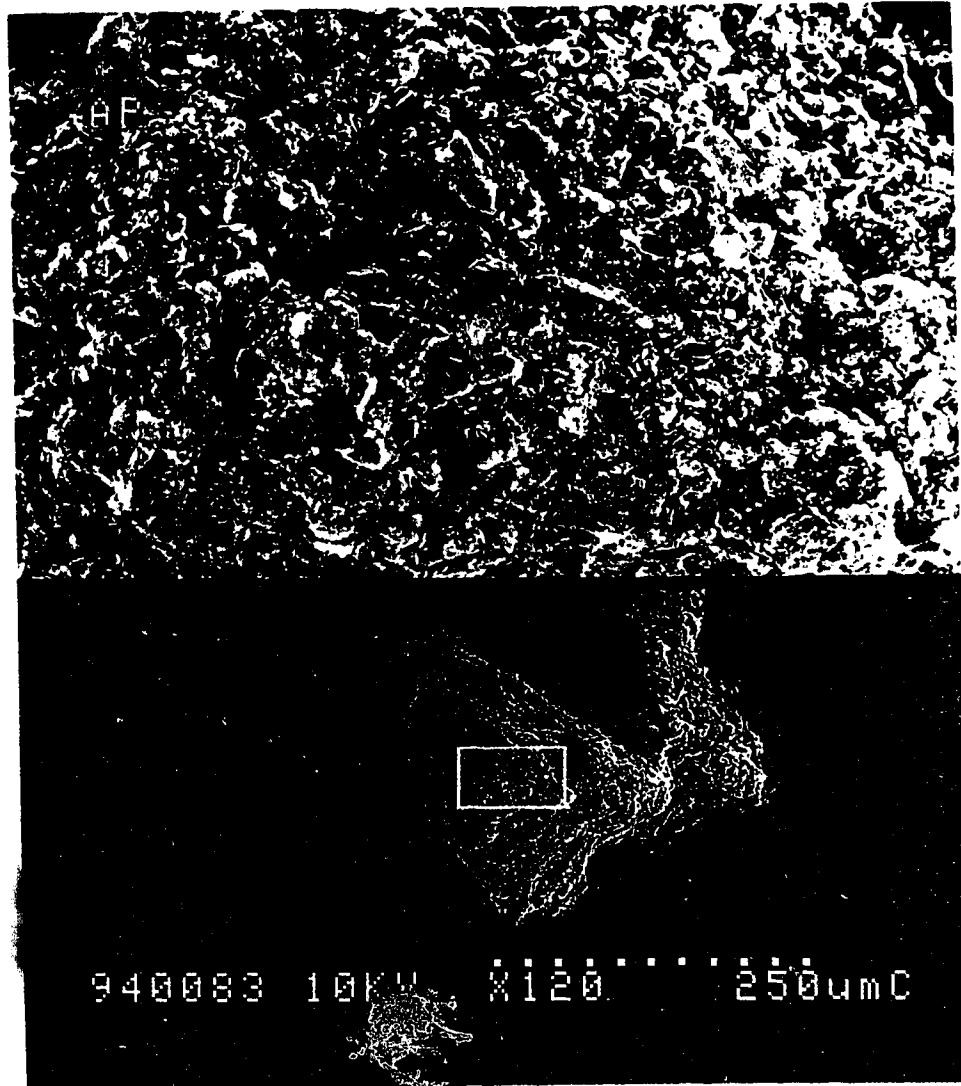


Plate 5.6 The Microstructure of a Polymeric Floc at a High Mixing Rate (kaolin = 20 mg/L, alum= 5 mg/L, polymer = 0.5 mg/L, NaHCO<sub>3</sub> = 100 mg/L,  $\overline{G}_c = \overline{G}_f = 400 \text{ s}^{-1}$ , and  $t_f = 30 \text{ min.}$ )

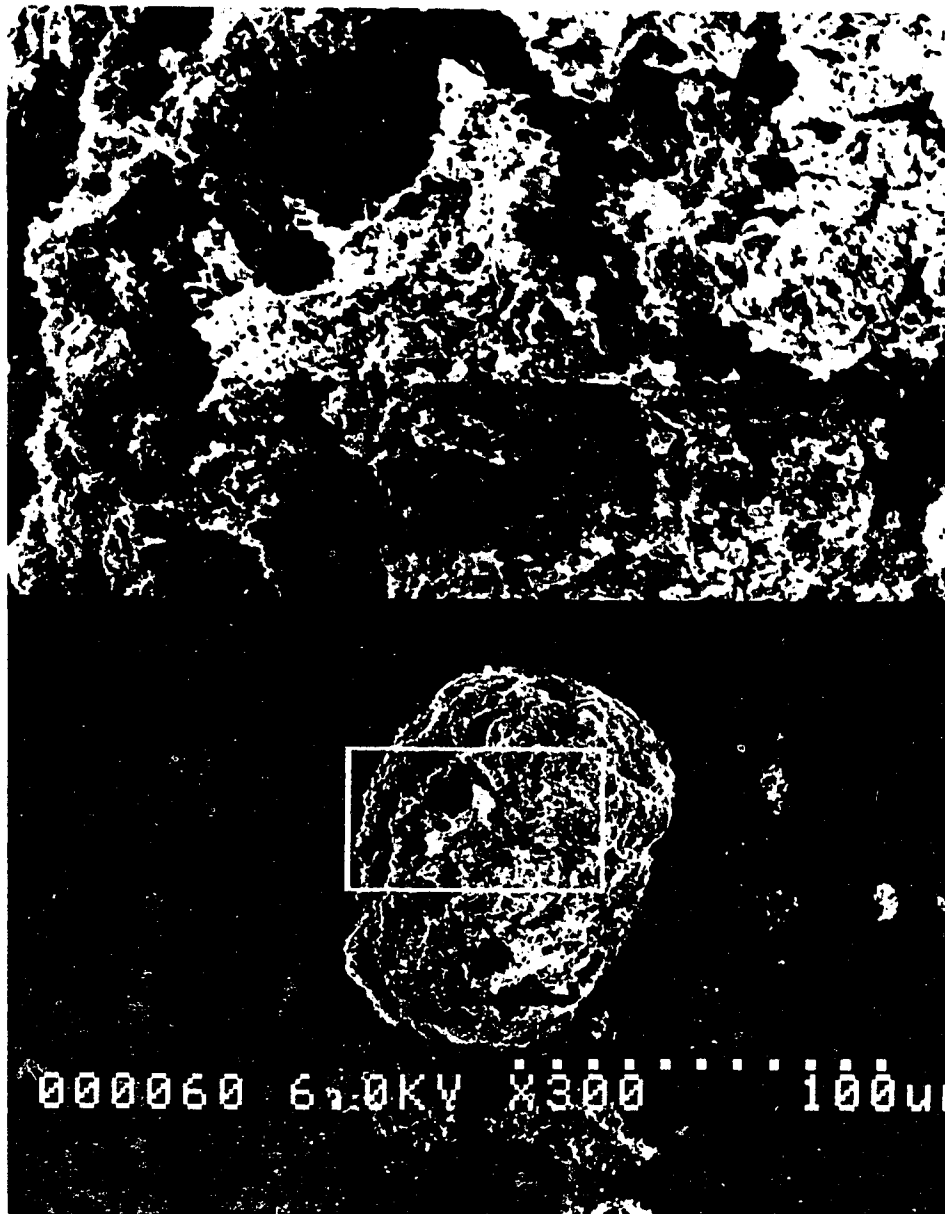


Plate 5.7 The Microstructure of of a Alum Flocc with Big Size ( $d \cong 70 \mu\text{m}$ ) (kaolin = 20 mg/L, alum= 5 mg/L, polymer = 0.5 mg/L,  $\text{NaHCO}_3 = 100 \text{ mg/L}$ ,  $\bar{G}_c = 200 \text{ s}^{-1}$ ,  $\bar{G}_f = 30 \text{ s}^{-1}$ ,  $t_c = 1 \text{ min}$ , and  $t_f = 30 \text{ min}$ .)

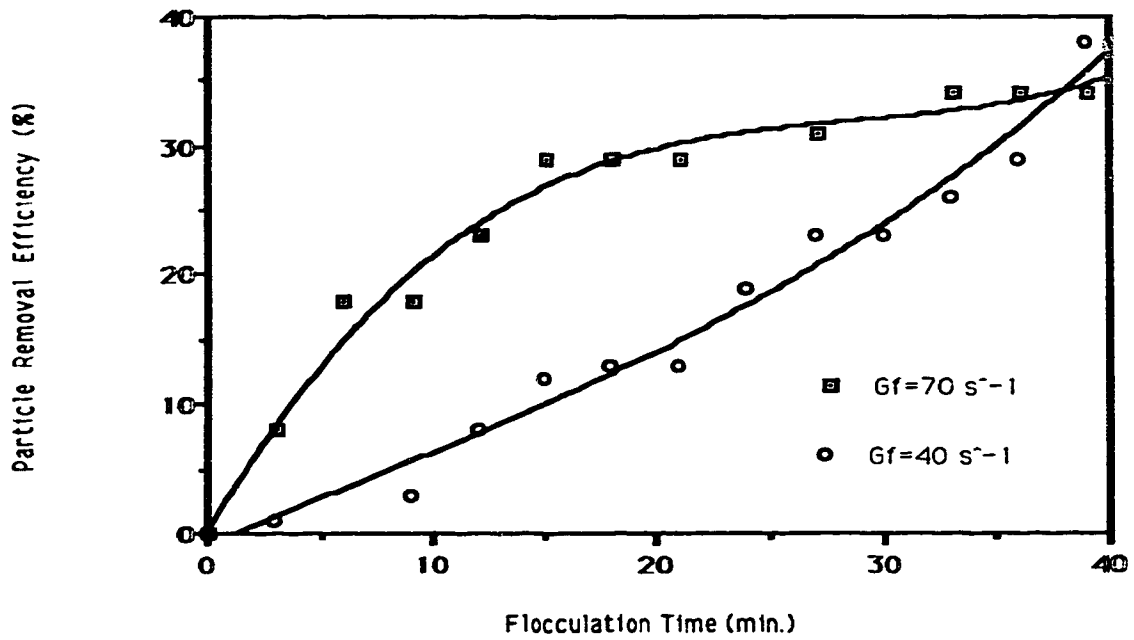


Figure 5.56 Effect of Mixing on Particle Removal Efficiency of Alum Flocculation (alum=5mg/L, kaolin=20 mg/L, pH=8,  $\text{NaHCO}_3=100 \text{ mg/L}$ ,  $\bar{G}_c=150 \text{ s}^{-1}$  for 1 min. )

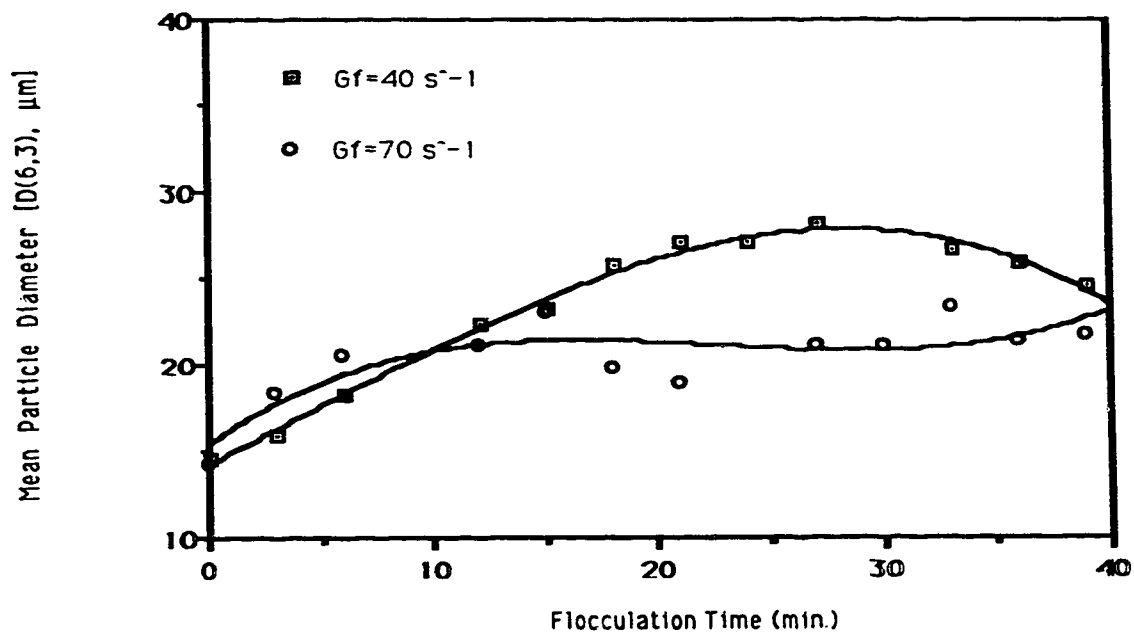


Figure 5.57 Effect of Mixing on the Growth Rate of the Alum Floc (alum=5mg/L, kaolin=20mg/L, pH=8,  $\text{NaHCO}_3=100 \text{ mg/L}$ ,  $\overline{G}_c=150 \text{ s}^{-1}$  for 1 min. )



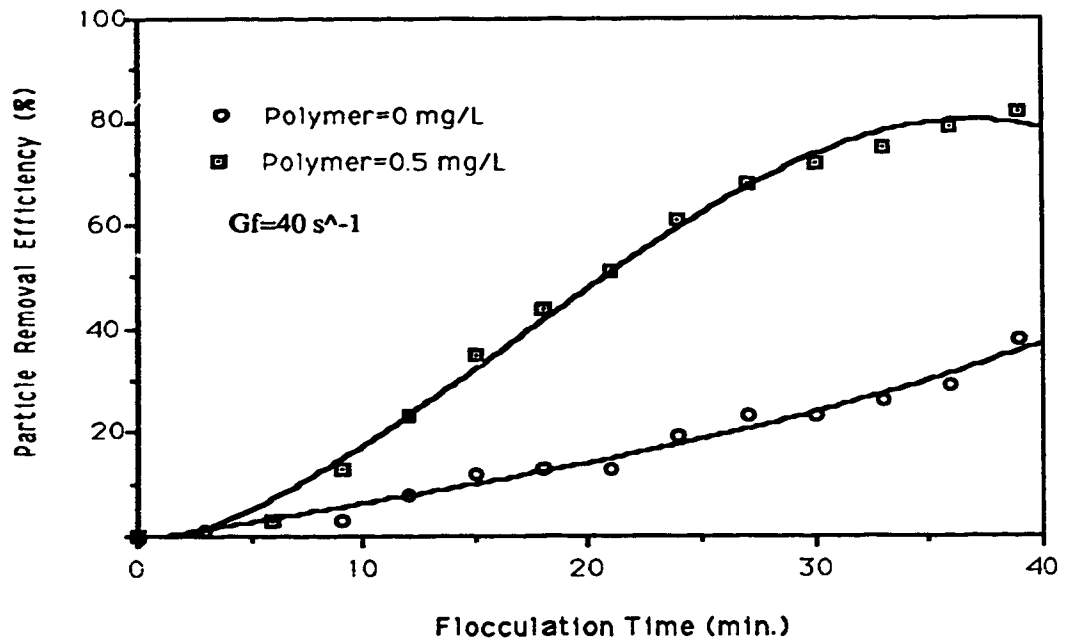


Figure 5.58 Effect of Polymer on Particle Removal Efficiencies at  $\bar{G}_f=40 \text{ s}^{-1}$   
 [kaolin=20 mg/L, alum=5mg/L,  $\text{NaHCO}_3=100 \text{ mg/L}$ , pH=8,  
 $\bar{G}_c=150 \text{ s}^{-1}$ ]

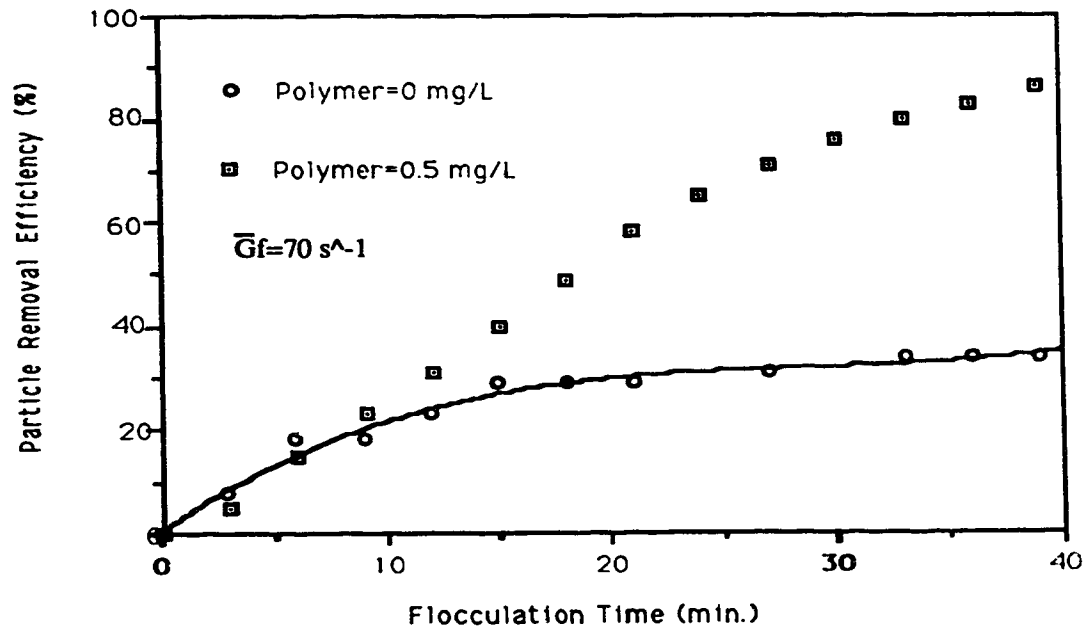


Figure 5.59 Effect of Polymer on Particle Removal Efficiencies at  $\bar{G}_f=70 \text{ s}^{-1}$   
 [kaolin=20 mg/L, alum=5mg/L,  $\text{NaHCO}_3=100 \text{ mg/L}$ , pH=8,  
 $\bar{G}_c=150 \text{ s}^{-1}$  for 1 min.,  $\bar{G}_f=70 \text{ s}^{-1}$  ]

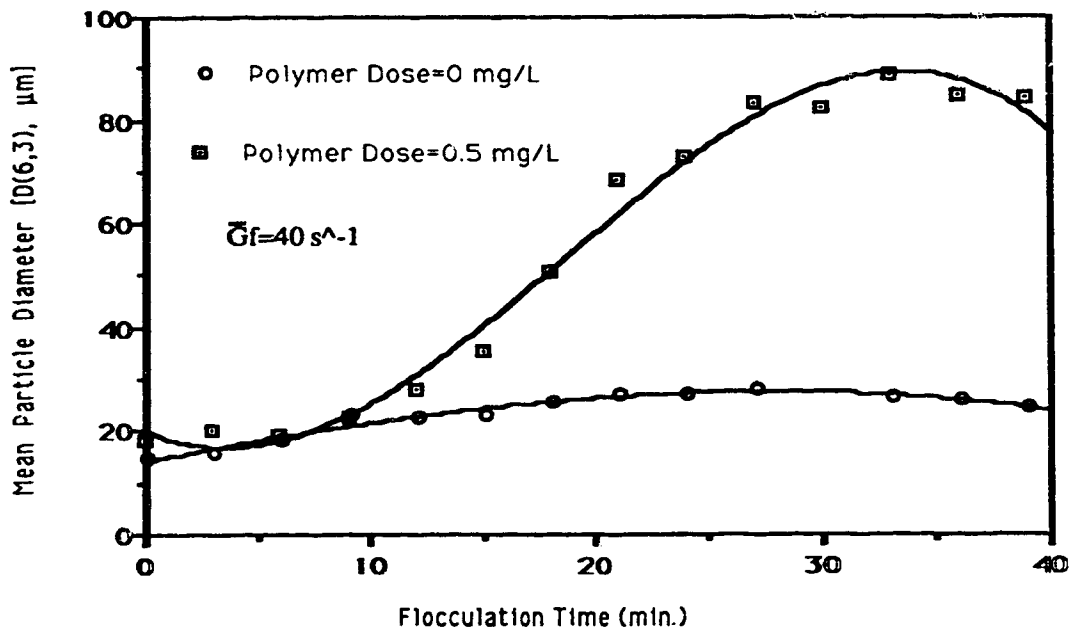


Figure 5.60 Effect of Polymer on the Rate of Floc Growth at  $\bar{G}_f=40 \text{ s}^{-1}$ [kaolin=20 mg/L, alum=5mg/L,  $\text{NaHCO}_3=100 \text{ mg/L}$ , pH=8,  $\bar{G}_c=150 \text{ s}^{-1}$  for 1 min. ]

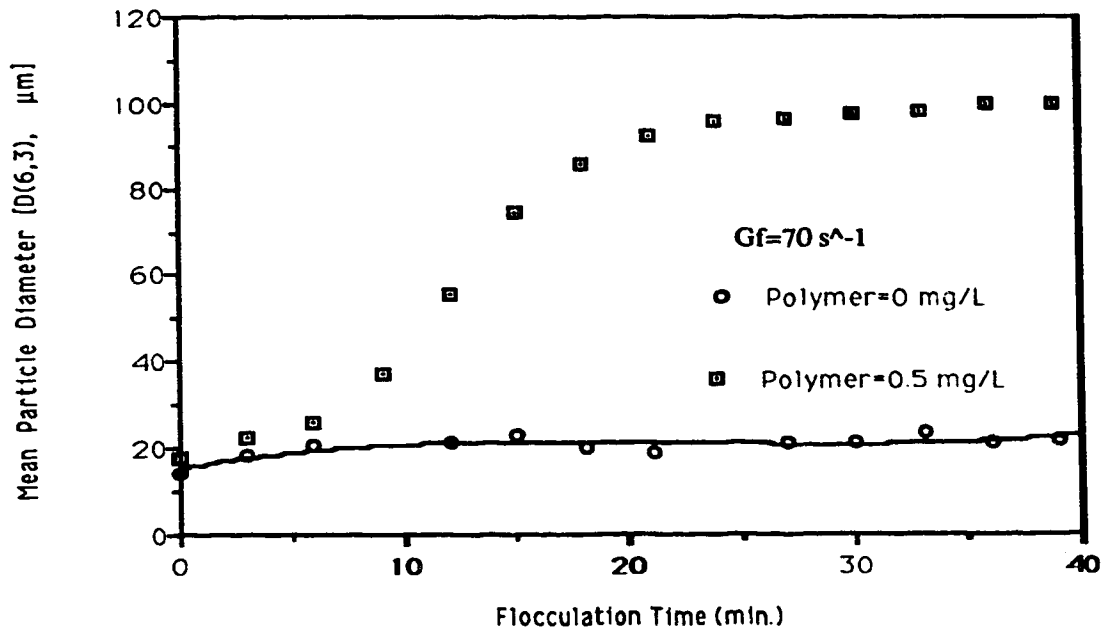


Figure 5.61 Effect of Polymer Dose on the Rate of Floc Growth at  $\bar{G}_f=70 \text{ s}^{-1}$   
kaolin=20 mg/L, alum=5mg/L,  $\text{NaHCO}_3=100 \text{ mg/L}$ , pH=8,  $\bar{G}_c=150 \text{ s}^{-1}$   
for 1 min.]

## 6 CONCLUSIONS

The significance of this study is to provide a method to transfer the raw data of particle size distributions into useful information for the selection, design, optimization, and operation of coagulation and flocculation processes in water treatment. The conclusive result is that rules, mechanisms, and kinetic models derived from alum flocculation studies are applicable to polymer aided flocculation. The experimental results also lead to following conclusions:

- 1 The experimental conditions play a central role in polymer-aided flocculation. The optimum process conditions for the coagulation and flocculation of 20 mg/L kaolin suspension are; alum = 5 mg/L, polymer = 0.5 mg/L, pH = 8,  $\text{NaHCO}_3$  = 100 mg /L.
- 2 At optimum process conditions,  $\bar{G}_f$  can be employed as a rate controlling factor. The optimum  $\bar{G}_f$  -value used in the polymer-aided flocculation occurs at  $\bar{G}_f=200$   $\text{s}^{-1}$ ;  $\bar{G}_f$  has a slight impact on the performance of flocculation at  $\bar{G}_f=200$  to 400  $\text{s}^{-1}$ ; and the floc break-up becomes substantial at  $> 400$   $\text{s}^{-1}$ . Moreover, the results demonstrate that the optimum mixing rate ( $\bar{G}_f=200$   $\text{s}^{-1}$ ) used in polymer-aided flocculation is significantly higher than that used in alum flocculation ( $\bar{G}_f=40$   $\text{s}^{-1}$ ). This is due to the increase in floc strength resulting from the use of polymer.
- 3 The performance of the polymer-aided flocculation can be evaluated by the maximum mean floc diameter ( $d_{\text{max}}$ ) and the floc buildup time( $t_b$ ). The rate of the polymeric floc growth can be monitored by: the mean floc growth rate ( $\frac{R_{t_2+t_1}}{2}$ )

$(\frac{R_{t_2+t_1}}{2})$  at given  $t_f$ ; floc growth constant ( $\mu_i$ ) in a given stage of floc growth process; and floc buildup time ( $t_b$ ) in overall floc growth process.

- 4 The rate of polymer-aided flocculation follows the first order kinetic model with respect to the primary particle concentration at  $0 < \bar{G}_f \leq 400 \text{ s}^{-1}$  and  $0 \leq t_f \leq 30$  minutes. The rate of polymeric floc growth may be described by a log-normal law at  $0 < \bar{G}_f \leq 800 \text{ s}^{-1}$ .
  
- 5 The use of polymer as a coagulant aid reduces alum dose, and forms a bigger denser floc. It dramatically improves the efficiency of fine particle removal, and lowers the cost of the treatment. Therefore, it is highly recommended for water treatment.

## **7 LIMITATIONS AND SUGGESTIONS OF THE STUDY**

The limitations and the suggestions of this study were summarized as follows:

- 1 **The errors arisen from the particle size analyzer.** The raw data generated from the particle size analyzer were subject to various sources of errors: (1) fluctuation in sampling and sample flow rate; (2) contamination of the sample line by residual particles; (3) time lag between acquiring and analyzing the samples; (4) floc breakup in the aperture tube, or at the orifice sensing zone of the instrument; (5) over-concentration of a sample due to the fluctuation of the initial particle concentration; (6) formation of microbubbles which were counted as particles.; (7) loss of few number concentration tested due to big flocs either being outside the sensor range, or settling out of the suspension.; and (8) fluctuations in the initial particle size distribution due to the agglomeration of kaolin particles. However, by controlled and identical procedures for dispersion, mixing, and sampling, the reproducibility of the results could be controlled. The results indicated that the reproducibility of kinetic data was fairly good
- 2 The investigation of kaolin-alum-polymer adsorption theories which was used to describe the mechanism of the first stage of the floc growth curve was unable to be completed by the kinetic analysis; thus, the study of the equilibrium thermodynamics is required in future work.
- 3 The fluid mechanism regimes which may affect flocculation-sedimentation performance should be included in further kinetic studies. This kinetic study was based on the assumption that mixing was isotropic, and a

average vessel parameter  $\overline{G}_f$  was used to control the mixing rate. The results did not include the impact of local hydrodynamics (especially in the impeller zone) and fluid flow patterns induced by different flocculation impellers at different mixing intensities.

- 4 Care should be taken as the mean particle sizes are compared. The sizes of the floc given in this study [ $D(6,3)$  and  $d_{max}$ ] were relative values. This allowed comparisons to be made between different experimental conditions if the identical methods of measurement and evaluation were used. However, the values did not represent the real dimensions of the floc as they were calculated based on particle size distributions.
- 5 Comparisons among alum flocculation, polymer-aided flocculation, and polymer flocculation which used only a polymer should be made in future work. Although the polymer flocculation experiments were conducted in different  $\overline{G}_f$ -values in this study, and results demonstrated the same trend of the variation of  $d_{max}$  with  $\overline{G}_f$  in polymer-aided flocculation, kinetic analyses, however, were not performed due to the time limitation.
- 6 Scale-up flocculation experiments should be performed in order to simulate the full scale application. Care should be taken when  $\overline{G}_f$  is used as a scale-up parameter. As the optimum  $\overline{G}_f$  value ( $\overline{G}_f = 200 \text{ s}^{-1}$ ) and the critical  $\overline{G}_f$  value ( $\overline{G}_f = 400 \text{ s}^{-1}$ ) determined from this study were based on the two-liter flocculator. It was reported that when  $\overline{G}_f$  was held constant, the performance of the flocculation deteriorated with increased size of the flocculator due to the variation of fluid impeller mechanism (Stanley, 1995). Therefore, it is important to search for another parameter to use as



**a scale-up criterion. This is currently under study by Stanley and other researchers (Stanley, 1995).**

## 8 REFERENCES

- Alderliesten (1984). "A Nomenclature for Mean Particle Diameters". Anal. Proc., v2?, May.
- Ali. W. (1985). "Chemical Aspect of Coagulation in Lakes". Ph. D Thesis, Johns Hopkins Univ. p222.
- American Society for Testing and Materials (1987). "Defining Size Calibration, Resolution, and Counting Accuracy of a Liquid-borne Particle Counter Using Near Monodisperse Spherical Particulate Material". Annual Book of ASTM Standards. Designation F658-87.
- American National Standards Institute (1990). "Hydraulic Fluid Power-calibration Method for Liquid Automatic Particle Counter Using Latex Spheres". ANSI/ (NFPA), T2.9.6 R1- 19.
- Amirtharajah, A. (1981). "Initial Mixing Proc. AWWA Seminar on Coagulation and Filtration: Back to the Basics".
- Amirtharajah, A. & Kawamura, S. (1983). "System Design for Polymer Use. Proc.". AWWA Seminar on Use of Organic Polyelectrolytes in Water Treatment.
- Amirtharajah, A. & Mills, K.M. (1982). "Rapis-Mix Design for Mechanisms of Alum Coagulation". Jour AWWA, v74, n4, p210.
- Amirtharajah, A. (1990). "Coagulation Processes: Destabilization, Mixing, and Flocculation". Water Quality and Treatment p283.
- Amirtharajah, A; and O'Melia, C. R. (1990). "Coagulation Processes: Destablization, Mixing, and Flocculation". Water Quality and Treatment, p336.
- Amirtharajah, A; Clark, M. M. and Trussell R. R. (1991). Mixing in Coagulation and Flocculation. AWWA Association Research Foudation.

- Argaman, Y. and Kaufman, W. J. (1968). "Turbulence in Orthokinetic Flocculation".  
SERL Rept. No. 68-5, Sanit. Eng. Research Lab., Univ. of California, Berkeley.
- Argaman, Y. & Kaufman, W.J. (1970). "Turbulence and Flocculation". J. San. Eng. Div.,  
ASCE 96, v2, n4, p223.
- Bache, D.H. & Al-Ani S.H.(1989). "Development of a System for Evaluating Flocculation  
Strength". Wat. Sci. Tech. v 21, p529-537.
- Baes, C. F. and Mesmer, R. E. (1976.) The Hydrolysis of Cations. John Wiley & Sons,  
New York.
- Barnett, P.R., Skougstad, M.W. and Miller, K.J. (1969). "Chemical Characterization of a  
Public Water Supply". J. Am. Water Works Assoc.,v 61, p60-67.
- Baes, C. F. and Mesmer, R. E. (1976). The Hydrolysis of Cations. John Wiley & Sons,  
New York.
- Beji Malek, Brown. (1981). "Virus Removal by Coagulation and Flocculation". AWWA  
J , V 73, n3, p164(5).
- Benedek, A. (1976). "Assessment of Polyelectrolytes for Phosphorus Removal". Env  
Canada Research Report No. 37.
- Benfield, Larry D., Joseph F. Judkins, and Borvon L. Weand, (1982), "Fundamentals of  
Surface and Colloidal Chemistry"; "Coagulation in Water Treatment"; and  
"Solubility Equilibria". Process Chemistry for Water and Wastewater Treatment,  
p191-200,211-235, 108-139.
- Bhaskar, G. V. ; Campanella, O. H. and Munro, P. A. (1993). "Effect of agitation on the  
Coagulation Time of Mineral Acid Casein Curd: Application of Smoluchowski's  
Orthokinetic Aggregation Theory". Chem. Eng. Sci. v48, n24, p4075 - 4080.
- Birkner, F. B. and Edzwald, J. K. (??) "Nonionic Polymer Flocculation of Dilute Clay  
Suspensions". J. AWWA, v61, n12, p645-651.
- Birkner, F. B. and Morgan, J. J. (1965). "Polymer Flocculation Kinetics of Dilute  
Colloidal Suspension". J. AWWA, v60, n2, p175 -191.

- Birkner, F.B. and Margon S.J. (1968). "Polymer Flocculation of Dilute Colloidal Suspensions". Journal AWWA, v60, p175.
- Black, A. P. ; Ball, A. I.; Boudet, R. A.; and Campbell, T. N. (1959). "Effectiveness of Polyelectrolyte Coagulant Aids in Turbidity Removal". J. AWWA, v31, n2, p247-262.
- Black, A. P. and Willems, D.G. (1961). "Electrophoretic Studies of Coagulation for the Removal of Organic Color". J. AWWA, v53, p589.
- Black, A. P. ; Birkner, F. B.; and Morgan, J.J. (1965). " Destabilization of Dilute Clay Suspensions with Labeled Polymers". J. AWWA, v57, n12, p1547.
- Black, A. P. ; Birkner, F. B.; and Morgan, J.J. (1966). " The Effect of Polymer Adsorption on the Electrokinetic Stability of Dilute Clay Suspensions". J. Coll. Sci., v21, p626-648.
- Bosanac, G., Grabaric, Z and Papic S. (1993). "Treatment of Wastewaters from Dye Industry". Environ Technol (Lett), v14, n4, p385(6).
- Botet, R., Jullien, R. and Kolb, M. (1986). Fractals in Physics, L. pietronero and E. Tosatti, Eds., Elsevier, Amsterdam.
- Bowine, Yames E. (1977). "Chemical Precipitation-Coagulation for Organic Color Removal from Groundwaters". Water Resources B, v13, n6, p1269(12).
- Brown, B.M. (1981). "Virus Removal by Coagulation and Flocculation". J. AWWA, V 73, n3, p164(5).
- Bruno, J. (1958). "Flocculation anf Gelation Phenomena". Organic Colloids, p223-230.
- Bowine, Yames E. (1977). "Chemical Precipitation-Coagulation for Organic Color Removal from Groundwaters". WaterResources B, v13, n6, p1269(12).
- Brown, A. and Leighton, J. (1966). "Some Solution to Sludge Treatment Problems at Fishmoor Treatment Plant". Institution of Public Health Engineers.
- Camp, T.R. & Stein, P.C. (1943). Velocity Gradients and Internal Work in Fluid Motion. J Boston Soc Civil Engrg., v30, n10, p217.

- Camp, T.R. (1953). "Flocculation and Flocculation Basins. Proc. ASCE, v79, n9, p1.
- Campbell, P. G., Bisson, C. M. (1983). Anal. Chem. v55, p2246-2252.
- Clark, M.M. (1985). "Critique of Camp and Stein's RMS Velocity Gradient". Journal of Environmental Engineering, ASCE. v111, n6, p741-754.
- Clark, M.M. et al. 1988. "Hydrodynamic Conditions of Aluminium-Humic Acid Flocculation". AWWA Annual Conf., Orlando, Fla.
- Clark, M.M. and Flora, J. R. (1991). "Floc Restructuring in Varied Turbulent Mixing". J. of Colloid and Interface Science, v147, n2, p407-421.
- Clark, M.M. (1993). "Mixing and Aluminium Precipitation". Environ. Sci. Technol. v27, p2181-2189.
- Clark, M.M., Srivastava, R. M., Lang, J.S., Trussel, R.R., McCollum, L.J., Baily, D., Christie, J.D., and Stolarik, G. (1994). "Selection and Design of Mixing Processes for Coagulation". American Water Works Association Research Foundation and American Water Works Association, Denver, CO. p150
- Cleasby, J.L. (1984). "Is Velocity Gradient a Valid Turbulent Flocculation Parameter?". Journal of Environmental Engineering, ASCE. v110, n5, p875-897.
- Committee Report. (1982). "Survey of Polyelectrolyte Coagulant Use in the United States". AWWA J. V74, N11, p600(9).
- Cohen, J. M. (1957). "Improved Jar Test Procedure". AWWA J. V49, p1425.
- Cruz, M., Jacobs and Fripiat, J.J., (1972). "The Nature of the Interlayer Bonding in Kaolin Minerals". Proceedings of the International Clay Conference, Madrid, p35 to 44.
- Dahl, B. W.; Zelinski, J. W.; and Taylor, O. W. (1972). "Polymer Aids in Dewatering and Elutriation". J. Water Poll. Control Fed. v42 n2 p201-211.
- Dale, H. P. (1973). "Polymers: Their Characteristics, Chemistry, and Production". The 54th Annual Conf. California Section AWWA, Oakland.

- Decook, K.L. (1980). "Hydrological and Environmental Controls on Water Management in Semiarid Urban Areas". NTIS Report Pb 81-109704 , Sept. 80 (77).  
Designation E-20-85. (1985). "Standard Particle for Particle Size Analysis of Particulate Substances in the Range of 0.2 to 75 Micrometres by Optical Microscopy". American Society for Testing and Materials, p17-24.
- Doe, P.W. (1968). "A Report on the Disposal of Sludge from Water Treatment Plants". British Waterworks Association.
- Donati, C. D. (1991). "Assessment of Coagulants for Water Treatment-Progress Report". Australian Centre for Water Treatment and Water Quality Research Internal Report.
- Donasch, K. et al. (1986). Chem. Tech., v38, p384.(French)
- Driscoll C. T. (1984). Int. J. Environ. Anal. Chem. 16 : 267-278.
- Driscoll C. T. 1985. Environ. Health Perspect. v63, p93-104.
- Durst, F; Macagno, M. (1986). Powder Technol. v45, p223-44.
- Eckenfelder, W. Wesley. (1987). Industrial Water Pollution Control. p29-61.
- Edz, J. K. et al. (1977). "Polymer Coagulation of Humic acid water". ASCE Journal Environ. Engineering Division", v103, n EE6, p989.
- EPA Report. (1975). "Coagulant Aids of Water Treatment". Journal AWWA, v68, n8, p468.
- Fair, G. M. & Gemmel, R. S. (1964). " A Mathematical Model of Coagulation". J. Colloid. Sci., v19, p360.
- Fountain, R.L. (1982). "Chemistry for Operators". Water Treatment Plant Operation. p120.
- Francois, R.J. and Van Haute, A.A. (1985). Water Research, v19, n10, p1249.
- Francois, R.J. (1985). "The Influence of Mixing Parameters and Water Quality on the Flocculation of Kaolinite with Aluminium Sulphate". Chemistry for the Protection of the Environment.

- Francois, R.J. (1987). "Strength of Aluminium Hydroxide Floccs". Wtr. Res., v21, n9, p1023.
- Francois, R.J. (1988). "Growth Kinetics of Hydroxide Floccs". J. AWWA, v80, n6, p92.
- Francois, R.J. (1989). "Influence of the Flocculation Process on Floc Strength and Floc Regrowth Ability". J. AWWA, In review.
- Friedlander, S. K. 1977. "Smoke, Dust, and Haze". Wiley-Interscience.
- Fuchs, N. (1934). "Uber Die Stabilitat und Aufladung der Aerosole". Zeitschrift Physik, v89, p736.
- Geothals, E. J. (1979). Polymeric Amines and Ammonium Salts.
- Ghosh, M.M.; Cox, C.D. and Prakash T.M. (1985). "Polyelectrolyte Selection for Water Treatment". J. AWWA, v77, n3, p67(7).
- Gillespie, T. (1960). "The Limited Flocculation of Colloidal Systems". J. Colloid. Sci., v15, p313.
- Gilman K.; Trattner R. and Cheremisinoff P.N. (1979-a). "Flocculants Ease Costs, Raise Quality of Wastewater: Part 1". Water & Sewage Works, v126, n7, p58.
- Gilman K.; Trattner R. and Cheremisinoff P.N. (1979-b). "Flocculants Ease Costs, Raise Quality of Wastewater Treatment". Water & Sewage Works, v126, n8, p54.
- Glaser, H.T. and Edzwald, J.K. (1979). "Coagulation and Direct Filtration of Humic Substances with Polyethylenimine". Environ. Science Tech., v13, p299.
- Glasgow, L. A. & Hsu, Y. P. (1982). "An Experimental Study of Floc Strength". J. AICHE, v28, n5, p779.
- Gregory, J. (1978). "Effect of Polymers on Colloid Stability". in K.J. Ives (ed.), The Scientific Basis of Flocculation, Sijthoff and Noordhoff, The Netherlands.
- Grim, R. E. (1962). Applied Clay Mineralogy. New York: McGraw-Hill Book Co.
- Gutcho, S. (1977). Waste Treatment with Polyelectrolytes and Other Flocculants, p1-37.

- Haff, J. D. (1976). "Removal of Humic Acid Using Alum and Synthetic Polyelectrolytes". AWWA 96th Annual Conf: water Technology and Research, V2, P17-22(10).
- Hahn, H.H. & Stumm, W. (1968). "Kinetics of Coagulation With Hydrolyzed Al(III)". Jour. Colloid Inter. Sci., v28, n1, p134.
- Hahn, H & Stumm, W. (1970). "The Role of Coagulation in Natural Waters ". Amer. Jour. Sci., v268, p354.
- Hanasaki, T; Ohnishi, H; Nikaidoh, A; Tanada S and Kawasaki, K. 1985. "Determination of Trace Polymer in Waste".
- Hargesheimer, E. E; Lewis C. M. and Yentsch, C.M. (1992). Evaluation of Particle Counting as a Measure of Treatment Plant Performance, p45-69.
- Hahn, H & Stumm, W. (1970). "The Role of Coagulation in Natural Waters ". Amer. Jour. Sci., v268, p354.
- Han, M & Lawler, D. F. (1992). "The (Relative) Insignificance of G in Flocculation". Journal American Water Works Association, v84, n10, p79-91.
- Hanson, A.T. & cleasby, J.L. (1990). "The Effect of Temperature on Turbulent Flocculation: Fluid Dynamics and Chemistry ". Journal American Water Works Association, v82, n11, p56-73.
- Hargesheimer, E.E.; Lewis, C. M.; and Yentsch, C. M. (1992). Evaluation of Particle Counting as a Measure of Treatment Plant Performance, p 45-69. AWWA Research Foundation.
- Harris , S. M.; Kaufman, W.J. and Krone, R. B. (1966). "Orthokinetic Flocculation in Water Purification". Proc. of the Amer. Soc. of Civil Eng., J. Sanit. Eng. Div., p95-111, December 1966.
- Hashimoto, K.; Hasegawa, T.; Onitsuka, T.; Goto, K.; and Tamboo, N. (1991). "Inorganic Polymer Coagulants of Metal-polysilicate Complex". Water Supply, v9, n1 p s65-s70.



- Healy, T. W. and La Mer, V. K. (1962). "The Adsorption-Flocculation Reactions of a Polymer with an Aqueous Colloidal Dispersion". J. Phys. Chem., v66, p1835-1837.
- Hek, De, Stol, H., R. J. and Bruyn, P. L. De. (1978). "Hydrolysis Precipitation Studies of Aluminium (III) Solution". J. Colloid Interface Sci., v64, n1, p72-89.
- Helfrich, G.; Haas, D.; Fox K. and Studstill, A. (1992). "Ferric Chloride as an Alternative Coagulant". Water Supply, v19, n4, p155-158.
- Hespanhol, I. and Selleck, R. E. (1975). "The Role of Polyelectrolytes in Flocculation Kinetics". Serl Report No. 75-2 Sanitary Engineering Research Laboratory.
- Higuchi, W. I., et al (19??). Kinetics of Aggregation in Suspensions. J. Pharm. Sciences, v54, p510.
- Hilson, M. A. (1970). Sludge Conditioning by Polyelectrolytes
- Hirtzel, C. S. and Rajagopalan. (1985). Colloidal Phenomena: Advanced Topics. Noyes.
- Hozumi, H. & Tambo, N. (1974). "A Rational Design of Suspended Solids Contact Clarifier". Kogko Yosui (Jour. Jan. Ind. Wtr. Supply), v193, n10, p23.
- Huck, P. M. and Murphy, R. L. (1978). "Kinetics Model for Flocculation with Polymers". J. Env. Eng. Div., EE4 104, p767.
- Hudson, H.E. Jr. and Wagner, E.G. (1981). "Conduct and Use of Jar Tests ". Journal of American Water Works Association, v73, n4, p218-224
- Hunter, K. A. and Liss, P.S. (1979). "The Surface Charge of Suspended Particles in Estuarine and Coastal Waters". Nature, v282, p823.
- James D. Haff. (1976). "Removal of Humic Acid Using Alum and Synthetic Polyelectrolytes". AWWA 96th Annual Conf: water Technology and Research, V2, P17-22(10).
- Jekel, M. R., and Heinzman, B. (1989). "Residual Aluminium in Drinking-water Treatment". Aqua, 38, p.281-283 Lewis(Ed.).

- Joyce, Thomas W., and Sailesh G. Lathia. (1978). "The Calcium-Magnesium Coagulation Process". TAPPL, v61, n10, p67-70.
- Kace J.S. & Linford H.B. (1975). "Reduced Cost Flocculation of a Textile Dyeing Wasterwater". JWPCE, v47, n7, p1971(7).
- Kaeding, U.W.; Drikas, M.; Drllaverde, P.J.; Martin, D. and Smith, M.K. (1992). "A Direct Comparision between Aluminium Sulphate and Polyaluminium Chloride as Coagulants in a Water Treatment Plant". Water Supply, v10, n4 p199-132.
- Kane, J. V.; La Mer V. K. and Lindford, H. B. (1963). "The Filtration of Silica Dispersions Flocculated by High Polymers". J. Phys. Chem., v67, p1977-1981.
- Katchalski, A. (1951). "Solutions of Polyelectrolytes and Mechanochemical Systems". J. Polymer Sci. v7, n4, p293-412.
- Kenneth J. Tascchi (1977) "Polyelectrolyte Usage in Industrial Wastewater Treatment". Industrial Water Engineering, v14, n7, p12(6).
- Keys, R. O. & Hogg, R. (1978). "Mixing Problems in Polymer Flocculation". Water 1979, AIChE Symp. Ser. 190, v 75, p63.
- Kim, W. (1963). "The Effect of Polyelectrolytes on Water Clarification". Ph.D. Thesis, Uni. of Calif., Berkeley (unpublished).
- Kim, W. ; Ludwig, H. F. and Bishop, W. D. (1965). "Cation-Exchange Capacity and pH in the Coagulation Process". J. AWWA, v57n3, p327.
- King, P.H. and Blankenship D.C. (1979). "Managing Organic Polymer Water Treatment Sludge". ASCE Environ Eng Natl Conf. San Francisco, p136(6).
- Klimpel, R.C. & Hogg, R. (1986). "Effects of Flocculation Conditions on Agglomerate Structure". Jour. Colloid Inter. Sci. v113, n1, p121.
- Krone, R. E. and Johnson, E. E.. (1965). "Organic Polyelectrolytes-A New Approach to Raw Sewage Flocculation". The 38th Annual Conf. of the WPCE.
- Kusuda,T. (1973). "Effect on Floc Preperities by Condition of Floc Formation". Proc. Japn. SCE, v217, n9, p33.

- Laapas, Freiberg, H and Forschungsh. (1985). A700, p99-108 (german). Chem. Abstr. 1985, v 103, 21724w.
- Lagvankar, A.L. & Gemmell, R.S. (1968). "A Size-density Relationship for Floccs". J. AWWA, v60, n9, p1040.
- La Mer, V. K.; Smellie, R. H.; and Lee, P. K. (1957). "Flocculation, Subsidence, and Filtration of Phosphate Slimes-IV. Flocculation by Gums and Polyelectrolytes and Their Influence in Filtration Rate". J. Coll. Sci., v12, p230-239.
- La Mer, V. K. and Healy, T. W. (1963). "Adsorption- Flocculation of Macromolecules at the Solid-Liquid Interface". Rev. Pure and Appl. Chem., v13, p1112-133.
- Langelier, W.F.; Ludwig, H. F. and Ludwig, R. G., (1953). "Flocculation Phenomera in Turbid Water Clarification". Trans. ASCE, v118, p147.
- Lawler, D. F. (1979). "A Particle Approach to the Thickening Process". Ph. D. Thesis, Uni. North Carolina, Chapel Hill. p259.
- Lawler, D. F. ; O'Melia, C. R.; and Tobiasson, J. E. (1980). "Integral Water Treatment Plant Design: From Particle Size to Water Characterization, Fate, Effects, and Removal ". Adv. Chem. Ser. 189, p353-389.
- Lawler, D. F. and Wilkes, D. R. (1984). " Flocculation Model Testing: Particle Sizes in a Softening Plant". J. AWWA, v76, n7, p90.
- LaZerta, B.D. (1984 ) Can. J. Fish Aquat Sci. v41, p766-776.
- Lee, W., Ettelt, A. (1975). "Dual Polymer Treatment of Variety Bakery Products wastewater". Purdue University 30th Industrial Waste Conf. May 6-8, P712(12).
- Leentvaar, J. and Rehun, M. (1983). "Strength of Ferric Hydroxide Floccs". Water Res. v17, p845.
- Leong, L. R. , Craddock, P.P. & Carol Ruth James, C. R. (1992). "Pilot Study to Meet Drinking Water Regulations". Environ. Eng. p504-509.
- Letterman, R.D.; Quon, J.E.; & Gemmell, R.A. (1973). "Influence of Rapid-Mix Parameters on Flocculation". J. AWWA, v65, p716.

- Letterman, R.D. & Pero R.W. (1990). "Contaminants in Polyelectrolytes Used in Water Treatment". J. AWWA, v82, n11, p87(11).
- Leu, R.J. & Ghosh, M.M. (1988). "Polyelectrolyte Characteristics and Flocculation". Jour. AWWA, v80, n4, p159
- Levine, S & Friesen, W. I. (1987). "Flocculation of Colloid Particles by Water-Soluble Polymers". Flocculation in Biotechnology and Separation Systems, p3-p20.
- Lieberman (1988). "Calibrations Requirements and Methods for Liquidborne Particle Counters". J. Enviro. Sci.(May/June): p34-36.
- Linda Rae Leong, Patti P. Craddock and Carol Ruth James (1992). "Pilot Study to Meet Drinking Water Regulations". Enviro. Eng. p504-509.
- Link, W. F. and Booth, R. B. (1960). "Physical Chemical Aspects of Flocculation by Polymers". Trans. Amer. Inst. Min. Met. Eng. v217, 364-371.
- Lyklema, J. 1978. "Surface Chemistry of Colloids in Connection with Stability". The Scientific Basis of Flocculation.
- Matsuo, T and Unno, H. (1981) "Forces Acting on Floc and Strength of Floc". J. Envir. Engrg., v108, EE3, p527.
- McGraw-Hill Book Co., New York, 2nd ed. (1979) "Chemical Unit Processes, "Wastewater Engineering: Treatment, Disposal, Reuse", p257-267.
- Michaelis, A. S. (1954.). "Aggregation of Suspended Solids by Polyelectrolytes". J. Ind. Eng. Chem., v46, n67, p1485-1490.
- Michaelis, A. S and Mowellos, O. (1955). "Polyelectrolyte Adsorption by Kaolinite". Ind. and Eng. Chem., v47, n9, p1801-1808.
- Mokb, A. W. (1992). "Comparison of Analytical Methods for the Determination of Aluminium in Drinking Water". Water Supply, v10, n4, p21-34.
- Morel, F. M. M. (1983). Principles of Aquatic Chemistry, Wiley-Interscience, New York.

- Mortensen, J. L. (1959). "Adoption of Hydrolyzed Polyacrylonitrile on Kaolinite II. Effect of Solution Electrolytes". Soil Sci. Soc. Amer. Proc., v23.
- Narkis, N. and Rebhun, M. (1977). "Stoichiometric Relationship Between Humic and Fulvic Acids and Flocculants". J. AWWA, v69, n6, p325.
- Namasivayam, C., and Kanagarathnam, A. (1992). "3<sup>+</sup> Hydroxide Sludge and Polymer Flocculants". J. Environ Sci Health-Environ Sci Eng, vA 27, n7, p11721(17).
- Niehof, R. A. and Loeb, G.I. (1972). "The Surface Charge of Particulate Matter in Sea Water". Limnology Oceanography, v17, p7.
- Nielsen, A. E. (1964). "Secondary Growth". Kinetics of Precipitation, p108.
- O' Melia, C. R. (1969) "A Review of the Coagulation Process". Public Works, p87-98.
- O' Melia, C.R. (1970). "Coagulation in Water and Wastewater Treatment". Water Quality Improvement By Physical And Chemical Processes, p219.
- O' Melia, C.R. (1972). "Coagulation and Flocculation" Physicochemical Processes for Water Quality Control, Chap. 2 .
- O' Melia, C. R. (1969). "A Review of the Coagulation Process". Public Works, p87-98.
- O' Melia, C. R. (1977). "Coagulation in Wastewater Treatment". The Scientific Basis of Flocculation, Sijthoff and Noordhoff, The Netherlands.
- O' Melia, C. R. and Bowman, K.S. (1984). "Origins and Effects of Coagulation in Lakes". Schweiz. Z. Hydrol. v46, p64-85.
- O' Melia, C. R. (1985). "The Influence of Coagulation and Sedimentation on the Fate of Particles, Associated Pollutants, and Nutrients in Lakes." In Stumm, W. [ed.], Chemical Processes in Lakes. Wiley-Interscience. p207-224.
- O' Melia, C. R. (1987). "Particle-Particle Interactions", p385-403. In W. Stumm[ed.], Aquatic Surface Chemistry. Wiley-Interscience.
- Overbeck, J. Th. G. 1952. "Kinetics of Flocculation". Chapter VII, Colloids Science. Irreversible Systems. Hydrophobic Colloids, v1, p278.

- Ontario Ministry of the Environment (1972) "Guideline for Conducting Treatability Studies for Phosphorus Removal at Waste Water Treatment Plant". Toronto.
- Packham, R. F. (1965). "Some Studies of the Coagulation of Dispersed Clays with Hydrolyzing Salts". J. Colloid Interface Science, v20, p81.
- Packham, R.F. and Ratnayaka, D.D. (1992). "Water Clarification with Aluminium Coagulants in the UK". Water Supply, v10, n4, p 35-47.
- Packer, D. S., et al (1971). "Physical Conditioning of Activated Sludge Floc". J. Wtr. Poll. Cont. Fed., v43, n9, p1817.
- Packer, D. S. (1972) "Floc Breakup in Turbulent Flocculation Process". J. San. Engrg. Div., SA v1, n2, p79.
- Pandya, J.D. & Spielman, L.A. (1982). "Floc Breakage in Agitated Suspensions: Theory and Data Processing Strategy". J. Colloid, Inter., vol 90, n2, p517.
- Parker, D.S. et al. (1971). "Physical Conditioning of Activated Sludge Floc". J. Wtr. Poll. Cont. Fed., v43, n9, p1817.
- Parker, D.S.; Kaufman, W.J.; Jenkins, F.J. (1972). "Floc Breakup in Turbulent Flocculation Processes". J. San.Eng. Div. ASCE 98, n2, p79.
- Pearson, P.C. (1976). "Factors Influencing oil Removal Efficiency in Dissolved Air Flotation Units". Water & Wastewater Equipment Manufacturers Assn 4th Annual Industrial Pollution Control Conf. H. Mar 30-Apr. p52 (36)
- Peterson, B. and Barlow, E. (1982). "Effects of Salts on the Rate of Coagulation and the Optimum Precipitation of Alum Floc". Industrial and Engineering Chemistry, v20, p51.
- Petroll, J.; De Jonge and Hung, J. (1985). J. Ind. Chem., v13, p323-35 (German). Chem. Abstr. 1986., v104, 70987s.
- Philipot, M. (1992). "Measures Taken in Drinking Water Treatment Plants in the Paris Suburbs to Comply with Regulations on the Use of Aluminium". Water Supply, v10, n4, p97-102.

- Popplewell, L. M.; Campanella, O.H.; Normand, M.D.; and Peleg, M. 1988. Power Technol. v54, p119-25.
- Pouillot, M. and Suty, H. (1992). "High-basicity Polymeric Aluminium Salts for Drinking- water Production". Water Supply, v10, n4, p133-153.
- Prendiville, P.W. and Chung, P.Y. (1992). "The Reduction of Aluminium Carryover into Distribution Systems by the Careful Control of Coagulation and Filtration". Water Supply, v10, n4, p77-81.
- Priesling, P.C. (1962). Ind. Eng. Chem., v54, n8, p38.
- Ramteke, D. S. (1990). "Drill Site Waste Treatment-Role of Coagulants with Polyelectrolytes". Indian J Env Protection, v10, n11, p80.
- Rebhun, M. (1990). Floc Formation and Breakup in Continuous Flow Flocculation and in Contact Filtration". Chemical Water and Wastewater Treatment, Hermann H. Hahn and Rudolf Klute (Eds.), p117-126.
- Reuter, J. M. and Landscheidt, A. (1988). "Polyelectrolytes for the Treatment of Tap and Filter Back Washing Water". Pretreatment in Chemical Water and Wastewater Treatment, p91 - 101.
- Reynolds, T. D. (1982). "Coagulation and Flocculation", and "Sedimentation". Unit operations and Processes in Environmental Engineering, p17-23, p69-119.
- Reynolds, Tom D. (1982). "Coagulation and Flocculation". and "Sedimentation". Unit Operations and Processes in Environmental Engineering, p17-23, 69-119.
- Riddick, T. M. (1961) "Zeta Potential: New Tool for Water Treatment". Chem. Eng., v68, n13, p121, v68, n14, p141.
- Ritchie, A.R. (1955). "Certain Aspects of Flocculation as Applied to Sewage Purification" Ph.D. Thesis, University of London.
- Robinson Jr. Correl N. (1974). "Polyelectrolytes as Primary Coagulants for Potable-Water System". I. AWWA, P 252-257.

- Rocheleau, A.W., Parker, D.G., Pessagno, D.G. and Gotza, E. M. (1970). "Phosphorus Removal Feasibility Study". Sarnia Sewage Treatment Plant. Dow Chemical of Canada Report.
- Ropp, R.C. 1985, Am. Lab. v17, n7 p76, 78-81,83.
- Ruehrvein , R. A. and Ward, D. W. 1952. "Mechanism of Clay Aggregation by Polyelectrolytes". Soil Sci. v73, p485-493.
- Saffman, P. G. and Turner, J.S. (1956). "On the Collision of Drops in Turbulent Clouds". J. Fluid Mechanics, v1, p16.
- Sastry,C.A. and Raghuver,S. (1991). "Colour Removal from Combined Wastewaters of Pulping, Bleaching and Soda Recovery Sections of Pulp and Paper Mill". Indian J. Environmental Protection, v11, n3, p161(6).
- Scarlett, B. (1982). "Particle Size analysis 1981". Chichster.
- Schofield, R. K. and Samson, H. R. (1953). "The Deflocculation of Kaolinite Suspensions and the Accompanying Charge-Over from Positive to Negative Chloride Adsorption" . Clay Minerals Bull. 2:9 , p45.
- Schofield, R. K. and Samson, H. R. (1954). "Flocculation of Kaolinite Due to the Attraction of Oppositely Charged Crystal Faces". Disc. Far. Soc., v18.
- Schwartz, M. (1975). "Ozone as a Treatment Process for Color Removal from Drinking Water". Water and Pollution Control,v114, n54, p14(7).
- Schwartz, M., and Moncrieff, D.J.W. (1976). "Ozone as a Treatment Process for Color Removal from Drinking Water". Water and Pollution Control. v114, n54, p14(7).
- Schwoyer, W. L. K. (1981). CRC. Polyelectrolytes for Water and Wasterwater Treatment, p91.
- Singley, J.E. (1972). "Theory and Mechanism of Polyelectrolytes as Coagulant Aids". Polyelectrolyte-aids to Better Water Quality, pII-1-II-5.



- Sheludko, A. (1966). "Preparation and Purification of Lyophobic Colloidal Systems". Colloid Chemistry, p1-8.
- Smellie, R. H. and LaMer, V. K. (1958). "Flocculation, Subsidence, and Filtration of Phosphate Slimes-VI. A Quantitative Theory of Filtration of Flocculated Suspensions". J. Coll. Sci., v23, p589-599.
- Smoluchowsky, M. (1916). "Drei Vorträge über Diffusion, Brownsche Molekular Bewegung und Koagulation von Kolloidteilchen". Physik. Z., v17.
- Smoluchowsky, M. (1917). "Versuch einer Mathematischen Theorie der Koagulations-Kinetik Kolloider Lösungen". Zeitschrift Physicalische Chemie., v92, p129.
- SPCUUS. (1982). "Survey of Polyelectrolyte Coagulant Use in the United States". J. AWWA, v74, n11, p600.
- Spielman, L. A. (1970). "Viscous Interactions in Brownian Coagulation". J. Colloid Interface Science, v33, p562.
- Spielman, L. A. (1978). "Hydrodynamic Aspects of Flocculation". in K. J. Ives (ed.), The Scientific Basis of Flocculation, Sijthoff and Noordhoff, The Netherlands.
- Stephen C. Pearson, Hercules (1976). "Factors Influencing Oil Removal Efficiency in Dissolved Air Flotation Units". Water & Wastewater Equipment Manufacturers Assn 4th Annual Industrial Pollution Control Conf. H. Mar 30-Apr. p52(36).
- Stanley, S.J. (1995). "Analysis and Measurement of Flocculant Mixing". Ph.D. Thesis, University of Alberta.
- Stumm, W. and Morgan, J. J. (1981). Aquatic Chemistry, 2nd ed., John Wiley & Sons, New York.
- Stumm, W and O' Melia , C. R. (1968). "Stoichiometry of Coagulation". J. AWWA, v5, p514-539.
- Suet-mei, Ho and Wing-shiu, Tso (1992). Water Supply, Vol. 10, No.4, p11-20.
- Swift, D. L. and Friedlander, S. K. (1964). "The Coagulation of Hydrosols by Brownian Motion and Laminar Shear Flow". J. Coll. Sci., v19, p621--647.

- Swope, H.G. (1977). "Zeta Potential Measurement". Water & Sewage Works, R-64.
- Tambo, N. et al . (1970-a). "The Strength of Floc Particles". Jour. Jpn. Wtr. Wks. Assn., v427, n4,p4.
- Tambo, N. et al . (1970-b). "Rational Design of Flocculation (I). Jour. Jpn. Wtr. Wks. Assn., v431, n8, p21.
- Tambo, N. et al . (1979). "A Mathematical Model of Turbulent Flocculation Process". Memories of the Faculty of Engineering, Hokkaido Univ., v15, n2, p163.
- Tambo, N & Hozumi, H. (1979). "Physical Characteristics of Flocs, II: Strength of Floc". Wtr. Res., v13, n4, p421.
- Tambo, N & Watanabe,Y. (1979). "Physical Aspect of Flocculation Process, I ". Wtr. Res., v13, n5, p409.
- Tambo, N. et al (1979). "A Mathematical Model of Turbulent Flocculation Process". Memories of the Faculty of Engineering, v15(2), p163
- Tambo, N. & Matsui, Y. (1989). "Performance of Fluidized Pellet Bed Separator for High Concentration Suspension Removal". J. Wtr. Supply Res. & Tech. (AQUA), v38, n1, p16.
- Tambo Norihito (1991). "Mixing, Breakup, and Floc Characteristics". Mixing in Coagulation and Flocculation, P257
- Tascchi, K. J. (1977). "Polyelectrolyte Usage in Industrial Wastewater Treatment". Industrial Water Engineering, v14, n7, p12(6).
- Theng, B.K.G. (1979). Formation and Properties of Clay-Polymer Complexes, p9.
- Timasheff, S. N. (1966). "Turbidity as Criterion of Coagulation". J. Coll. and Interf. Sci., v21, p489-497.
- Tim Brodeur (1976). "Use of Anionic Polymer to Replace Aluminium Sulfate in a Softening Plant". AWWA 96th Annual Conf: Water Technology and research, Jun 20-25, v2, p20-2(10).

- Thomas, D.G. (1964). "Turbulent Disruption of Flocs in Small Size Suspension". J. AIChE. , v10, n4, p517-523.
- Tomi, D.T. & Bagster, D.F. (1975). "A Model of Floc Strength Under Hydrodynamic Forces". Chem. Engrg. Sci., v30, n3, p269.
- Tomi, D.T. & Bagster, D. F. (1978). "The Behavior of Aggregates in Stirred Vessels, I: Theoretical Consideration on the Effects of Agitation". Trans. Inst. Chem. Eng., v56, n1, p1.
- Tucson and Decook, K.L. (1980). "Hydrological and Environmental Controls on Water Management in Semiarid Urban Areas". NTIS Report Pb 81-109704 , Sept 80 (77).
- Valioulis, I. R. and List, E. J. (1984). "Collision Efficiencies of Diffusing Spherical Particles: Hydrodynamic, van der Waals and Electrostatic Forces". Advances Colloid Interface Science, v20,p1.
- Van de Ven, T. G. M. and Mason, S. G. (1977). "The Microheology of Colloidal Suspensions. VII: Orthokinetic Doublet Formation of Spheres". Colloid Polymer Science, v255, p468.
- Vladimir, P. , Knor, Z. and Cerny, S. (1974). "The Mechanism of Physical Adsorption", "The Mechanism of Chemisorption". Adsorption on Colloids, p419-491.
- Vold, M.J. (1963). "Computer Simulation of Floc Formation in a Colloidal Suspension". J. Colloid Inter. Sci. v18, n7, p684.
- Wadell, H. (1932). "Volume, Shape, and Roundness of Rock Particles". J. Geol., v40, p443.
- Wadell, H. (1933). "Sphericity and Roundness of Rock Particles". J. Geol., v41, p310.
- Wang L.K.; Wang M.H. and Kao J.F. (1978). "Application and Determation of Polyelectrolytes". Purdue Univ Ind Waste 33 rd Conf, Lafayette, p935 (9).
- Watanabe, Y. & Tambo, N. (1971). "A Study on the Aluminium Floc Density". J. Jpn. Wtr. Wrs. Assn. v445, n10, p2.

Weber, W. (1972). Physicochemical Processes for Water Quality Control. Wiley-Interscience, New York.

Weilenmann, U and O' Melia , C. R. (1989). "Particle Transport in Lakes: Models and Measurements". Limnol. Oceanogr. v34, n1 p1-18.

World Health Organization. (1984). Guidelines for Drinking Water Quality, v1, p79-80 and v2, p249-252.

## 9 APPENDIX

### Appendix A Reactor Calibration Plot

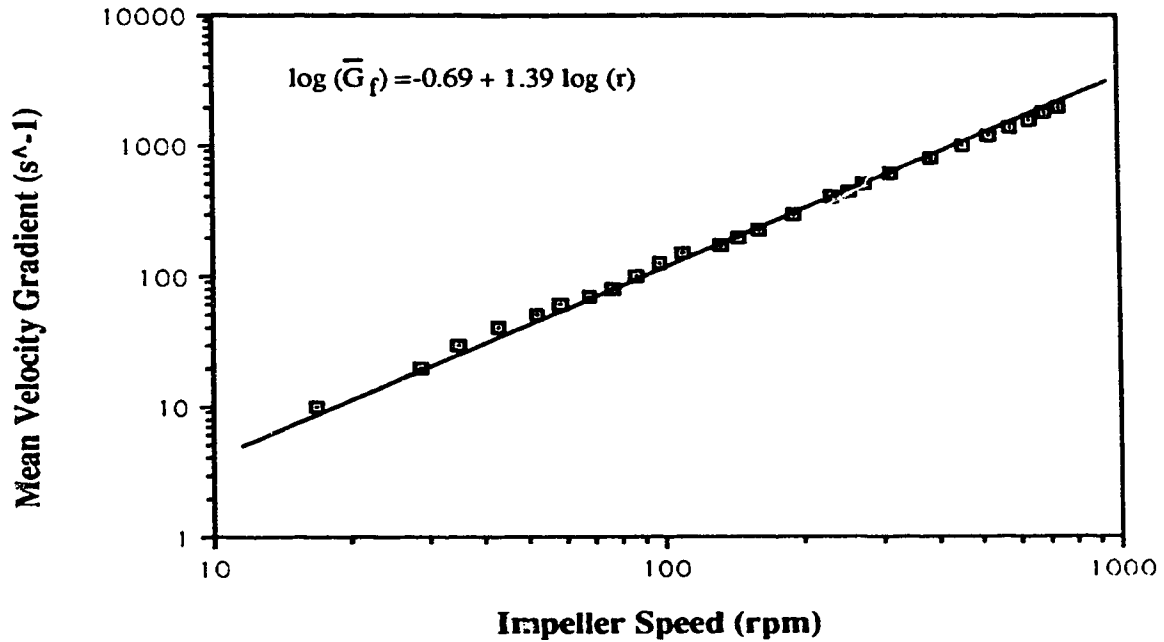
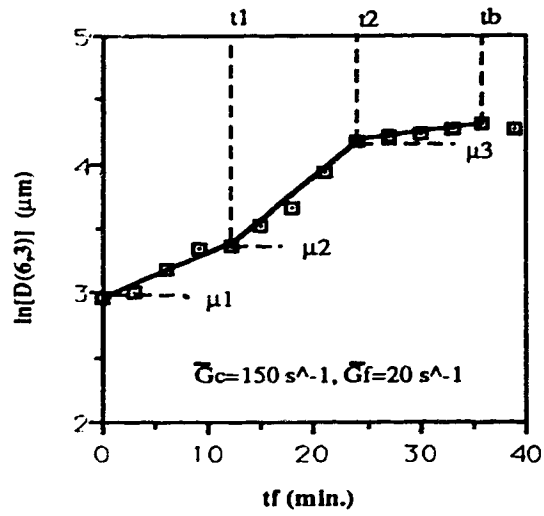


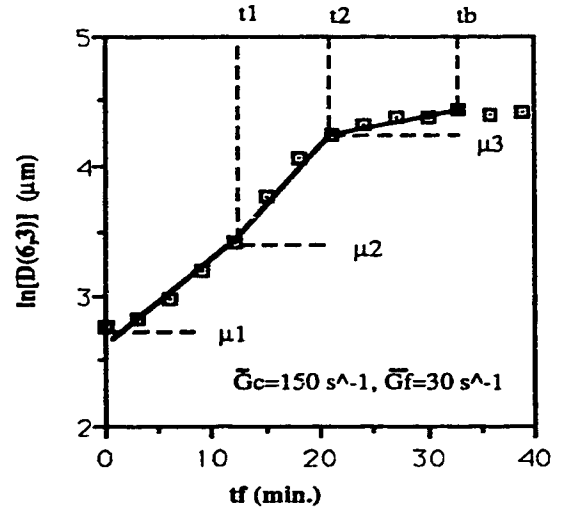
Figure A Calibration Curve Between Impeller Speed and Mean Velocity Gradient for Flat Paddle in 2L Hudson Jar

### Appendix B Polymeric Floc Growth Curves on Semilogarithmic Scale

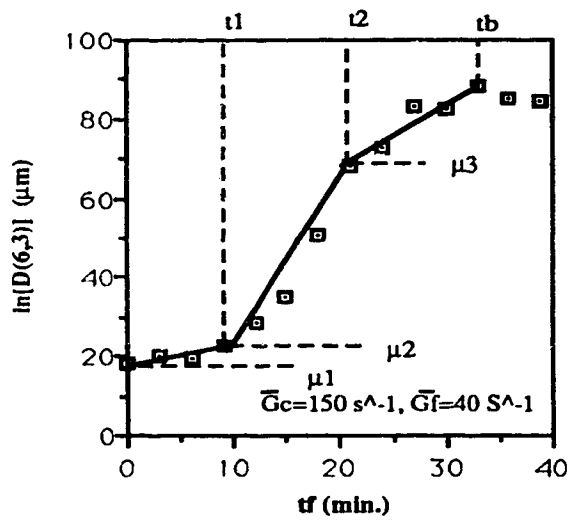
Experimental Conditions: kaolin=20 mg/L, pH=8,  $NaHCO_3$ =100 mg/L, alum=5 mg/L, polymer=0.5 mg/L, fast mixing time=1 min.



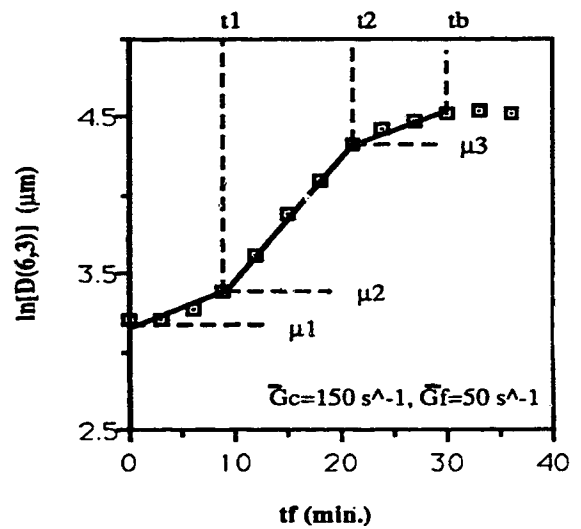
(a)



(b)

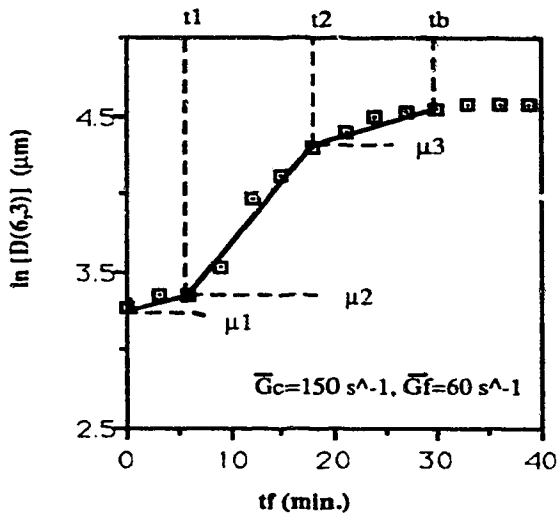


(c)

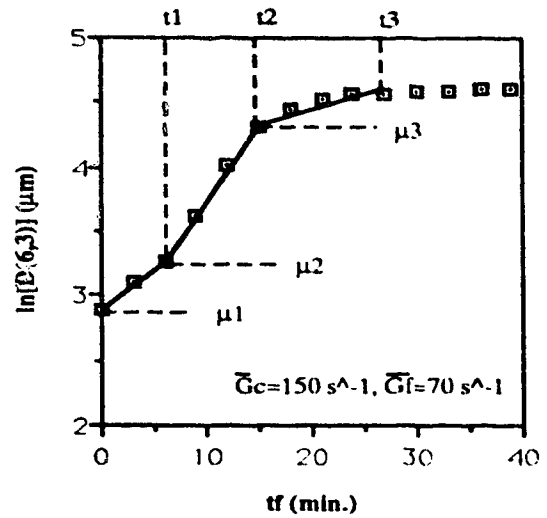


(d)

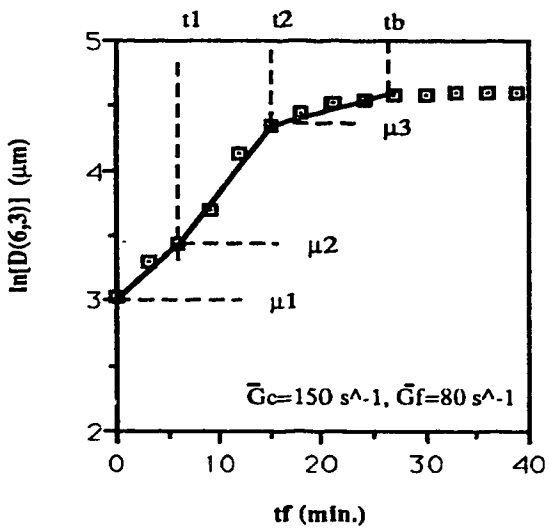
Figure B-1 Floc Growth Curves on Semi-logarithmic Scale ( $20 \leq \bar{G}_f \leq 50 \text{ s}^{-1}$ )



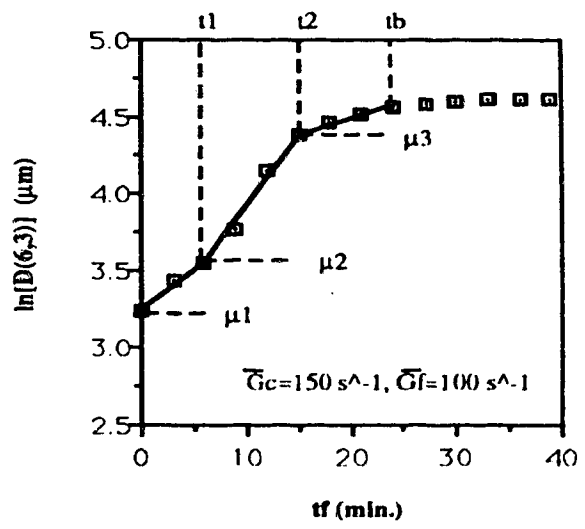
(a)



(b)



(c)



(d)

Figure B-2 Floc Growth Curves on Semi-logarithmic Scale ( $60 \leq \bar{G}_f \leq 100 \text{ s}^{-1}$ )

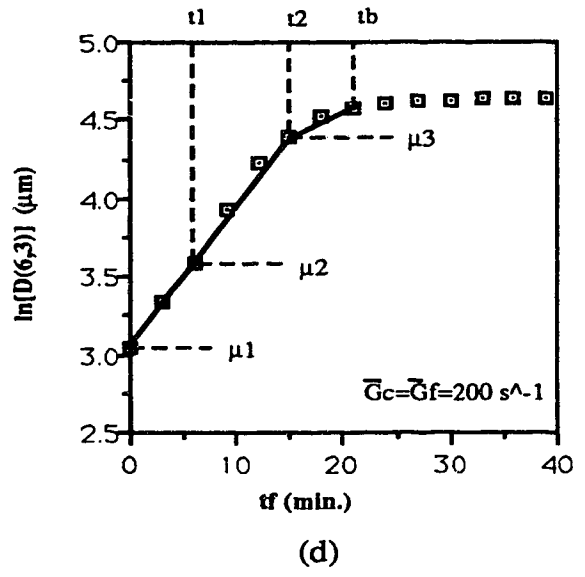
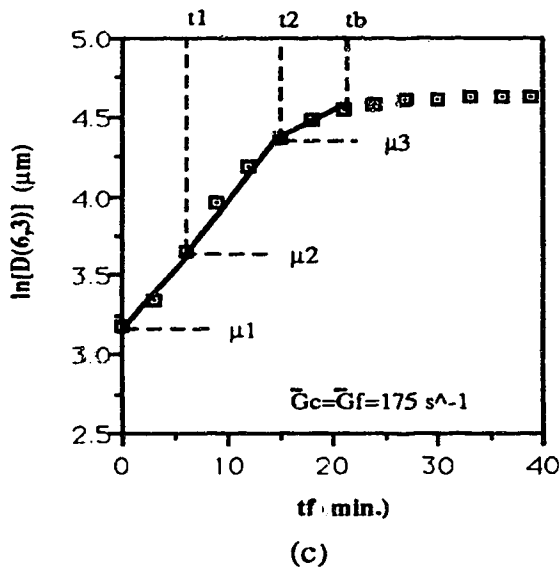
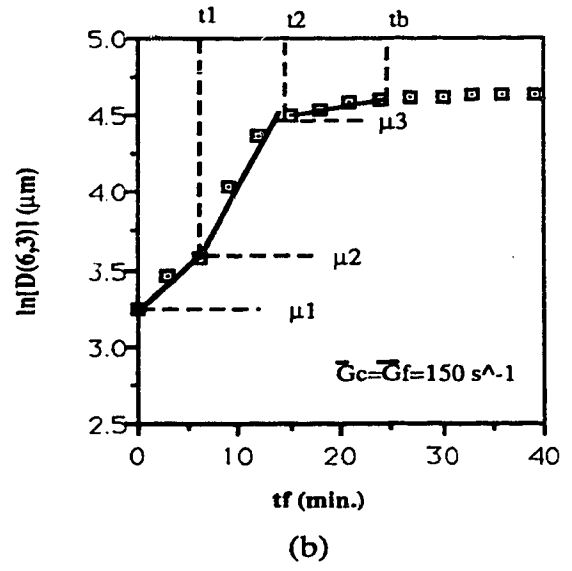
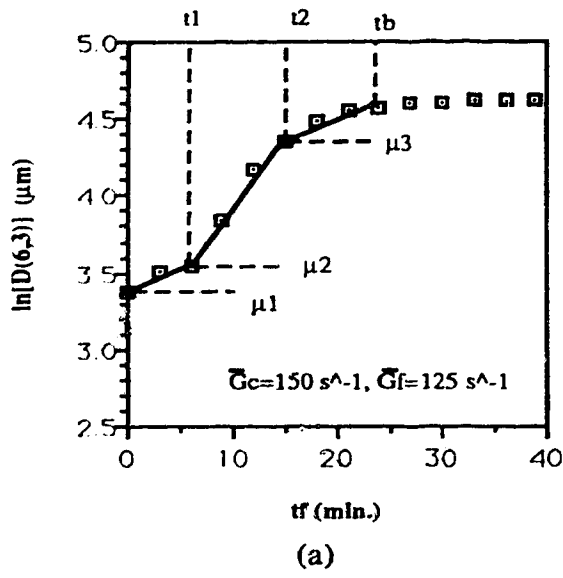


Figure B-3 Floc Growth Curves on Semi-logarithmic Scale ( $125 \leq \bar{G}_f \leq 200 \text{ s}^{-1}$ )



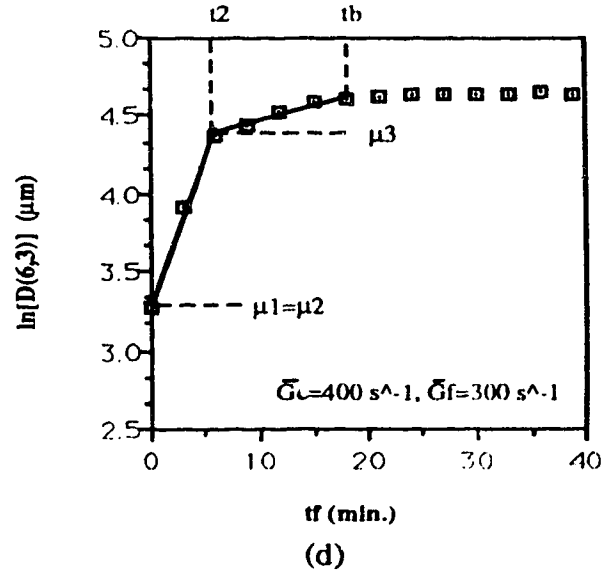
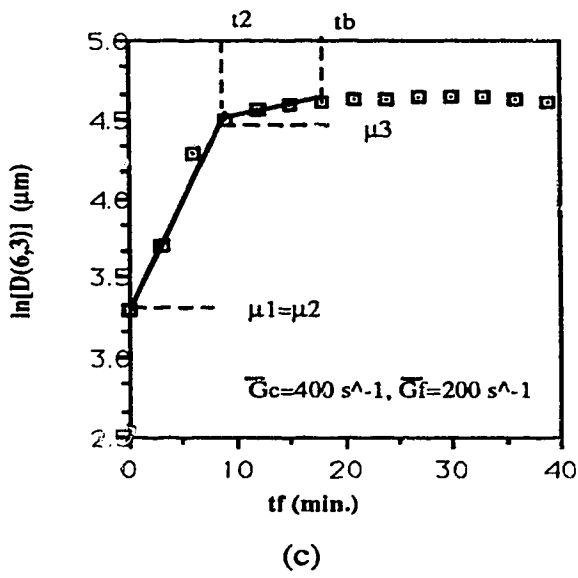
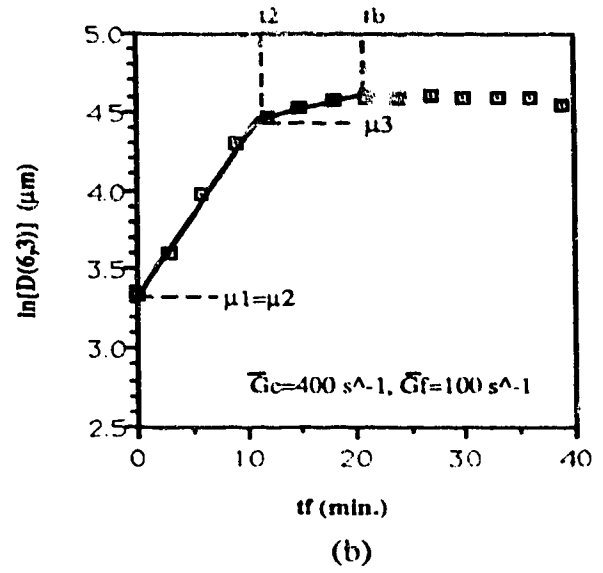
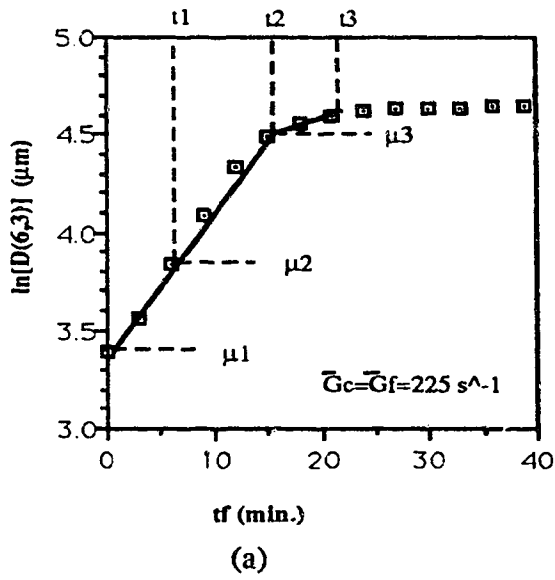
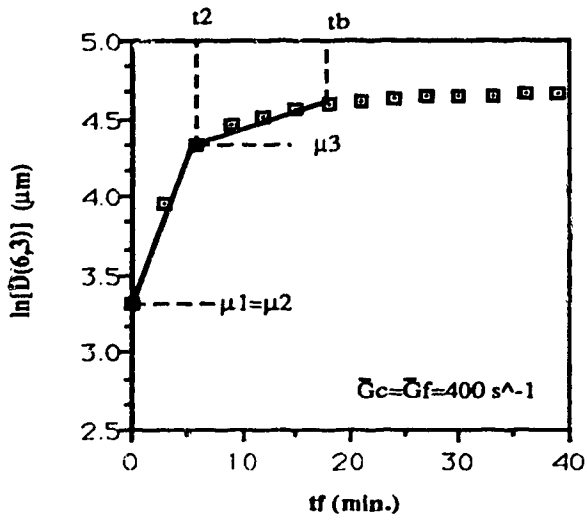
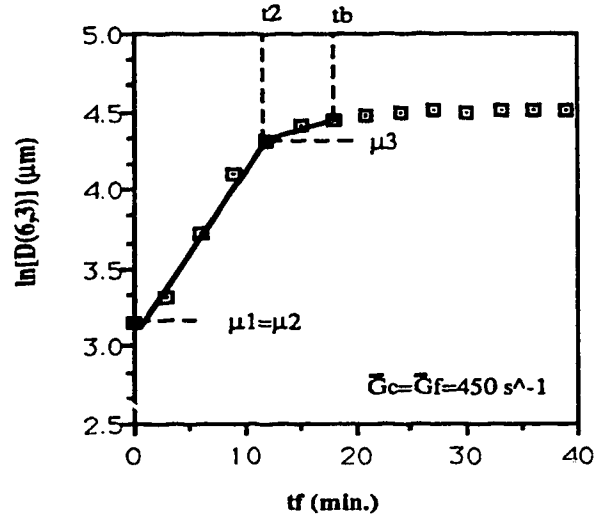


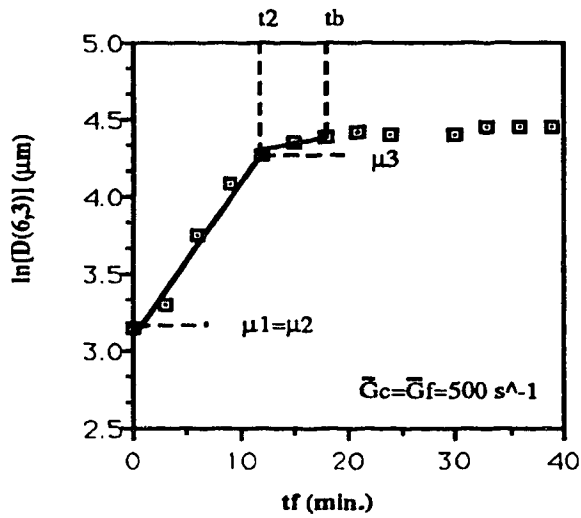
Figure B-4 Floc Growth Curves on Semi-logarithmic Scale ( $100 \leq \bar{G}_f \leq 300 \text{ s}^{-1}$ )



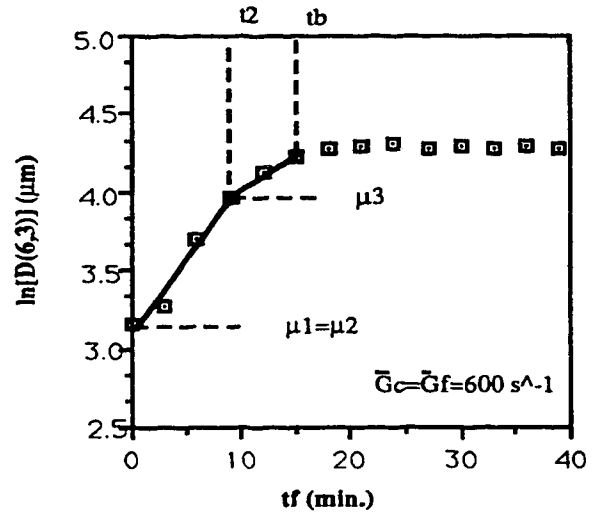
(a)



(b)



(c)



(d)

Figure B-5 Floc Growth Curves on Semi-logarithmic Scale ( $400 \leq \bar{G}_f \leq 600 \text{ s}^{-1}$ )

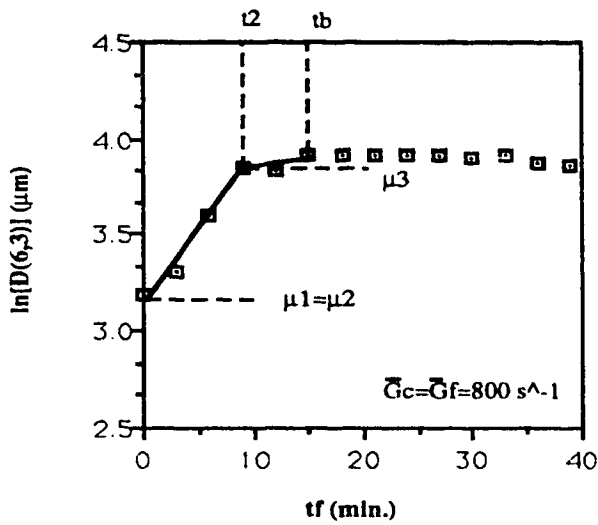


Figure B-6 Floc Growth Curve on Semi-logarithmic Scale ( $\bar{G}_f \leq 600 \text{ s}^{-1}$ )

### Appendix C Model for Effect of Mixing on First Order Rate Constant

Two mathematical models for the first order rate constant were tested. The general expressions of the above two models are given as:

$$\text{Model 1: } K = M * (\bar{G}_f)^N + C \quad (M, N \text{ and } C \text{ are constants}) \quad (\text{C.1})$$

$$\text{Model 2: } K = A \text{ Ln} (\bar{G}_f) + B \quad (A \text{ and } B \text{ are constants}) \quad (\text{C.2})$$

The model simulation and residual examination processes are presented in the following tables and figures.

#### C.1 Model (Equation C. 1) Simulation and Residual Examination Processes

**Table C.1 Model (C.1) Simulation Process**

**Model C. 1:  $K=M*(\bar{G}_f)^N + C$  (M, N and C are constants)**

ITERATION	LOSS	PARAMETER VALUES		
0	0.4965402D-03	0.7466D+01	0.4394D-02	-.7547D+01
1	0.4965148D-03	0.7583D+01	0.4327D-02	-.7664D+01
2	0.4965083D-03	0.7571D+01	0.4334D-02	-.7652D+01
3	0.4964913D-03	0.7644D+01	0.4293D-02	-.7725D+01
4	0.4964777D-03	0.7709D+01	0.4257D-02	-.7790D+01
5	0.4964529D-03	0.7777D+01	0.4222D-02	-.7858D+01
6	0.4964313D-03	0.7857D+01	0.4179D-02	-.7938D+01
7	0.4964278D-03	0.7854D+01	0.4181D-02	-.7935D+01
8	0.4964112D-03	0.7923D+01	0.4145D-02	-.8004D+01
9	0.4964057D-03	0.7967D+01	0.4122D-02	-.8048D+01
10	0.4963977D-03	0.7967D+01	0.4123D-02	-.8048D+01

DEPENDENT VARIABLE IS K

SOURCE	SUM-OF-SQUARES	DF	MEAN-SQUARE
REGRESSION	0.087	3	0.029
RESIDUAL	0.000	12	0.000
TOTAL	0.088	15	
CORRECTED	0.012	14	

RAW R-SQUARED (1-RESIDUAL/TOTAL) = 0.994  
 CORRECTED R-SQUARED (1-RESIDUAL/CORRECTED) = 0.960

PARAMETER	ESTIMATE
M	7.967
N	0.004
C	-8.048

Model C.1:  $K= 7.967(\bar{G}_f)^{0.004} - 8.048$

Table C. 2 Model (C. 1) Simulation Data [  $K= 7.967 (\bar{G}_f)^{0.004} - 8.048$  ]

$\bar{G}_f$ (s <sup>-1</sup> )	K (Counts/ml*min.)	ESTIMATE	RESIDUAL
20	0.018	0.02	-0.002
30	0.02	0.032	-0.012
40	0.049	0.041	0.008
50	0.052	0.048	0.004
60	0.058	0.054	0.004
70	0.054	0.059	-0.005
80	0.072	0.063	0.009
100	0.067	0.071	-0.004
125	0.074	0.078	-0.004
150	0.083	0.085	-0.002
175	0.096	0.090	0.006
200	0.102	0.095	0.007
225	0.102	0.099	0.003
300	0.105	0.109	-0.004
400	0.113	0.120	-0.007

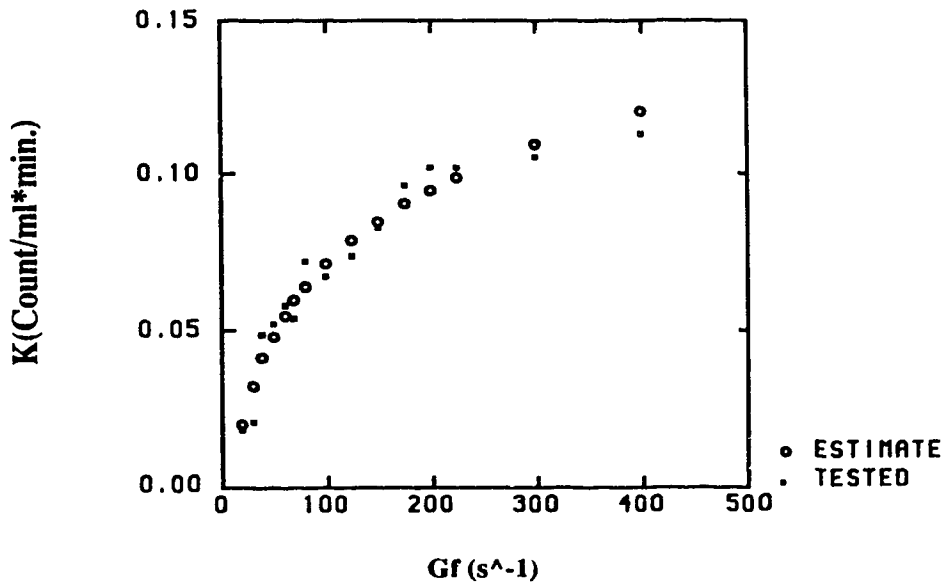


Figure C.1 The Model Simulation Diagram at  $\bar{G}_f=80 \text{ s}^{-1}$  [  $K= 7.967 (\bar{G}_f)^{0.004} - 8.048$  ]

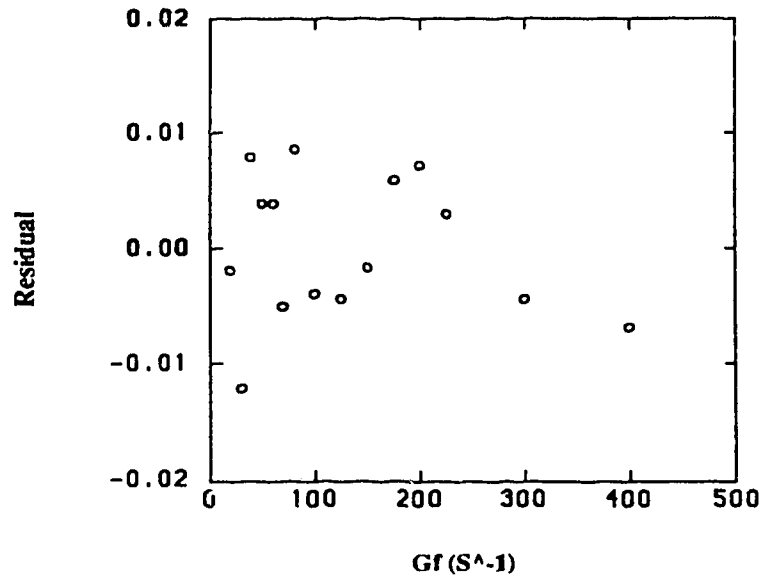


Figure C.2 The Residuals Plotted against the Independent Parameter

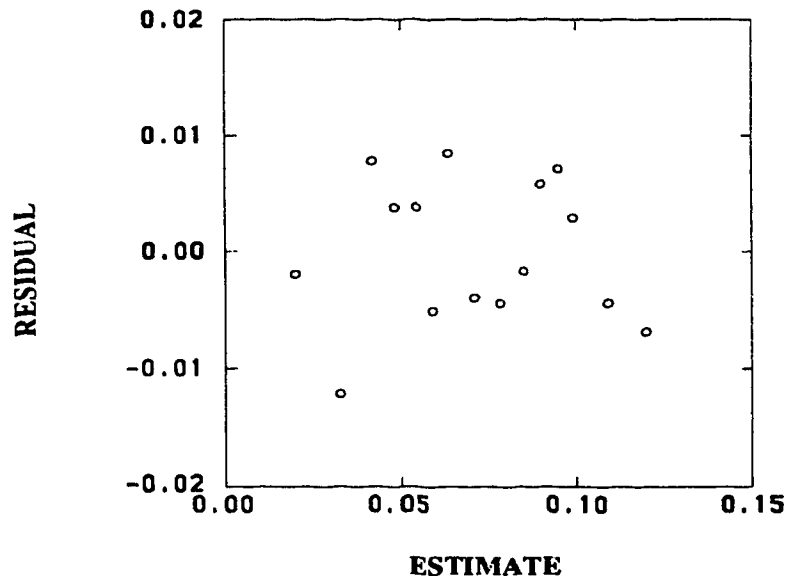


Figure C.3 The Residuals Plotted against the Estimate Parameter (K)

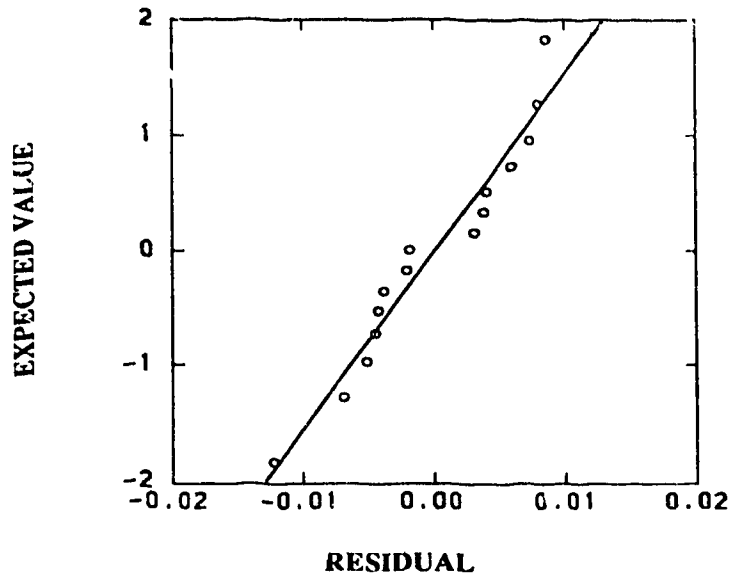


Figure C.4 The Normal Plot of the Residuals

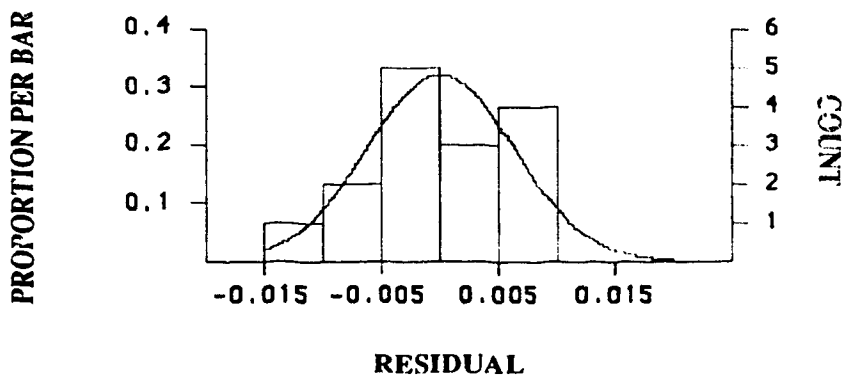


Figure C.5 The Histogram Plot of the Residual

## C.2 Model (Equation C.2) Simulation and Residual Examination Processes

Table C.3 Model (C.2) Simulation Process

**Model C.2:  $K=A \text{ Ln } (\bar{G}_f) +B$  (A and B are constants)**

ITERATION	LOSS	PARAMETER VALUES	
0	0.3608902D+01	0.1000D+00	0.1000D+00
1	0.1778583D+01	-.7100D-01	0.6345D-01
2	0.5500339D-03	0.3121D-01	-.7168D-01
3	0.4945157D-03	0.3332D-01	-.8167D-01
4	0.4942738D-03	0.3347D-01	-.8238D-01
5	0.4942738D-03	0.3347D-01	-.8238D-01
6	0.4942738D-03	0.3347D-01	-.8238D-01

DEPENDENT VARIABLE IS K

SOURCE	SUM-OF-SQUARES	DF	MEAN-SQUARE
REGRESSION	0.087	2	0.044
RESIDUAL	0.000	13	0.000
TOTAL	0.088	15	
CORRECTED	0.012	14	

RAW R-SQUARED (1-RESIDUAL/TOTAL) = 0.994  
 CORRECTED R-SQUARED (1-RESIDUAL/CORRECTED) = 0.960

PARAMETER	ESTIMATE
A	0.033
B	-0.082

Model:  $K= 0.033 \text{ Ln } (\bar{G}_f) - 0.082$  [counts/(ml·min.)]



Table C.4 Model (C.2) Simulation Data [  $K = 0.033 \ln(\bar{G}_f) - 0.082$  ]

$\bar{G}_f (s^{-1})$	K [counts/(mi*min.)]	Estimate	Residual
20	0.018	0.018	0
30	0.02	0.031	-0.011
40	0.049	0.041	0.008
50	0.052	0.049	0.003
60	0.058	0.055	0.003
70	0.054	0.060	0.006
80	0.072	0.064	0.008
100	0.067	0.072	-0.005
125	0.074	0.079	-0.005
150	0.083	0.085	-0.002
175	0.096	0.090	0.006
200	0.102	0.095	0.007
225	0.102	0.099	0.003
300	0.105	0.109	-0.004
400	0.113	0.118	-0.005

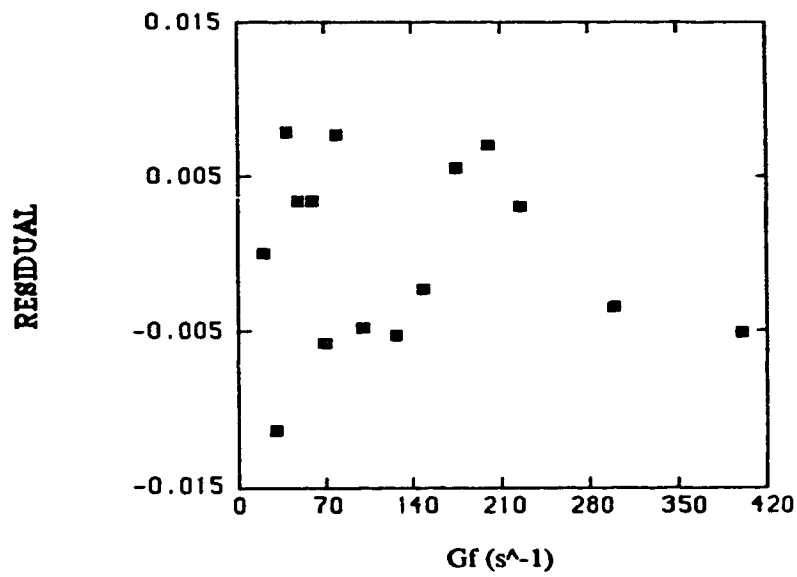


Figure C.6 The Residuals Plotted against the Independent Parameter ( $\bar{G}_f$ )

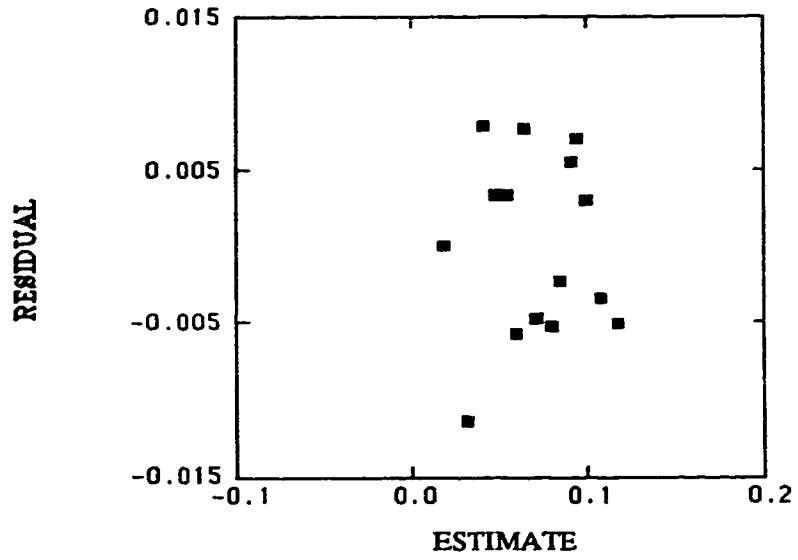


Figure C.7 Residuals Plotted against Fitted Values [  $\text{Ln}(\bar{G}_f)$  ]

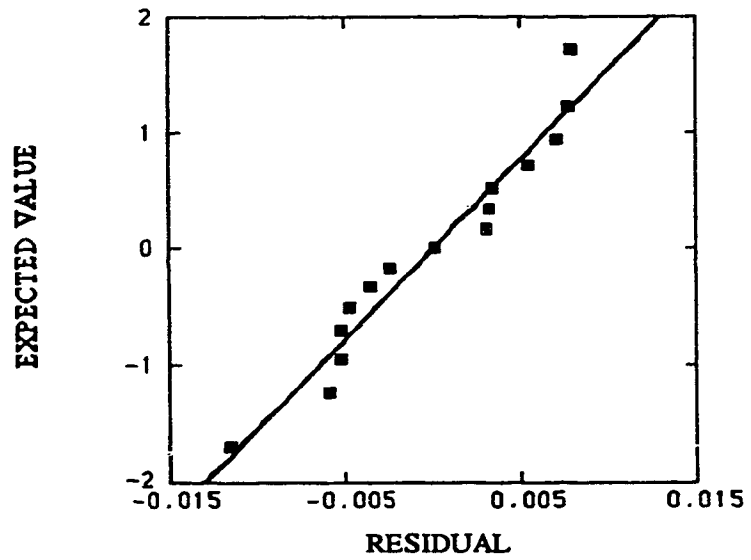


Figure C.8 The Normal Plot of the Residuals

## Appendix D Determination of the Power Law Slope Coefficient

The values of the power law slope coefficients ( $\beta$ ) were determined graphically from the slope of the straight lines. It is presented in Figures D-1 to D-10.

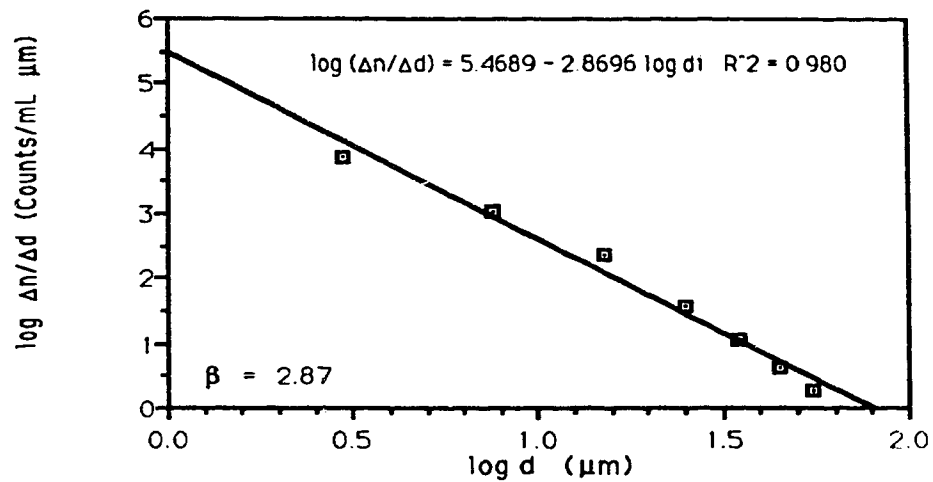


Figure D-1

The log-log Curve for Particle Size Distribution Function ( $\bar{G}_{ft} = 43200$ ,  $\bar{G}_f = 20 \text{ s}^{-1}$ ,  $t_b = 36 \text{ min.}$ )

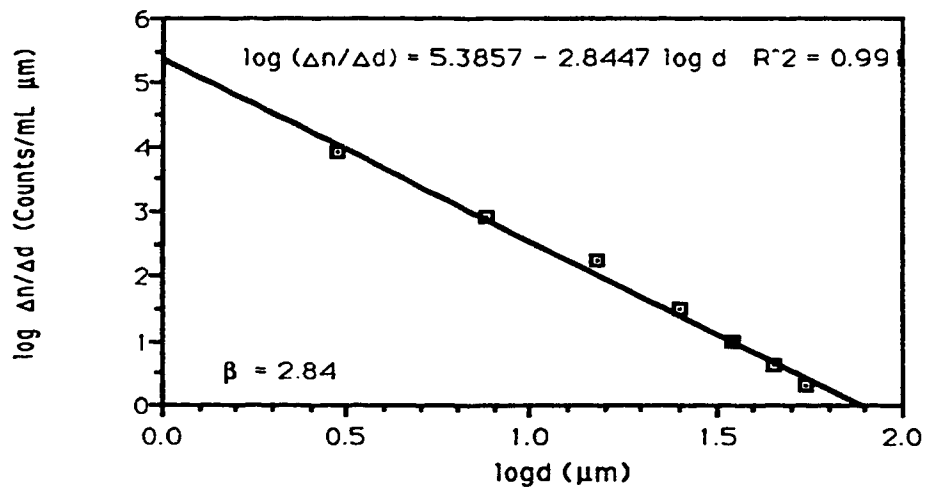


Figure D-2 The log-log Curve for Particle Size Distribution Function ( $\bar{G}_{ft}=59400$ ,  $\bar{G}_f=30 \text{ s}^{-1}$ ,  $t_b=33 \text{ min.}$ )

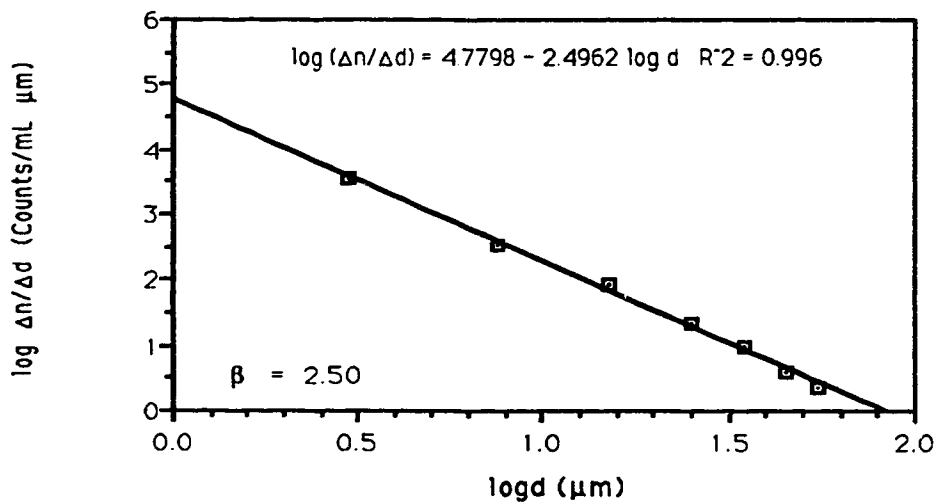


Figure D-3 The log-log Curve for Particle Size Distribution Function ( $\bar{G}_{ft}=79200$ ,  $\bar{G}_f=40 \text{ s}^{-1}$ ,  $t_b=33 \text{ min.}$ )

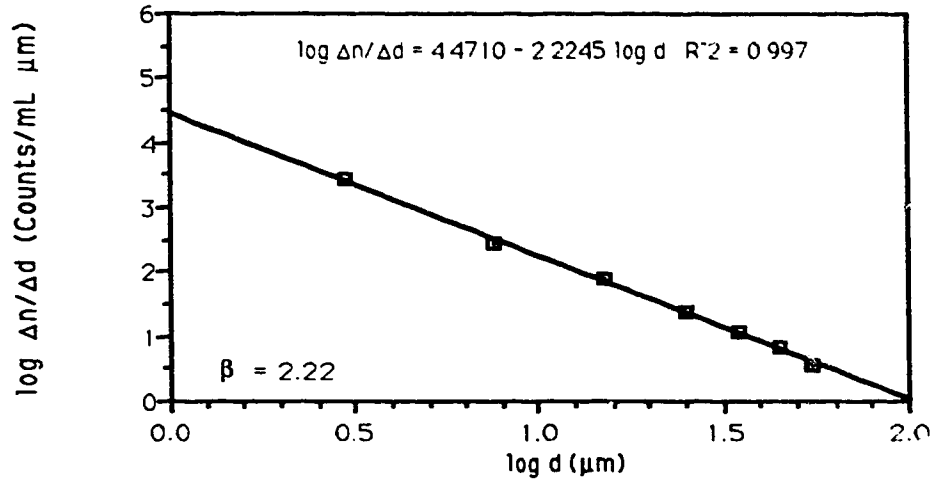


Figure D-4 The log-log Curve for Particle Size Distribution Function ( $\bar{G}_f=90000$ ,  $\bar{G}_f=50 \text{ s}^{-1}$ ,  $t_b=30 \text{ min.}$ )

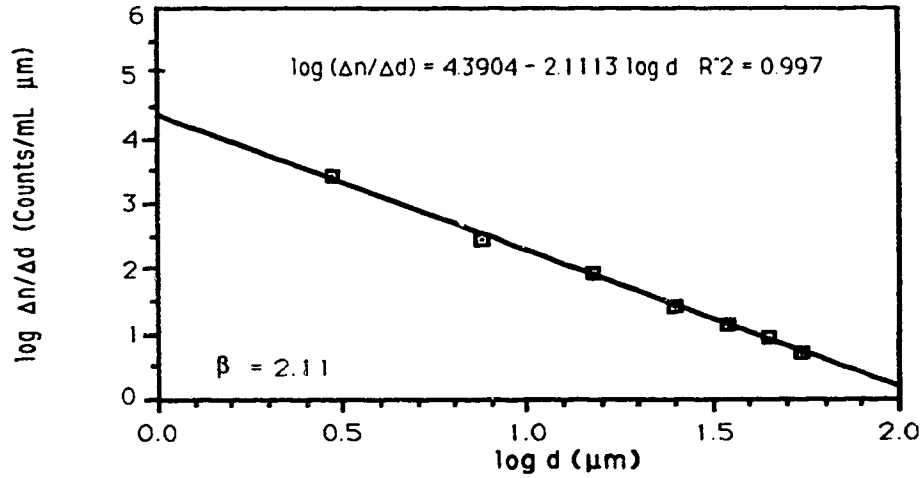


Figure D-5 The log-log Curve for Particle Size Distribution Function ( $\bar{G}_f=108000$ ,  $\bar{G}_f=60 \text{ s}^{-1}$ ,  $t_b=30 \text{ min.}$ )

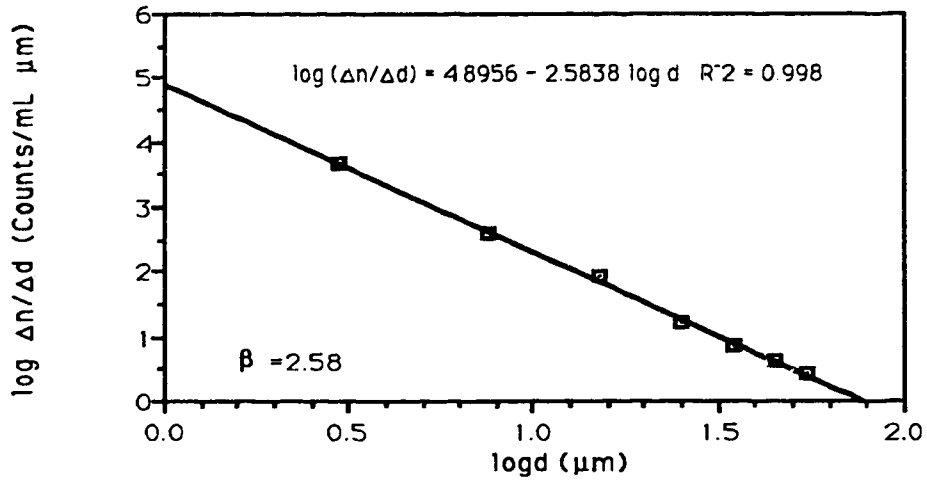


Figure D-6 The log-log Curve for Particle Size Distribution Function ( $\bar{G}_t=113400$ ,  $\bar{G}_f=70 \text{ s}^{-1}$ ,  $t_b=27 \text{ min.}$ )

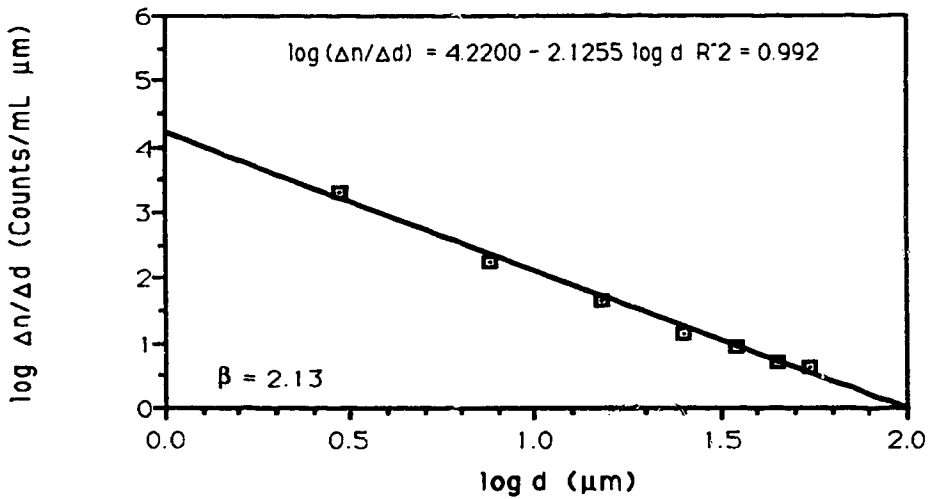


Figure D-7 The log-log Curve for Particle Size Distribution Function ( $\bar{G}_t=125500$ ,  $\bar{G}_f=80 \text{ s}^{-1}$ ,  $t_b=27 \text{ min.}$ )

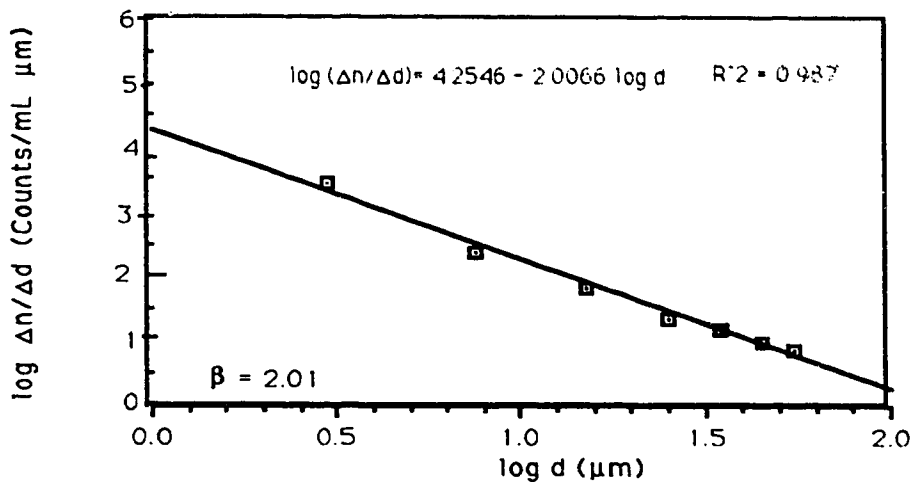


Figure D-8 The log-log Curve for Particle Size Distribution Function ( $\bar{G}_f=144000$ ,  $\bar{G}_f=100 \text{ s}^{-1}$ ,  $t_b=24 \text{ min.}$ )

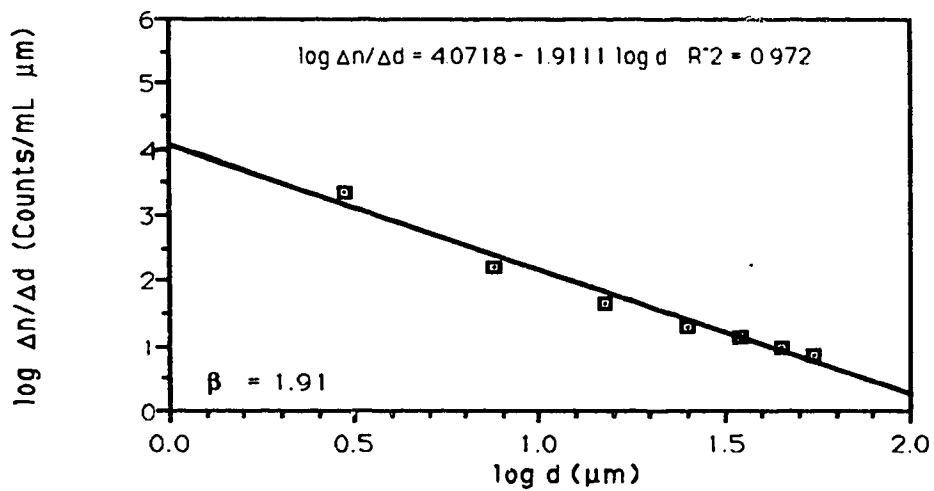


Figure D-9 The log-log Curve for Particle Size Distribution Function ( $\bar{G}_f=180000$ ,  $\bar{G}_f=125 \text{ s}^{-1}$ ,  $t_b=24 \text{ min.}$ )

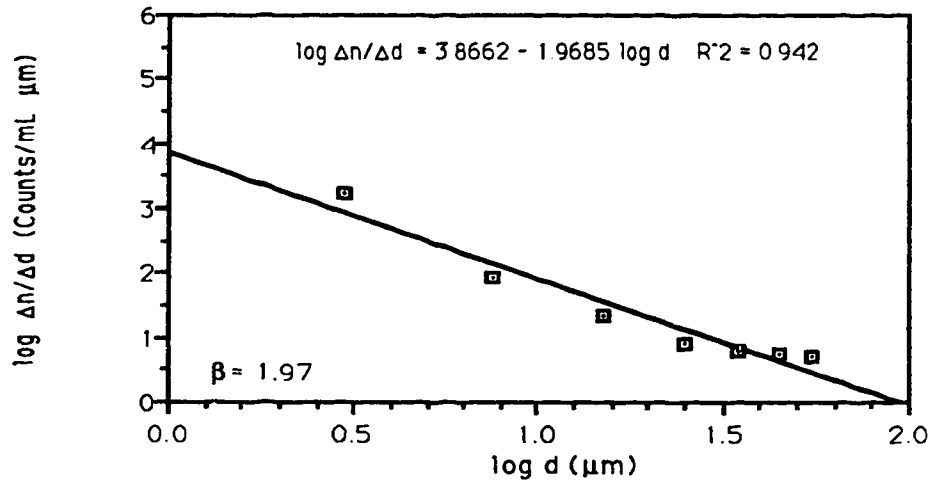


Figure D-10 The log-log Curve for Particle Size Distribution Function  
 ( $\bar{G}_f=216000$ ,  $\bar{G}_f=150 \text{ s}^{-1}$ ,  $t_p=24 \text{ min.}$ )

### Appendix E Determination of $d_{\max}$ Growth Constant

The following model:

$$d_{\max}=a*(\bar{G}_f)^m +b \quad (0 < \bar{G}_f \leq 400 \text{ s}^{-1}, a, b \text{ and } m \text{ are constants}) \quad (\text{E.1})$$

was used to fit the data of  $d_{\max}$  growth constant  $m_i$  ( $i=1,2$  and  $3$ ) in each stage.

#### E.1 Determination of the First Stage $d_{\max}$ Growth Constant $m_1$



Table E.1 Model Simulation for  $m_1$

Model 1:  $d_{\max} = a * (\bar{G}_f)^m + b$  ( $0 < \bar{G}_f \leq 70 \text{ s}^{-1}$ )

ITERATION	LOSS	PARAMETER VALUES	
0	0.8175154D+01	0.2028D+02	0.3185D+00
1	0.8172759D+01	0.2023D+02	0.3191D+00
2	0.8172739D+01	0.2024D+02	0.3190D+00
3	0.8172739D+01	0.2024D+02	0.3190D+00

DEPENDENT VARIABLE IS  $d_{\max}$

SOURCE	SUM-OF-SQUARES	DF	MEAN-SQUARE
REGRESSION	49182.125	2	24591.063
RESIDUAL	8.173	5	1.635
TOTAL	49103.409	7	
CORRECTED	4285.807	6	

RAW R-SQUARED (1-RESIDUAL/TOTAL) = 1.000  
 CORRECTED R-SQUARED (1-RESIDUAL/CORRECTED) = 0.998

PARAMETER	ESTIMATE
a	20.237
m	0.319

$$d_{\max} = 20.237 (\bar{G}_f)^{0.319} + 22.56 \text{ (}\mu\text{m)}$$

Table E.2 Model Simulation for  $m_1$  ( $0 < \bar{G}_f \leq 70 \text{ s}^{-1}$ )

$\bar{G}_f \text{ (s}^{-1}\text{)}$	Tested $d_{\max} \text{ (}\mu\text{m)}$	Estimate $d_{\max}$	Residual
0.001	22.56	24.808	-2.248
20	74.84	75.221	-0.381
30	83.49	82.48	1.01
40	88.57	88.229	0.341
50	93.68	93.066	0.614
60	97.13	97.281	-0.151
70	99.84	101.041	-1.201

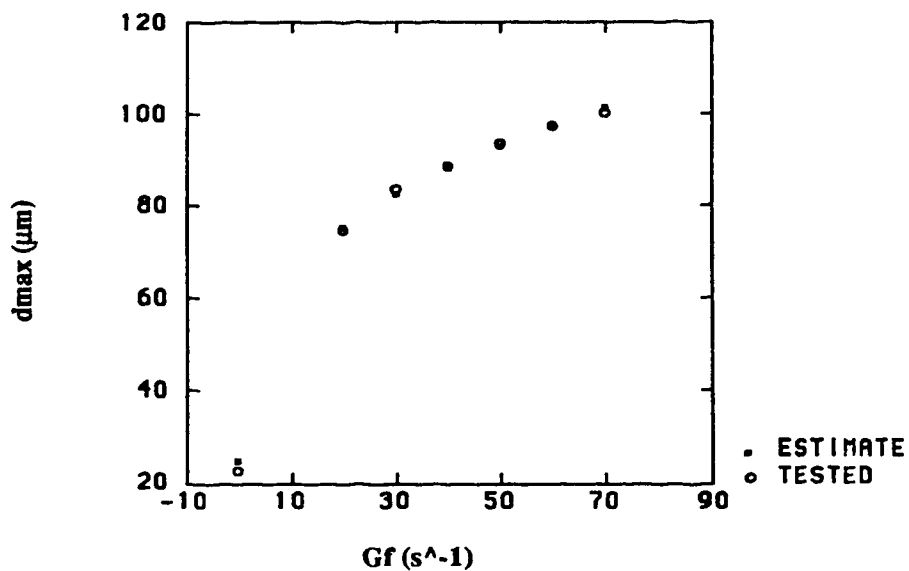


Figure E.1 Effect of Mixing on  $d_{max}$  ( $0 < \bar{G}_f \leq 70 s^{-1}$ )

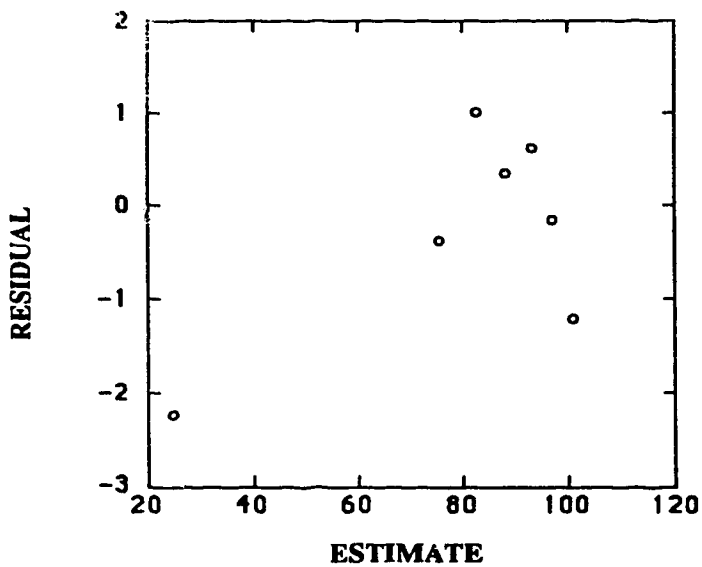


Figure E.2 The Residuals Plotted against Fitted Values of  $d_{max}$  ( $0 < \bar{G}_f \leq 70 s^{-1}$ )

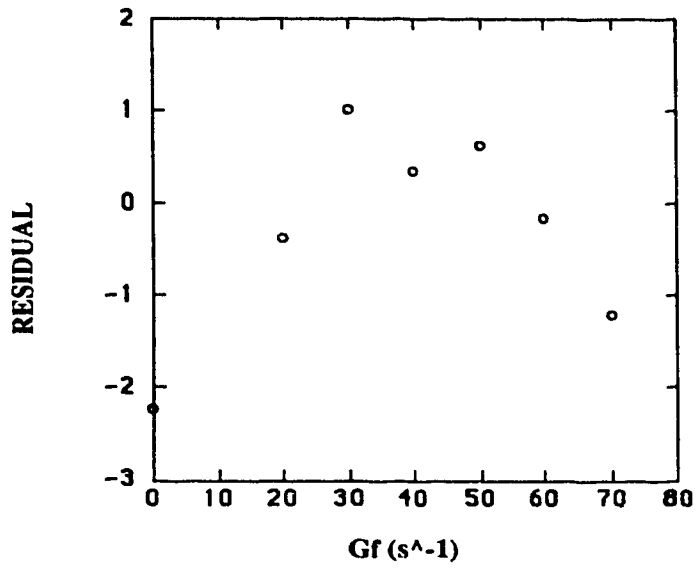


Figure E.3 Residual Plotted against the Independent Parameter ( $0 < \bar{G}_f \leq 70 \text{ s}^{-1}$ )

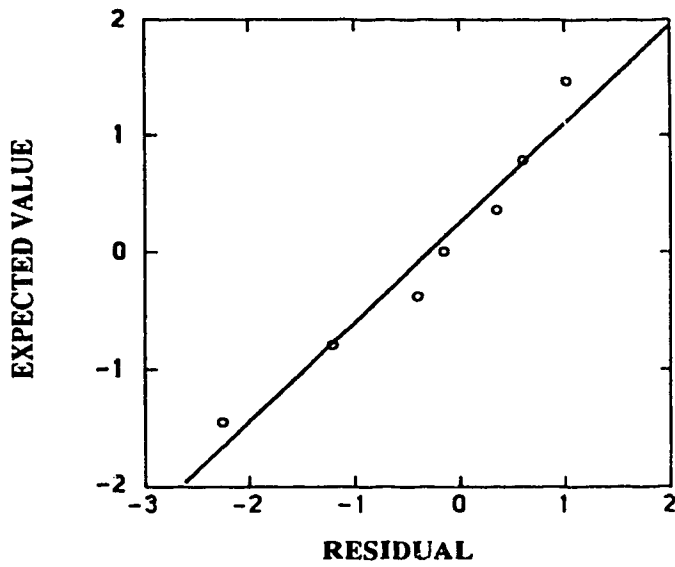


Figure E.4 The Normal Plot of the Residuals ( $0 < \bar{G}_f \leq 70 \text{ s}^{-1}$ )

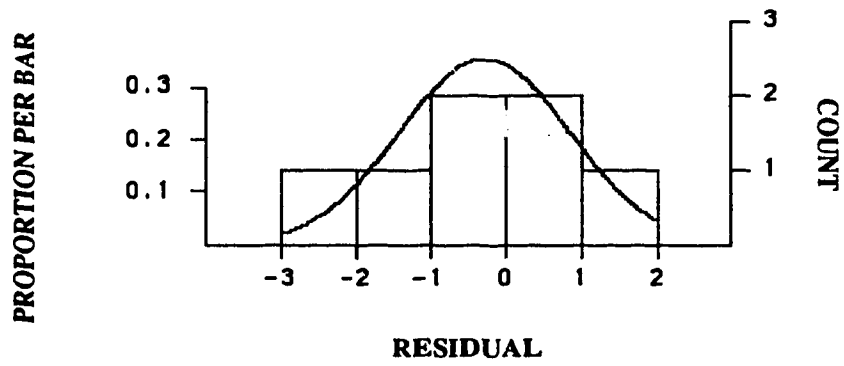


Figure E.5 The Histogram Plot of the Residuals ( $0 < \bar{G}_f \leq 70 \text{ s}^{-1}$ )

## E.2 Determination of $d_{\max}$ Growth Constant $m_2$

Table E.3 Model Simulation for  $m_2$

Model 2:  $d_{\max}=a*(\bar{G}_f)^m + b$  ( $70 < \bar{G}_f \leq 400 \text{ s}^{-1}$ )

ITERATION	LOSS	PARAMETER VALUES	
0	0.2749397D+05	0.1000D+00	0.1000D+00
1	0.7110137D+04	0.3604D+00	0.1015D+00
2	0.7949956D+03	0.1042D+00	0.7856D+02
3	0.1570806D+03	0.1412D+00	0.5529D+02
4	0.1468458D+02	0.1314D+00	0.6176D+02
5	0.1342938D+02	0.1299D+00	0.6246D+02
6	0.1162865D+02	0.1226D+00	0.6432D+02
7	0.4789240D+01	0.1076D+00	0.6670D+02
8	0.2081682D+01	0.8436D-01	0.7053D+02
9	0.1900514D+01	0.8494D-01	0.7015D+02
10	0.1825453D+01	0.8319D-01	0.7051D+02
11	0.1820260D+01	0.8230D-01	0.7065D+02
12	0.1819293D+01	0.8184D-01	0.7072D+02
13	0.1819281D+01	0.8182D-01	0.7072D+02
14	0.1819281D+01	0.8182D-01	0.7072D+02

DEPENDENT VARIABLE IS  $d_{\max}$

SOURCE	SUM-OF-SQUARES	DF	MEAN-SQUARE
REGRESSION	61538.139	2	30769.070
RESIDUAL	1.819	4	0.455
TOTAL	61540.078	6	
CORRECTED	12.476	5	

RAW R-SQUARED (1-RESIDUAL/TOTAL) = 1.000  
 CORRECTED R-SQUARED (1-RESIDUAL/CORRECTED) = 0.854

PARAMETER	ESTIMATE
m	0.082
b	70.722

$d_{\max}=20.237 (\bar{G}_f)^{0.082}+70.722$

Table E.4 Model Simulation for  $m_2$  ( $70 < \bar{G}_f \leq 400 \text{ s}^{-1}$ )

$\bar{G}_f \text{ (s}^{-1}\text{)}$	Tested $d_{\text{max}} \text{ (}\mu\text{m)}$	Estimated $d_{\text{max}}$	Residual
80	99.020	99.686	-0.666
100	100.030	100.220	-0.190
125	100.840	100.764	0.076
150	102.040	101.215	0.825
200	102.490	101.941	0.549
400	103.170	103.763	-0.593

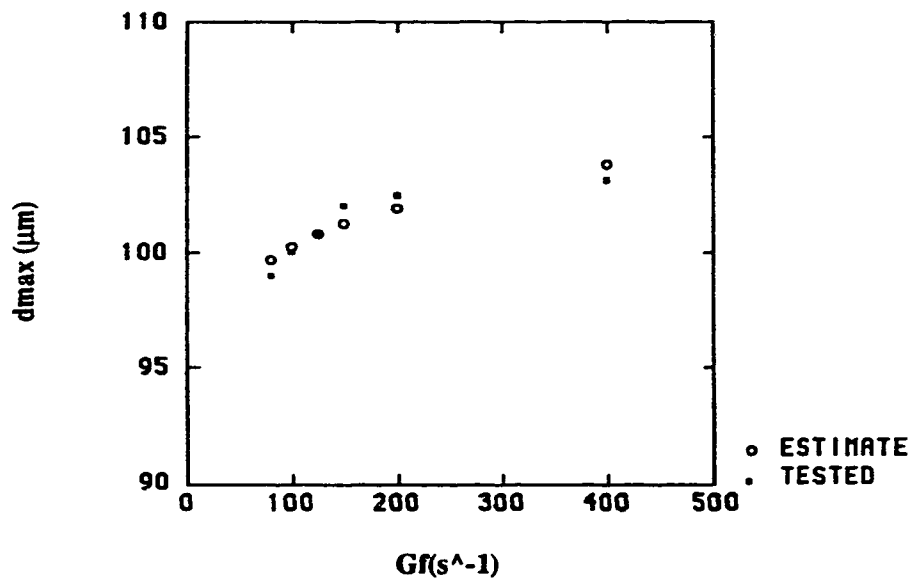


Figure E.6 Effect of Mixing Rate on the Maximum Floc Diameter ( $70 < \bar{G}_f \leq 400 \text{ s}^{-1}$ )

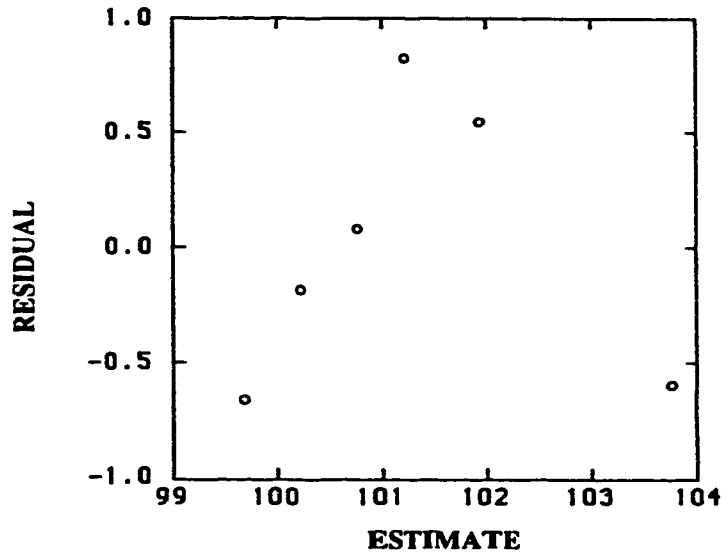


Figure E.7 The Residuals Plotted against Fitted Values of  $d_{\max}$  ( $70 < \bar{G}_f \leq 400 \text{ s}^{-1}$ )

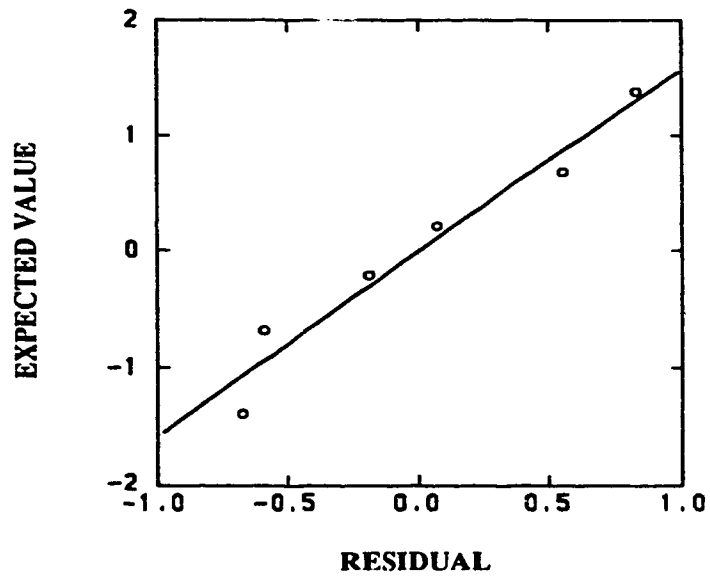


Figure E.8 The Normal Plot of the Residuals ( $70 < \bar{G}_f \leq 400 \text{ s}^{-1}$ )

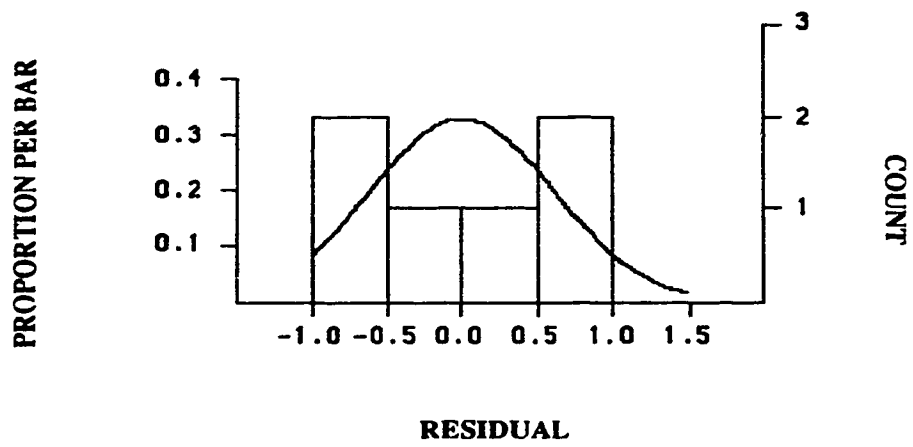


Figure E.9 The Histogram Plot of the Residuals ( $70 < \bar{G}_f \leq 400 \text{ s}^{-1}$ )



### E.3 Determination of $d_{\max}$ Growth Constant $m_3$

Table E.5 Model Simulation for  $m_3$

Model 3:  $d_{\max} = a \cdot \bar{G}_f^m + b$  ( $400 < \bar{G}_f \leq 1000 \text{ s}^{-1}$ )

ITERATION	LOSS	PARAMETER VALUES		
0	0.3118529D+04	0.5570D+01	-.1508D+00	0.7077D+02
1	0.3088437D+04	0.1453D+02	-.2313D+00	0.6824D+02
2	0.3015512D+04	0.2665D+02	-.1560D+00	0.6348D+02
3	0.3012356D+04	0.3464D+02	-.1360D+00	0.6068D+02
4	0.2877600D+04	0.6544D+02	-.2143D+00	0.5365D+02
5	0.2830419D+04	0.6585D+02	-.1898D+00	0.5281D+02
6	0.2762257D+04	0.8364D+02	-.1742D+00	0.4707D+02
7	0.1675424D+04	0.3470D+03	-.1945D+00	-.2770D+02
8	0.1162863D+04	0.6552D+03	-.2020D+00	-.1162D+03
9	0.2615363D+03	0.9212D+03	-.1951D+00	-.1936D+03
10	0.1268767D+03	0.1071D+04	-.1934D+00	-.2369D+03
11	0.2518197D+02	0.1205D+04	-.1946D+00	-.2753D+03
12	0.1429583D+02	0.1287D+04	-.1950D+00	-.2988D+03
13	0.1373190D+02	0.1278D+04	-.1949D+00	-.2963D+03
14	0.1370714D+02	0.1277D+04	-.1949D+00	-.2960D+03
15	0.1370687D+02	0.1278D+04	-.1949D+00	-.2961D+03
16	0.1370687D+02	0.1278D+04	-.1949D+00	-.2961D+03

DEPENDENT VARIABLE IS  $d_{\max}$

SOURCE	SUM-OF-SQUARES	DF	MEAN-SQUARE
REGRESSION	34894.864	3	11631.621
RESIDUAL	13.707	3	4.569
TOTAL	34909.063	6	
CORRECTED	3146.412	5	

RAW R-SQUARED (1-RESIDUAL/TOTAL) = 1.000  
 CORRECTED R-SQUARED (1-RESIDUAL/CORRECTED) = 0.996

PARAMETER	ESTIMATE
a	1277.593
m	-0.195
b	-296.114

$d_{\max} = 1277.593 (\bar{G}_f)^{-0.195} - 296.114$  ( $400 < \bar{G}_f \leq 1000 \text{ s}^{-1}$ )

Table E.6 Model Simulation for  $m_3$  ( $400 < \bar{G}_f \leq 1000 \text{ s}^{-1}$ )

$\bar{G}_f \text{ (s}^{-1}\text{)}$	$d_{\text{max}} \text{ (}\mu\text{m)}$	ESTIMATE	RESIDUAL
400	103.17	101.07	2.101
450	90.09	92.05	-1.961
500	83.77	84.157	-0.387
600	72.67	70.875	1.759
800	49.71	50.854	-1.144
1000	37.14	36.081	1.059

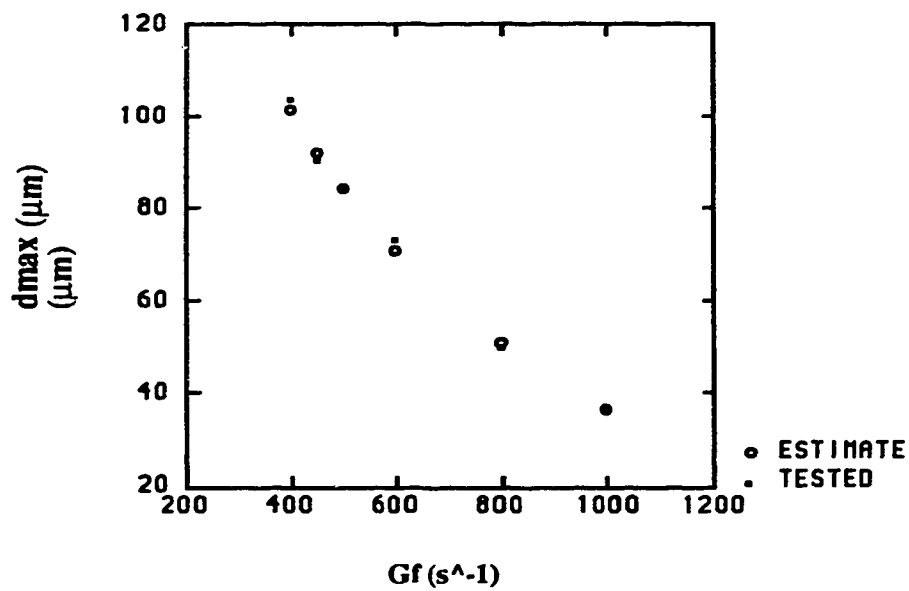


Figure E.10 Effect of Mixing on the Maximum Mean Floc Diameter ( $400 < \bar{G}_f \leq 1000 \text{ s}^{-1}$ )

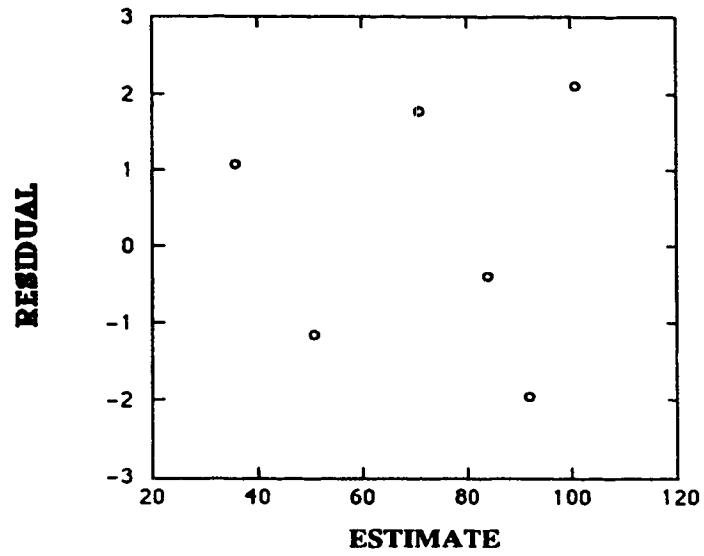


Figure E.11 The Residuals Plotted against Fitted Values ( $d_{\max}$ ) ( $400 < \overline{G}_f \leq 1000 \text{ s}^{-1}$ )

Appendix F The Data of Determination of Experimental Conditions

Table F-1 Particle Size Distributions at Different Stages (polymer=0.5 mg/L, alum=5 mg/L, pH=8, NaHCO<sub>3</sub>=100 mg/L,  $\bar{G}_e=150 \text{ s}^{-1}$  for 1 min.,  $\bar{G}_r=34 \text{ s}^{-1}$  for 30 min.)

Initial Particle Size Distribution (Before Coagulation)						
Particle Diameter( $\mu\text{m}$ )			Number of Particles			
Channel setting	Range d1 to d2	Arithmetic Mean (d)	Channel Width( $\Delta d$ )	Differential Counts/mL(d1 to d2)	Normalized Differential Counts/mL	Cumulative (NP $\geq$ d1) Counts/mL
2	2 to 5	3.5	3	34770.0	11590.0	58010.0
5	5 to 10	7.5	5	21824.0	4365.0	23240.0
10	10 to 20	15	10	1383.4	138.3	1416.0
20	20 to 30	25	10	28.8	2.9	32.6
30	30 to 40	35	10	3.5	0.4	3.8
40	40 to 50	45	10	0.2	0.0	0.3
50	50 to 60	55	10	0.1	0.0	0.1
60	60 to 150	105	90	0.0	0.0	0.0
Particle Size Distribution (After Flocculation)						
Particle Diameter( $\mu\text{m}$ )			Number of Particles			
Channel setting	Range d1 to d2	Arithmetic Mean (d)	Channel Width( $\Delta d$ )	Differential Counts/mL(d1 to d2)	Normalized Differential Counts/mL	Cumulative (NP $\geq$ d1) Counts/mL
2	2 to 5	3.5	3	6005.0	2002.0	9685.0
5	5 to 10	7.5	5	2527.0	505.0	3680.0
10	10 to 20	15	10	975.0	98.0	1153.0
20	20 to 30	25	10	138.0	14.0	179.0
30	30 to 40	35	10	29.0	3.0	41.0
40	40 to 50	45	10	9.0	0.9	12.0
50	50 to 60	55	10	3.0	0.3	4.0
60	60 to 150	105	90	0.9	0.0	0.9
Particle Size Distribution (After Sedimentation)						
Particle Diameter( $\mu\text{m}$ )			Number of Particles			
Channel setting	Range d1 to d2	Arithmetic Mean (d)	Channel Width( $\Delta d$ )	Differential Counts/mL(d1 to d2)	Normalized Differential Counts/mL	Cumulative (NP $\geq$ d1) Counts/mL
2	2 to 5	3.5	3	3282.0	1094.0	4784.0
5	5 to 10	7.5	5	1156.0	231.0	1502.0
10	10 to 20	15	10	327.0	33.0	346.0
20	20 to 30	25	10	19.0	2.0	19.0
30	30 to 40	35	10	0.3	0.0	0.6
40	40 to 50	45	10	0.0	0.0	0.3
50	50 to 60	55	10	0.1	0.0	0.3
60	60 to 150	105	90	0.2	0.0	0.2

Table F-2 Effect of pH on Particle Settling Rates (polymer=0.5 mg/L, alum=5 mg/L, NaHCO<sub>3</sub>=100 mg/L,  $\bar{G}_c=150 \text{ s}^{-1}$  for 1 min.,  $\bar{G}_f=34 \text{ s}^{-1}$  for 30 min.)

Settling Time (min.)	Turbidity(NTU)					
	pH=6.5	pH=7	pH=7.5	pH=8	pH=8.5	pH=9
Initial (-10)	11	11	11	11	11	11
0	10.5	12	10.5	12.5	9	10.5
10	6	6	4	4.5	4	7.5
20	5	5.5	4	2.5	4	7.5
30	3.7	4.5	3	1.2	4	7.5

Table F-3 Effect of pH on Particle Settling Rates (polymer=0.5 mg/L, alum=5 mg/L, NaHCO<sub>3</sub>=100 mg/L,  $\bar{G}_c=150 \text{ s}^{-1}$  for 1 min.,  $\bar{G}_f=34 \text{ s}^{-1}$  for 30 min.)

Settling time (min.)	Turbidity (NTU)					
	pH=7	pH=7.5	pH=8	pH=8.5	pH=9	pH=10
initial	18	19	19	18	18	18
0	11	13	12	10	22	24
10	4	1.5	0.5	2	11	14
20	2.5	1.5	0.2	2	9.5	12.5
30	2.5	1.5	0.2	2	9.5	12.5

Table F-4 Effect of pH on Particle Removal Efficiency (polymer=0.5 mg/L, alum=5 mg/L, NaHCO<sub>3</sub>=100 mg/L,  $\bar{G}_c=150 \text{ s}^{-1}$  for 1 min.,  $\bar{G}_f=34 \text{ s}^{-1}$  for 30 min.)

pH	Removal Efficiency (%)
7.0	66
7.5	83
8.0	92
8.5	89
9.0	30
10.0	22

Table F-5 Effect of Alkali Doses on Particle Settling Rates (polymer=0.5 mg/L, alum=5 mg/L pH=8,  $\bar{G}_c=150 \text{ s}^{-1}$  for 1 min.,  $\bar{G}_f=34 \text{ s}^{-1}$  for 30 min.)

Settling Time (min.)	Turbidity (NTU)					
	C=0 mg/L	C=25 mg/L	C=50 mg/L	C=75 mg/L	C=100 mg/L	C=125mg/L
initial	20.5	19.5	20.5	18.5	20.5	17.5
0	9.5	9.5	9.5	9.5	8.5	10.5
10	4.5	4.5	4.5	4.5	0.5	4.5
20	2.5	2.7	2.0	1.5	0.1	1.8
30	2.2	2.5	1.5	1.0	0.1	1.5

Note: C= the Concentration of NaHCO<sub>3</sub>

**Table F-6 Effect of Alkali Doses on Particle Removal Efficiency and Mean Particle Diameter (polymer=0.5 mg/L, alum=5 mg/L pH=8,  $\bar{G}_c=150 \text{ s}^{-1}$  for 1 min.,  $\bar{G}_f=34 \text{ s}^{-1}$  for 30 min.)**

NaHCO <sub>3</sub> Conc. (mg/L)	Particle Removal Efficiency (%)	Mean Particle Diameter D(6,3) (μm)
0	70	54.8
25	74	60.44
50	outlier	63.53
75	79	68.74
100	90	75.78
125	70	65.04

**Table F-7 Data for the Evaluation of Mean Particle Diameter (  $d_i$  = channel settling, polymer=0.5 mg/L, alum=5 mg/L pH=8, NaHCO<sub>3</sub>=100 mg/L,  $\bar{G}_c=150 \text{ s}^{-1}$  for 1 min.,  $\bar{G}_f=34 \text{ s}^{-1}$  for 30 min.)**

Flocculation Time (min.)	Mean Particle Diameter (μm)			
	D (1,0)	D (3,0)	D (4,3)	D (6,3)
0	5.47	7.10	11.25	16.77
3	5.86	8.14	14.22	18.50
6	5.90	9.43	20.22	25.17
9	5.94	10.11	24.22	30.29
12	5.76	11.75	32.8	38.88
15	5.30	12.17	38.47	44.41
18	5.04	11.14	37.19	43.93
21	4.92	10.64	35.28	42.32
24	4.71	10.15	33.62	40.64
27	4.68	10.40	35.51	42.44
30	4.24	8.69	30.69	38.93

**Table F-8 Data for the Evaluation of Mean Particle Diameter ( $d_i$ =arithmetic mean of each channel size range, polymer=0.5 mg/L, alum=5 mg/L, pH=8, NaHCO<sub>3</sub>=100 mg/L,  $\bar{G}_c=150 \text{ s}^{-1}$  for 1 min.,  $\bar{G}_f=34 \text{ s}^{-1}$  for 30 min.)**

Flocculation Time (min.)	Mean Particle Diameter ( $\mu\text{m}$ )			
	D (1,0)	D (3,0)	D (4,3)	D (6,3)
0	8.32	10.48	15.48	25.27
3	8.82	11.53	17.81	26.22
6	8.72	12.55	22.88	32.24
9	8.76	13.24	29.12	45.15
12	8.42	15.29	35.56	67.66
15	7.83	16.71	66.28	82.77
18	7.54	15.5	64.77	82.4
21	7.37	14.62	59.75	78.89
24	7.09	13.69	54.02	74.24
27	7.05	14.23	59.56	78.62
30	6.50	11.89	49.42	71.81

**Table F-9 The Data of Polymeric Floc Settling Rate (polymer=0.5 mg/L, alum=5 mg/L, pH=8, NaHCO<sub>3</sub>=100 mg/L,  $\bar{G}_c=150 \text{ s}^{-1}$  for 1 min.,  $\bar{G}_f=34 \text{ s}^{-1}$  for 20 min.)**

Settling Time (min.)	Turbidity (NTU)
initial	22.5
0	2.5
2	1.8
4	1.8
6	1.8
8	1.2
10	1.0
20	0.9
30	0.6

**Table F-10 Effect of Lag Time of Polymer Addition on Process Performance**

Parameter	Lag Time of Polymer Addition			
	LT=0 min.	LT=5 min.	LT=10 min.	LT=15 min.
(Before Coagulation) Cuml. Counts/mL	57506	62862	59901	59525
(After Sedimentation) Cuml. Counts/mL	9078	10740	11623	9868
Removal Efficiency (%)	84	84	81	84
Max. Floc Size (µm)	100	120	110	120
Stage	Mean Particle Diameter, D(6,3) (µm)			
	LT=0 min.	LT=5 min.	LT=10 min.	LT=15 min.
Before Coagulation	19.84	20.8	15.76	13.96
After Flocculation	56.12	62.95	57.87	36.36
After Sedimentation	30.34	22.48	35.31	16.88
Settling Time (min.)	Turbidity(NTU)			
	LT=0 min.	LT=5 min.	LT=10 min.	LT=15 min.
Initial	17.8	22.8	17.8	18.8
0	4.8	4.8	5.3	4.8
10	2.8	2.8	2.8	2.3
20	2.3	1.8	2.8	1.3
30	2.3	1.8	2.8	1.3

Note: LT = the Lag Time of Polymer Addition



## Appendix G Kinetic Data of Polymer-Aided Flocculation

Tabl e-G-1 The Data of Mean F article Diameter D(6,3) at  $\bar{G}_c=150\text{ s}^{-1}$ , and  $\bar{G}_f= 20$  to  $150\text{ s}^{-1}$  )

$t_f$ (min.)	Mean Particle Diameter D(6,3)				
	$\bar{G}_f=20\text{ (s}^{-1}\text{)}$	$\bar{G}_f=30\text{ (s}^{-1}\text{)}$	$\bar{G}_f=40\text{ (s}^{-1}\text{)}$	$\bar{G}_f=50\text{ (s}^{-1}\text{)}$	$\bar{G}_f=60\text{ (s}^{-1}\text{)}$
0	19.47	15.77	18.38	24.79	26.08
3	20.08	16.96	20.08	24.90	28.35
6	24.18	19.77	19.2	26.39	28.48
9	28.10	24.48	22.45	29.84	33.94
12	28.94	30.10	28.28	37.37	53.01
15	33.50	42.96	35.29	48.86	61.83
18	38.57	57.75	50.68	60.21	73.70
21	50.86	68.69	68.33	76.03	81.58
24	65.23	75.33	72.80	82.93	88.73
27	67.11	79.46	83.36	87.25	91.90
30	69.05	78.53	82.37	92.35	94.09
33	71.08	83.49	88.57	93.08	96.78
36	74.84	81.29	84.82	92.71	96.83
39	71.44	82.56	84.34		97.79
$t_f$ (min.)	Mean Particle Diameter D(6,3) ( $\mu\text{m}$ )				
	$\bar{G}_f=70\text{ (s}^{-1}\text{)}$	$\bar{G}_f=80\text{ (s}^{-1}\text{)}$	$\bar{G}_f=100\text{ (s}^{-1}\text{)}$	$\bar{G}_f=125\text{ (s}^{-1}\text{)}$	$\bar{G}_f=150\text{ (s}^{-1}\text{)}$
0	17.84	20.46	25.43	29.29	25.86
3	22.38	27.42	31.01	33.39	32.07
6	26.07	31.33	34.72	34.39	35.74
9	37.25	40.06	42.91	46.72	56.82
12	55.28	62.22	63.01	64.78	78.95
15	74.48	77.47	79.92	78.12	89.86
18	85.74	84.92	86.81	88.82	94.00
21	92.33	92.11	91.75	94.63	97.84
24	95.64	94.51	96.08	96.72	100.25
27	96.18	98.48	97.97	98.99	101.16
30	97.44	97.72	99.60	100.18	101.81
33	98.26	99.38	100.66	100.84	102.59
36	99.78	99.41	100.81	102.20	102.35
39	99.88	99.56	101.09	102.03	102.28

**Table G-1-b Mean Particle Diameter  $D(6,3)$  at  $\bar{G}_c = \bar{G}_f = 175$  to  $225 \text{ s}^{-1}$**

Flocculation Time (min.)	Mean Floc Diameter [ $D(6,3)$ , $\mu\text{m}$ ]		
	$\bar{G}_f=175 \text{ s}^{-1}$	$\bar{G}_f=200 \text{ s}^{-1}$	$\bar{G}_f=225 \text{ s}^{-1}$
0	23.95	21.04	29.82
3	28.23	28.33	35.37
6	38.88	36.06	46.43
9	52.51	51.14	59.51
12	66.17	68.44	76.67
15	78.72	80.48	89.59
18	88.24	92.69	95.02
21	94.04	96.54	99.32
24	96.65	99.66	101.18
27	100.31	101.27	102.27
30	100.98	101.56	103.33
33	102.22	103.20	103.48
36	102.76	103.54	103.90
39	102.52	104.18	103.93

**Table G-1-c Mean Particle Diameter  $D(6,3)$  at  $\bar{G}_c = 400 \text{ s}^{-1}$ ,  $\bar{G}_f = 100$  to  $400 \text{ s}^{-1}$**

$t_f$ (min.)	$\bar{G}_f=400 \text{ (s}^{-1}\text{)}$	$\bar{G}_f=300 \text{ (s}^{-1}\text{)}$	$\bar{G}_f=200 \text{ (s}^{-1}\text{)}$	$\bar{G}_f=100 \text{ (s}^{-1}\text{)}$
0	27.40	26.58	27.11	28.51
3	52.28	49.95	40.66	36.54
6	76.51	78.83	72.91	53.49
9	86.30	85.11	89.12	73.53
12	91.58	92.16	96.29	87.29
15	95.61	98.04	99.29	93.13
18	99.05	100.68	101.27	97.05
21	100.10	102.34	102.01	98.72
24	102.14	103.3	102.89	99.26
27	103.25	103.71	103.24	99.75
30	103.76	104.05	103.33	98.80
33	103.99	104.06	103.21	98.93
36	104.47	104.34	101.56	98.15
39	104.52	103.70	100.94	94.96

Table G-1-d Mean Particle Diameter D(6,3) at  $\bar{G}_c = \bar{G}_f = 450$  to  $800 \text{ s}^{-1}$

$t_f$ (min.)	$\bar{G}_f=450 \text{ (s}^{-1}\text{)}$	$\bar{G}_f=500 \text{ (s}^{-1}\text{)}$	$\bar{G}_f=600 \text{ (s}^{-1}\text{)}$	$\bar{G}_f=800 \text{ (s}^{-1}\text{)}$
0	23.46	23.46	23.46	24.11
3	27.52	27.27	26.25	27.28
6	41.49	42.61	40.37	36.44
9	60.42	59.07	52.88	46.81
12	75.11	71.20	61.82	46.46
15	82.89	77.60	67.98	50.01
18	84.78	80.26	71.67	50.44
21	87.94	82.75	72.67	49.94
24	89.91	81.66	73.90	50.55
27	90.40	73.50	71.90	50.09
30	90.08	81.51	73.58	49.78
33	90.75	84.95	72.25	50.58
36	90.80	85.71	73.09	48.60
39	90.72	86.03	72.36	47.73

Table G-1-e Mean Particle Diameter D(6,3) at  $\bar{G}_c = \bar{G}_f = 1000$  to  $1600 \text{ s}^{-1}$

$t_f$ (min.)	$\bar{G}_f=1000 \text{ (s}^{-1}\text{)}$	$\bar{G}_f=1200 \text{ (s}^{-1}\text{)}$	$\bar{G}_f=1400 \text{ (s}^{-1}\text{)}$	$\bar{G}_f=1600 \text{ (s}^{-1}\text{)}$
0	15.60	28.68	15.91	24.18
3	27.10	38.38	23.49	20.55
6	32.09	38.00	27.22	19.72
9	32.75	42.52	29.38	22.97
12	34.86	34.92	23.64	24.52
15	36.59	39.59	25.63	18.47
18	35.29	36.39	28.41	19.71
21	35.99	38.02	26.01	21.63
24	37.45	37.87	28.40	21.60
27	36.50	36.11	24.28	20.49
30	35.86	38.53	22.51	26.28
33	38.33	35.82	25.70	24.87
36	33.87	34.72	21.52	23.09
39	35.32	35.39	23.19	22.22

**Table G-2 Effect of Sample Volume on the Rate of Polymeric Floc Growth**

Flocculation Time (min.)	D(6,3) (μm)		
	Gf=70 s <sup>-1</sup> (68 rpm, V=2L)	Gf=99 s <sup>-1</sup> (68 rpm, V=1L)	Gf=100 s <sup>-1</sup> (86 rpm, V=2L)
0	17.84	27.44	25.43
3	22.38	32.34	31.01
6	26.07	38.11	34.72
9	37.25	57.66	42.91
12	55.28	76.63	63.01
15	74.48	85.04	79.92
18	85.74	93.06	86.81
21	92.33	94.05	91.75
24	95.64	96.39	96.08
27	96.18	98.05	97.97
30	97.44	98.00	99.60
33	98.26	97.17	100.66
36	99.78	97.81	100.81
39	99.88		101.09

**Table G-3 Effect of Mixing on the Maximum Mean Floc Diameter (d<sub>max</sub>)**

$\bar{G}_f$ (s <sup>-1</sup> )	d <sub>max</sub> (μm)	$\bar{G}_f$ (s <sup>-1</sup> )	d <sub>max</sub> (μm)
0	22.56*	125	100.84
20	74.84	150	102.04
30	83.49	200	102.49
40	88.57	400	103.17
50	93.68	450	90.09
60	97.13	500	83.77
70	99.84	600	72.67
80	99.02	800	49.71
100	100.03	1000	37.14

Note: d<sub>max</sub>=22.56 μm is the average of the mean floc diameters D(6,3) at t<sub>f</sub>=0 min., and different  $\bar{G}_f$  values.

Table G-4 Effect of Mixing on Transfer Points and Polymeric Floc Buildup Time

$\bar{G}_c$ (s <sup>-1</sup> )	$\bar{G}_f$ (s <sup>-1</sup> )	t <sub>1</sub> (min.)	t <sub>2</sub> (min.)	t <sub>3</sub> ( t <sub>b</sub> ) (min.)
150	20	12	24	36
150	30	12	21	33
150	40	9	21	33
150	50	9	21	30
150	60	6	18	30
150	70	6	15	27
150	80	6	15	27
150	100	6	15	24
150	125	6	15	24
150	150	6	15	24
175	175	6	15	21
200	200	6	15	21
225	225	6	15	21
400	100	NE	12	21
400	200	NE	9	18
400	300	NE	6	18
400	400	NE	6	18
450	450	NE	12	18
500	500	NE	12	18
600	600	NE	9	15
800	800	NE	9	15
1000	1000	NE	6	15

Note: NE stands for "not exist" due to the mergence of the first two stages

**Table G-5-a Effect of Mixing on Mean Floc Growth Rate ( $\bar{G}_c=150\text{ s}^{-1}$ ,  $\bar{G}_f=20\text{ to }150\text{ s}^{-1}$ )**

$t_f$ (min.)	Mean Floc Growth Rate ( $\Delta d/\Delta t$ , $\mu\text{m}/\text{min.}$ )				
	$\bar{G}_f=20\text{ s}^{-1}$	$\bar{G}_f=40\text{ s}^{-1}$	$\bar{G}_f=60\text{ s}^{-1}$	$\bar{G}_f=100\text{ s}^{-1}$	$\bar{G}_f=150\text{ s}^{-1}$
1.5	0.20	0.57	0.77	1.86	2.07
4.5	1.37	outlier	0.043	1.23	3.29
7.5	1.31	1.08	1.82	2.73	7.03
10.5	outlier	1.94	6.77	6.70	7.38
13.5	1.52	2.34	2.53	5.64	3.64
16.5	1.69	5.13	3.96	2.30	1.38
19.5	4.10	5.88	2.63	1.65	1.23
22.5	4.79	1.49	2.38	1.44	0.80
25.5	0.63	1.59	1.06	0.63	0.30
28.5	0.65	2.06	0.73		

**Table G-5-b Effect of Mixing on Mean Floc Growth Rate ( $\bar{G}_c=400\text{ s}^{-1}$ ,  $\bar{G}_f=100\text{ to }400\text{ s}^{-1}$ )**

$t_f$ (min.)	Mean Floc Growth Velocity ( $\Delta d/\Delta t$ , $\mu\text{m}/\text{min.}$ )			
	$\bar{G}_f=400\text{ (s}^{-1}\text{)}$	$\bar{G}_f=300\text{ (s}^{-1}\text{)}$	$\bar{G}_f=200\text{ (s}^{-1}\text{)}$	$\bar{G}_f=100\text{ (s}^{-1}\text{)}$
0	0.00	0.00	0.00	0.00
1.5	8.29	7.7	4.52	2.68
4.5	8.08	9.3	10.75	5.62
7.5	3.26	outlier	5.40	6.68
10.5	1.76	2.35	2.39	4.59
16.5	1.15	0.88	0.66	1.31
19.5	outlier	0.55	0.25	0.56
22.5	0.68	0.32	0.29	0.18
25.5	0.37	0.14	0.12	
28.5	0.17	0.11	0.03	

Table G-6 Effect of  $\bar{G}_f$  on the Maximum Mean Floc Growth Rate  $[(\Delta d/\Delta t)_{\max}]$ , and on the Critical Flocculation Time ( $t_0$ ) ( $\bar{G}_c=150 \text{ s}^{-1}$ ,  $20 \leq \bar{G}_f \leq 150 \text{ s}^{-1}$ ;  $\bar{G}_c=400 \text{ s}^{-1}$ ,  $150 < \bar{G}_f \leq 400 \text{ s}^{-1}$ )

$\bar{G}_f$ ( $\text{s}^{-1}$ )	$t_0$ (min.)	$(\Delta d/\Delta t)_{\max}$ ( $\mu\text{m}/\text{min.}$ )
20	22.5	4.79
40	19.5	5.88
60	10.5	6.77
100	10.5	6.70
150	10.5	7.38
200	4.5	10.75
300	4.5	9.63
400	1.5	8.29

Table G-7 Effect of Mixing on Floc Growth Constant  $\mu_i$  ( $i=1, 2$  and  $3$ )

$\bar{G}_c$ ( $\text{s}^{-1}$ )	$\bar{G}_f$ ( $\text{s}^{-1}$ )	$\mu_1$ ( $\text{min.}^{-1}$ )	$\mu_2$ ( $\text{min.}^{-1}$ )	$\mu_3$ ( $\text{min.}^{-1}$ )
150	20	0.038	0.068	0.011
150	30	0.055	0.092	0.015
150	40	0.022	0.094	0.021
150	50	0.030	0.078	0.021
150	60	0.015	0.083	0.020
150	70	0.063	0.118	0.021
150	80	0.071	0.105	0.020
150	100	0.052	0.096	0.020
150	125	0.027	0.093	0.024
150	150	0.051	0.103	0.012
400	200	0.090	0.139	0.014
400	300		0.181	0.021
400	400		0.171	0.021
450	450		0.104	0.020
500	500		0.100	0.020
600	600		0.096	0.042
800	800		0.076	0.011